M. Hall

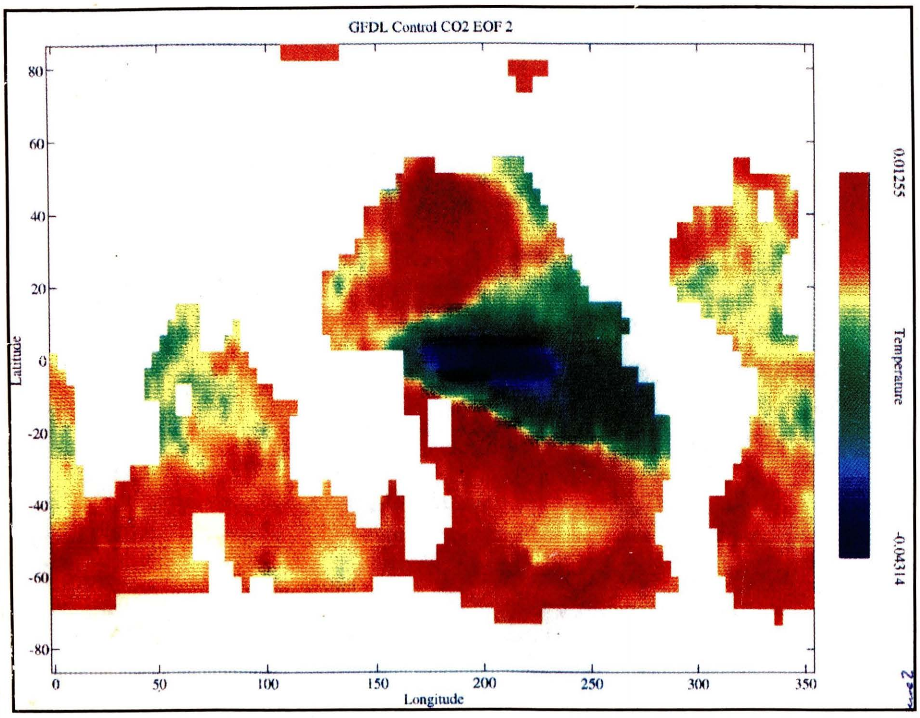

International Conference on Underwater Acoustics

UNSW

5 -7 December 1994

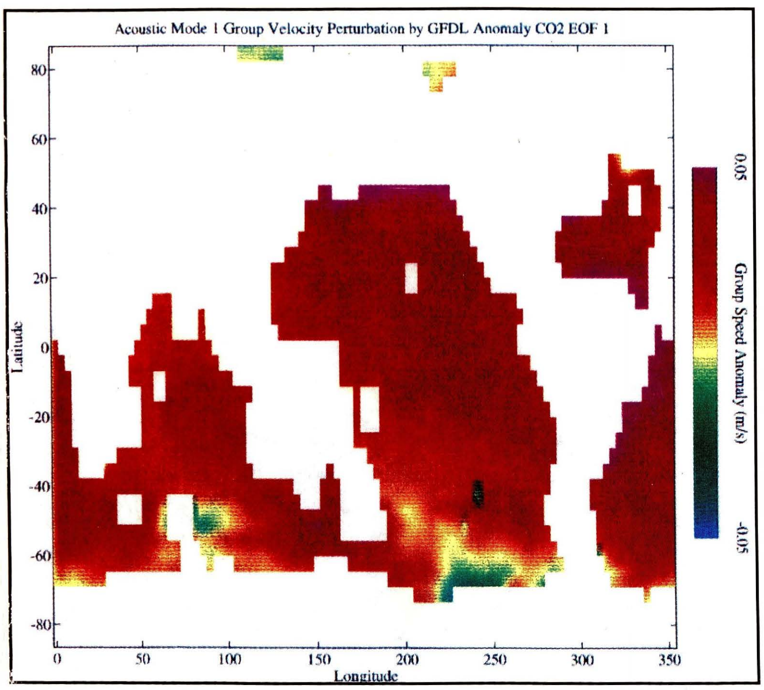

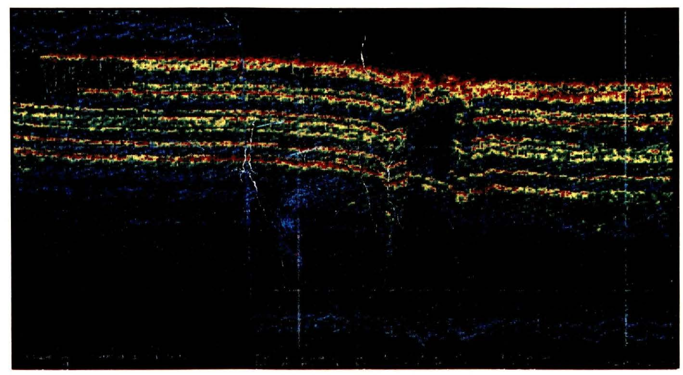

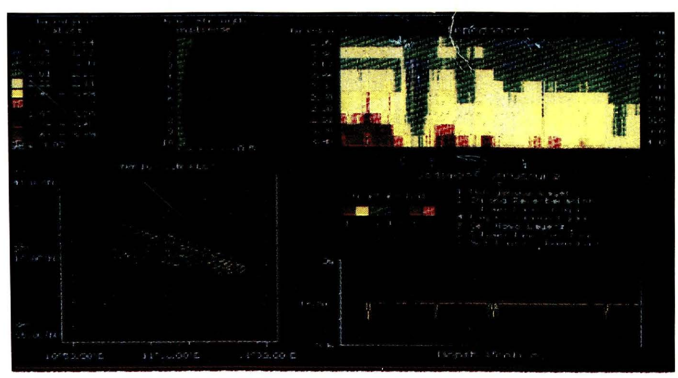

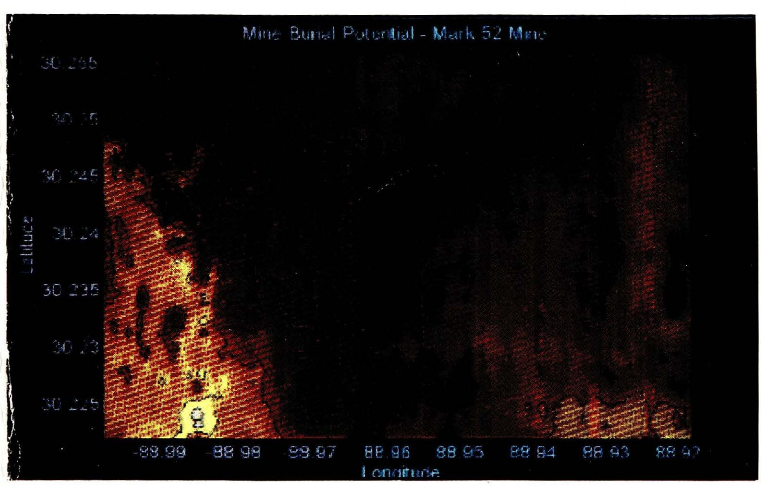

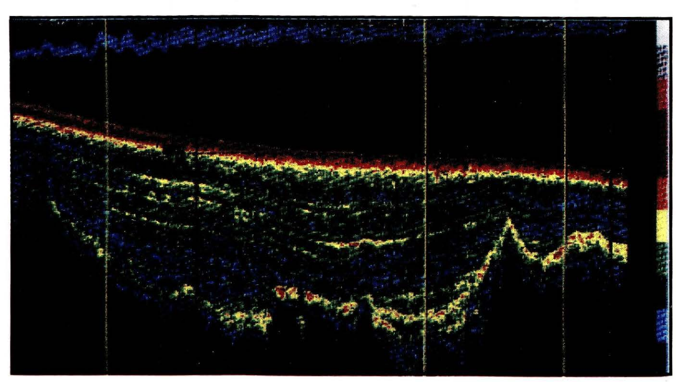

Australian Acoustical Society

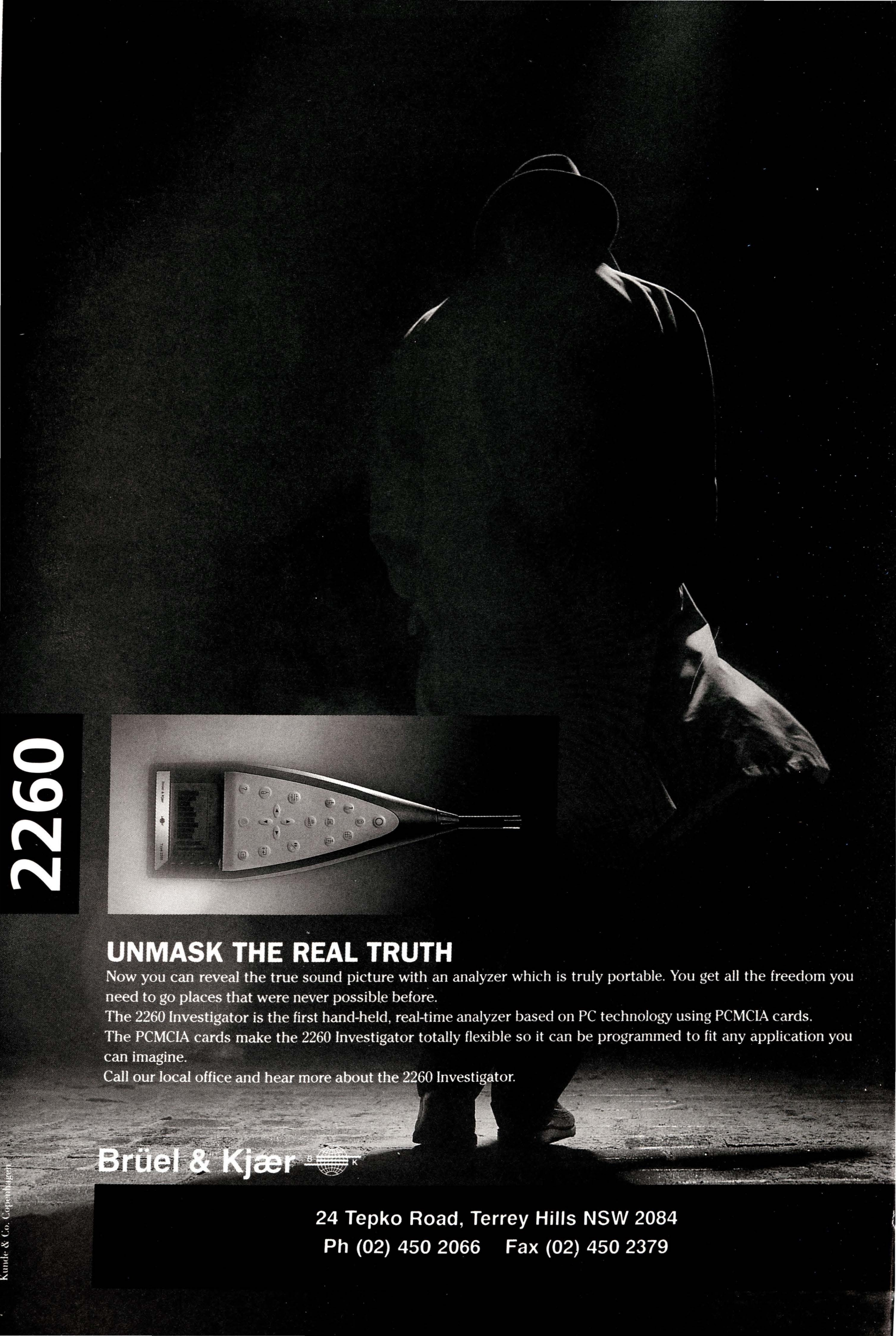
2260
UNMASK THE REAL TRUTH
Now you can reveal the true sound picture with an analyzer which is truly portable. You get all the freedom you need to go places that were never possible before.
The 2260 Investigator is the first hand-held, real-time analyzer based on PC technology using PCMCIA cards.
The PCMCIA cards make the 2260 Investigator totally flexible so it can be programmed to fit any application you can imagine.
Call our local office and hear more about the 2260 Investigator.
Brüel & Kjær
24 Tepko Road, Terrey Hills NSW 2084
Ph (02) 450 2066 Fax (02) 450 2379
Kunde & Co, Copenhagen

Australian Acoustical Society

International Conference on Underwater Acoustics

Acoustic Imaging and Remote Sensing
held at the University of New South Wales
5th-7th December

Co sponsored by
Australian Academy of Science
GEC - Marconi

ISBN 0-909882-15-0

Published by Australian Acoustical Society
Darlinghurst Public School - Annex Bld
Liverpool / Barkham St.
Darlinghurst 2010
Australia

Printed by
Cronulla Printing Co.
16 Cronulla St.
Cronulla 2230

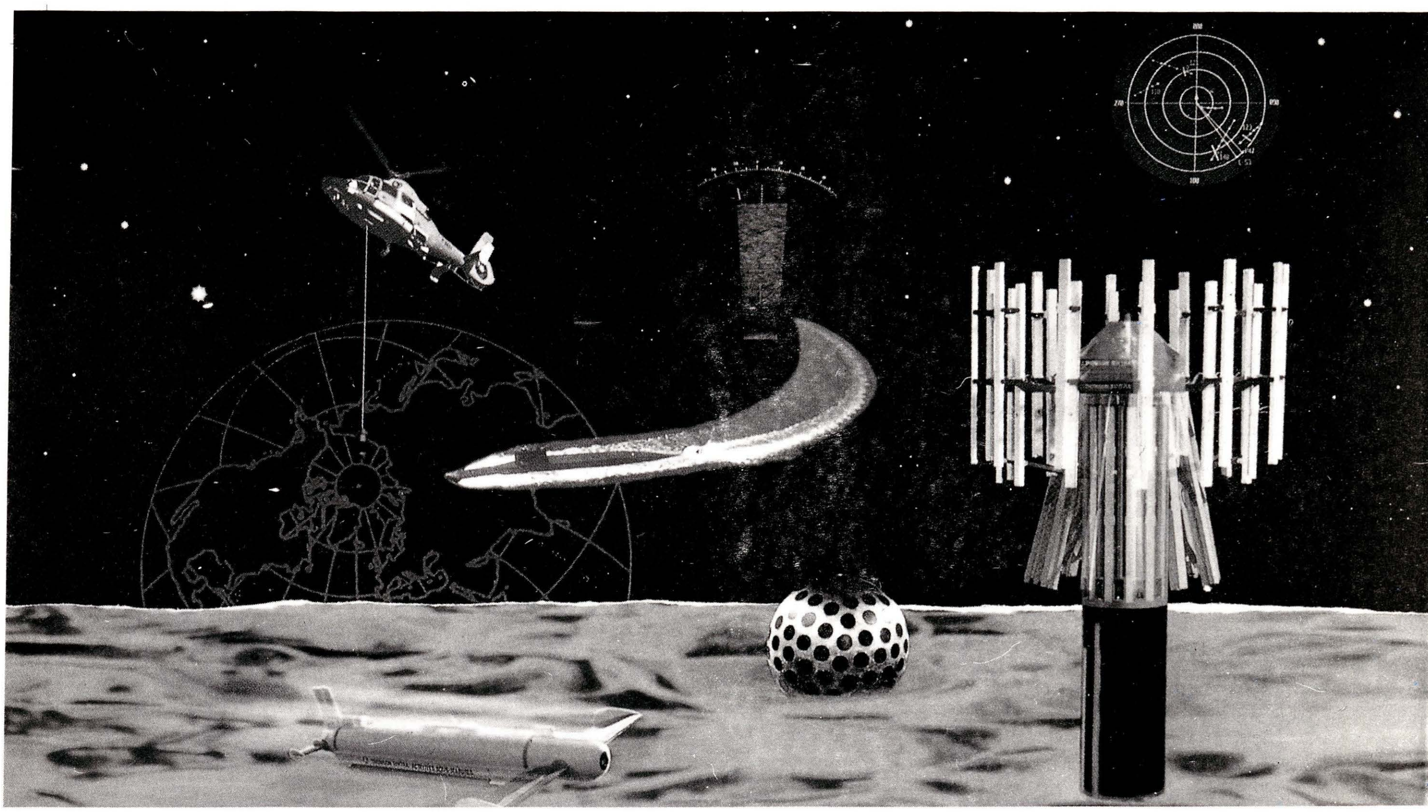

THOMSON SINTRA PACIFIC. THE PEOPLE WHO TAKE TECHNOLOGY INTO UNCHARTED WATERS.

The sea is a big theatre. We're a vital part of a big team. At Thomson Sintra Pacific we participate in the design, development and production of very advanced systems for every area of underwater detection. This activity includes submarine, surface and airborne systems, minehunting and undersea calibration systems.

The driving force is R&D. At Adelaide in South Australia, for example, we run Australia's leading centre for sonar technology research and development. First class developments in high performance arrays and training technology are now coming on to the world market from this centre. We are active research participants in government sponsored co-operative research centres and involve leading scientific researchers from Australian universities in our work. The synergy of such R&D resources ensures we continually renew our position as the leading supplier of military underwater detection systems.

At North Ryde in Sydney we are producing the next generation of sonars for submarines and surface ships to approved military standards of quality. We conduct scientific studies for customers and for internal applications. These diverse activities require knowledge at the leading edge.

As a member of the Thomson Sintra ASM team we are present in most major countries around the world. The sea covers the globe. So do we.

THOMSON-CSF
World-Class Electronics

THOMSON SINTRA PACIFIC *Pty Limited* (ACN 003 335 377), *Unit* 18, 112-118 *Talavera Road*, NORTH RYDE, NSW, 2113. *Tel* (02) 805 0755 *Fax* (02) 805 0698

Preface

After the previous two successful conferences on underwater acoustics held at the University of New South Wales in 1984 and 1989, it was considered that it was time for another such meeting; there having been many recent developments in research and technology. The theme of this presented conference is similar to that of the previous two, but a greater emphasis has been placed on acoustic imaging and remote sensing.

The role of underwater acoustics is vital to many of Australia's national needs, from the economic exploitation of marine resources to national defence. Recent advances in acoustic imaging and remote sensing technology have added new capabilities to both of these fields of endeavour, for example, the assessment of marine biological resources and the mapping of the seabed, and to many other areas so it is appropriate that they feature strongly in any scientific and technological conference on the subject.

A number of distinguished scientists were invited to present their recent advances and to act as a focus in bringing together other scientists from academia, the defence and the commercial world in an atmosphere conducive to learning and the exchange of ideas and information.
Some 60 papers were presented from authors working in Australia, New Zealand, the US, China, South Africa, England and Scotland.

The Conference was divided into several sections which were organised by convenors as follows:

Medical Ultrasonics —- David Robinson

Acoustic Imaging —- Ian Jones

Seabed Characterisation —- Marshall Hall

Sensing —- John Penrose

The Noise Environment —- Doug Cato

Fisheries —- Rudy Kloser

Acknowledgements and thanks for sponsoring the Conference are due to the **Australian Acoustical Society,** to the **Australian Academy of Science** and to **GEC-Marconi.**

Thanks are also due to commercial supporters of the conference, **Bruel and Kjaer (Australia), Geo Instruments Pty Ltd, Unisearch, Kingdom Pty Ltd** and **Thompson-Sintra.**

I would also like to acknowledge the help and advice given by the Section Convenors listed above and by the other members of the Conference executive committee, Marshall Hall and Stephen Samuels.

J. I Dunlop
School of Physics
University of New South Wales
Sydney 2052, Australia

Front Cover: Top: Dzieciuch figure 2 page 119, Centre Left: Dzieciuch figure 3 page 120, Lower Left: Richardson et al figure 1 page 90, Centre & Lower Right: Lambert et al figures 1,2,3 pages 68 ,69

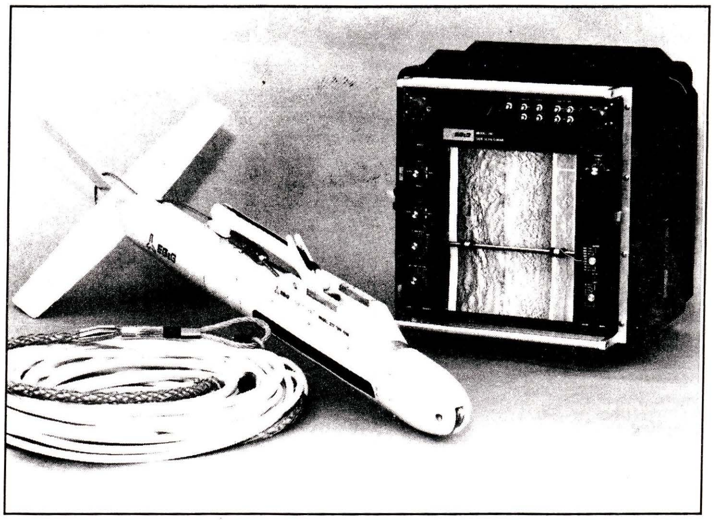

EG&G Model 260 Side Scan Sonar with the 272 Dual Frequency Tow Fish.

OS-200 Portable CTD for Profiling or Mooring. For Oceanography, and Environmental Studies.

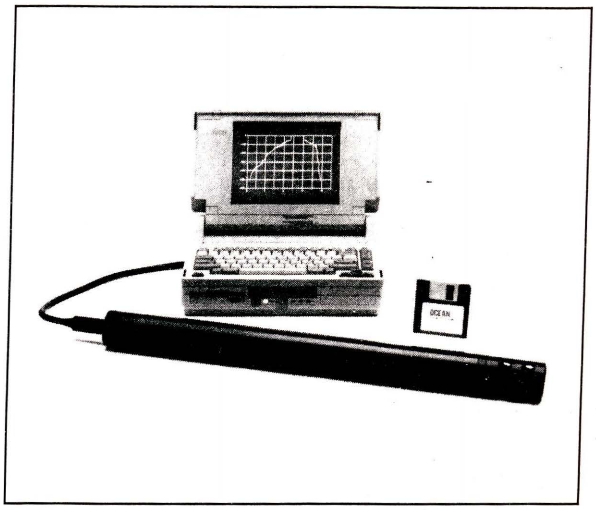

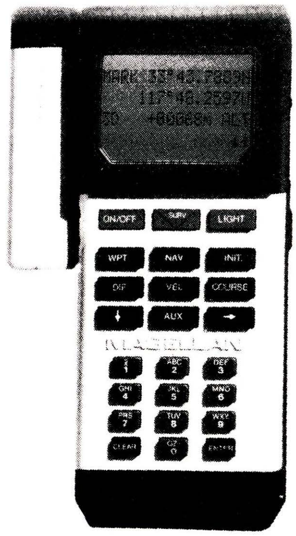

Model 5000Pro Magellan GPS Receiver, with 5 channels. Differential and Carrier Phase are optional.

Transmissometer from Sea-Tech for the measurement of Light Transmission in Water.

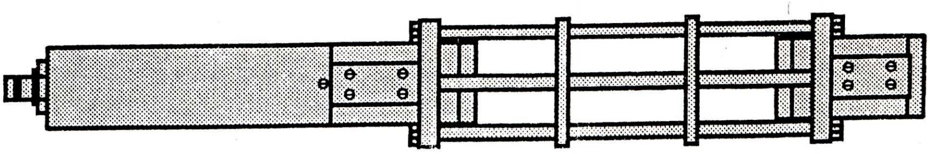

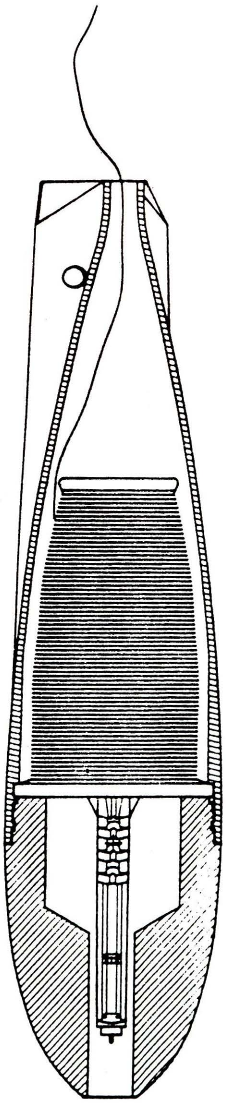

Expendable Bathythermograph Probe (XBT) for the measuring of temperature, from Sparton of Canada.

Contents

Page

Acoustic Imaging

Acoustic Imaging - Seabed

UNDERWATER SENSING

An Industrial Training Course

This package has been designed for training newly recruited engineers and for retraining personnel whose job function has changed. It has been produced at the Open University in the UK and sponsored by a consortium of contractors and the UK Defence Research Agency.

The course comprises five separate multimedia modules - one on each of the following topics and featuring a leading authority presenting relevant state of the art concepts:

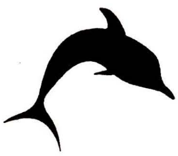

1. **Basic Acoustics & Propagation**
2. **Sonar Signal Processing**
3. **Oceanography**
4. **Sonar Transducers**
5. **Sonar Performance Analysis**

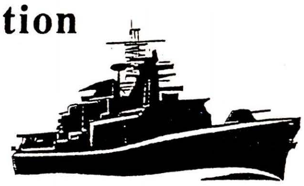

Each module comprises approx 8 hours of video and 4 hours of audio cassettes as well as extensive tutorial manuals. The course is intended for graduate scientists and engineers who are assumed to have some technical and mathematical ability. Non-graduate employees with sufficient experience in the industry should be able to benefit from the material.

The Acoustics & Vibration Centre, at the Australian Defence Force Academy, via Unisearch (UNSW), is the agent for Australia and Asia.

Further details and demonstration:

Marion Burgess
Acoustics & Vibration Centre
Aust. Defence Force Academy
Canberra ACT 2600
Australia

tel: Int + 61 6 268 8241
fax: Int + 61 6 268 8276
email: m-burgess@adfa.oz.au

Reflections on Early Experiences in Ocean Acoustics

A.C. Kibblewhite
Department of Physics, University of Auckland, Private Bag 92019, Auckland, New Zealand

ABSTRACT

Acoustics is a fundamental branch of physics which is important to many disciplines. Specialists in modern acoustics are found in Departments of Physics, Engineering, Oceanography, Mathematics, Psychology, Music and Architecture. Studies being undertaken range from noise suppression to concert hall acoustics.

Ocean acoustics, which is concerned with the science of sound in the sea, began many centuries ago. Leonardo da Vinci was aware of the efficiency with which sound propagated in the ocean and measurements to determine the velocity of sound in the sea were first attempted about 170 years ago. However significant advances in the subject had to await the technological developments of the 20th century.

Underwater acoustics is concerned with a medium which is inhomogeneous, bounded by complex interfaces and seemingly determined to protect its secrets. Experimental programmes in this field have traditionally involved the deployment of sources and receivers from ships. They have always placed severe demands on personnel and equipment alike. Prime objectives have been the monitoring of the soundfield and relating this to the ocean parameters which control the refraction, scattering and attenuation of sea water, and to the reflection properties of the boundaries. The accumulation of this information has required the dedication of many people, the methodical development of a wide range of instrumentation of increasing sophistication and the expenditure of much blood, sweat and tears in operations at sea.

The development of the subject has also involved intensive theoretical analysis. For many years ray theory provided the basis for most of the studies of propagation in the sea. However, as with all scientific research, the arrival of modern computers has had a dramatic impact on ocean acoustics. Numerical modelling of acoustic phenomena has become common place. Using the more exact wave theoretical description of propagation, previously intractable acoustic problems can now be examined with remarkable speed and efficiency to provide a quantitative appreciation of the processes involved. The maturity acoustic modelling has now achieved is demonstrated by the recent publication of the first text book on computational ocean acoustics[1].

The developments in marine acoustics as a whole are demonstrated afresh at meetings such as this. The recent Boston meeting of the Acoustical Society of America[2] was particularly notable in this respect, in that a special session on the possible use of naval SOSSUS facilities for general ocean acoustics demonstrated quite dramatically how far the combination of current underwater instrumentation and modern data processing capability has taken the fields of Acoustical Oceanography and Underwater Acoustics[37]. In an innovative attempt to attract non-military use of the US Navys Undersea Surveillance System, the Navy gave some evidence of its remarkable capability and its potential to service many important projects concerned with the worlds oceans. One example cited involved the tracking of a specific marine mammal for weeks at a time over oceanic distances. Another concerned the ability to detect and position illegal drift-net fishing activities.

Our knowledge of the oceans and underwater acoustics has not always been at this level of sophistication. It was only 40-50 years ago that acousticians were struggling to understand the ocean properties controlling long range propagation. It is important, particularly for those introduced to the subject in recent years, to reflect occasionally on the developments (and tribulations) of the past, on which today's achievements are based. The Organisers of this Conference had this in mind in asking me to base this talk on the early New Zealand activities in ocean acoustics. At first it seemed presumptuous to select such a theme but I finally accepted that the subject was probably appropriate to this Australasian meeting because the work to be described involves some of the first studies in ocean acoustics carried out in the Southern Hemisphere. The paper will certainly serve to emphasise the differences in instrumentation, shipping and background knowledge between now and then, and the influences these had on planning experimental programmes.

While the experiences will be related from a personal perspective, it is important to acknowledge that many individuals were involved with the studies to be reported. I believe all will regard their association with these early activities as being a very positive experience in their lives. All that was done in those early days was very much in the pioneering mould. The frustrations of bad weather, equipment breakdown and scientific ignorance were often demanding on morale but a great spirit nevertheless pervaded the whole team. We had some bitter disappointments and some gratifying achievements. This paper is appropriately dedicated to those who participated.

The paper will deal with the establishment of the New Zealand research group in the 1950s and the first hesitant underwater acoustic measurements that were made. The installation of a permanent hydrophone system will be outlined and some of the important contributions to marine acoustics which arose from it will be described.

Basic to these studies was the measurement and understanding of propagation in New Zealand waters and the classification of the prevailing sea-noise levels and the sources responsible for them. A large number of propagation studies were carried out in local waters all of which were to add to the understanding of shallow-water propagation[4-6]. Because of the low shipping densities in coastal waters, it was expected that ambient noise levels would be among the lowest recorded anywhere. While this is effectively so, the presence of various unforeseen acoustic sources had to be identified and classified before the true picture became clear. Some of these proved to be biological[7]. Others proved to be geophysical. The identification of one probably represents the first time an underwater volcano was discovered and located by acoustic means[8]. The source of another remained unresolved for many years until much better instrumentation was to become available[9]. Studies of it are still active today. With New Zealand so centrally placed in the Southern Ocean it was natural to extend the coastal studies to deep-water as technology developments allowed. Numerous long-range propagation studies were mounted to examine the transmission characteristics of the Southern Ocean[10], the Tasman Sea[11], the South Pacific Ocean[12-15] and the Antarctic[16]. Some of these experiments were joint studies with United States laboratories. They were among the first to demonstrate the potential of oceanographic acoustics in that several distinct water mass boundaries were identified acoustically. They were also to demonstrate the existence of clear transmission paths from New Zealand to the west coast of North America through the Pacific Ocean and from New Zealand to South Africa through the Southern Ocean. These results were to give some credence to the basic premise of the Heard Is. experiment which was to be mounted 30 years later. Some of the results of the experiments will be reviewed.

REFERENCES

1. F.B. Jensen, W.A. Kuperman, M.B. Porter, H. Schmidt, Computational Ocean Acoustics, American Institute of Physics, New York (1994).

2. 127th meeting of the Acoustical Society of America, 6-10 June 1994, Cambridge, Massachusetts.

3. Session 2pAO: Acoustical Oceanography and Underwater Acoustics: Use of Naval Facilities for Ocean Acoustics.

4. A.C. Kibblewhite and R.N. Denham Propagation in Surface Sound Channel, J.Acoust.Soc.Am, 38-71 (1965).

5. A.C. Kibblewhite and R.N. Denham, Experiment on Sound Propagation in Shallow-Water under Isovelocity Conditions, J.Acoust.Soc.Am. 40, 1137-1344 (1966).

6. A.C. Kibblewhite and R.N. Denham, Experiment on Sound Propagation in Shallow-Water with Velocity Structure, J.Acoust.Soc.Am. 44, 104-112 (1968).

7. A.C. Kibblewhite, R.N. Denham and D.J. Barnes, Unusual Low-Frequency Signals Observed in New Zealand Waters, J.Acoust.Soc.Am. 41, 644-655 (1967).

8. A.C. Kibblewhite, The Acoustic Detection and Location of an Underwater Volcano, N.Z.J1,Sci. 9, 178-199 (1966).

9. A.C. Kibblewhite and K.C. Ewans, Wave-Wave Interactions, Microseisms and Infrasonic Ambient Noise in the Ocean, J.Acoust.Soc.Am. 78, 981-994 (1988).

10. A.C. Kibblewhite and R.N. Denham, Long-Range Propagation in the Southern Ocean, J.Acoust.Soc.Am. 38, 629-643 (1965).

11. A.C. Kibblewhite and R.N. Denham, Long-Range Sound Propagation in the South Tasman Sea, J.Acoust.Soc.Am. 41, 401-411 (1967).

12. A.C. Kibblewhite and R.N. Denham, Hydroacoustic Signals from the CHASE V Explosion, J.Acoust.Soc.Am. 45, 944-956 (1969).

13. A.C. Kibblewhite and R.N. Denham, The CHASE V Explosion - Submarine Topographic Reflections from the Vicinity of Pitcairn Is., Deep Sea Research, 18, 905-911, 1971.

14. A.C. Kibblewhite and R.N. Denham, Project Apteryx - A Study of Long-Range Sound Transmission in the Pacific Ocean, Part I: Background to the Experiment. J.ofUnderwater Acoustics (USN) 21, 297-311 (1971).

15. A.C. Kibblewhite and R.N. Denham, Low-Frequency Acoustic Attenuation in the South Pacific Ocean, J.Acoust.Soc.Am. 49, 810-815 (1971).

16. A.C. Kibblewhite and D.A. Jones, Ambient Noise Under Antarctic Sea Ice, J.Acoust.Soc.Am. 59, 790-798 (1976).

Theoretical Developments Relating to the Seismo-Acoustic Effects of Ocean Wave Interactions

A.C. Kibblewhite & C.Y. Wu
Department of Physics, University of Auckland, Private Bag 92019, Auckland, New Zealand

The role of nonlinear wave-wave interactions as a dominant source of ultra-low-frequency (ULF) ocean noise and microseisms was first identified by Longuet-Higgins[1]. In his very comprehensive analysis, which remains the definitive paper to this day, he considered many aspects of the phenomenon and further confirmed the essential physics of the process in an elegant laboratory experiment[2]. In a subsequent contribution of significance Hasselmann[3] provided a statistical description of the source field. A great deal of activity was to follow and the literature of the 1960's is rich with accounts of related papers.

In the 1980's a renewed interest in ULF acoustics led to a series of studies, based on vastly improved technology, designed to clarify the characteristics of the process involved in a field environment [4-13].

Among the results reported was a set of wind-dependent pressure spectra[4]. The spectral levels reported were consistent with other measurements made around that time, and the spectra and their behaviour with respect to wind speed appeared to conform very closely to the predictions of wave interaction theory. While satisfying, the significance of this agreement with theory remained uncertain because of some of the basic assumptions involved in establishing the relationship for the wave-induced pressure field. For instance in the traditional theoretical analysis only the second order of the perturbation solution is considered. While a reasonable approximation no justification for this restriction is provided. Further, only the homogeneous component of the induced pressure field(for which the horizontal wave number, k, is less than $\omega\ \alpha_1$, ω being the angular frequency and α_1 the sound velocity in water), is considered, the neglect of the inhomogeneous component $k > \omega\ \alpha_1$ being justified by the infinite ocean depth assumed. The deep-water assumption also justifies the use of the deep-water approximation of the ocean-wave dispersion relation but no attempt has been made to see how the pressure and seismic fields relate to its general form.

The resolution of these and related issues is not only important to any meaningful quantitative analysis of field measurements but it is equally critical to the proper understanding of the physics involved. Some of these theoretical issues have now been considered[11-19]. In particular the nature of the inhomogeneous component of the pressure field has been examined. Wind-dependent spectra calculated using the new generalised expressions for the pressure field have shown how important this component can become in the upper levels of the water column[13,17,18] An analysis based on these revised expressions has also been used to examine the propagation of wave-induced seismic energy outside an active region of finite size[16]. In addition, a more general theory of sound generation in the vicinity of the sea surface has been developed which describes inherents virtually all wave related sound source mechanisms[14,15].

Significant as these developments have been certain ambiguities persist, which are critical to the complete understanding of the ULF noise field in shallow-water environments. Key among these is the use of the deep-water dispersion relation in all theoretical developments. The nature of the second-order interactions when the deep-water approximation is no longer valid, also remains to be examined. Furthermore at ultra-low and very-low frequencies the effects of the first-order pressure field and the difference-frequency component of the second-order wave interaction process, which has not yet been analysed hitherto can become comparable with those of the sum-frequency second-order component in shallow-water regions[17], and should be taken into account in considering the total pressure field. These topics have been examined in recent theoretical studies[22,23], which present an exact and unified analysis of the wave-induced ULF pressure and seismic fields in an environment of any water depth and any layered seabed structure and give a complete description of the behaviour of the spectrum throughout the whole horizontal wave plane.

REFERENCES

1. M.S. Longuet-Higgins, ` A theory of the origin of microseisms', Philos.,Trans. ,Roy. ,Soc. ,London , Ser. ,A243 , 1-35 (1950)

2. M.S., Longuet-Higgins, ` Can sea waves cause microseisms?', Symposium on Microseisms, September 1952, NAS-NRC Pub. No.306, pp. 74-93,(1953)

3. K., Hasselmann, `A statistical analysis of the generation of microseisms', Rev., Geophys. 1, 177—210(1963)

4. A.C.,Kibblewhite and K.C., Ewans, `Wave-wave interactions, microseisms and infrasonic ambient noise in the ocean', J.,Acoust.,Soc.,Am. 78, 981-994,(1985).

5. A.C., Kibblewhite and K.C., Ewans, `A study of ocean and seismic noise at infrasonic frequencies', Ocean-Seismo Acoustics Series IV, Vol.,16, pp, 731—741, Eds. T., Akal and J.M., Berkson, Plenum Press (1986).

6. S.C., Webb and C.S., Cox, `Observations and modelling of seafloor microseisms', J., Geophys.,Res., 91 7343—7358 (1986).

7. R.G.,Adair, `Microseisms in the deep ocean: observations and theory', Doctoral dissertation, University of California at San,Diego, La,Jolla, CA (1985).

8. R.G.,Adair, J.A.,Orcutt and T.H.,Jordan, `Low frequency noise observations in the deep ocean', J.,Acoust.,Soc.,Am. 80(2), 633-645 (1986).

9. A.C,,Kibblewhite and C.Y.,Wu, `The generation of infrasonic ambient noise in the ocean by non-linear interactions of ocean surface waves', J.,Acoust.,Soc.,Am., 85, 1935-1945 (1989).

10. A.C.,Kibblewhite and C.Y.,Wu, `A re-examination of the role of wave-wave interactions in ocean noise and microseisms', J.,Acoust.,Soc.,Am., 85, 1946—1957 (1989).

11. H.,Schmidt and W.A.,Kuperman, `Estimation of surface noise source level from low-frequency seismo-acoustic ambient noise measurements', J.,Acoust.,Soc.,Am. 84,2153—2162 (1988).

12. M.A.H.Hedlin and J.A.Orcutt, `A comparative study of island, sea floor, and sub-sea floor ambient noise levels', Bull. Seis. Soc. Am. Vol.,79, No.1, pp. 172-179, February (1989).

13. A.C.,Kibblewhite and C.Y.,Wu, `The theoretical description of wave-wave interactions as a noise source in the ocean', J.,Acoust.,Soc.,Am. 89, 2241—2252 (1991).

14. D.H. Cato, 'Sound generation in the vicinity of the sea surface: Source mechanisms and the coupling to the received sound field.', J. Acoust. Soc. Am. 89, 1076-1095(1991)

15. D.H. Cato, `Theoretical and measured underwater noise from surface orbital motion.', J. Acoust. Soc. Am. 89, 1096-1112(1991)

16. A.C. Kibblewhite and C.Y. Wu, `Acoustic source levels associated with the nonlinear interactions of ocean waves', J. Acoust. Soc. Am. 94, 3358-3378, (1993).

17. A.C. Kibblewhite and C.Y. Wu, `An analysis of the ULF acoustic wave field in the ocean', Proceedings of the Conference on Natural Physical Sources of Underwater Sound $-$ Sea Surface Sound (2), Ed. B.R. Kerman, Kluwer Academic Publishers, pp189-202 (1993)

18. J.A. Orcutt, C.S. Cox, A.C. Kibblewhite, W.A. Kuperman, H. Schmidt, `Observations and causes of ocean and seafloor noise at ultra-low and very-low frequencies', Proceedings of the Conference on Natural Physical Sources of Underwater Sound $-$ Sea Surface Sound (2), Ed. B.R. Kerman, Kluwer Academic Publishers, pp203-232 (1993)

19. M.J. Buckingham, ' Infrasonic ambient noise in the ocean due to atmospheric pressure fluctuations on the surface', J. Acoust. Soc. Am. 88(2), 984-994, (1990).

20. A.C. Kibblewhite and C.Y. Wu, `A study of reflection loss: (I) A multilayered visco-elastic seabed at very low frequencies' J. Acoust. Soc. Am., 96 (1994)(inpress).

21. A.C. Kibblewhite and C.Y. Wu, `A study of reflection loss: (II) Involving a porous layer and a demonstration of the Biot slow wave', J. Acoust. Soc. Am., 96 (1994)(inpress).

22. A.C. Kibblewhite and C.Y. Wu, `A solution for the seismo-acoustic effects induced by ocean waves applicable in shallow-water regions', Proceedings of the Conference on Natural Physical Sources of Underwater Sound $-$ Sea Surface Sound (3),(in press)

23. A.C. Kibblewhite and C.Y. Wu, 'Seismo-acoustic effects of ocean gravity waves', Research Report, Department of Physics, University of Auckland, New Zealand, (1994)(In preparation).

The Correlation of Sea Surface Generated Noise with Speed in Two Oceanic Regions

Douglas H. Cato and Sandra Tavener
Maritime Operations Division Defence
Science and Technology Organisation PO Box 44, Pyrmont, NSW 2009

This paper discusses the correlation of sea surface generated noise with wind speed in two oceanic regions: one in open water (depth 400m) off Perth and the other in the partly enclosed waters (depth 40 m) of Spencer Gulf. Significantly different dependence on wind speed was observed in the two regions. The effect on the correlation of separating the noise and wind measurements in space and time is also discussed. Since surface generated noise is the prevailing noise in the ocean, this study provides an indication of the effectiveness of predicting noise at sea using wind data from weather stations (which may be some distance from the site of interest), or forecasting the noise at some later time from current wind observations.

It has long been known that the prevailing ambient noise in the ocean is generated by sea surface motion (Knudsen, et al, 1948). The noise correlates better with wind speed than with other readily observable parameters such as surface wave height (Wenz, 1962; Perrone, 1969) and has come to be known as "wind dependent noise". More recent studies have shown that the source of noise, at least above 100 Hz, is the oscillation of bubbles formed by wave breaking (Banner and Cato, 1988; Medwin and Beaky, 1989; Pumphrey and Ffowcs Williams, 1990; Updegraff and Anderson, 1991a and b). Wave breaking is evident as white caps and since a clear dependence of white cap coverage on wind speed has been established (Monahan, 1971, for example) a dependence of noise on wind speed is to be expected.

The surface generated noise field results from sources spread over a wide area of the sea surface. The effect of the reflectivity of the sea surface results in the sources radiating as a distribution of vertical dipoles. A simple model which excludes the effect of the sea floor indicates that 90% of the received noise intensity comes from sources within a horizontal range equal to three times the hydrophone depth. The effect of bottom reflections would be to significantly increase this range. Since the wind field is usually turbulent (gusting), a point measurement of wind speed is not likely to be representative of the whole area contributing to the noise, so that the correlation of noise with wind speed is likely to be somewhat imperfect. On the other hand, this correlation could be expected to degrade relatively slowly as the point of the wind measurement is separated from the hydrophone position. If the spatial distribution of the advected wind turbulence is "frozen" and statistically homogeneous in the horizontal plane, the effect of separation in space and time would be interchangeable and related by the speed of advection of the wind turbulence (the geostrophic wind speed). Since the spatial distribution changes slowly, the real situation would be a reasonable approximation to this. It would also follow that the spatial averaging resulting from the contribution of a significant area of sources to the noise field would also be effectively a temporal average. Spectral measurements of the wind turbulence suggest that much of the effect of gustiness would be averaged out (Van der Hoven, 1957).

This paper presents some measurements of noise and wind speed in Australian waters where traffic noise is low, and discusses the wind-wind and wind-noise correlation over various distance scales up to 55 km. Measurements were made using systems comprising a hydrophone on the sea floor (400 m depth off Perth and 40 m depth in Spencer Gulf) and an anemometer mounted on a buoy moored nearby. Comparisons are also made with wind speeds measured at coastal weather stations.

The results show that the measured dependence of noise on wind speed is significantly different for the two regions. Possible reasons for the differences are discussed. Correlation of noise level at a frequency of 1 kHz with the logarithm of wind speed showed a general decrease with spatial or temporal separation, as would be expected. The rate of decrease being broadly similar when spatial and temporal separations are related by the mean geostrophic wind speed. Noise and wind speed measured nearby showed similar correlation coefficients in both regions (0.92 off Perth and 0.93 in Spencer Gulf). At 55 km separation off Perth the coefficient was 0.86, and at 51 km separation in Spencer Gulf it was 0.76.

REFERENCES

Banner, M. L. and Cato, D. H. (1988). Physical mechanisms of noise generation by breaking waves - a laboratory study. In Sea Surface Sound (see Kerman, 1988).

Cato, D. H. and Jones, I. S. F. (1988). Noise generated by the motion of the sea surface - theory and measurement. In Sea Surface Sound (see Kerman, 1988).

Ferguson, B. G. and Wyllie, D. V. (1987). Comparison of observed and theoretical responses of a horizontal line array to wind induced noise in the deep ocean. J. Acoust. Soc. Am., 82, 601-605.

Kerman, B. R. (1988). (editor) Sea Surface Sound. Kluwer, Dordrecht.

Kerman, B. R. (1993). (editor) Natural Physical Sources of Underwater Sounds - Sea Surface Sound (2). Kluwer, Dordrecht

Knudsen, V. O., Alford, R. S. and Emling, J. W. (1948). Underwater ambient noise. J. Mar. Res., 7, 410-429.

Medwin, H. and Beaky, M. M. (1989). Bubble sources of the Knudsen sea noise spectra. J. Acoust. Soc. Am., 89, 1124-1130.

Monahan, E.C. (1971) Oceanic whitecaps. J. Phys. Oceanogr., 1, 139-144.

Perrone, A. J. (1969). Deep ocean ambient noise spectra in the North West Atlantic Ocean. J. Acoust. Soc. Am., 34, 762.

Pumphrey, H. C. and Ffowcs Williams, J. E. (1990). Bubbles as sources of ambient noise. IEEE J. Oceanic Eng. 15, 268-274.

Updegraff, G. E. and Anderson, V. C. (1991a). An instrument for the in situ measurements of sea surface noise from a depth of 1 m under low wind conditions. J. Acoust. Soc. Am., 89, 2253-2263.

Updegraff, G. E. and Anderson, V. C. (1991b). Bubble noise and wavelet spills recorded 1 m below the ocean surface. J. Acoust. Soc. Am., 89, 2264-2279.

Van der Hoven, I. (1957). Power spectrum of horizontal wind speed in the frequency range from 0.0007 to 900 cycles per hour. J. Meteorol., 14, 160-164.

Wenz, G. M. (1962). Acoustic ambient noise in the ocean: spectra and sources. J. Acoust. Soc. Am., 34, 1936-1956.

Underwater Acoustic Noise Levels in Lake Cethana

David R Edwards, Edward O'Brien and Iain Edmondson
Australian Maritime Engineering Cooperative Research Centre Launceston Node
PO Box 986, Launceston, Tasmania 7250, Australia

This paper describes the noise measurements made in Lake Cethana, Northern Tasmania, as the first step in establishing the suitability of this lake as a possible site for a proposed towed array test facility and gives the noise spectrum results obtained. The results are compared with typical ambient noise data for Australian waters.

1. INTRODUCTION

Lake Cethana is a long deep artificial lake which is managed by the Hydro-Electric Commission (HEC) of Tasmania as part of the State's hydro-electric generating network. The lake, situated approximately 80 km west of Launceston, is one of the sites used by the Australian National Underwater Training Centre Ltd (ANUTC), a company established to train surface supported air and mixed-gas divers.

Lake Cethana is being investigated as a potential site for a towed array testing facility under an Australian Maritime Engineering Cooperative Research Centre (AMECRC) project. As a first step in assessing the suitability of the lake for this role, underwater acoustic noise measurements have been carried out with and without the HEC generators in operation. Depth soundings of the lake have also been made. A map of the northern end of Lake Cethana is included.

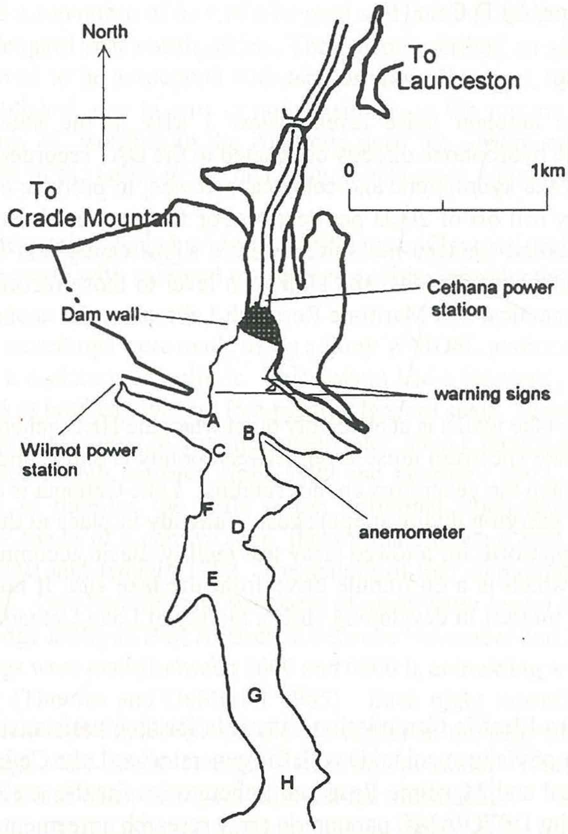

DAT recorder
cuts off
below 1KHz

Figure 1. Map of Lake Cethana

2. DEPTH SOUNDINGS AND THE NOISE SPECTRUM LEVEL

Figure 1 shows the north end of Lake Cethana with the location of various measurement positions shown. With the lake water level approximately 2m below the dam spillway, the lake depth varies mainly between 60m and 80m with the shallowest point being 52m approximately, between the points D and E. The deepest recording was 90m at a point between the signs in front of the dam wall. The depth soundings of the lake were made with a narrow beam echo sounder along the approximate centre line of the lake from the dam wall to point H.

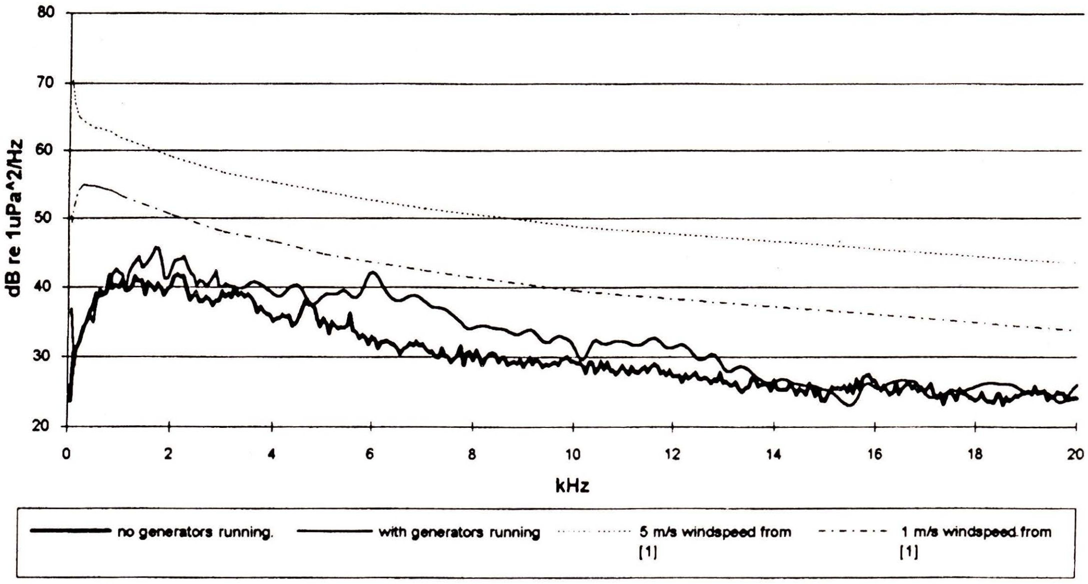

Figure 2. Measurements made at point G with and without the generators running

Figure 2 shows the noise level at point G with and without the generators running. Between the frequencies of 2 kHz and 13 kHz there is approximately 5 dB difference between the two levels. For comparison, the two upper curves show typical ambient noise data for Australian waters for the wind speeds shown. These data have been taken from Figure 1 of a paper by D Cato [1].

3. DISCUSSION OF RESULTS

The rapid decrease in the ambient noise levels below 1 kHz in the above results is because the measurements were made with the hydrophone directly connected to the DAT recorder. The low input impedance of the DAT acts, with the sum of the hydrophone and cable capacitance, to produce a lower cutoff frequency of about 1kHz with a low-frequency roll off of 20dB per decade. For frequencies above 1 kHz the ambient noise levels are encouraging. The recorded Cethana measurements are significantly less than the typical results for Australian oceanic waters at similar wind speeds, and similar in level to those recorded in Woronora Dam [2], which is used by the DSTO Aeronautical and Maritime Research Laboratory for acoustic experimentation.

4. SUMMARY

Lake Cethana is a long deep lake which is acoustically quiet when the HEC generators are not running. With the generators in operation, the lake spectrum noise level between points D and E and at point G are marginally increased compared to the case when the generators are not running. Lake Cethana is one of the sites used by the ANUTC and a 22m x 11m barge carrying diving support gear is already in place at the dam wall end of the lake which could be used as a winch platform for a towed array test facility. Basic accommodation is available at the old HEC camp at Gowrie Park which is a 20 minute drive from the lake site. It now needs to be established whether or not there is sufficient interest in developing such a facility at Lake Cethana.

5. ACKNOWLEDGEMENTS

The authors thank the Hydro-Electric Commission,Tasmania for their assistance, and particularly for their co-operation regarding the timing of visits to coincide with the generators at Lake Cethana being on or off. They also thank the DSTO Aeronautical and Maritime Research Laboratories for the use of the Rockland Analyser, which is on loan to AMC for a joint DSTO/AMC parametric array research agreement, and Dr Doug Cato for his encouragement and advice regarding this project. The support of Dr Allan Carpenter, Director of Australian Sonar Systems and AMECRC Sub-Program leader for this and other projects is also acknowledged.

6. REFERENCES

1. Cato, D.H., Review Of Ambient Noise In The Ocean: Non Biological Sources, Bulletin of Australian Acoustical Society, Volume 6, 1978

2. Cato, D.H., Private Communication

Agonistic and Advertising Vocalisations of the Leopard Seal, Hydrurga leptonyx

T. Rogers, D.H. Cato*, and M.M. Bryden
Department of Veterinary Anatomy, University of Sydney, NSW 2006
* also at Defence Science and Technology Organisation, PO Box 44, Pyrmont, NSW 2009

Leopard seals, Hydrurga leptonyx, are circumpolar in distribution, and are found generally between 50 S and 79 S (Bonner and Laws 1964), though the northern limit of their distribution is unknown and strandings on east and west coasts of Australia are are a regular occurrence. Birth occurs between October and mid November in the Antarctic pack ice (De Master et al. 1979; Siniff and Stone 1985), and mating three to four weeks later, in December and early January (Sinha and Erickson 1972; Siniff and Stone 1985).

Little is known of the reproductive behaviour of the leopard seal. Ice floes provide numerous platforms to whelp and suckle pups, in areas of abundant food supply with unrestricted access to the sea. However, because the floes constantly break up through the summer, pack ice-breeding seals, including the leopard seal, tend to have short breeding seasons (Riedman 1990). During the breeding season, leopard seals are solitary and are found at low densities (Erickson et al. 1971), this may lead to difficulties when finding a mate. Leopard seals are very vocal at this time (Thomas and DeMaster 1982), therefore acoustic behaviour may play an important role in the breeding strategy of these seals.

Ray (1970) published a sonagram of part of a leopard seal call but Stirling and Siniff (1979) were the first to quantitatively describe leopard seal vocalisations. They also described an alternate pattern of "singing" and breathing, which was believed to be associated with territoriality. However, the behavioural functions of these calls have never been established, due in part to poor visibility in the marine environment and the particular, mainly logistical, difficulties of working in the Antarctic pack ice. More often than not, it is impossible to determine the identity or sex of the caller or the behavioural context in which calls are being used.

This study aimed to determine the behavioural significance of leopard seal calls, by linking the behavioural context in which calls were made with seasonal occurrence and the reproductive state of the seals.

Underwater acoustic recordings were made using a Sony WMD6C audiocassette recorder from a Bruel and Kjaer 103 hydrophone and a custom preamplifier. This system had a frequency response from 40 to 15,000 Hz. Vocalisations were recorded of both captive and free-ranging leopard seals. Most recordings of captive seals were made at Taronga Zoo, Sydney. Ten 20 minute underwater sound recordings and concurrent behavioural observations were made each month between April 1990 and February 1993. Biweekly blood samples were collected during this time to monitor the seals serum hormonal fluctuations. Five hours of opportunistic underwater recordings were made of a captive lone, mature male leopard seal at Marineland, New Zealand in November and December 1991 and January 1992. The sounds of free ranging leopard seals were recorded in the Antarctic over two summers. One hundred and ten hours of underwater leopard seal calls were recorded in a 60 km area along the fast-ice edge in Prydz Bay, Antarctica between November and January in 1992/93 and 1993/94. Underwater sound recordings were made between 1600 and 0300 h, coinciding with the period when leopard seals are most vocal underwater (Thomas and DeMaster 1985). Each night recordings were made at the locations where leopard seals had been seen hauled out on the ice earlier in the day, from aerial surveys. One hour of underwater sound recordings were made at each site, when possible. Recordings were made when wind conditions were below 15 Kt. and when there was minimal ice movement.

Sounds were analysed only when the caller was positively identified as a leopard seal. Calls were grouped according to their acoustical characteristics. A random sample of each call type with good signal to noise ratio was selected and analysed using a Kay Elemetrics 5500 Sona-Graph spectrum analyser. To calculate the source levels of the different call types, representatives were used where the distance between the seal and the hydrophone was known at the time the recording were made. It was difficult to see the position of calling seals in the field however on occasions seals could be seen in-between calling bouts at the surface, breathing. The source level, the equivalent sound pressure level at a distance of 1m from the source, was calculated from measurements of the received level at known distances by correcting for the propagation loss from 1 m. All calculations of received levels were made using a Bruel and Kjaer digital frequency analyser (Type 2131) and a Hewlett-Packard (3582A) spectrum analyser.

Twelve different vocalisations were identified, nine of which have not been described previously. All calls were in the low to middle frequency range (35 to 4800 Hz). From the captive study the vocalisations were categorised into two groups, agonistic and advertising calls, according to their behavioural significance. Agonistic calls are those associated with interactions between the two seals, such as aggressive or defensive behaviour and the advertising sounds were linked with sexual receptivity in the captive female leopard seal and are believed to be used as 'solicitation calls'.

The agonistic and advertising calls have different acoustic features. Agonistic calls were heard occasionally in the field, whereas advertising calls were heard for long periods each day. It is proposed that leopard seals hold underwater 'territories' prior to, and during, the breeding season and that they use the advertising calls for a dual purpose: to advertise sexual receptivity and proclaim territorial presence.

REFERENCES

Bonner, W.N., and Laws, R.M. 1964. Seals and sealing. In Antarctic research: A review of British scientific achievement in Antarctica. Edited by R. Priestey, R.J. Adie and G. Robins. Butterworths, London.

DeMaster, D., Thomas, J., Stone, S., and Andriashek, S. 1979. Biological studies of seals in ice habitat. Antarct. J. U.S. 14(5): 179 - 180.

Erickson, A.W., Siniff, D.B., Cline, D.R., and Hofman, R.J. 1971. Distributional ecology of Antarctic seals. In Symposium on Antarctic ice and water masses. Edited by G. Deacon. SCAR Cambridge. pp 55 - 76.

Riedman, M. 1990. The pinnipeds: seals, sealions, and walruses. University of California Press, Oxford.

Ray, G.C. 1970. Population ecology of Antarctic seals. Vol 1. In Antarctic ecology. Edited by M.W. Holdgate. Academic Press, New York. pp. 398-414.

Sinha, A.A., and Erickson, A.W. 1972. Ultrastructure of the placenta of Antarctic seals during the first third of pregnancy. Ant. J. Anat. 141: 263 - 280.

Siniff, D.B., and Stone, S. 1985. The role of the leopard seal in the tropho-dynamics of the Antarctic marine ecosystem. In Antarctic nutrient cycles and food webs. Edited by W.R. Siegfried, P.R. Condy and R.M. Laws. Springer-Verlag. pp 555 -559.

Stirling, I., and Siniff, D.B. 1979. Underwater vocalisations of leopard seals (Hydrurga leptonyx) and crabeater seals (Lobodon carcinophagus) near the South Shetland Islands, Antarctica. Can. J. Zool. 57: 1244 - 1248.

Thomas, J.A., and DeMaster, D.P. 1982. An acoustic technique for determining diurnal activities in leopard (Hydrurga leptonyx) and crabeater (Lobodon carcinophagus) seal. Can. J. Zool. 60: 2028 - 2031.

A New Sound Type: Low Frequency (< 2kHz) Narrow-Band Sounds Produced by Bottlenose Dolphins

Ken W. Schultz, Douglas H. Cato*, Peter J. Corkeron, M. M. Bryden
Department of Veterinary Anatomy, University of Sydney, NSW 2006, Australia.
* Also at Defence Science and Technology Organisation,
P.O. Box 44, Pyrmont, NSW 2000, Australia.

The bottlenose dolphin, *Tursiops truncatus,* is perhaps the most familiar of all dolphins being seen frequently near shore and held in captivity worldwide. Bottlenose dolphins have been studied extensively, particularly aspects such as social systems, cognition, sonar and other sound production. The dynamic social structure of dolphins suggests that there is significant communication between animals and the varied nature of their sound repertoire has lead to speculation about the complexity of their acoustic communication.

The many studies of the sounds produced by the bottlenose dolphin, have lead to their classification into two broad categories: pulsed sounds (including clicks and burst-pulses) and narrow-band whistles. The clicks are very short in duration (of the order of 50 microseconds) and have a broad bandwidth (up to 200 kHz). Their effectiveness for echolocation has been well established (Au, 1993). The whistles are narrow-band harmonic sounds of durations typically in the range 0.1 to 1.5 seconds.

Whistles and burst-pulses are considered to be used in communication, though relatively little is known about the significance of these sounds in spite of the considerable amount of investigation. It has been demonstrated that some whistles are used to identify the individual responsible, i.e. as signature whistles (Caldwell, Caldwell and Tyack 1990; Sayigh, Tyack, Wells and Scott 1990; and Smolker, Mann and Smuts 1993). Burst-pulses are usually associated with social activity in groups of dolphins.

This paper presents a new sound type recorded from bottlenose dolphins, *Tursiops truncatus,* in eastern Australian waters: low frequency narrow-band (LFN) harmonic sounds. These sounds were defined as less than 2 kHz although most were of frequencies less than 1 kHz. A *Bruel and Kjaer* 8105 hydrophone, custom built pre-amplifier and Sony TCD-D10 PRO digital tape recorder were used for recordings. The system had a frequency response of 20 Hz to 22 kHz (limited by the tape recorder). Underwater recordings were made from groups of free-ranging bottlenose dolphins engaged in various behavioural activities. A Kay Elemetrics DSP Sona-Graph model 5500-1 and LeCroy 9304 M quad 175 MHz digital oscilloscope were used to analyse the spectrographic structure and waveform of the LFN sounds.

The production of LFN sounds by bottlenose dolphins has not been described previously. McCowan and Reiss (1991) recorded "thunks" which were sounds of frequencies less than 2 kHz, but these sounds were harsh noisy sounds (i.e. not narrow-band). Dos Santos, Caporin, Moreira, Ferreira and Coelho (1990) presented sonagrams of low frequency sounds called "brays" consisting of a pair of sounds, the first part of which could be physically of the same nature as LFN sounds (i.e. continuous narrow-band), the second a form of pulsed sound. However, LFN sounds in the present study were produced generally as a series of LFN sounds and showed no consistent association with pulsed sounds.

These sounds differed significantly from narrow-band whistles, which were higher in frequency and longer in duration. It has been accepted, generally, that whistles range in frequency from 4 to 20 kHz, although ranges vary between studies (e.g. Caldwell, Caldwell and Tyack 1990, Schultz and Corkeron in press). Sections of some whistles extending as low as 1 kHz and higher than 24 kHz have been noted (Caldwell, Caldwell and Tyack 1990), but whistles with fundamental frequencies entirely below 2 kHz have not been described.

The rate of LFN sound production (number of sound emissions per individual per minute) was calculated from samples of recordings of bottlenose dolphins engaged in a wide range of behavioural activities, namely; socialising (S), socialising and slow travel (S+T), socialising and milling (S+M), feeding (F), milling (M), slow travel (T), slow travel and resting (T+R) and medium travel (TM). LFN sounds were produced in significantly higher rates during behaviours involving socialising (S, S+T and S+M) than other behaviours in which their production was negligible. The presence of LFN sounds in 41 out of 42 of the sampled recordings involving socialising dolphins (S, S+T and S+M) and their significantly higher rate of production during these behaviours demonstrates a social importance of these sounds for bottlenose dolphins in the present study area.

The absence of these sounds in most studies of the acoustic behaviour of bottlenose dolphins may be a result of geographic differences in repertoires. Alternatively, their absence in other studies may have resulted from insufficient sampling such as the use of filters or hydrophones restricting the frequency range of the recording equipment to above 1 kHz (to reduce background noise) and/or limited recordings of bottlenose dolphins during certain behavioural contexts (especially socialising).

REFERENCES

Au, W. W. L. 1993. *The Sonar of Dolphins.* Springer-Verlag, New York.

Caldwell, M. C., D. K. Caldwell and P. L. Tyack. 1990. Review of the signature whistle hypothesis for the Atlantic bottlenose dolphin. Pages 199-234 in S. Leatherwood and R. R. Reeves, eds. *The Bottlenose Dolphin.* Academic Press, Inc. San Diego, California.

McCowan, B. and D. Reiss. 1991. Maternal disciplinary behaviour toward captive-born infant bottlenose dolphins *(Tursiops truncatus)*: Harsh low frequency signals during mother-infant interactions. Page 46 in Abstracts of the Ninth Biennial Conference on the Biology of Marine Mammals, Chicago, Illinois.

dos Santos, M. E., G. Caporin, H. O. Moreira, A. J. Ferreira and J. L. B. Coelho. 1990. Acoustic behavior in a local population of bottlenose dolphins. Pages 585-598 in J. Thomas and R. Kastelein, eds. *Sensory Abilities of Cetaceans.* Plenum Press, New York.

Sayigh, L. S., P. L. Tyack, R. S. Wells and M. D. Scott. 1990. Signature whistles of free-ranging bottlenose dolphins Tursiops truncatus: stability and mother-offspring comparisons. *Behavioral Ecology and Sociobiology* 26: 247-260.

Schultz, K. W. and P. J. Corkeron. in press. Interspecific differences in whistles produced by inshore dolphins in Moreton Bay, Queensland (Australia). *Canadian Journal of Zoology.*

Smolker, R. A., J. Mann and B. B. Smuts. 1993. Use of signature whistles during separations and reunions by wild bottlenose dolphin mothers and infants. *Behavioral Ecology and Sociobiology* 33: 393-402.

Patterns of Fish Calls and Choruses in Northern Australia

Robert D. McCauley1 and Douglas H. Cato2
1Department of Marine Biology, James Cook University, Townsville, Qld., 4811.
2Defence Science and Technology Organisation, P.O. Box 44, Pyrmont, NSW 2009.

Sound is used extensively by marine animals and contributes significantly to the ambient noise of the ocean. In particular, biological choruses that result when large numbers of animals vocalise, cause high levels of ambient noise for sustained periods. Such choruses have been found to be wide spread in Australian waters, particularly in tropical shallow waters, often increasing background noise by 20-30 dB (Cato, 1978). Choruses may be produced by invertebrates, fish or marine mammals.

Fish have been found to produce high levels of transient and sustained underwater-noise throughout northern Australian waters mostly in the frequency band 50 Hz to 2 khz (Cato, 1980; Kelley at al, 1985; McCauley, 1989, 1992). Individual fish calls may have source levels of up to 150 dB re 1 microPa at 1 m, while choruses of fish sounds may produce continuous spectrum levels as high as 100 dB re 1 microPa2/Hz. Calls and choruses have spectral peaks mainly between 50 and 1300 Hz, depending on species concerned, fish size and calling depth.

In northern Australia, calling fish have been recorded from around inshore and offshore reefs and shoals, inter-reef waters on the continental shelf, and from deep oceanic waters. Specific call types correlate with habitat type, reflecting species distribution patterns on small (kilometres) and large (northern Australian) scales. Calls may be produced intermittently, spaced seconds to minutes apart but repeated ad nauseam, or may be produced in continuous choruses where individual calls overlap and cannot be easily distinguished. Intermittent calls of Some species may occur frequently enough to significantly raise time averaged sea noise levels. In such instances calling rates of up to 150 calls per 10 minute period are not uncommon. Choruses may be sustained for hours on end and occur daily in set time periods. Both intermittent calls and choruses may be evident seasonally over times scales of weeks to months.

Most of the acoustically important sources studied to date show marked temporal patterns in calling habits with different species displaying unique patterns. For fish which do not produce continuous choruses, highest call rates occur most often (but not always), during darkness with crepuscular peaks common for many species. Continuous choruses are nearly always heard during the hours of darkness. Calling often shows several seasonal peaks of activity, although some species such as nocturnal reef planktivores call regularly throughout the year on a daily basis. Some species display lunar trends in calling activity, superimposed over seasonal trends. For example nocturnal reef planktivores produce choruses up to 10 dB higher in level during new moon periods, as compared to choruses produced during times of full moon.

The most acoustically dominant fish species produce calls by excitation of the gas filled swimbladder. Vibration patterns are applied to the swimbladder most commonly by attached or surrounding muscles or in some species by striking the swimbladder with a dorsal or pectoral spine. Calls vary considerably in structure between species. Within a species or species group calls are stereotyped around a common structure. Two examples of common calls are: (a) a long drumming sound produced Frequently but not in continuous choruses by sciaenids during August to March in inter-reef waters across northern Australia (composed of 22-38 pulses each of 12-50 ms duration to give a call of length 1-2.81 s with a spectral peak between 240-450 Hz); (b) short trumpet sounds produced between August to May by members of the family Teraponidae and heard in evening choruses in coastal waters, probably around most of Australia but to date confirmed in the north from the Kimberleys to Hervey Bay (for Terapon theraps a single pulse of 130-190 ms with a strong harmonic interval of 105-115 Hz and a spectral peak between 400-1300 Hz).

Often several 'varieties' of a call may be heard. Variations generally comprise lengthening a call by a specific time increment (for example in increments of around 60 ms in Terapon theraps) or by changing the muscle contraction rate and so the observed harmonics (for example Terapon theraps approximately halves its muscle contraction rate to make an alarm call). Some fish also appear able to control swimbladder damping to produce different calls. For example reef- associated nocturnal-planktivore choruses are composed of many short lightly damped pulses, whereas heavily damped pulses can be elicited from some of these species when they are disturbed in their daytime resting places.

For the acoustically dominant species studied, the most common call types show only small variations in structure at any given time and place, but may show significant variations in structure at the same location at different times during a calling season. For example the sciaenid drumming described above shows significantly longer and more pulses per call off Townsville at the start of a calling season (August) than at the end (February-March).

In many habitat types several acoustically important species co-exist.

For example in inshore inter-reef waters of North Queensland two fish species which produce frequent intermittent calls over protracted periods (months) and two species groups which produce choruses on a daily basis may be heard. Although some competition between calling sources can be discerned, particularly between the intermittent calling species, taken as a whole the calling patterns for each species are remarkably co-ordinated so as to reduce acoustic competition. This is achieved primarily through offset of maximum call răte or chorus time on a daily and seasonal basis, but also through small scale separation of optimal calling zones.

Indirect evidence from some of the choruses and the findings of other workers suggest that much of the fish calling described can be attributed to breeding or spawning events. This would explain much of the seasonality in calling behaviour. Calls may be used to attract mates, particularly in visually restricted environments, and/or as a cue in spawning behaviour. The production of calls or choruses continually throughout the year suggests other functions underlying calling behaviour for some species. Such functions could include maintaining loose aggregations or schools during periods of low visibility (for example in the nocturnal planktivore choruses), or in maintaining contact between small groups or solitary animals over distances of hundreds of metres to kilometres.

REFERENCES

Cato, D.H. (1978) "Marine biological choruses observed in tropical waters near Australia", J. Acoust. Soc. Am. 64, 736-743.

Cato, D.H. (1980) "Some unusual sounds of apparent biological origin responsible for sustained background noise in the Timor Sea." J. Acoust. Soc. Am.68, 1056-1060.

Kelly, L.J., Kewley, D.J. and Burgess, A.S. (1985) "A biological chorus in deep water northwest of Australia." J. Acoust. Soc. Am. 77, 508-511.

McCauley, R.D. (1989) "Aspects of marine biological sound production in northern Australia." James Cook University, Townsville.

McCauley, R.D. (1992) "Aspects of marine biological sound production in northern Australia II: Temporal and spatial variability in observed calling patterns of some acoustically dominant inter reefal, inshore fishes." James Cook University, Townsville.

Has data on transmission of
choruses in Cleveland Bay out to 8 km
(2 KHz)

16 m $f_{co} = \frac{c}{4h} = \frac{1540}{4 \times 16} \sim 200$ Hz

$c = f\lambda$

Management of Deep-Water Fisheries Resources, An Acoustic Solution

R.J. Kloser
CSIRO Division of Fisheries, GPO Box 1538, Hobart Tas. 7000

BACKGROUND

The exploitation by commercial fishing of deep-water resources in southern Australian and New Zealand has increased substantially over the past years. One such species, orange roughy (*Hoplostethus atlanticus*) is vulnerable to over exploitation due to its aggregating behaviour, slow growth and longevity. Estimating stock size is vital for good management to maintain orange roughy as a sustainable fishery. The aggregating behaviour of orange roughy makes it suitable to monitor by acoustic methods. Echo integration theory and methods are well established, (Johannesson and Mitson 1983; MacLennan and Simmonds 1992) and recently these techniques were applied to orange roughy in Australian waters using hull-mounted acoustics (Elliott & Kloser 1993).

Several factors limit the usefulness of hull-mounted or near-surface deployed acoustic systems for the assessment of deepwater fish. The major factor, which arises from the association of orange roughy with steep bottom topography, is the large acoustic dead-zone caused when the acoustic beam reverberates off the side of the hill, such that fish at greater depths within the beam cannot be distinguished from the bottom echo. Other factors include acoustic attenuation from near-surface bubbles, which varies with sea conditions (Dalen & Lovik 1981); the effects of ship motion (Stanton 1982); uncertainties in the sound absorption constant (Fisher and Simmonds 1977; Francois and Garrison 1982) and beam thresholding (Foote 1991). These factors may be reduced or entirely alleviated by deploying the acoustic transducer on a deep towed body (Fig. 1).

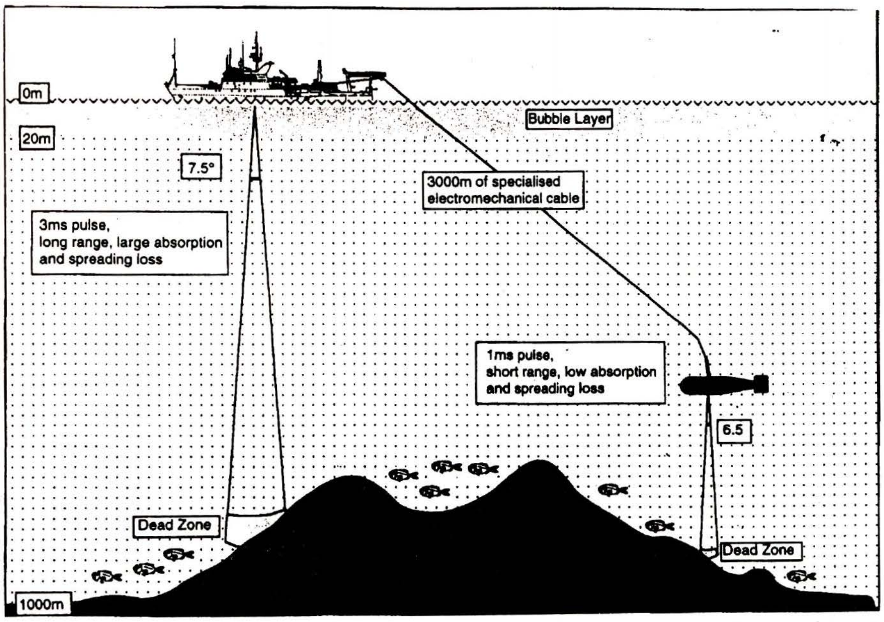

Figure 1. Diagram showing differences between acoustic surveys for deepwater fish with hull-mounted and deep-towed transducers.

Through use of a deep towed-body acoustic system with split-beam transducer, single acoustic targets can be resolved and their acoustic target strength (TS) measured. TS is directly proportional to the biomass obtained from echo integration, so it is a critical parameter in an absolute estimate of biomass. The split beam method of obtaining TS has been adopted due to its better noise performance (Ehrenberg 1983) and its ease of calibration.

ACOUSTIC EQUIPMENT AND CALIBRATION

The acoustic equipment located on board the research vessel *FRV Southern Surveyor* consists of a scientific Simrad EK500 echo sounder connected to both a standard Simrad 38kHz (7 degrees full angle) split beam hull mounted transducer and an EDO Western 38kHz (6.5 degrees full angle) split beam transducer rated to 1000m mounted in a towed body. The towed body used was built in-house to perform echo integration surveys to 600m depth at 5-6 knots and in-situ target strength measurements down to 1000m at 2-3 knots with 2000 m of cable out. The towed body is a dead weight type 750kg, housing the transducer, transmitter, pre-amplifiers and a monitoring package. The monitoring pressure case measures physical parameters such as towed body pitch, roll, depth and operating voltage, displayed continuously aboard by a computer. The towed body is connected to the vessel by 3000 m of electromechanical cable that consisted of 5 single conductors required for power, trigger and monitoring signals and 4 twisted shielded pairs that carried the pre-amplified split-beam acoustic signals. The acoustic ping and summary data is logged on a Sun IPX workstation via ethernet and the serial port.

The acoustic design of connecting the EDO split beam 38kHz transducer to the Simrad EK500 is complicated by the cable characteristics. Cable attenuation (20dB) and noise is overcome by placing the transmitter and preamplifiers in the towed body. The 2.5kW, 38kHz transmitter is transformer matched (60ohms) to all 112 elements of the transducer and diode isolated for reception. On reception the transducer is divided into a split beam configuration, and four high impedance preamplifiers with line drivers amplify the acoustic signals up the cable. Twisted shielded paired (tsp) cabling with isolating and matching transformers at the cable ends reduce far end crosstalk to less than -80dB. The acoustic system can detect a single fish, TS -36dB down to 640m using a 10dB signal to noise ratio. This assumes that the transmit power is 2.5kW, sea state noise 20dB/uPa/Hz, bandwidth 3kHz and sound absorption 10dB/km.

Calibration of acoustic equipment was performed using a standard -36dB, 60mm copper sphere (Foote 1983 and Simrad 1992) to obtain the target strength and on axis echo integration constants. The on axis echo integration technique lumps together the electrical and acoustic constants of the system such as transmitter power, transducer transmit and receiving efficiency, ideal beam angle and receiver gain. The coefficients in the EK500 were adjusted to meet the theoretical TS of the standard sphere (-36dB) and the area backscattering coefficient Sa dependant on target depth. Further the towed transducer was calibrated from 100-1000 m to correct for the depth dependent changes in transducer sensitivity and to examine any change in beam pattern. This was performed by suspending a sphere fore and aft 10m under the towed body and lowering it through the water column. The sea water parameters of absorption (α) and sound velocity (c) were calculated from temperature and salinity profiles obtained from a Neil Brown conductivity-temperature-depth recorder (CTD), using the formulae of Francois and Garrison (1982b) for α and MacKenzie (1981) for c.

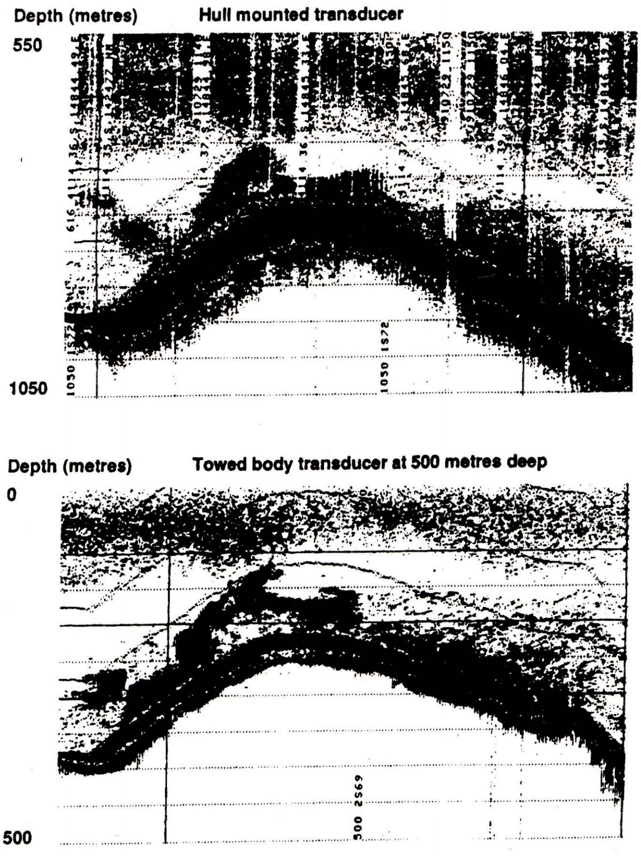

Figure 2. Echogram from hull-mounted (top) and towed transducer (bottom). They are of the same ground. Note the greater definition of the acoustic marks from the deep-water transducer and the diminished dead-zone.

RESULTS

EQUIPMENT

Figure 2 shows echograms from the towed and hull mounted transducers when conducting the same transect across a seamount with orange roughy schools. The towed transducer is at a depth of 500m with 2000m of wire out. The echogram shows the enhanced performance of the towed system with greatly reduced noise and dead zone height. The reduction in the dead-zone is demonstrated by the reduced width of the bottom echo for the towed transducer. School structure is also more defined due to the decreased sampling volume of the towed body. However, it should be noted that the surface calibration of the hull mounted acoustic system has been stable over a four year period with only a 5% (0.2dB) change in values, whereas the towed acoustic system has undergone changes of 26%. These changes are due mainly to failures in towed body circuit boards at sea. Deep water calibration of the towed transducer shows a sensitivity loss with depth of approximately 26% (0.5dB) per 100m. A slight hysteresis is observed on the up and down cast for the calibration and is thought to be due to a temperature lag.

SURVEYS

Acoustic surveys have been conducted from 1990-93 on a spawning aggregation of orange roughy on the St. Helens seamount off the east coast of Tasmania (Kloser et al 1994). The initial stock assessment results for orange roughy in 1990 on the St. Helens seamount significantly reduced the huge (50-1000 thousand tonnes) uncertainty surrounding the stock size. As the stock is fished down the technique becomes sensitive to species composition with more care required in the analysis of results. The trend from acoustic surveys from 1990-93 of biomass on the hill shows a consistent decline. The hull-mounted echo integration estimates were consistently lower than the towed body by a factor of 1.5-1.7, most likely due to a combination of sampling threshold effects at the edge of the acoustic beam and uncertainty in the absorption coefficient when sampling over large depths. The TS of orange roughy is still not precisely known due to the avoidance response of the fish to sampling gear. From our knowledge at present it is concluded that the in-situ TS for a 35cm standard length orange roughy is likely to be in the range of -48 to -53dB.

REFERENCES

Dalen, J., Lovik, A.(1981). The influence of wind-induced bubbles on echo integration surveys. Journal of the Acoustics Society of America. 69: 1653-1659.

Ehrenberg, J. E. (1983). A review of in situ target strength estimation techniques. FAO Fisheries Report 300: 85-90.

Elliot, N.G., Kloser, R.J.(1993) Use of acoustics to assess a small aggregation of orange roughy, Hoplostethus atlanticus (Collett), off the eastern coast of Tasmania.Aust. J. Mar. Freshwater Res., 44: 473-82.

Fisher, F. H., V.P. Simmons (1977) Sound absorption in sea water. Journal of the Acoustics Society of America 62: 558-564.

Foote, K.G.(1991) Acoustic sampling volume. Journal of the acoustical society of America 90 (2), Pt. 1, 959-964.

Foote, K.G.(1982). Optimizing copper spheres for precision calibration of hydroacoustic equipment. Journal of the acoustical society of America 71: 742-747.

Francois, R. E., Garrison, G.R. (1982). Sound absorption based on ocean measurements. II. Boric acid contribution and equation for total absorption. Journal of the acoustical society of America 72, 896-907.

Johannesson, K.A., Mitson, R.B. (1983) Fisheries Acoustics: A practical manual for aquatic biomass estimation. FAO Fish. Tech. Pap. 240: 249 pp.

Kloser, R., Koslow, J.A.,Williams, A.(1994) Acoustic biomass assessment of a spawning aggregation of orange roughy (Hoplostethus atlanticus) off southeastern Australia from 1990-93. Final report to FRDC. 90/25: 59-81.

MacKenzie, K.V. (1981). A nine-term equation for sound speed in the oceans. Journal of the acoustical society of America 70, 807-812.

MacLennan, D.N., Simmonds, J.E. (1992) Fisheries Acoustics. Chapman&Hall.

Simrad (1992) Simrad EK500 Scientific Echo Sounder Instruction Manual. Simrad Subsea P2170E.

Stanton, T. K. (1982). Effects of transducer motion on echo-integration techniques. Journal of the Acoustics Society of America. 72: 947-949.

An Adaptable Acoustic Data Acquisition System for Fish Stock Assessment

Roger F Coombs
Ministry of Agriculture & Fisheries, MAF Fisheries, Marine Research,
Greta Point, PO Box 297, Wellington, New Zealand

ABSTRACT

The scientific echosounders available commercially for fish stock assessment are typically designed for use in long-established northern hemisphere fisheries in depths down to 500m. They incorporate real-time processing to give biomass estimates, but no facilities for saving raw data. This is unsatisfactory for the fisheries around New Zealand, many of which are only a few years old and may be in waters over 1000m deep. This system is an adaptable and expandable echosounder designed to preserve as much of the information present at the terminals of the transducer or transducers, as possible. Analysis of the data to give biomass estimates and other information about fish and fish distributions is carried out later. The data can thus be analysed in many different ways and re-analysed as ideas change and new techiques develop. The system is low-noise, has a wide dynamic range, supports multiple transducers and the concurrent collection of ancilliary data such as vessel position. It is implemented using multiple digital signal processors (Motorola DSP56001) which carry out filtering, data compression and other signal processing and pass data to a controlling computer which provides a user control interface, data presentation and data storage and management.

Laboratory And Field Measurements of the Acoustic Target Strength of Free Swimming Antartic Krill

T.J. Pauly *, J.D. Penrose **
*Australian Antarctic Division Channel Hwy Kingston 7050 Tasmania
**Centre for Marine Science and Technology Curtin University of Technology
Kent St. Bentley 6102 Western Australia

Sustainable utilisation of fishery resources and predator prey studies require monitoring techniques suitable for stock biomass assessment. The use of acoustic echo integration techniques for distribution and biomass estimates now constitutes the major field technique for assessing biomass. When such techniques are used estimates of the acoustic target strength (TS) of scatterers are required to convert integrated back scattered energy to biomass estimates.

Repeatable measurements using insitu techniques have proven difficult with larger swimbladder bearing species and the weaker non swimbladder bearing scatterers have proved more difficult.

Early programs to determine such target strength values used tethered specimens in laboratory test tank experiments (Haslett (1962)). Later work has used free swimming targets in either tank or caged field locations (Foote *et al.* (1990)) and in-situ measurements at sea (Hewitt and Demer(1991)). Foote (1991) has provided a recent review of target strength measurement methods. The purpose of the present paper is to report on a suite of measurements made on free swimming Antarctic krill, *Euphausia superba*, in a laboratory test tank and similar measurements made at sea.

Antarctic krill, the focus of the present work, are recognised as a major component of the Antarctic food chain. The distribution and abundance of krill has been a subject of continued interest over the last decade and a focal point for the Commission for the Conservation of Antarctic Marine Living Resources (CCAMLR) as the management of the harvesting of krill has been a key issue for the Commission.

The extraction of target strength values from measurements made from freely moving krill calls for some method of dealing with the uncertainties arising from unknown target angular position within the sound beam. In addition, for targets large enough to enter the geometric sound scattering regime, the detailed morphology and attitude in the beam of the target provides an additional source of fluctuation in individual backscattered sound pressure. Two major approaches have been developed to enable the target strength of single point targets to be estimated from signals subject to such stochastic processes. One approach (termed by Foote (1991) the "Indirect" approach, which may be traced to Craig and Forbes (1969) and was later applied by Peterson, Clay and Brandt (1976) and Ehrenberg et al.(1981)) uses a statistical treatment of an ensemble of echoes to yield target strength estimates. This approach enables data derived from a simple single transducer operating in mono-static mode to be processed, provided a set of assumptions relating to the scattering regime are applicable. The second "Direct" approach requires a modified beam structure; various forms involving dual or split beam geometries. Such techniques offset one of the uncertainties inherent in the Indirect approach, that associated with the location of the target with respect to the axis of the beam pattern, at the cost of requiring a more complex and generally larger transducer configuration.

The work reported here utilised the Indirect approach in which a simple piston transducer was used for tank measurements and the set of assumptions defined by Peterson, Clay and Brandt (1976) invoked as a basis for a signal processing methodology.

A single beam sounding system acting on a population of point scatterers returns an ensemble of echoes which, once corrected for transmission effects, may be regarded as arising from a combination of two stochastic processes, corresponding to the position and attitudes of individual targets in the beam. An ensemble of returns from individual targets may be processed to yield a target strength estimate for an individual target provided a suite of assumptions associated with the scattering process are made.

This methodology has been the subject of a detailed performance analysis (Palumbo *et al.* (1993)) and evaluation (Penrose and Pauly (1993)). In this analysis, simulated data developed using Monte Carlo techniques was used to assess signal processing performance under a number of non-ideal operating conditions likely to be experienced in tank or field measuring programs of target strength. Thus the influences on derived target strength of variations: in the size distribution of target populations; in the spatial density of scatterers; in target attitude effects on scattering statistics and of beam shape uncertainties were evaluated. This work and Monte Carlo simulation of range determination uncertainties and of the influence of backscatter signal to noise ratio have been used in assessing the error budget applicable to the results reported here.

A series of experiments were conducted in a purpose built tank (figure 1) at the Australian Antarctic Division Kingston Laboratories in Tasmania with a data acquisition system (figure 2) designed and built at CMST Curtin University of Technology. The krill swam freely within the tank, triggering the data acquisition system when entering the beam provided a back scattered signal (figure 3) of magnitude sufficient for detection above the system noise level threshold was generated. The digitised echo-traces, received voltage as a function of time, were stored for later processing.

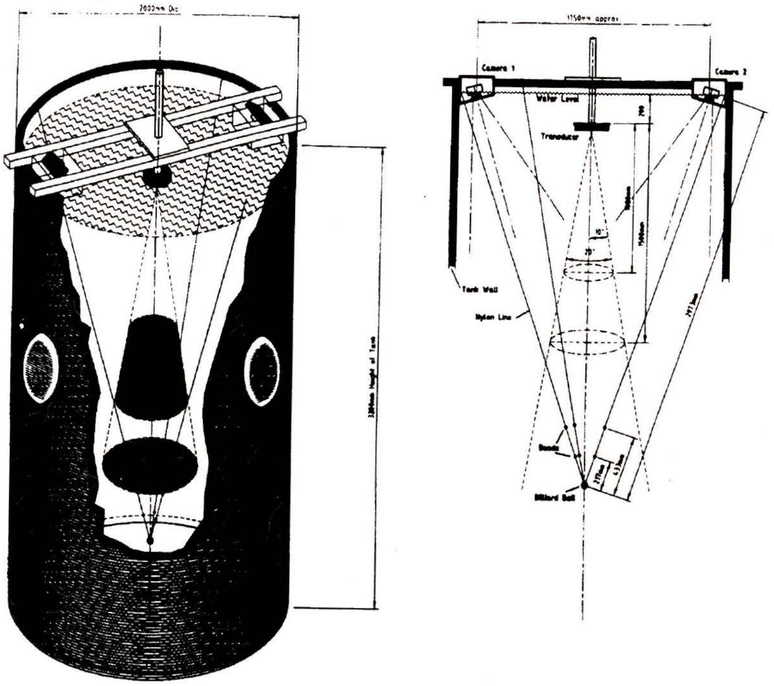

Figure 1. Laboratory tank system schematic and experimental configuration showing acoustic and photogrammetry geometry.

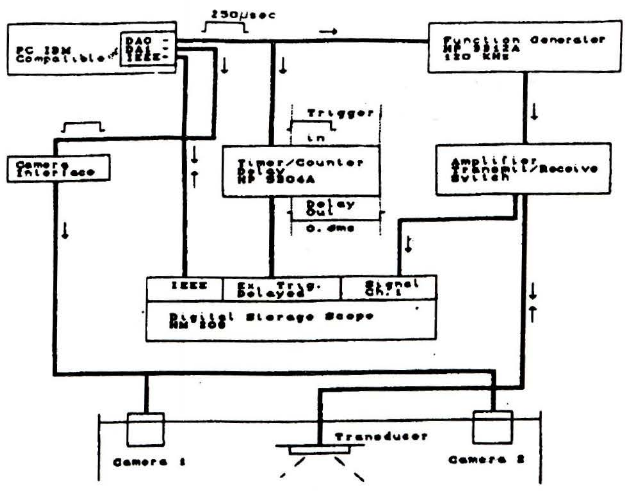

Figure 2. Acoustic data acquisition and photogrammetry control systems.

Field measurements were conducted from the Australian Antarctic research and supply vessel, <u>Aurora Australis</u>, using a modified version of the data acquisition system used for laboratory measurements. A 120kHz transducer mounted in a towed body was deployed in a disperse scattering layer of krill for ~12 hours collecting an ensemble of single target echoes.

Calibration experiments, using calibration target spheres (Foote (1983)), were conducted for both laboratory and field programmes to determine beam patterns and system transmit/receive sensitivity.

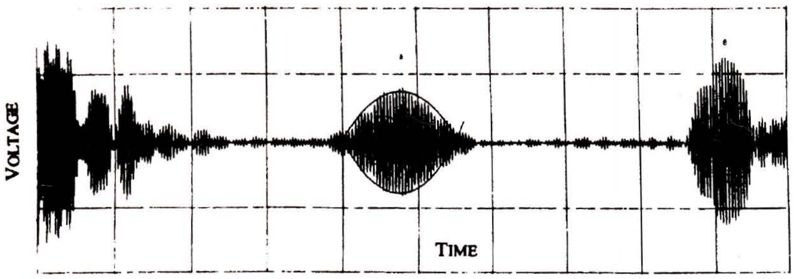

Figure 3. Data sample of a single echo voltage as a function of time. A single krill target return at A and the fixed calibration target at B.

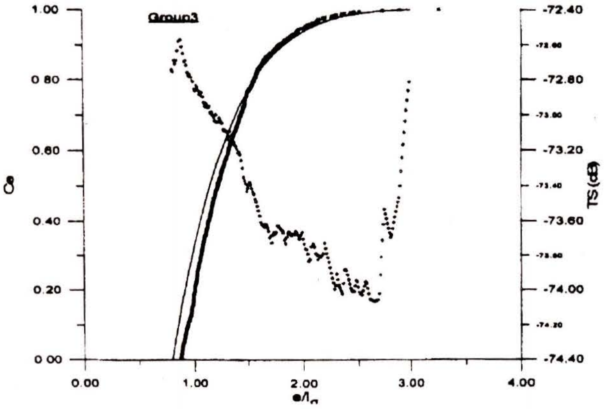

Figure 4. Experimental and theoretical cumulative distributions for a typical echo ensemble and the TS determined at each data point.

Pre-processing algorithms were developed to screen data sets for noise and multiple echo returns. Calibration and echo ensemble data sets were then processed using a modified RANKED ARRAY methodology to compute mean TS for each data set. The mean TS estimate is derived from the theoretical and experimental distributions for each data set (Figure 4).

The mean target strength estimates of Antarctic krill determined in this programme are considerably lower than the majority of estimates previously made. They show reasonable agreement with recent estimates produced by Foote *et al.* (1990). Recent model TS estimates (eg. Stanton (1989)) are generally lower (~2dB). These measurements combined with results from other recent measurement programmes (eg. Foote *et al.* (1990), Wiebe *et al.*(1990)) have been significant in bringing about change in the accepted length verses TS relationships by organisations such as CCAMLR. Previous relationships resulted in values as much as 8 dB or larger for a given target length than these result. This has major implications when considering biomass estimates based on surveys using echo integration techniques with results correspondingly varying six fold or more.

REFERENCES:

Craig, R.E. and Forbes, S.T. "Design of a sonar for fish counting," FiskDir. Skr. Ser. Havaunders. **15**, 210-219 (1969).

Ehrenberg, T.J., Carlson, J.J., Traynor J.J. and Williamson, N.J. "Indirect measurement of the mean acoustic scattering cross section of fish," J. Acoust. Soc. Am. **69**, 955-962 (1981).

Foote, K.G. "Use of elastic spheres as calibration targets," Nakken, O. and Venema, S.C. (eds). Symposium on Fisheries Acoustics, Bergen, Norway. FAO Fisheries Rep. **300**, 52-58, (1983).

Foote, K.G., Everson, I., Watkins, J.L. and Bone, D.G. "Target strength of Antarctic krill (Euphausia superba) at 38 and 120 kHz," J. Acoust. Soc. Am. **87**, 16-24, (1990).

Foote, K.G. "Summary of methods for determining fish target strength at ultrasonic frequencies," ICES J. mar. Sci., **48**, 2111-217 (1991).

Haslett, R.N.G. "Determination of the acoustic backscattering patterns and cross sections of Fish," Br. J. Appl. Phys. **13**,349-357, (1962).

Hewitt, R.P. and Demer, D.A. "Target strength of Antarctic Krill," Nature **353**, 310, (1991).

Palumbo, D., Penrose, J.D. and White, B.A. "Target strength estimation from echo ensembles," J. Acoust. Soc. Am. **94**, 2766-2775 (1993).

Peterson, M.L., Clay C.S. and Brandt S.B. "Acoustic estimates of fish density and scattering function," J. Acoust. Soc. Am. **60**, 618-622 (1976).

Penrose, J.D. and Pauly, T.J. "An evaluation of Target Strength Estimation from Echo Ensembles," Moura, J.M.F. and Lourtie, I. M. G. (eds). Acoustic Signal Processing for Ocean Exploration, Funchal, Maderia, Portugal. NATO ASI Series C: Mathematical and Physical Sciences **388**, 433-440, (1993).

Stanton, T.K. "Sound scattering by cylinders of finite length. III. Deformed cylinders," J. Acoust. Soc. Am. **86**, 1499-1510, (1989).

Wiebe, P.H., Greene, C.H., Stanton, T.K. and Bruczynski, J. "Sound scattering by live zooplankton and micronekton: empirical studies with a dual-beam acoustical system," J. Acoust. Soc. Am. **87**, 16-24, (1990).

Echo - Managing Fisheries Acoustic Data

Jason R.Waring, Rudy J. Kloser
CSIRO Division of Fisheries, P.O. Box 1538, Hobart, 7000, Tasmania, Australia
Tim Pauly
Australian Antarctic Division, Channel Highway, Kingston, 7050, Tasmania, Australia.

BACKGROUND

Acoustic methods using echo integration are currently being used to manage fisheries world wide. The theory and methods are well established and are detailed in many references recently summarised by MacLennan and Simmonds (1992). The technique generates large digitised data sets that require management, quality assurance and need to be readily available for processing and analysis. Automated computational techniques are required in areas such as noise filtering, bottom and surface exclusion, school pattern recognition and multi-frequency analysis. To perform these processes, flexible software is required (Foote 1991).

In the Australian context the CSIRO Division of Fisheries and the Australian Antarctic Division currently use acoustic methods to provide biomass assessments on resources such as orange roughy in the deep-water and krill in the Antarctic. These biomass surveys use Simrad EK500 scientific echo sounders at several frequencies, 12kHz, 38kHz, 120kHz and 200kHz, operating hull mounted and towed transducers. The acoustic data from these transducers are combined with navigational, pitch-roll, towed body depth and other vessel information. The amount of data collected can exceed a giga byte per day. Such large volumes require complex data management systems for archival storage and processing.

The CSIRO and the Antarctic Division embarked on a software development program (Echo) that would greatly simplify data management and processing, assist in the analysis and provide a platform for development of future methods.

COMPUTING ENVIRONMENT

Early in the design phase of Echo a stable development platform was required that would not be hardware limited. We chose a number of standard platforms such as a Sun Unix workstation, X-Windows user interface and Oracle data base. The programming language C++ was chosen because of its object oriented structures which provide considerable flexibility when extending the program's capabilities.

SYSTEM DESIGN AND IMPLEMENTATION

Echo was designed in three separate modules. These are:

1. Acquisition and Instrument Control
2. Storage Management
3. Quality Assurance and Processing

An overview of Echo system design is represented in Figure 1.

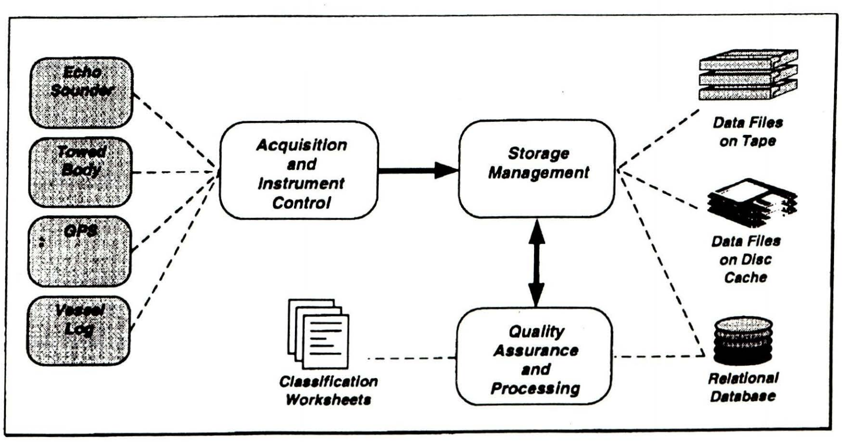

Figure 1. Echo System Design

1. Acquisition and Instrument Control

This module is designed to acquire and store data to disc. Preprocessing of the data before registration with the database is also required. Each instrument is provided with a dedicated program that understands its communication protocol. These interfacing programs pass the data on to an Acquisition Coordinator, which is primarily responsible for storage to disc. An additional facility allows co-operative programs to communicate with the Acquisition Coordinator and request that certain data telegrams be relayed to them when available. All monitors and real-time display programs use this communication mechanism. Specifically, the EK500 interfacing program communicates via an ethernet connection with the instrument and provides facilities to remotely control the EK500, monitor the acquisition of data and display echograms in real-time.

2. Storage Management

The Echo Storage Management System (ESMS) is responsible for the registration, management, retrieval and exporting of all acoustic data. An Oracle relational database is used to assist in the management of this information. Registration involves importing logged data into the database (either from an historical source or from the acquisition system). Data records are placed chronologically within uniquely named binary files, which are associated with the database according to cruise, survey, instrument, data type and data channel.

An inherent problem in managing acoustic data is that because of the large data volumes it is not always possible to store all data files to local disc. It is necessary to place registered data files on archival tapes. The ESMS was designed to keep track of the physical storage location of data files on archival tapes and local discs. To facilitate efficient retrievals, data files are grouped according to rules of likely retrieval before archival. Descriptive information is also provided for each tape, which assists users during retrieval.

ESMS provides a number of local disc "caches" that permit sections of data to be recalled from tape and stored locally on the workstation. Two types of caches are supported, volatile and non-volatile. Volatile caches provide a temporary storage space for applications to load their data which is automatically removed when the application registers that it is longer required. The non-volatile cache is managed by the user and data files are loaded on demand remaining in the cache until the user requests their removal.

3. Quality Assurance and Processing

While the ESMS can manage a wide variety of data types, processing is restricted to selected data types, Echo is currently limited to the processing of echogram data files (See Fig. 2).

During the logging and registration with the ESMS data quality is not checked. It is necessary to assure the data quality before processing. This is achieved by applying calibration and filtering coefficients and defining regions of unwanted data (e.g. Bottom and surface exclusion), to assist with this a 'classification worksheet' has been designed. The classification worksheet also allows the user to attach special meaning to selected regions (e.g. a school of orange roughy) which is of critical importance for some processing techniques. Processing involves integration of the echogram data within defined layers or regions over a survey area. Layers may be locked to the transducer, sea surface or sea bottom. Results are written to files in a tabular format allowing for further analysis using a spread sheet or data base software.

DISCUSSION

Echo is a fisheries research tool for the management and processing of echo sounder data. The development of Echo has proved successful, meeting user expectations and the medium term objectives.

These include

- Processing of single frequency echogram information to assist in the estimation of biomass.
- Provides a management framework for acoustic data. Prior to the development of Echo the logistics of managing acoustic data was tiresome and error prone. Scientific staff no longer need to be skilled in use of a cryptic operating system simply to access their data.
- Open architecture accommodates future requirements.

The development of echo was undertaken with other key considerations in mind that were not so tangible. In particular it was a key goal that the management structure be sufficiently broad to facilitate the acquisition and storage of any data from a new instrument with minimum difficulties. Other benefits are still more obscure but no less significant. The decision to use C++ was prudent as it ensured that the package is not permanently tied to a particular database or Graphical User Interface.

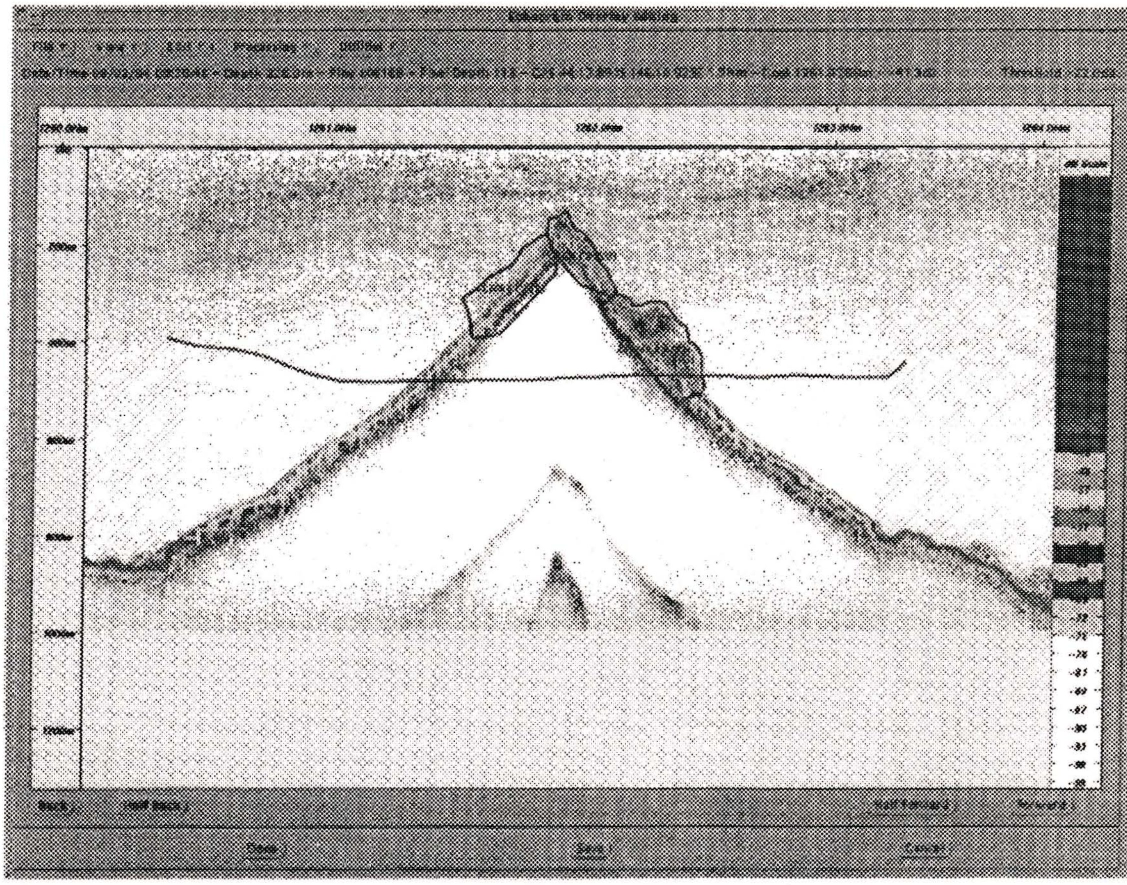

Figure 2. Echogram

FUTURE DEVELOPMENTS

The completion of Echo is not envisaged. It is a research tool and as such will continue to develop according to the needs of the research. In the short-to-medium term echo will be extended to accommodate techniques for multi-frequency analysis, spatial modeling and semi-automated classification.

REFERENCES

Foote, K.G., Knudsen, P., Korneliussen, R.J., Nordbo, P.E., Roang, K.(1991). Postprocessing system for echo sounder data. Journal of the acoustical society of America 90 (1): 37-47.

MacLennan, D.N., Simmonds, J.E. (1992) Fisheries Acoustics. Chapman & Hall.

Impact of Ultrasound on Clinical Practice

Peter Warren
Director, Department of Medical Imaging, Royal Hospital for Women, Sydney;
President, Australasian Society for Ultrasound in Medicine.

Historically, the use of ultrasound in medicine was developed by obstetricians, cardiologists and physicians who applied the method to overcome the limitations of existing procedures in their specialties. Commercial equipment became available in the mid-1970s and its adoption in Australia was rapid - in no small measure due to the international reputation of and detailed technical advice available from the Ultrasonics institute, which had carried out pioneering research in the area. It is now available in all but the smallest hospitals, most radiology practices, and in many obstetric, cardiology, vascular and other practices.

Since its formation in 1970 the Australasian Society for Ultrasound in Medicine has brought together in one organisation many disparate groups including technicians, scientists and engineers, and practitioners from all corners of medicine. It has provided for them a framework for professional advancement and the promotion of high standards of practice. The society has some 2000 members and is growing fast.

The economic trend throughout the world is to demand truly cost-effective health care and this has coincided with remarkable advances in imaging technology generally, particularly in ultrasound technology. In volume terms the use of diagnostic ultrasound in a global context is outstripping all other forms of medical imaging and within the next year or two it will become the commonest medical imaging modality in the world. Although we are forever getting bombarded with the notion of "high-cost" technology we seldom get presented with an impartial view of both sides of the balance sheet - the fact that much modern imaging is aimed at keeping patients out of hospital, minimising their stay in hospital, sometimes obviating the need for an anaesthetic and enabling them to return earlier to their families and work. In our hospital, for example, the availability of ultrasound to assess bleeding in early pregnancy has brought about the closure of a whole ward and most patients with bleeding in late pregnancy no longer need to be hospitalised as was the case only twenty years ago.

The technological advances in ultrasound imaging have provided not only images with fine detail and good contrast resolution but also a range of machines including small, portable, relatively inexpensive equipment which enables the doctor to use it as an extension of the usual physical examination performed at a consultation. This means that the technology can be taken to the patient readily be it in their homes, in a remote outback settlement or in the intensive care unit of a university teaching hospital. Despite extensive research for over thirty years no irreversible tissue or biochemical damage has been demonstrated when ultrasound in diagnostic doses is used according to established guidelines. No untoward cumulative effects have been identified and this means that the technique can be applied frequently to assist directly in management decisions. This saves time and hence money.

In clinical practice ultrasound is used to confirm a clinical impression, to answer a specific question and to resolve ambiguity raised by other differing opinions or other tests. It is available as a broad screening test for defined patient groups at risk of a specific disease process as well as being used to follow-up known lesions. It assists greatly certain operative procedures, particularly those associated with tissue biopsy and aspiration of fluid collections. In recent years it has assumed a major role in the assessment of blood flow characteristics and tissue perfusion which, being relatively non invasive, has not only encouraged earlier diagnosis but can assist directly in planning an approach to surgery or other treatment.

The first major applications were in obstetrics. An accurate knowledge of gestational age is one of the corner stones of modern antenatal care. In the days of x-rays this was confined to a very crude assessment in the second half of pregnancy. With ultrasound a pregnancy may be identified within two weeks of conception and the embryo measured accurately ten days after that to give a gestational age assessment which is accurate to within half a week. At the same time heart motion can be recorded. Most major fetal abnormalities can be identified in the first half of pregnancy and appropriate management effected. In the second half of pregnancy assessment of fetal growth and welfare can be assessed with both structural and functional information acquired by ultrasound. Its efficacy is such that throughout the world many learned societies and health authorities recommend that obstetricians screen routinely all pregnancies with ultrasound.

In gynaecology the woman with vaginal bleeding, a pelvic mass or pain will frequently be spared an unnecessary operation or painful and less diagnostic x-ray procedure by the use of ultrasound.

The ability to provide real-time images of the beating heart and a colour rendition of the blood-flow patterns has had an enormous impact on patient management in clinical cardiology. Measurements made of the volume of the various chambers of the heart and of the Doppler spectrum in particular areas can provide much quantitative information on which management decisions can be based. At the same time the number of expensive and somewhat hazardous invasive radiological examinations has been reduced greatly.

Colour and spectral Doppler techniques allow a rapid, safe, painless and effective evaluation of the vascular system. A clot in the leg veins or a plaque in the carotid artery can now be assessed without the need for catheterisation or contrast injection. Many niche applications also have been identified.

In conclusion, in the mid 1990s diagnostic ultrasound is in robust health and is the most versatile imagine modality available from the point of view of both cost and breadth of application. It provides a visual form of tissue characterisation with a high degree of reliability in trained hands. In the future, from the point of view of the sophisticated tertiary referral examination, we look forward to even better imaging performance, probably assisted by the use of contrast agents, and the assessment of aspects of tissue function will also become more established. Scientists and medical practitioners working in diagnostic ultrasound have gone a long way towards understanding the areas of activity of each other in a way which hitherto did not exist in diagnostic imaging. The trained medical practitioner knows not only how to drive the ultrasound machine but also the physical principles involved in its use. At the same time the research scientist is familiar with its applications and with a basic knowledge of disease processes. The synergy which has evolved between scientists and medical practitioners with the use of ultrasound is almost unique and has provided an example for co-operation between professional groups in other areas of health care delivery.

The State of Art in Medical Ultrasonic Imaging

David Carpenter
Ultrasonics Laboratory, CSIRO, 126 Greville St. Chatswood NSW 2067

Since the mid 1980's there has been a range of new technical developments in medical ultrasound equipment to improve imaging quality and Doppler capability. In imaging these have been predominantly in the areas of transducer developments, beam forming and image processing. There have been new display techniques but these have been predominantly in the area of Doppler blood flow measurement.

The use of array transducers commenced in the 1970's and were of two types known as linear arrays or phased arrays. The linear array uses a long array of transducer elements, typically from 64 up to several hundred in number. A group of these elements are selected electronically to form the aperture for a given line of sight. This group of elements is then switched along the array, moving by one element at a time to make each new line of sight in the overall scan which has a rectangular format. The phased array also uses a group of elements to make up the transducer aperture but the transmitting signals to each element have electronic delays applied such that the wavefronts from each element add to give an ultrasonic beam which is steered in a particular direction. Each scan line uses a different set of delays and hence the overall scan has a sector format similar to a phased array radar or sonar system. (Wilkinson, 1981) These early systems gave fairly poor images as they used a small number of elements in each aperture (eg. 8 or 16), had primitive focussing systems and made no attempt to reduce sidelobe levels. Another system developed at this time was the annular array transducer which was a circular disc transducer cut into concentric circular elements. This allowed a tracking focus to be used on reception such that the returning echo signals were always in focus and the system was called dynamic focussing.

Current developments have seen the number of elements in the aperture (or number of channels in the beamformer) increase to 128 or more in the top-end machines. The dynamic focussing technique from the annular array systems has been applied to the linear and phased array scanners and there has been a dramatic improvement in the sidelobe performance of modern systems by the use of dynamic apodisation techniques on both transmission and reception and the improvement in the basic piezoelectric materials used to manufacture the arrays (Smith, 1992). A system called multifocus has been developed for the transmitted line of sight in that the line is transmitted several times, each time with a different depth of focus. Only the received echoes from the region of focus for each transmission is used to form the final image and the result is a continuously focussed transmit beam, similarly to the effect produced by the dynamic focussing on reception. While this multifocus system involves additional scan time in that multiple transmit pulses are used, techniques are being use to reduce this problem by using low power and higher frequency for the near foci so that the next transmit pulse can be sent shortly after the echoes from the focal point of the previous pulse are received. with these techniques frame rates of 12 images per second can be achieved while using 5 different transmit foci. Another technique to increase frame rate is to use parallel processing of 4 different receive apertures either from a single broader transmit beam or from sending 4 different transmit pulses at the same time but in spatially different directions. With this technique frame rates of 158 frames per second have been achieved.

With the linear and phased array transducers these electronic focussing techniques are used only in the scanning plane and a simple lens is used to reduce the beamwidth in the cross-axis (or slice thickness) plane. New transducers are now being developed called 1½ D arrays in which the elements are divided into 3 or 5 sections across the array to allow a degree of electronic focussing in the cross-axis plane. Techniques to vary the transducer aperture are also being employed to give a constant F-number system regardless of the depth of the focal point in tissue and hence ensure that a uniform display of tissue texture resolution is achieved in all parts of the scan.

Until recently separate transducers were needed for each of the main operating frequencies of 3.5, 5.0, 7.5 and 10 MHz. The introduction of composite transducer materials has allowed the development of transducers with almost 100% bandwidth. Probes to cover the range 4 to 7 MHz and 5 to 10 MHz are now available on the top-end machines. These composite materials offer a number of other advantages in that their acoustic impedance is about 1/3 of that of the synthetic ceramics and hence a much closer match to tissue is achieved. This improves coupling efficiency into the body and reduces reverberation artifact at the transducer surface.

The wide bandwidth of these transducers is allowing various image processing techniques such as parallel processing of different parts of the spectrum of the returned echoes to improve resolution and to enhance the contrast between tissue types. This is particularly useful for tumour detection. The availability of digital signal processing (DSP) chips has allowed the incorporation of new techniques in both imaging and Doppler processing into machines that are portable, or at least transportable.

The use of contrast agents is common in X-ray but it is only recently that ultrasonic contrast agents have been developed and approved for human use. These agents are typically micro bubbles or micro bubbles tagged wit a chemical agent and by injecting into the blood stream enhance the imaging and Doppler techniques in defining blood vessels and flow regions in the heart, brain, kidneys and other organs.

The conventional upper limit of ultrasonic imaging was considered to be 10 MHz but new developments are seeing imaging within blood vessels with miniature transducers that will fit on the end of a catheter. This intravascular imaging is being carried out at 20 to 30 MHz to give excellent resolution of plaque and the various layers within vessel walls (Roelandt,1993). Other high frequency imaging at 50 to 70 MHz is in the research stage and is showing exquisite detail in the eye and in skin lesions such as melanoma.

A major change that has occurred over the past 6 to 7 years is the increased use of internal probes. Probes are now available for almost every orifice of the body. In particular the use of endovaginal probes in obstetrics and gynaecology can show details in the fetus at 6 weeks gestation that previously could only be seen at 12 to 14 weeks gestation (Davison, 1986; Kossoff, 1991). The use of an internal scanning probe has two major advantages. Firstly, it can be placed closer to the area of interest and therefore a higher frequency of operation can be used for higher resolution as there is less tissue attenuation. Secondly, there is less beam distortion as the beam does not have to pass through the various subcutaneous layers of skin, fat and muscle. Where an internal probe cannot be used there is considerable research on aberration correction techniques being carried out, both in Australia and overseas, to remove this distortion due to the subcutaneous tissues (Kossoff, 1989; Carpenter, 1993).

An area that is occupying considerable research effort is the display of medical ultrasonic images in three dimensions. Some preliminary systems are showing clinical results at this time. As in most 3D systems the problem is twofold in firstly the data acquisition phase and secondly the method of display. Data can be obtained from a volume of interest within the body by various scan techniques. A conventional mechanical sector scanner can be sectored in the opposite plane to obtain echo information from a volume of tissue. The other approach is to build a 2D array of transducer elements which can be scanned over a volume by a number of different scan regimes. Clearly this approach is very flexible but the number of transducer elements and hence the complexity can rise rapidly. Currently there are research systems with up to 512 elements in the 2D array. As ultrasound imaging is not just a surface display technique there needs to be considerable image processing to decide which layers of the data are displayed in the final image. There are clearly a number of display techniques for the 3D images such as stereoscopy, surface rendering, holography, etc. which can be used for the final display.

In conclusion, a number of recent surveys are predicting ultrasound as the fastest growing medical imaging modality in the 1990's and this should assure further growth in the technological developments of the modality.

REFERENCES

Carpenter D.A., "The Effect of Overlying Tissues in Medical Ultrasonic Imaging", PhD Thesis submitted to University of New South Wales, 1993.

Davison G. "Transvaginal Assessment of Pregnancy in the First Trimester", Proc. Australian Society for Ultrasound in Medicine - 16th Scientific Meeting. pp. 66-67, 1986.

Kossoff G., Carpenter D.A., Robinson D.E., Ostry D. and Ho P.L. "A Sonographic Technique to Reduce beam Distortion by Curved interfaces" Ultrasound in Med. and Biol., Vol. 15, No. 4, pp. 375-382, 1989.

Kossoff G., Griffiths K.A. and Dixon C.E., "Is the Quality of Transvaginal Images Superior to Transabdominal Ones Under Matched Conditions?" Ultrasound in Obstetrics and Gynaecology, Vol. 1, pp. 35-41, 1991.

Roelandt J., Gussenhoven W.J. and Bomm N. "Intravascular Ultrasound", Developments in Cardiovascular Medicine 143. ISBN 0-7923-2301-7, Kluwer, 1993.

Smith W.A., "New Opportunities in Ultrasonic Transducers Emerging from Innovations in Piezoelectric Materials" Proc. New Developments in Ultrasonic Transducers and Transducer Systems, S.P.I.E. Vol. 1733, 1992.

Wilkinson R.W., "Principles of Real-Time Two-Dimensional B-Scan Ultrasonic Imaging" J. Medical Engineering and Technology, Vol. 5, No.1, Jan. 1981.

Doppler Techniques In Medical Ultrasound

Thanasis Loupas, Robert Gill
Ultrasonics Laboratory, CSIRO Division of Radiophysics,
126 Greville St, Chatswood, NSW 2067

Doppler applications in medical ultrasound date from 1957, when simple continuous wave techniques were first used by Japanese investigators to detect blood flow in the heart. For many years, Doppler ultrasound remained in the domain of cardiologists and vascular surgeons. Simple continuous wave (cw) instruments were used to obtain audible Doppler shift signals from moving blood, which were interpreted aurally by experienced operators.

In the late sixties and early seventies, two major advances in instrumentation occurred. Pulsed Doppler instruments were developed, allowing the interrogation of blood flow in the heart and vessels with far greater precision, and real-time spectral analysis became feasible, permitting the Doppler signal to be displayed in the form of a sonogram. This meant that objective measurements could be made, and records of examinations kept for documentation and comparison with subsequent examinations.

CONTINUOUS WAVE DOPPLER

Continuous wave instruments are remarkably simple (see Figure). The probe contains two transducer elements with diverging fields. One transmits a continuous stream of ultrasound (solid line) while the other (broken line) receives the echoes generated by any objects which lie in the region of overlap of the two beam patterns (shaded). These echoes are amplified and quadrature detected against the transmitted frequency. Low pass filtering results in detection of the Doppler shift and direction of flow. At the frequencies used (2 - 10 MHz) and with typical blood velocities (0 - 3 m/sec), the Doppler shift conveniently falls into the audible frequency range.

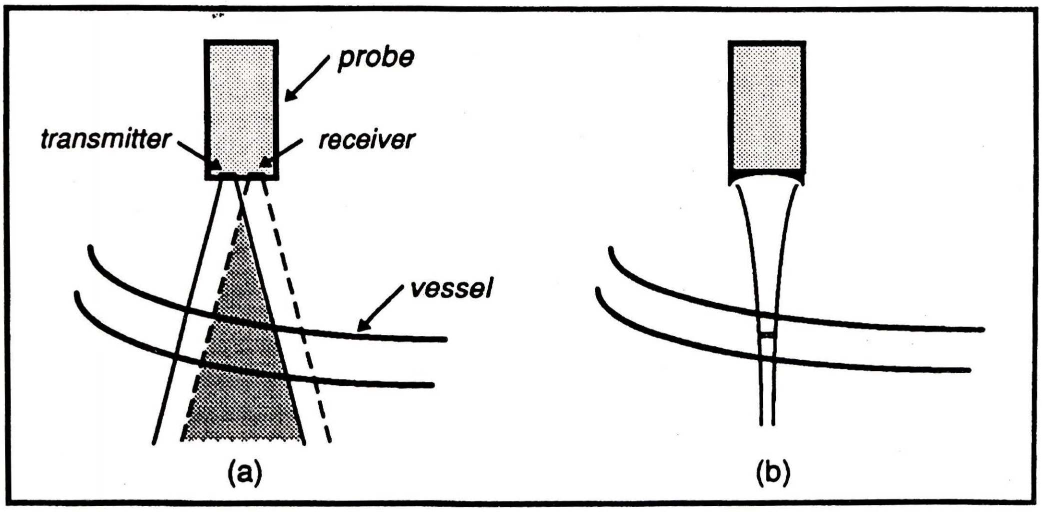

(a) CW and (b) pulsed Doppler probes used to examine a blood vessel.

PULSED DOPPLER

The major limitation of cw instruments is their lack of spatial selectivity. In a typical application, several blood vessels fall within the region of beam overlap, making interpretation of the Doppler signals difficult. This deficiency led to the development of pulsed Doppler systems. A single focused transducer is used alternately as transmitter and receiver, as in ultrasound imaging. Time gating (ìrange gatingî) is applied to selectively pass through to the Doppler detector only those echoes originating from the range of interest. Low pass filtering of the phase-detected echoes from a number of successive bursts (typically 50 to 200) results in the generation of an audible Doppler shift signal.

Depending on the frequency used and the depth of the range gate in the body, the ìsample volumeî of the pulsed Doppler system may be as small as a few millimetres in width and depth. Accurate placement of such a small region dictates that these systems are virtually always integrated into ultrasonic imaging machines (creating ìduplexî systems), permitting the images to guide the user in positioning the Doppler sample volume.

Since the pulsed Doppler system effectively samples the Doppler shift at a rate equal to the transmitter pulse repetition frequency (PRF), it is subject to frequency aliasing whenever the Doppler shift exceeds the Nyquist limit of PRF/2. Baseline shifting is commonly used on the spectral display to ìunwrapî the sonogram in cases of modest aliasing. Alternatively, the PRF can be increased (up to the limit set by the depth of the range gate and speed of sound in the body). Unfortunately, many of the diseases of interest (eg narrowing of vessels in atherosclerosis and reduced opening of heart valves in cardiac disease) produce very high velocities, and at times it is necessary to resort to cw Doppler to eliminate the aliasing.

SONOGRAM DISPLAY

The real-time spectral ìsonogramî display has become standard for both cw and pulsed Doppler systems, due to the richness of the information which it can display. It shows the range of Doppler shifts - and hence velocities - present at each instant, and the relative quantity of blood travelling at each velocity. A variety of parameters can be measured from the sonogram. These include the maximum, minimum and mean Doppler shift, acceleration and deceleration times, and the relative timing of portions of the cardiac cycle.

Note that absolute velocity values can be computed from the Doppler shift only if the angle between the direction of blood flow and the interrogating ultrasound beam is known. A number of indices have therefore been defined in an attempt to characterise arterial flow waveforms. These use the ratios of various Doppler shift values (eg {max - min} / {mean}) to provide a measure of waveform shape which is independent of both the angle and ultrasound frequency. An important limitation of the sonogram display is "intrinsic" spectral broadening caused by the use of large aperture strongly focused transducers. This can be mistaken for the spectral broadening associated with disturbed flow, and it leads to over-estimation of velocity.

COLOUR FLOW IMAGING

In the mid 1980s yet another major innovation occurred. Colour flow imaging techniques were developed. These generate a colour overlay on the grey scale ultrasound image, with the colour representing Doppler shift values. Highly efficient methods, commonly based on autocorrelation, are used to estimate the mean Doppler shift for each pixel from a small number of transmit pulses (typically 4 - 16 pulses per line of sight). At least as challenging as the frequency estimation is the suppression of clutter from stationary and slowly moving tissue, since this may be 40 - 60 dB above the signal from moving blood. More recently, other velocity estimators have been developed for colour flow imaging, for example using two-dimensional autocorrelation or cross-correlation of echoes from successive transmit pulses.

Despite its limited spatial and velocity resolution and poor frame rate, colour flow imaging has gained widespread acceptance in the clinical environment. It is used in a ìpathfinderî role to display the blood vessels in a given region and to find specific vessels. It is also used to distinguish between blood vessels and other tubular structures (such as bile ducts), and between arteries and veins. As part of the initial examination of a patient suspected of arterial disease, it is used to survey the vessels of interest, highlighting areas with abnormal velocities. Almost universally pulsed Doppler with the sonogram display are then used to derive more accurate diagnostic information.

A variation on the theme of flow imaging has emerged recently. This is "power mode" imaging, in which the colour of each pixel represents the estimated power of the Doppler signal at that point. This mode has a number of advantages over conventional colour flow imaging. It produces a far more uniform background in areas where there is no significant blood flow, facilitating the detection of flow in small vessels. Longer acquisition times can be used, since pulsatile velocity variations are not of interest, increasing the sensitivity. In addition, the absence of information on flow velocity and direction makes the colour display substantially easier to interpret in some clinical circumstances.

FUTURE OF DOPPLER ULTRASOUND

Over the past decade, Doppler instrumentation has improved, and the range of applications has increased, to the extent that Doppler has become an integral part of the ultrasound examination. It is used to diagnose disease of the heart, arteries and veins, often replacing more invasive (and therefore risky) tests such as X-ray contrast studies and cardiac catheterisation. It is also used to investigate organ function, for example in the kidneys and liver, and to detect the abnormal vessels generally associated with malignancies. At present Doppler instrumentation is limited by the processing power available in ultrasound machines, although this is advancing very rapidly. Future developments will include faster data acquisition using simultaneous formation of multiple beams, more effective algorithms for spectral and velocity estimation and improved spatial resolution through the use of two-dimensional array transducers.

Aberration Correction in Ultrasonic Imaging

David Carpenter
Ultrasonics Laboratory, CSIRO, 126 Greville St. Chatswood NSW 2067

Problems in the quality of medical ultrasonic images have long been ascribed to the subcutaneous tissue layers in the body wall. All medical ultrasound scanners, and many other ultrasonic systems, operate on the assumption that ultrasonic waves travel in straight lines and at constant velocity. In the subcutaneous tissues these assumptions do not hold because of the differing velocities in skin, fat and muscle and the shape of these structures. The impetus to correct distortions due to the subcutaneous layers has come from three main clinical areas:

- There are artifacts in abdominal and obstetric scanning in which double or triple representations of structures were seen due to refraction by the rectus muscles (Buttery and Davison, 1984).
- Low quality images are often obtained from very obese or very muscular patients (Shirley et al., 1978).
- An improvement in image quality is obtained when internal scanning probes were used such that the ultrasound beam did not have to traverse the subcutaneous tissues (Davison, 1986).

Research has been carried out in a number of centres worldwide since the late 1980's to both model the effects and to attempt to correct them. All correction methods have been applied to the image-forming part of the imaging process. Researchers in the USA at General Electric (O'Donnell and Flax, 1988) and at Duke University, North Carolina (Nock et al, 1989) have used various backward propagation methods whereby a feature in the image is used to attempt to correct the image. These techniques are most effective when a suitable image feature is available such as a highlight (point target) , or a scattering region (fully developed speckle). They are also best adapted to small stochastic variations in the propagation path. When discrete refraction, leading to gross image distortion, is present the backward propagation modelling techniques can converge to an "incorrect" image or fail to converge at all.

At the Ultrasonics Laboratory in Sydney a forward propagation technique has been developed to correct for the refraction at the fat/muscle boundaries in the subcutaneous tissues. The correction principle developed is a forward propagation technique in which the scanning beam from an array transducer is pre-distorted such that a well-formed beam is obtained after the ultrasonic beam has traversed the subcutaneous tissues. This is possible as the shape of the overlying layers can be obtained from an initial scan and the values of propagation velocity for fat and muscle are known. From this information the amount of time-delay error can be calculated for each element in the scanning aperture and then the corrections can be applied to generate a corrected beam (Kossoff et al., 1989; Carpenter, 1993). The principle is shown in Figure 1. The area can then be rescanned with the appropriate corrections applied to each scanning beam to give a corrected image.

This approach is satisfactory for model studies and scanning tissue phantoms but rescanning is not possible for live subjects where there is tissue movement, due to respiration and cardiac motion, between the two scans.

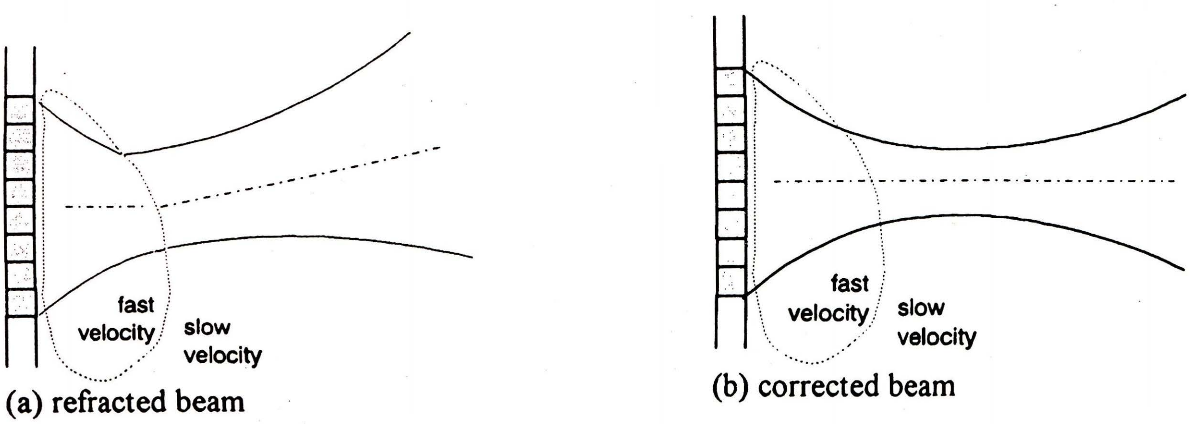

Figure 1. Diagram showing the principle of the correction technique

To overcome the need to rescan, a synthetic- aperture technique has been developed. This technique has been used in fields such as radar, sonar and NDE (Brown, 1969) but is less common in medical ultrasound. The principle is to transmit with a single element of the array and receive with all the elements of the aperture which uses that element as shown in Figure 2. In this system a given element is fired and the 8 channels to the right of the element are received and stored. The same element is then fired again and the 8 channels to the left are stored. This is then repeated for each element in the array and the receive data stored in computer memory. A complete image can then be reconstructed, as data for every possible transmitt/receive combination are available in the stored data set.

An acquisition system was built to allow the use of synthetic-aperture scanning to reconstruct images from live patients (Carpenter, 1993). The system uses a basic 5.0 MHz, 8 channel ultrasound scanner, 8-channels of time-gain-compensation (TGC), 8 channels of A/D conversion and 4 MByte of fast memory to store the RF echo data. The data can then be downloaded to a Sun workstation for processing.

Software has been written to reconstruct the image from the stored RF data. The subcutaneous muscle and fat layers are outlined manually by the operator, and the software can then calculate the time delay under each element in the array used to form the scan. From this stored RF data and the calculated corrections, an image can be reconstructed which is corrected for the refraction due to the subcutaneous layers.

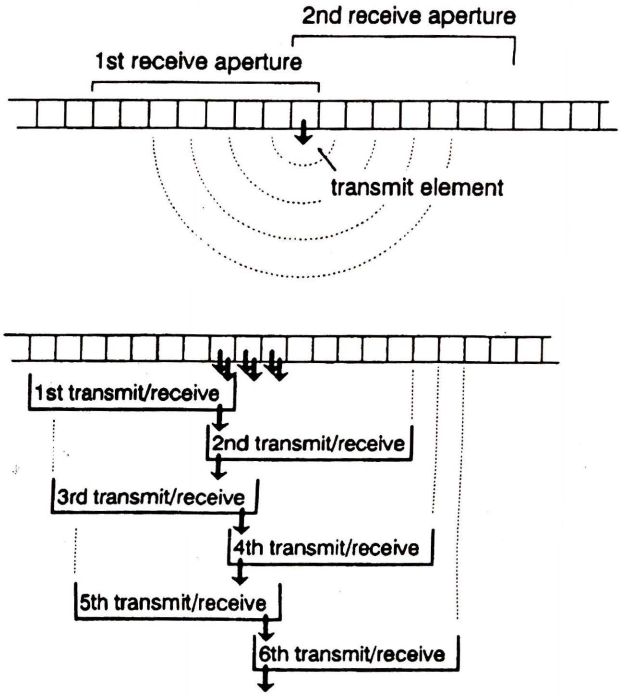

Figure 2. Diagram of the synthetic-aperture scanning technique.

Model studies have shown that an ultrasound beam, which has been broadened and deviated by refraction in the subcutaneous layers, can be corrected using a forward propagation technique. Abdominal images have been taken on a range of volunteer subjects, both male and female, ranging in age from 17 to 48 years. We were able to correct distortions which gave double images of the blood vessels and incorrect sizes and shapes to other abdominal structures. The superior mesenteric artery (SMA) and the aorta were used as test targets within the body as it is relatively easy to get double images of these structures due to refraction of the scanning beam by the rectus muscles. Similar correction has been applied in obtaining corrected images of tissue phantoms where the display of the internal structures has been distorted by using an overlying layer, simulating a wedge of fat.

The need for the operator to outline the fat and muscle structures is not practical in the clinical situation and work is proceeding to detect the shape of the overlying layers automatically. The present scanner, while useful to prove the concept, is restricted in penetration and quality by the low number of channels and the operating frequency. The system is presently being expanded to a 32-channel system that will operate at both 3.5 and 5.0 MHz.

It has been demonstrated that our forward propagation correction method can remove gross image distortion due to discrete refractive effects. Undoubtedly stochastic refractive effects will co-exist in the real world. The "ultimate" correction system will probably include a combination of forward modelling and some iterative technique based on image quality, or other methods currently under consideration.

REFERENCES

Brown R.M., "An Introduction to Synthetic-Aperture Radar", IEEE Spectrum, Vol. 6, 52-62, September 1969.

Buttery B. and Davison G., "The Ghost Artifact", J. Ultrasound Med.Vol. 3, pp 49-52, 1984.

Carpenter D.A., "The Effect of Overlying Tissues in Medical Ultrasonic Imaging", PhD Thesis, University of New South Wales, 1993.

Davison G. "Transvaginal Assessment of Pregnancy in the First Trimester", Proc. Australian Society for Ultrasound in Medicine - 16th Scientific Meeting. pp. 66-67, 1986.

Kossoff G., Carpenter D.A., Robinson D.E., Ostry D. and Ho P.L. "A Sonographic Technique to Reduce beam Distortion by Curved interfaces" Ultrasound in Med. and Biol., Vol. 15, No. 4, pp. 375-382, 1989.

Nock L., Trahey G.E. and Smith S.W. "Phase Aberration Correction in Medical Ultrasound using Speckle Brightness as a Quality Factor" J. Acoust. Soc. Am. Vol. 85:(5), May 1989.

O'Donnell M. and Flax S.W., "Phase Aberration Corrections using Signals from Point Reflectors and Diffuse Scatters: Basic Principles" IEEE Trans. on Ultrasonics, Vol. 35, No. 6, November 1988.

Shirley I.M., Blackwell R.J., Cusick G., Farman D.J. and Vicary F.R. " A User's Guide to Diagnostic Ultrasound" Pitman Medical, 1978.

A Neural Computing Implementation of the Scaled Mean Square-Error Filter for the Elimination of Speckle Noise in Ultrasonic Images

X.L. Zhou and L. Guan
Machine Vision and Real-Time Image Processing Group
Department of Electrical Engineering,
The University of Sydney, Sydney, NSW 2006, Australia

Since the emergence of A-scan, B-scan, and time-position (M-mode) recording, ultrasonic imaging has become a more and more significant method in medical diagnosis and biological research.

It is understandable that the performance of an imaging system affects the quality of the recorded images. Ultrasonic imaging is no exception. The existence of speckle phenomenon is just one of the examples, which may mislead to a wrong conclusion in pathology. Therefore, it is important to improve the image quality as much as possible before the analysis of the ultrasonic images in the knowledge domain of medicine or biology.

In this paper, a new image filtering technique is applied to the processing of ultrasonic images. More exactly, the pattern of the speckle phenomenon in the image is first identified in term of noise correlation and then a vector neuron evolution algorithm is used to execute a newly proposed scaled mean square-error (SMSE) filter. The proposed method has the following desirable features:

1. The SMSE filter is a further improvement upon the standard or parametric minimum mean square-error (MMSE) filters. The standard MMSE filter considers the complete information carried by correlation and the resultant images tend to be too smooth. The parametric filter attenuates the effect of total correlation, but the improvement is limited due to the linear nature of the method. The SMSE filter introduced uses a scaling policy to de-emphasize gradually the correlation factor off the diagonal in a nonlinear fashion. Eventually, the oversmooth phenomenon associated with the standard MMSE and the parametric MMSE filter is significantly reduced.

2. The vector neuron evolution algorithm is a newly developed neural computing technique. According to this processing scheme, each image pixel is represented by a neuron, and all the neurons of the same row/column evolve simultaneously. Therefore, the probability that the algorithm reaches the global optimal solution is significantly higher than its scalar counterparts when the solution lies in an enlongated valley. Thus the vector neuron evolution algorithm can provide more satisfactory results.

When applying the proposed method to the enhancement of the ultrasonic images, one additional problem must be addressed. That is the identification of the correlation of the images and that of the speckle noise. Since they are not obtainable from the recorded data, an estimation procedure is devised. The proposed statistics of the noise is obtained from a relatively smooth background. The statistics of the image is obtained from a rough estimation based on a blurred image with reduced noise which obviously approximates the original image better than the recorded noisy image.

The proposed technique is applied to the enhancement of an ultrasonic image "artery", as shown in Figure 1. From the result illustrated in Figure 2, it can be seen that the noise is effectively eliminated without affecting the quality of the image.

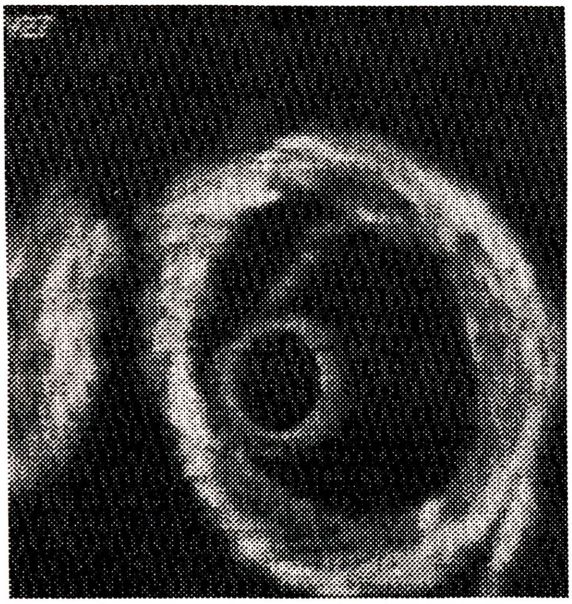

Figure 1. Input Noisy Image

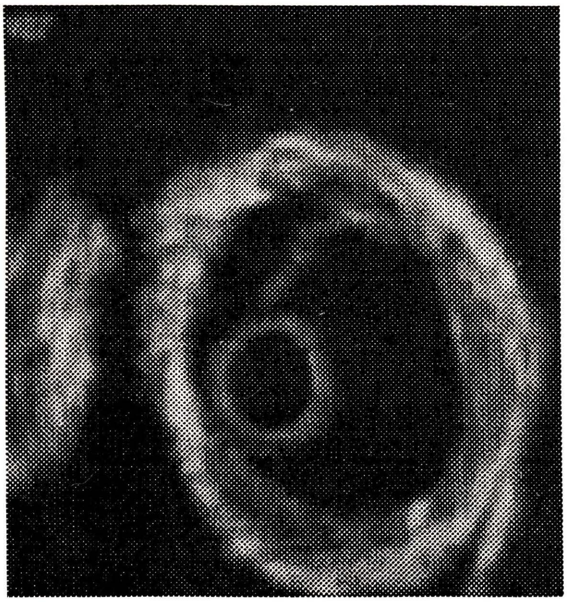

Figure 2. Output Improved Image

Acoustic Daylight: Imaging in the Ocean with Ambient Noise

Michael J. Buckingham
Marine Physical Laboratory, Scripps Institution of Oceanography, La Jolla, California 92093-0213
and
Institute of Sound and Vibration Research, The University, Southampton, SO9 5NH, England

ABSTRACT

Detection of targets in the ocean using sound is traditionally achieved with either passive or active techniques. Passive relies on sound emission from the target itself, whereas an active system transmits a pulse and listens for the returning echo. A third technique was introduced recently, which is neither active nor passive: Acoustic Daylight relies on the ambient noise field in the ocean to provide the acoustic illumination necessary to detect a target. The presence of a target in the field scatters some of the incident energy. By using an acoustic lens (reflector, refractor or phased array) to focus the scattered radiation onto an image plane filled with acoustic sensors, and after applying the appropriate signal processing, a pictorial image of the object space can be produced on the screen of a desk top computer. Such images show (optical) colour, which is directly related to the frequency dependence of the acoustic reflectivity of the objects in the image. A refresh rate of up to 30 Hz is also possible, providing for moving images.

The Acoustic Daylight concept was first tested in the ocean about two years ago, when a simple experiment was conducted off Scripps Pier in southern California 1 . A single-beam acoustic lens in the form of a parabolic reflector with a hydrophone at the focus was placed on the sea bed and, as neoprene targets were placed in the beam, the perceived noise level increased by a nominal 3 dB. The targets were indeed visible just through the illumination from the ambient noise.

Encouraged by this result, a more sophisticated imaging system was constructed, known as ADONIS (Acoustic Daylight Ocean Noise Imaging System). ADONIS consists of a spherical reflector with a hydrophone array of 126 elements in the focal surface. Each element has an associated beam, and each beam corresponds to a "super pixel" or s-pixel in the screen image. The s-pixels are arranged in an elliptical configuration on the screen, representing a one-to-one mapping with the elements in the array. If a beam intersects a target in the ocean, the noise level changes to produce an intensity contrast with the remaining beams. The intensity variations seen in the s-pixels produce the screen image. An obvious analogue is a photographic negative, where the image is formed through (optical) density variations.

The ADONIS array was deployed in the ocean off Point Loma during the last two weeks of August 1994. Neoprene targets were arranged in various configurations at a range of 38 m from the receiver. When the dish was scanned past the targets at a rate of 22.5 per minute, recognizable, moving colour images were visible on the output screen 2 . These images were produced in real-time, using a Macintosh IIfx fitted with a DSP board. The acoustic contrast levels in the images were consistent with a numerical simulation 3 and a wave-theoretic analysis 4 of Acoustic Daylight imaging.

The evolutionary development of Acoustic Daylight imaging will be presented, along with the latest results from the recent ADONIS deployment.

REFERENCES

1. M.J. Buckingham, B.V. Berkhout, and S.A.L. Glegg, "Imaging the oceanwith ambient noise", Nature 356, 327-329 (1992).
2. M.J. Buckingham, et al., "Experimental imaging in the ocean with acoustic ambient noise", Nature, submitted September 1994, (1994).
3. J.R. Potter, "Acoustic imaging using ambient noise: Some theory and simulation results", J. Acoust. Soc. Am. 95, 21-33 (1994).
4. M.J. Buckingham, "Theory of acoustic imaging in the ocean with ambient noise", Journal of Computational Acoustics 1, 117-140 (1993).

A Comparison of Ultrasonic Imaging for Underwater and Medical Applications

David E. Robinson
Ultrasonics Laboratory, Div. of Radiophysics, CSIRO;
126 Greville St, Chatswood, NSW 2067

Medical ultrasonic imaging is fast becoming the most used medical imaging modality. It is widely available in radiology, cardiology and obstetrics practices. It is a pulse-echo imaging technique which shares many common concepts with sonar and radar. Despite this commonality, there are also significant differences which make direct transfer of concepts, conclusions and common belief from one field to another dangerous. There is also considerable commonality with exploration seismology, but in this case the differences are more distinct. This paper will outline some of the differences in imaging requirement and basic imaging assumptions between medical and sonar imaging. The paper will discuss some of the differences, and their consequences in the understanding of the two techniques. The differences are detailed in Table 1, and the consequences discussed.

CONVENTIONAL PULSE-ECHO RANGING - (SONAR & RADAR)

The principles of sonar or radar imaging are well established. In its conventional PPI form, the image obtained is a two-dimensional map of impedance discontinuities (reflectors) in the scanned volume projected onto a reference plane. There is no resolution in the direction perpendicular to the reference plane, and the interrogating beam is sufficiently wide to encompass all of the scanned volume. When the relationship between the target and the interrogating beam are suitable, the effect of a three-dimensional display can be obtained. This is particularly apparent with side-scan sonar and radar, where the perspective view of the ocean bottom or land surface is enhanced by the appearance of shadows behind obstructions to the beam. However this is only quasi-3D and cannot be relied upon for imaging irregular target fields.

In the reference or image plane, azimuthal resolution is obtained by the diffraction effect of the transducer aperture. Conventional systems operate in the far field, and the resolution cell is a cone with its apex at the transducer. For a synthetic aperture system, some allowance must be made for the difference in slant range to the target from different parts of the aperture, and this is equivalent to weak focussing. The resolution is then limited by the size of the physical transducer. The range resolution is obtained from the bandwidth of the interrogating pulse. This is usually a long chirp, typically many hundreds of wavelengths long.

The imaging range required can be quite long, up to many kilometers. At one kilometer, the echo delay time for sonar is 1.3 seconds, implying minutes for unambiguous imaging with many beams. Faster imaging requires multiple parallel beamforming and transmit pulse coding, and is still limited by the transit time.

The use of the image information is for target detection and tracking, and target classification. Target detection requires a low false-alarm rate, meaning that grating lobes, side-lobes and clutter must be small compared with the expected target strength. Target classification looks at echo character, such as the echo spectrum, or the echo shape. In each case, the target echo is normally larger than the interfering noise signals. Target motion (or transmitter motion) can provide useful data for signal processing and aid the detection process. The image obtained is a representation of the surface of target, either the surface of the ocean bottom, or of targets within the water column.

MEDICAL IMAGING

The principles of medical ultrasonic imaging are also well established. The image represents a two-dimensional slice through the scanned anatomy. The resolution perpendicular to the image plane is made as good as possible to reduce the slice thickness of the image. To obtain three-dimensional information, multiple thin slices are obtained. At the present stage of technology, the combination of the data into three dimensions is performed in the brain of the interpreter.

The echo dely time for a 20 cm depth of tissue is 260 μs, and a 128 beam image can be formed in 30 ms, yielding 30 frames per second. Ultrasonic imaging transducers are hand-held, and the combination of a real-time image and tactile feedback of the image plane enhances the mental three-dimensional reconstruction process.

Typically, the depth to aperture ratio of the imaging system is in the range from 2 to 5, and the image is formed in the first 20% of the near field. Thus medical imaging is normally carried out in the mid to strong focus regime. Four to ten transmit focal zones may be used to encompass the 20 cm of tissue. The receive focus is usually dynamic, being adjusted during receipt of the echoes to track the image range. For a strongly focussed beam, the image blur function is a bicone with its apex at the focal point. The locus of beam width at the focal point for different focal distances lies on a cone with its apex at the transducer aperture plane.

In contrast with sonar and radar, the required target information resides in the low-level echoes originating within the tissues. Diagnostic information is obtained from the appeasrence and uniformity of the image texture resulting from the scattered energy from the tissue structures which are smaller than the resolution cell of the imager. Echoes from the boundaries of the organs, and interfering echoes from adjacent highly reflecting structures containing air and bone constitute the noise in the system. Typically, the noise signals are considerably larger than the required image signals, but displaced in time and location in the image. The dynamic range required to be displayed to ensure that the tissue echoes are properly displayed is of the order of 80 dB.

The transmit signal used is a short pulse, typically of the order of 3 cycles in length, with a fractional bandwidth of .4 to .8. That is, a 3.5 MHz system could have a bandwidth of 2 MHz. Beam-forming is achieved by time-shifting rather than phase-shifting, and is usually implemented in the time domain. Particular attention is paid to the dynamic range of the transmitted pulse, as any residual energy transmitted outside the required pulse period will be displayed by the high receiver dynamic range as a structure immediately behind a strong reflector. It may then be interpreted as a genuine structure, the presence of which could affect the diagnosis.

The medium in which the imaging is carried out is assumed to be homogeneous. In reality this is not the case, the sound speed and acoustic impedance vary greatly. Bone and air produce strong reflection and refraction, and for most practical purposes can be considered a barrier to ultrasonic imaging. In soft tissue, the variation in density is small, but in sound speed it is considerable. Cartilaginous tissue and skin are at 1800 to 2000ms^{-1}, muscle is around 1600ms^{-1}, organs such as spleen, liver, and blood 1540ms^{-1}, and fat around 1450ms^{-1}. Despite the unattractive prospect, ultrasonic imaging has proven to be remarkable robust against aberrations in the medium. Aberrations certainly do exist, and affect the image quality, but usually the effects are recognisable, often avoidable, and are sometimes used as diagnostic signs.

DIFFERENCES

As I hope to have demonstrated, the fundamental principles of sonar and medical imaging are quite similar, but the details and the language used to describe them are substantially different. I have listed some of the specific differences in the operating regimes of the two systems in Table 1.

Table 1. Differences in operating regimes of underwater and medical imaging systems.

PARAMETER	UNDERWATER	MEDICAL
Imaged region	Volume	Thin slice
Object feature of interest	Surface shape	Interior structure
Acoustic field regime	Far field	Near field, focussed.
Interrogating pulse	Chirp (hundreds of cycles)	Short pulse (a few cycles)
Signal feature of interest	Peak value (detection) Spectrum (classification)	Distribution of low-level echoes (image texture)
Sound travel time	1.3 s (sonar, 1km) 5 ms (Acoustic Vision, 4m)	260μs (20cm of tissue)
Imaging rate	Many sec/frame, or Single ping	30 frames/sec
Display	Slow sweep	Real-time video

The difference with the greatest impact is that medical imaging operates deep in the near field using broad-band short pulse excitation. This combination means that grating lobes are not a consideration, but the available focal depth of field certainly is. Attempting to use a fixed focus system loses at least an order of magnitude in lateral resolution, and various focussing approaches, both in transmit and receive are necessary.

The characteristics of interest in the image bring another difference. Typically, the top 30dB or more of the dynamic range is compressed (almost to the point of hard limiting). The available grey-scale display range is used to display small changes in amplitude and texture in the smaller echoes originating within the organ tissues. This places stringent requirements on the entire image-forming chain to avoid image contributions due to amplifier saturation, beam side-lobes, transducer ringing etc.

The region of intersection of the sonar and medical imaging technologies is in the application of high frequency ultrasonic imaging for underwater vision in turbid water. A combination and modification of classical sonar and classical medical imaging approaches, taking due consideration of the areas of dissimilarity as well as the similarities, promises to provide an interesting hybrid capable of quite spectacular performance.

$k = .5$ dB/cm/MHz

$= 50$ dB/m/MHz

$k_p = .05$ dB/m/kHz

$\therefore h \simeq .08$ dB/cycle

High Resolution Underwater Imaging

Ian S F Jones
AMRL, DSTO, Pyrmont, NSW

The transmission of electromagnetic radiation in the ocean is poor, with long wavelengths suffering strong attenuation and short wavelengths liable to scatter by suspended particles. There is a band of acoustic frequencies where scattering and attenuation are low and wavelength is short enough to allow construction of imaging devices of modest size. This acoustic oceanic window, which is in the low megahertz frequencies is shown in Figure 1.

To achieve resolution of the order of public television, but less than photography, one requires of order 10^3 by 10^3 pixels. Television provides a two dimensional image, but with acoustics, it is practical to provide a true three dimensional image. The same resolution as above in the viewing direction implies 10^9 voxel resolution. Both the processing and the display of such information presents a challenge. However the needs of underwater inspection in turbid conditions, where divers and current technology visual (video) systems are ineffective, demands an innovation.

An innovation plan has been prepared to produce an underwater acoustic imaging system with a timed application of research, development and commercialisation resources. The constraints and progress of the research and development undertaken so far is reported.

To make a practical imaging system at this time, four major technical decisions must be taken. Firstly the wavelength that finds the best window in the turbid ocean water must be determined. The range of operating temperatures are important in this decision because molecular attenuation is significant. Secondly, sparse random array technology is needed to keep the number of acoustic signals within practical limits. Thirdly, one bit digitisation and the noise penalty this implies must be embraced. Fourthly, massively parallel processing must be used if an image is to be produced in near real time. With these constraints, there is considerable scope to optimise the design of an imaging system.

The display of three dimensional data presents a challenge. The exterior surfaces of most underwater objects are continuous and this allows opportunities for pattern recognition algorithms to enhance and render the exterior surfaces in a three dimensional image. The ability to view the object from a number of directions may be useful, as may perspective images.

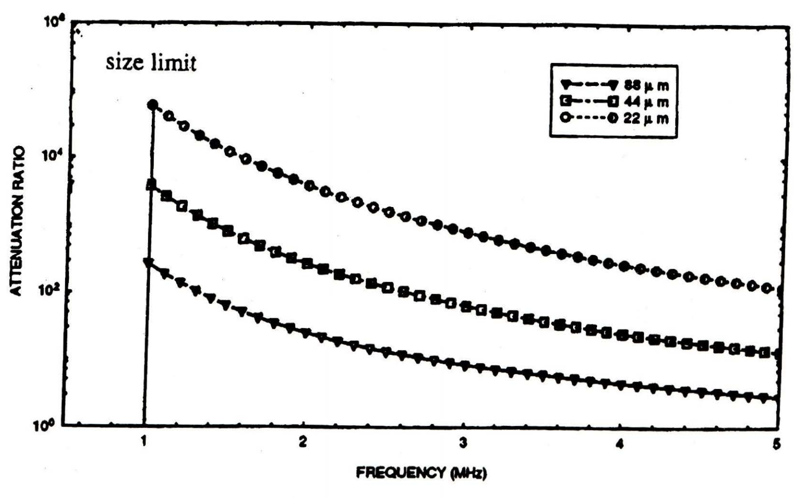

Diagram of acoustic window in the ocean for various levels of turbidity. The vertical axis is the ratio of attenuation by scattering of blue light to that of acoustics over a path of one meter. The array size limitation is for a field of view one quarter the acoustic path length. The ratio is independent of concentration of sediment and depends only on particle size.

The Application of High Frequency Sonar in Mine Countermeasures

CMDR R R Baker, RAN
Commander Australian Mine Warefare and Clearance Diving Forces, Sydney, Australia

The high attenuation of remote sensing signals in water, other than sound, means that probing beneath the ocean surface is dominated by acoustics. For identifying and locating inert objects, high frequency sonars are the main device, supplemented with divers and video cameras on Remote Operating Vehicles.

An important operational problem for Navies is the detection, classification and identification of underwater explosive mines. The mine can be used to disrupt commerce and endanger naval forces. The survey of areas is carried out by side scan sonars while mine detection uses forward looking sonars in the frequency range 30 kHz to 100kHz. Classification needs frequencies of hundreds of kilohertz and narrow beamwidth to obtain the necessary resolution. Identification is often made with the use of optical sensors, ie divers or video cameras. One difficulty is that in turbid waters optical devices can become useless. This has driven the Australian Defence Organisation to undertake an innovation program in conjunction with industry.

The resolution needed for the three steps is as follows. For detection the resolution cell needed is of order 2m by 2m at ranges from several hundred meters to about 1000m. For classification the cell size needs to be smaller than the object and so about 0.5m at several hundred meters is appropriate. Identification occurs at close range and requires 1 to 10 mm resolution.

The use of these sonar systems in a military environment poses additional problems for the platform designer and the system operator.

FTV: A 3-dimensional Sonar Imaging System for Mapping Zooplankton Trajectories

Jules S. Jaffe, Duncan McGehee
Marine Physical Lab, Scripps Institution of Oceanography, La Jolla, CA 92093©0238

ABSTRACT

Over the last several years, our research group in the Marine Physical Laboratory at SIO has beendeveloping several new underwater imaging systems for measuring both spatial and dynamic characteristics of underwater organisms. Our primary goal has been to create what we consider to be a "next generation" of ocean technology. To us, this means cameras that have fast repetition ratesand good spatial resolution. We have been developing both sonar technology as well as optical methods in an effort to resolve phenomena on scales ranging from centimeters to meters. These include fine scale distribution of phytoplankton, behavior of zooplankton, interactions between zooplankton, and interactions between zooplankton and phytoplankton. We now have several working prototypes. This article describes the technical aspects of the sonar system. We have called the system Fish T.V., or FTV, in order to emphasize our basic goal of developing a real-time 3-dimensional imaging sonar for aquatic use. With this sonar system, we have successfully been able to track the 3-dimensional trajectory of a small ($2 cm$) freshwater shrimp in a large tank. Quantitative estimation of the accuracy of the sonar system when compared to trajectories measured directly via optical means has confirmed the success of the technique.

INTRODUCTION

The use of sonar systems to look at zooplankton is certainly not new and various researchers have concentrated their efforts on using these tools both for broad survey and size characterization. Currently, two commercial systems, one manufactured by Biosonics (Seattle, WA) and the other by Simrad (Norway) are routinely used in both echocounting and echointegration studies. Although much has certainly been learned from data processed from both of these systems, neither can count or track multiple organisms at high frame rates when target densities exceed even moderate amounts. Our efforts in developing new sonar systems have been dedicated to creating a system which has the capability of resolving, in both space and time, single organism tracks. From a technical point of view, the solution to this problem is clear: multibeam sonar imaging systems with high repetition, or frame, rates.

SYSTEM DESCRIPTION

The system that we have designed in order to achieve the goal of both finer spatial resolution and more frequent sampling in time utilizes two arrays of 8 sonar transducers each in order to create a 3-dimensional image of "targets" in the field of view of the sonar. One aspect of sonar imaging systems, similar to the type that we designed, is that the two cross range dimensions have fixed resolution in angle rather than distance. Our system, FTV (for Fish TV) has beams which are approximately 2 degrees by 2 degrees. In the third direction, range, the resolution is determined essentially by the "effective" pulse length. We are currently using a pulse of range duration of approximately 3 cms. The system operates at a frequency of 450 kHz.

At a distance of 4 meters, the system has resolution cells which are about 15 cms. x 15 cms. x 3 cms. The repetition rate of the system is variable, but can be as high as 5 frames/second. Since the system has eight 2 degree by 2 degree beams, it images a "wedge" of space which is 16 degrees by 16 degrees. The depth of the wedge can also be varied to a range as large as 20 meters. Presently, we have tested the system to a range of 4 meters; at this distance, a single animal of size .5 cm can be localized and tracked in 3 dimensions.

SYSTEM OPERATION

The system is designed so that it can be used in several different modes. In one mode, a set of temporal waveforms can be displayed, similar to an oscilloscope, so that the user can judge the quantitative characteristics of the individual time evolving signals. Alternately, the system can be used in a continuous acquisition mode where a facsimile of the 3-dimensionally collected data is displayed. As a third mode, the data can be continuously acquired without display. The first mode is used mostly for system debugging, and the second mode is used exclusively during system operation so that the user may have some idea of the characteristics of the data. The third mode is used in order to maximize system frame rate, as no processing of the received data is needed for display. The real-time display presents 3 views of the 3-dimensional matrix, corresponding to an integration of the data along each of the three principle axes. For example, given a 3-dimensional coordinate system x, y, z, where z is range, the top view is a presentation of the data where each of the eight values along the y direction have been integrated into a single value, the side view is integration along the x axis and the front view is integration along the z axis. Looking at the top, side, and front views, the sizes of the 2-dimensional displayed images are 8 x 512, 8 x 512, and 8 x 8. In this case we have assumed a range depth of 512 bins (3.84 m).

In using the system, various options are available the design of which were motivated by the desire to maintain some degree of flexibility. For example, a variable acquisition delay permits the 15 m range gate of the system to be place an arbitrary distance from the transducer. Thus, the system should be viewed as collecting a range "slice" of 15 meters at an arbitrary distance. In addition, the system has some processing algorithms built into it which reduce the appearance of any noise which is occurring. Note that this only affects the display and does not influence the data which is transferred to the hard disk.

In addition, the user may vary the transmit pulse width and the pulse amplitude. It is also possible to control the transmit pulse repetition rate to minimize reverberation effects in a test tank or guard against ghost images from large objects beyond the range of the acquired volume. The rate at which an entire volumetric frame is acquired can also be controlled for various volumetric survey applications. The number of volumetric frames to be saved can be varied, allowing the user to save from one frame to as many as the hard disk can hold. Also, the range depth of the system can be adjusted from 0 to 2048 range bins. In this way, trade-offs between repetition rate and system range depth can be made. Finally, as mentioned already, arbitrary transmit waveforms may be calculated and loaded into the arbitrary waveform generator. This allows the user to maximize the performance of the system through the use of pulse compression waveforms and permits experimentation with various pulse compression techniques.

RESEARCH RESULTS

Over the past years, the system has undergone numerous field tests. In one instance, we operated the system which was mounted on a Phantom IV ROV from the SIO Research Vessel Robert Gordon Sproul. Here, the system was utilized at depths ranging up to 80 meters. Two deployment modes were used. In one mode, the ROV was raised and lowered in the water column to measure both the amount of scatterers and also their 3-dimensional spatial distribution. In the other mode, the system was kept at a fixed depth so that the trajectories of various targets could be measured. Figure 1 shows the result of processing 42 frames of data and the resultant trajectories of 6 targets that were tracked simultaneously within the field of view of the system. The time interval between successive frames was one second. As can be seen, the system has been used to track simultaneous targets at high frame rates.

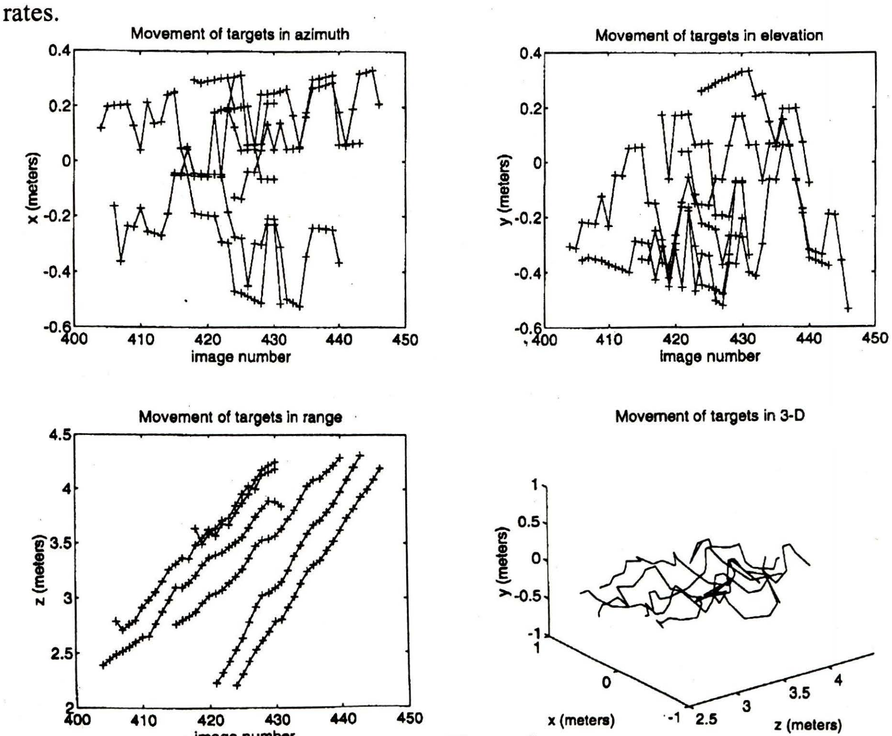

Figure 1

Acknowledgements

This work is a result of research sponsored in part by the National Science Foundation under Grant OCE 89-14300, in part by ONR grants N00014-93-I-0121, N00014-89-J-1419 and in part by NOAA, National Sea Grant College Program, Department of Commerce, under Grant No. NA89AA-D-SG138, project number R/OE-24, through the California Sea Grant College.

Evaluation of the Klein Multiscan sidescan sonar

Stuart Anstee
Maritime Operations Division, Defence Science and Technology Organisation
PO Box 44, Pyrmont, NSW 2009, Australia

DSTO has recently taken delivery of the first production version of the new Multiscan sonar manufactured by Klein Associates Inc. of the United States. The Multiscan is a multiple-beam, dynamically focussed sidescan sonar operating at a high frequency (390 kHz) in order to image swaths on the sea bottom up to 300 m wide at high resolution.

The Multiscan system was acquired with the intention of assessing its use in mine hunting and route-survey applications, with a view to future application by the Australian Navy. Areas of research interest include: (i) measurements of its susceptibility to reverberation noise sources and transducer motions; (ii) the scope for optimisation of the dynamic beam forming mechanisms and signal processing; (iii) the application of image processing techniques to the sonar display; (iv) assessments of the resolution and range performance of the sonar; and (v) measurement of the position and orientation of the towfish with respect to the ship.

The sonar consists of two packages, the wet end "towfish", and the dry end sonar processing, control and display package. The towfish is a 3 m long torpedo-shaped towed body weighing between 164 and 490 kg submerged, depending on the ballast used. Multiple-element transducers are mounted exterior to a pressure vessel containing pre-amplifiers, time-varying gain amplifiers and analogue beamformers capable of simultaneously forming five parallel across-track beams from returning echoes. The analogue beam outputs are digitised and multiplexed in the towfish and then sent up a coaxial copper serial cable to the dry-end. The main functions of the dry-end package are control of the towfish time-varying gain and beamforming, archiving of the data to 8mm Exabyte tape and display of the demultiplexed data via a video monitor and a thermal printer. Options to mark, zoom and measure objects on the display are driven by a graphical interface.

Benefits of the Multiscan sonar over currently deployed dual-frequency Klein 595 sidescan sonars in Australian Naval Service are expected in a number of areas, including increased coverage of the sea bottom at higher velocity and greater resolution than was previously available; superior signal processing and reduced noise levels due in part to digital data transmission in the cable; increased stability of the towfish against motion fluctuations; and better display of the data. Set against this are much increased cost and possible difficulties of deployment from small vessels. In addition, many of the advantages due to improved signal processing and digital transmission of data appear now in smaller single-beam sidescan systems.

The multiple-beam capability of the Multiscan devolves from the formation of five narrow, parallel beams simultaneously along the track, rather than the single narrow beam of a conventional sidescan sonar. This allows the possibility of faster surveying and/or better along-track resolution, depending on the separation of the beam centres and the beamwidth. During each ping, dynamic focussing and steering, updated with increasing range from the towfish, maintains each beam parallel to the others. The beamwidth is maintained approximately constant at 20 cm by dynamic control of element weightings: more elements are switched on as range increases, giving a greater effective length for the array. The full array length of 1.4 m, divided into 10 cm sections, allows control of beamwidth out to ranges of approximately 80 m in this fashion, after which the beam diverges with beamwidth approximately 0.14°.

Trials with a prototype Multiscan device conducted in Bigbury Bay in the English Channel have already shown that along-track resolution of the order of the beamwidth is possible (Huff and Weintroub, 1992). It is intended that further experiments will be conducted using the production device to establish its optimal working range, and to establish the resolutions attainable using various range scales and hence beam separations. The Multiscan allows range scales of 75, 100 and 150 m each side of the towfish, dictating pulse intervals of 0.1, 0.13 and 0.2 seconds respectively. The beam separations are then dependant on the towing velocity, which may be up to 10 knots. For example, at 100 m range scale a 12 cm beam separation is achieved with a velocity of 9 knots. Huff and Weintroub (1992) and simulations by the author agree that decreasing the spacing between beams along-track does not offer much improvement in resolution along-track for spacings below the beam width. The effects of towing speed will be considered in the light of further experimental evidence.

Experiments with Klein 595 systems deployed in shallow waters (say 25 m depth) such as are encountered in harbours shows that reverberation from surface waves can reduce sonar performance greatly in only moderately choppy conditions. Trials of transducer baffles have shown that significant reduction of this surface return is possible. The problem is expected to recur in shallow-water trials of the Multiscan and design issues with respect to sonar baffles are examined, including geometries and materials.

The susceptibility of model Multiscan-type images to towfish motions has been examined, (Anstee 1994a, 1994b) with the conclusion that if fine detail is not required, the Multiscan is approximately half as sensitive to all transducer motions as a single-beam Klein 595 device, and has approximately the same sensitivity when details at the limits of along-track resolution are of interest. Multiscan images are sensitive to yaw rates of the order of 1° to 2° per second. Some representative images of image distortion from the modelling are presented. As the Multiscan towfish has far greater translational and rotational inertia than a Klein 595 towfish, it is expected that motion-induced image distortions should be less severe in the Multiscan images. Available experimental evidence from sea trials will be presented.

Optimisation of the dynamically-formed beam patterns has been investigated with the intention of sidelobe reduction, control of beam width and correction for the effects of towing velocity and towfish motion. Simulations employing iterative refinement of conventional weighting functions (eg., cosine, Gaussian) and simulated annealing have shown some optimisation is possible, however, binary (on/off) element shading is surprisingly effective. The effects of towing velocity and the method of pulse emission are shown, and simulations of the standard and optimised beam patterns are compared.

With the possibility of measurement of towfish attitude and orientation comes the possibility of correction for towfish motions by dynamic alteration of the beamforming algorithm. Simulations have shown that a simple yaw-correction algorithm, which steers the receive beams to counteract the yaw recorded at the moment of pulse emission, is effective for yaw rates up to 2° per second, but is limited by the maximum steering angle of the receive beams, which is less than 2°. Other more complicated yaw-compensation algorithms are also discussed.

Image processing techniques have been applied to noisy data collected from a prototype Multiscan sonar, both to correct for electrically-induced noise and to correct for translations of the towfish away from straight-line motion. Some results are presented.

Finally, determination of towfish position and orientation relative to the towing vessel is an ongoing research area. Under consideration are internal instrumentation including motion, attitude and depth sensors; location of the towfish by a transponder beacon; and location of the towfish by cable direction and layback. The Klein Multiscan offers some scope for data transmission via the digital towfish-to-ship coaxial link.

REFERENCES

Anstee, S.D., (1994a) The effects of towfish motion on sidescan sonar images. *MRL Report MRL-RR-1-94.* DSTO Aeronautical and Maritime Research Laboratory, Cordite Avenue, Maribyrnong, Victoria 3032, Australia.

Anstee, S.D., (1994b) The effects of towfish motion on sidescan sonar images: extension to a multiple-beam device. *MRL Technical Note MRL-TN-660.* DSTO Aeronautical and Maritime Research Laboratory, Cordite Avenue, Maribyrnong, Victoria 3032, Australia.

Huff, L.C. and Weintroub, J., (1992) Field measurements of a multibeam dynamically focused side scan sonar's along track resolution. *Proceedings of the 1992 US hydrographic conference, Baltimore, Maryland, February 25-28, 1992,* pp 97-102.

A 3D Acoustic Imaging System for Non-Destructive Evaluation.*

D.J Battle, R.P Harrison
Australian Nuclear Science and Technology Organisation, PMB 1 Menai NSW 2234.

M. Hedley
Sydney University Department of Electrical Engineering, JO3, Sydney University NSW 2206

The Non-Destructive Evaluation (NDE) community has been interested in acoustic imaging ever since rudimentary reflection mode measurements proved useful for detecting flaws. The variety, complexity and effectiveness of acoustic inspection techniques have steadily increased over the years to the point where ultrasonics is now a widely used tool in industry and research. Now more than ever, it is important to be able to image defects in high investment and safety critical structures in order to make quantitative judgements.

The purpose of this paper will be to outline some research undertaken to investigate the performance of a particular diffraction tomography algorithm and in addition demonstrate various effective means of visualising three dimensional acoustic data. In conclusion, some of the design parameters of a prototype acoustic imaging system for NDE will be previewed for discussion.

The goal of the present research is to establish an economical solution to industrial requirements for acoustic imaging in heavy section components and welds. It is believed that quantitative images of acceptable quality will be possible from a relatively inexpensive system based on Fourier domain reconstruction principles coupled with either a miniaturised scanner or solid state array sensor. The governing philosophy is to keep expensive custom electronics to a minimum while maximising the use of off-the-shelf microcomputer technology, the cost/performance ratio of which continues to diminish at an astonishing rate.

The present development work is aimed at evaluating the performance of backpropagation image reconstruction algorithms. The main calculations are handled by a Fujitsu VP2200 vector processor with a peak performance of 1.0 Gflops. Reconstruction times of approximately five minutes for wide band 3D images over 128 x 128 x 128 voxels and fifty frequencies are entirely satisfactory, although speed improvements to the basic algorithm could reduce processing times by as much as an order of magnitude if this was required. Data input is via a PC controlled laboratory scanning system utilising ultrasound at frequencies between 1 MHz and 100 MHz. Image data from the vector processor is post-processed for visualisation by a Silicon Graphics RS3000 workstation running the AVS (Application Visualisation System) X-windows package which has proved an invaluable means of visualising 3D data sets. A special feature of the Silicon Graphics machine which makes it ideally suited to visualisation is the provision of hardware rendering and shading support, which enables 3D geometries to be manipulated in near real time. Figure 1. shows the general arrangement of computing resources employed at present, and how these might be transformed into a practical imaging system.

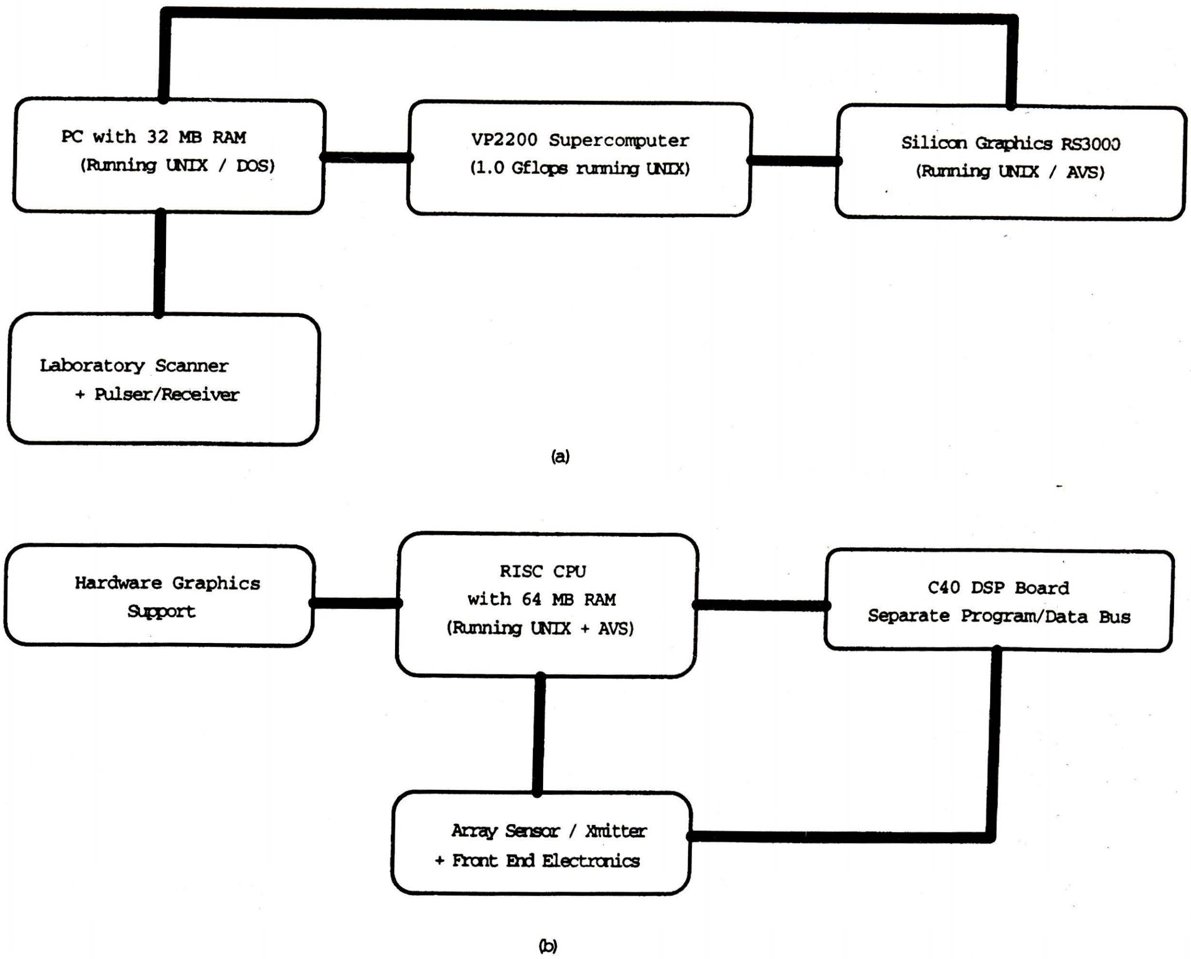

Figure 1. (a) Schematic of existing 3D acoustic imaging system. (b) Target system.

Three dimensional imaging of any form is computationally intensive, and therefore any practical computer based imaging system must have large memory resources coupled with a large data bandwidth. It is anticipated that sustained transfer rates of 10 MBytes per second into memory would be desirable. In particular the readily available TMS C40 range of DSP devices support a Harvard architecture with separate program and data buses, and could easily meet the speed requirements of data acquisition and image reconstruction. For the present, data acquisition is mono-static; requiring a single focussed transducer to sequentially occupy the positions of individual transmit/receive units in a fictitious array. The focal length of the probe is positioned at the top surface of the sample to be imaged so as to imitate the wide angular response of a small transducer element in intimate contact with the surface. It is intended that a solid state 2D array used as a replacement for the scanner would be entirely passive. The resolution performance of the system would then drop by half if only one transmitting unit were used in a bi-static imaging arrangement, although there is scope for using an additional (small) number of transmitters to recover the resolution performance lost by using a passive array. It is intended that no more than a 64 x 64 element array be employed, covering an aperture of perhaps 20 to 40 mm square.

Figures 2 (a) and (b) show raw time domain data acquired for a test sample consisting of a 10 cm thick aluminium block drilled from the back with three 1 cm deep holes with diameters of 2.0, 4.0 and 5.0 mm. Figures 3 (a) and (b) show respectively a raytraced plan view of the reconstructed holes and a perspective shaded iso-surface rendering of the same data. The centre frequency for the experiment was 2.25 MHz ($\lambda \approx 2.7mm$). The signal bandwidth used in the reconstruction was from 1 MHz to 3 MHz. Additional results will be presented with the full paper.

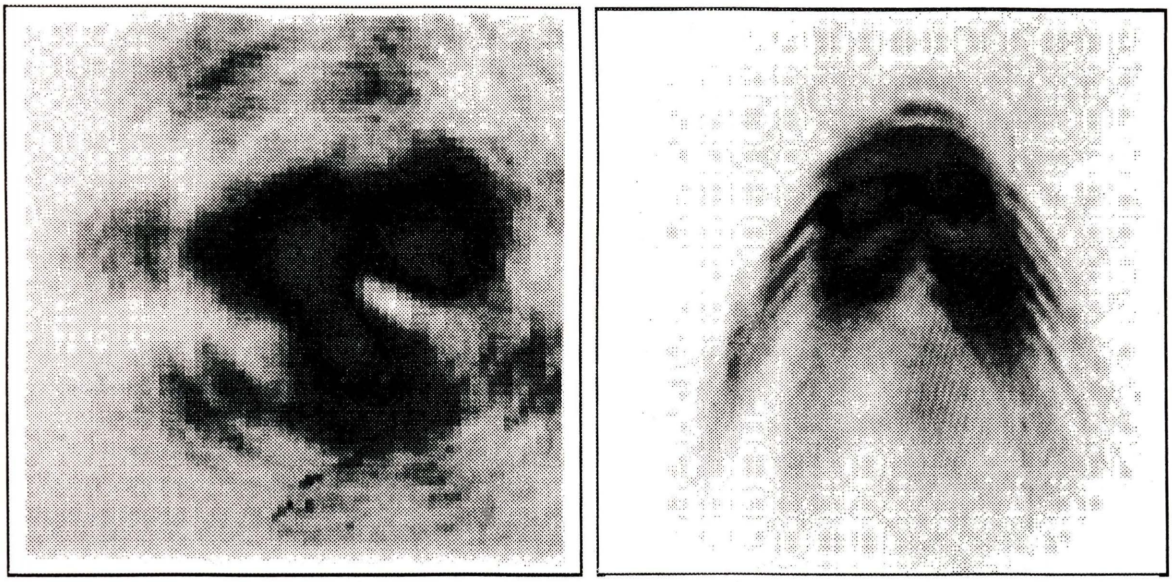

(a) **(b)**

Figure 2. Raytraced visualisations of unprocessed time domain data from a wide-band acoustic imaging experiment with a drilled aluminium block. (a) A plan view showing the diffractred hole images. (b) A perspective view of the same data field depicted in (a). The scanned aperture size was 64 mm square and the time (vertical) extent of the data was 10.24 us.

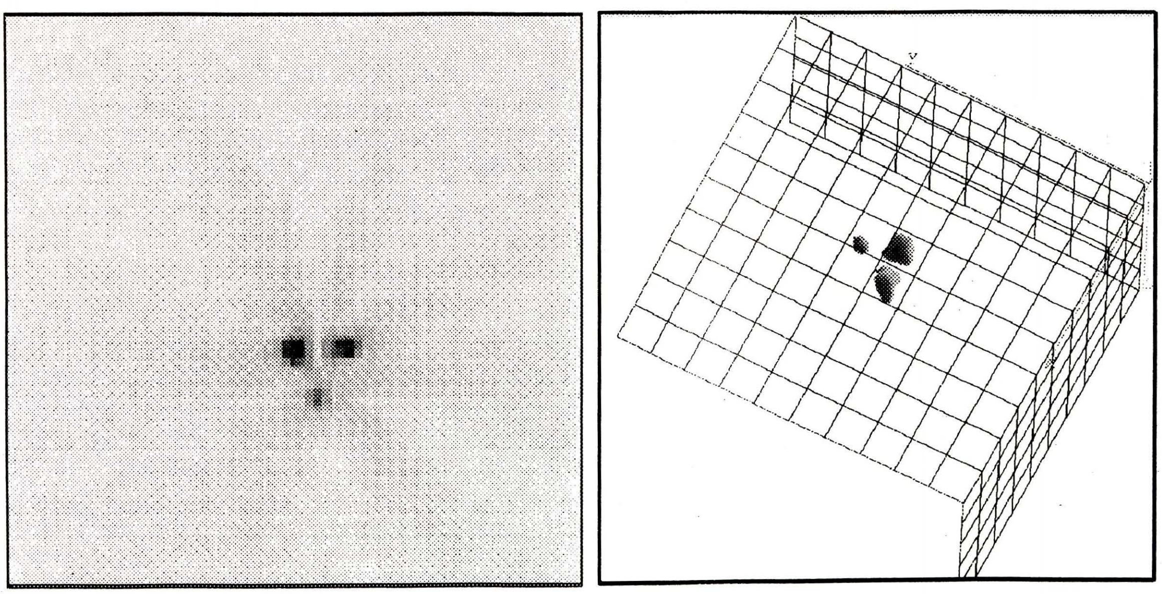

(a) **(b)**

Figure 3. The reconstructed hole pattern. (a) A plan view. (b) A perspective isosurface rendering of the hole data. A geometrical surface is fitted over voxels exceeding a certain threshold intensity value and then shaded according to a user defined lighting direction. Rendering time was approximately 5 s.

Emergent Signal Processing in Acoustic Imaging.*

D.J Battle, R.P Harrison
Australian Nuclear Science and Technology Organisation, PMB 1 Menai NSW 2234.

M. Hedley
Sydney University Department of Electrical Engineering, JO3, Sydney University NSW 2206

A common requirement of most types of acoustic imaging is that of significant computing power (of one form or another). Digital acoustic image reconstruction allows great flexibility at a diminishing cost, however it is an open question as to which reconstruction algorithms are most efficient at extracting image information from sensor data. Conventional methodologies suffer from common deficiencies, due to the fundamental nature of acoustic imaging, which is that of an inverse rather than a direct problem. The mathematical consequences of this are complex and have to be dealt with appropriately if truly satisfactory approaches to image reconstruction are to be developed. This paper will review some broad concepts that may be applicable to acoustic image reconstruction with the advent of inexpensive high speed computers.

Recent emphasis on array technology in achieving real time imaging with sonar and radar has spawned research in diverse areas of estimation theory, information theory and image processing. One arguably obvious principle that has emerged concerns information conservation. In general, if an image is reconstructed from remotely sensed data alone, its information content (measured in bits) is equivalent to that of the original data. No amount of linear enhancement or filtering can increase this latent information content; it can only alter the way it is perceived [1].

Rather than simply alter the presentation of an image, some signal processing methods are, however, able to incorporate *a priori* knowledge about an imaging problem and thus actually add information to an image without breaking the conservation rule. These methods are usually termed parametric, model based or constraint based, and are responsible for many of the so-called hi-resolution and super-resolution algorithms in use and under development.

TRANSFER FUNCTION MODEL FOR IMAGING

The concept of an imaging system as having a linear systems interpretation of a transfer function [2] coexists with its interpretation as an information channel which is often non-linear. A consequence of this is that many constraint based restoration procedures are iterative rather than direct, and thus the benefits of enhanced information content often come at the price of considerable computation. Figure 1. shows a simple schematic for point spread function (psf) formation in terms of a signal input (a delta function), a transfer function and an output psf signal which characterises the transfer function. Matched filtering is usually applicable under this model whereby the output signal is able to be processed by an approximation to the inverse of the transfer function to arrive at an image of the object distribution, assumed to be a collection of individual point scatterers.

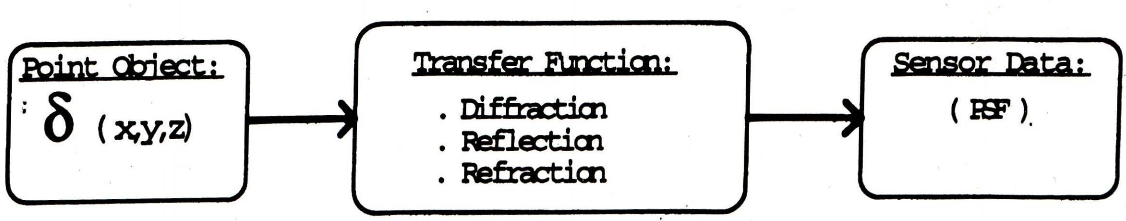

Figure 1. Transfer function model for imaging system

SINGULAR VALUE DECOMPOSITION (SVD)

In practice, the approximation of the inverse to an imaging transfer function is usually ill- conditioned and not straight forward. In the Fourier domain, where inversion of the transfer function implies simply taking its reciprocal, the dilemma arises at small or zero values of the denominator which cause numerical instability. This form of ill-conditioning is also observed if the transfer function is modelled as a matrix such that

$$g = [H]\,f$$

where the g and f are vectors containing stacked rows or columns of image pixels and the matrix H operates on f to form g [3]. SVD of the matrix H is able to be carried out such that H^{-1} is the product of three trivial inverses which can be represented as a weighted sum of outer products between columns of orthogonal matrices U and V such that

$$[H]^{-1} = \sum_{i=1}^{R} 1/w_i\, U_i\, V_i^T$$

where R is the rank of H. This holds except for the case where one or more of the so called singular values w_i are zero or so small as to corrupt the inverse matrix with round-off or noise error. In that case the particular product is poorly represented in the data and can simply be excluded from the sum. An important property of the SVD is that it gives a least squares solution for a given degree of truncation, so inverse point spread functions can be approximated and used to yield image reconstructions optimal in a least squares sense. Other interesting possibilities for SVD are in the area of aberration correction when imaging through inhomogeneous media. Spatially varying point spread functions are able to model such effects, however some practical difficulties need to be overcome, as the size of the SVD calculations scales with N^4, where N^2 is the number of image pixels.

MAXIMUM ENTROPY METHODS (MEM)

Maximum entropy methods have been successfully employed in a variety of remote sensing and image reconstruction/restoration situations [4]. These methods represent a consistent way of handling the effects of missing information such that unknown values of a signal correlation function are assumed to have maximum entropy (randomness) with respect to those values for which better estimates exist [5]. MEM makes intuitive sense when it is considered that entropy is a measure of uncertainty, which is at a maximum in the absence of information. MEM image restoration achieves artefact suppression and super-resolution effects in high SNR circumstance. While the non-linear optimisation procedures required for this are not easily built into image reconstruction algorithms, considerable research is focussed on this area.

Maximum entropy spectral estimation procedures follow the same philosophy to estimate the power spectra of signals from limited sets of discrete observations [6]. These techniques are theoretically capable of superior frequency resolution by virtue of adaptive windowing which limits spectral leakage between frequency bands. MEM spectral estimates hold great promise in acoustic imaging where limited numbers of sensors are employed and resolution specifications are stringent. MEM is conceptually extendable to two dimensions and improved hybrid algorithms are reported which handle uniform background power spectra in addition to point like spectral features [7].

PROJECTION ONTO CONVEX SETS (POCS)

POCS is a another non-linear technique for constraint based introduction of *a priori* information which makes use of successive transformations between vector spaces. At each transformation, deterministic constraints known to be applicable in each space are applied and the iterations proceed until a convergence criterion is satisfied. The transformation spaces most often considered are the spatial domain and the frequency domain and some examples of constraints are:

- image positivity
- a known bound on integrated pixel intensity
- a known region of spatial support
- a known region of spectral support

Numerous other constraints are also applicable [8] and are able to be incorporated in one iterative loop. This type of algorithm is best suited to situations where a considerable amount is known about the object(s) being imaged and can give good results within a small number of iterations.

CONCLUSION

The main paper will seek to demonstrate the performance of various linear and non-linear algorithms and in particular demonstrate the effects of incorporating *a priori* information into reconstructions from limited sensor data.

REFERENCES

1. Klug, A., Crowther, R. A. "Three - Dimensional Image Reconstruction from the Viewpoint of Information Theory", Nature. Vol. 238. August 25, (1972), pp 435-440.

2. Powers, J., Guyomar, D. "A Transfer Function Model for Propagation in Homogeneous Media", Proc. Int. Sym. Pattern Recognition and Acoustical Imaging., California (1987), Vol 768. pp 253-258.

3. Shim, Y. S., Cho, Z. H. "SVD Pseudoinversion Image Reconstruction", IEEE Trans. ASSP. Vol. 29, (1981), No. 4, pp 904-909.

4. Wernecke, S. J., D'Addario, L. R., "Maximum Entropy Image Restoration", IEEE Trans. Comp. Vol. 26, (1977) No. 4, pp 351-364.

5. Jaynes, E. T., "On The Rationale of Maximum-Entropy Methods", Proc. IEEE. Vol. 70, (1982) No. 9, pp 939-952.

6. Laeri, F. "Some Comments on Maximum Entropy Spectral Analysis of Time Series", Comp. in Phys., Nov/Dec (1990), pp 627-636.

7. Sato, T., Yokota, T. "2-D Spectral Estimation Combing Parametric Estimation of Background and Maximum Entropy Estimation", IEEE Trans. ASSP. Vol 32, (1984) No. 2, pp 220-228.

8. Sezan, M. I., Stark, H. "Image Restoration by the Method of Convex Projections: Part 2- Applications and Numerical Results" IEEE Trans. Med Im. Vol 1, (1982) No. 2, pp 95-101.

An Experimental Synthetic Aperture Imaging Sonar

Brett Haywood
Department of Electrical Engineering, University of Sydney

ABSTRACT

The application of synthetic aperture techniques to seabed imaging sonars has been limited. Relatively slow area mapping rates and the instability of an underwater towfish both present major obstacles for a prospective implementation. The experimental sonar described in this paper addresses both of these issues. The mapping rate is improved using a multi-element receive array and frequency diversity in the transmissions. The motion of the towfish is measured in six degrees of freedom using both accelerometers and gyroscopes. Although the sonar described does not operate in real-time, the techniques it presents may allow such an implementation in the future.

INTRODUCTION

Sidescan sonar is the tool predominantly used to image the seabed. Such a sonar images swathes of seabed to each side of a platform as it is towed through the ocean. The image represents the strength of backscattered energy from the seabed for pulses of acoustic energy directed towards it. For such a sonar two important issues of interest are the resolution of the resulting image and the rate at which an area can be mapped. A compromise between the two is necessary as a higher resolution image necessitates a slower mapping rate if the image is not to have gaps in the coverage.

The resolution of a sidescan sonar image can be examined independently in two dimensions, the along-track and the across-track. In the across-track direction the resolution is determined by the length of the acoustic pulse. In the along-track direction the resolution is inversely proportional to the length of the transducer, whilst also proportional to the range from the transducer. For a fixed transducer length the resolution cell becomes increasingly distorted with range, its across-track dimension remains constant while the along-track increases with range.

The synthetic aperture sonar (SAS) operates in a similar manner to the conventional sidescan sonar, imaging swathes to each side as it is towed through the ocean. They differ in that the SAS stores the acoustic returns from successive transmissions. Once the desired aperture has been traversed the stored data is processed and a line in the image produced. In a conventional sidescan sonar each transmission would directly produce a line in the image.

The primary motivation for synthetic aperture processing is the improvement in along-track resolution over a conventional sidescan sonar. By increasing the synthetic array length with range, it is possible to maintain a constant along track resolution. As such, the resolution cell remains of constant dimension, regardless of range. This concept could be applied to a conventional sidescan sonar, though it would require a long array with an extremely large number of elements. Such an array would need to be housed in a large and cumbersome towfish.

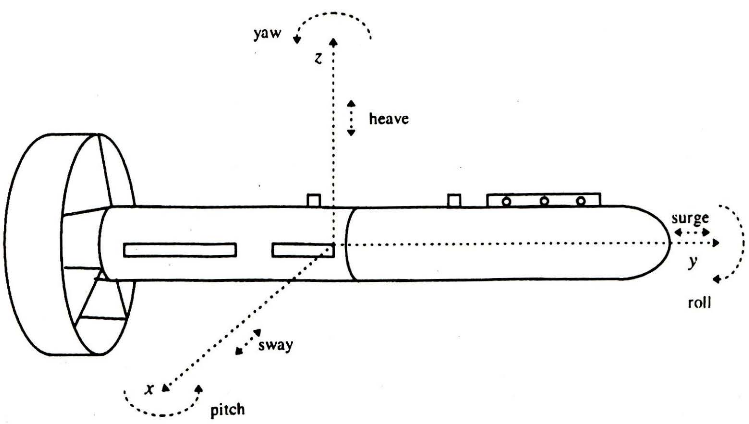

Figure 1. Experimental sonar towfish.

Synthetic aperture radar (SAR) techniques have evolved considerably since the first description of the technique by Carl Wiley in 1951. The same is not so for SAS. The ocean medium presents substantial complexities for the operation of a SAS and these have hindered development to date. A small number of prototypes have been deployed in experiments, though most of these have been operated in controlled environments.

A group at Tokyo Institute of Technology worked in the area from the early 1970ís through to the mid 1980ís (Sato *et al*, 1973). Their efforts were restricted to test tanks where the environment could be easily controlled. The first attempt to image the sea floor was by Loggins and Christoff (Loggins, Christoff and Pipkin, 1982). They towed a transducer along a rail system to remove phase degrading effects due to platform motion. A similar experiment by Gough and Hayes (Gough and Hayes, 1989) in turbulent water also explored the use of broadband signals in the formation of synthetic apertures. The most recent experimentation in the area (Douglas and Lee, 1993) involved the use of a stable towfish and concentrated upon compensating for small deviations to the ideal trajectory by using acoustic data.

The experimental sonar described here will allow an extension to the present state of development of synthetic aperture sonars. A more general approach to motion compensation is attempted with the measurement of platform motion in six degrees of freedom. To supplement this, and allow for relative movement between the ocean and seabed, motion compensation using acoustic data is also to be included in data processing. To improve the area mapping rate an array of receivers is utilised. In addition, a number of independent narrowband transmissions are made and combined in the final image to give an averaged response with frequency.

EXPERIMENTAL SONAR

The sonar developed for this work consists an underwater towfish and a data acquisition and control system. The underwater and surface components are tethered by two cables, providing separate data paths for both motion and acoustic data during experimentation.

The towfish is based upon a commercial side scan sonar, a Klein 595 from Klein Associates Inc. Placed between the original body and the tail is a new section that houses acoustic transducers and electronics for signal conditioning. The original body houses the motion measurement package and associated electronics.

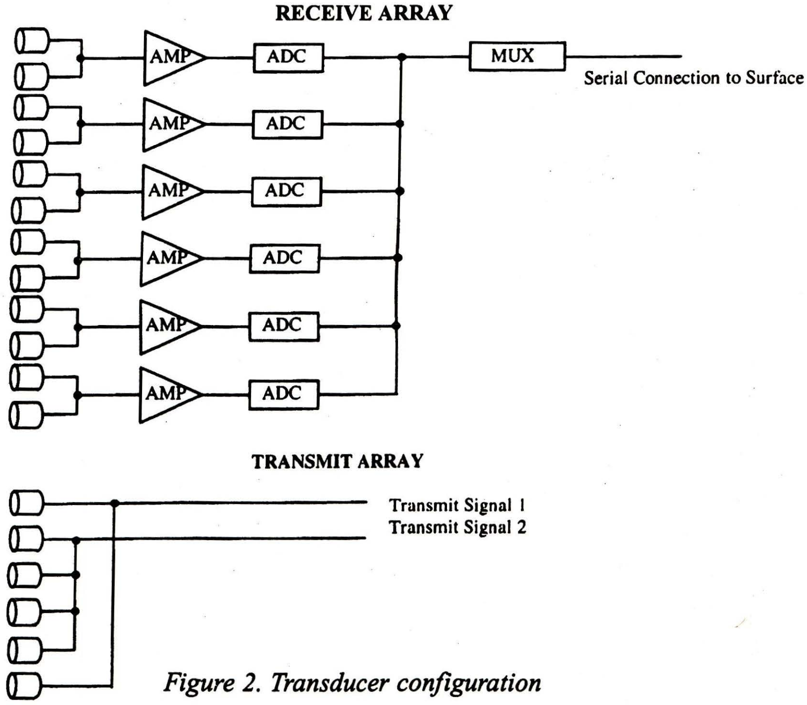

Figure 2. Transducer configuration

Three translations and three rotations are measured by the towfish motion package. The three translations are sway, surge and heave, with corresponding rotations of pitch, roll and yaw. These are shown in Fig. 1. The translations are measured as accelerations with piezo-electric accelerometers, these measurements are differentiated in subsequent processing to obtain a measure of displacement. The measurements represent deviations from steady-state behaviour, so the forward motion of the towfish must be added to the surge measurement. The rotations are measured as angular velocities by the gyroscopes, these are also differentiated to obtain angular displacements. The raw measurements are updated every 0.02s and transmitted to a data acquisition PC on the surface.

The acoustic section of the towfish houses separate transmit and receive arrays as shown in Fig. 2. Individual transducer elements are the same for both arrays, being of a broad bandwidth design and having a flat frequency response from 55kHz to 80kHz. The transmit array is a linear configuration of six of these elements in two sub-arrays. The middle four elements represent one sub-array, while the outer two elements represent the other. This arrangement allows a constant beamwidth over the frequency range by exciting the two sub-arrays with amplitude weighted signals. The receive array consists of twelve elements, also in a linear arrangement. Here six sub-arrays are formed from pairs of elements lying beside each other. Signals on the six receive sub-arrays are amplified and digitised in the canister. This data is multiplexed onto the one serial link and transmitted to the surface recording system.

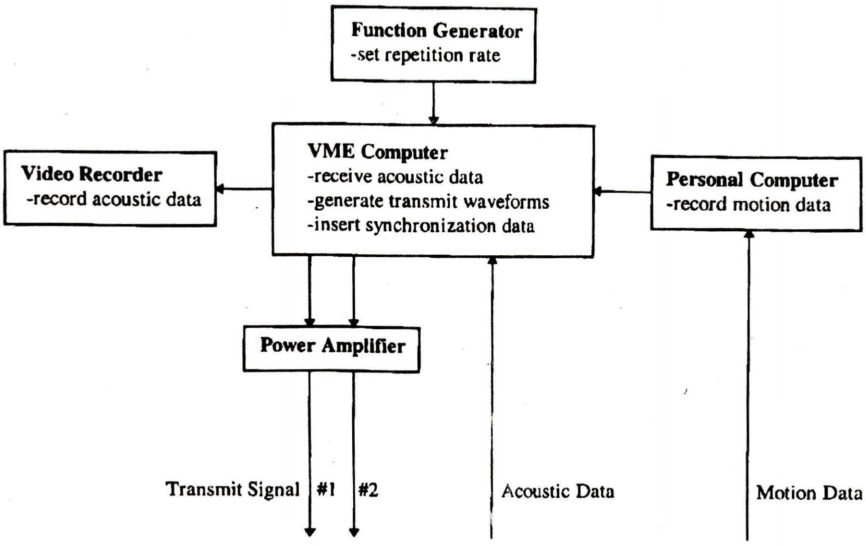

Figure 3. Signal flow in data acquisition system.

The surface recording and control system consists of a VME computer and a high bandwidth video recorder. Specialised circuit cards in the VME computer receive acoustic data from the towfish and continuously present it to the recorder. Multiplexed into the acoustic data are transmit flags and motion synchronization information. These cards also digitally synthesise the two transmit waveforms. The waveforms are amplified before cable connection to the transmit arrays. The transmit pulse repetition frequency is accurately set with a function generator. A representation of this is given in Fig. 3.

Subsequent to an experiment the data is transcribed in the laboratory for later processing. Acoustic data is reproduced through the VME computer onto a workstation. Motion data from the PC is also transferred to the workstation and merged with the acoustic data.

CONCLUSION

A seabed imaging sonar utilising synthetic aperture techniques allows performance improvements over the conventional sidescan sonars currently in use. These improvements are at a cost of substantial processing complexity. The design of an experimental synthetic aperture imaging sonar has been discussed. When completely developed it will allow the investigation of techniques to reduce the processing complexity and perhaps make a practical implementation more possible in the future.

REFERENCES

Douglas, B. L., Lee, H. (1993) "Synthetic Aperture Sonar Imaging with a Multiple Element Receiver Array," *Proc. ICASSP 93,* Vol. 5, pp. 445-448.

Gough, P. T., Hayes, M. P. (1989) "Test Results Using a Prototype Synthetic Aperture Sonar," *J. Acoust. Soc. Am.,* Vol. 86, No. 6, Dec., pp. 2328-2333.

Loggins, C. D., Christoff, J. T. and Pipkin, E. L. (1982) "Results from Rail Synthetic Aperture Experiments," *J. Acoust. Soc. Am .* Suppl. 1, Vol. 1, No. 71.

Sato, T., Mitsuhiro, U. and Fukuda, S., (1973) "Synthetic Aperture Sonar," *J. Acoust. Soc. Am.,* Vol. 54, No. 3, Aug., pp 799-802

ACKNOWLEDGMENTS

This work is supported by the Aeronautical and Maritime Research Laboratory, Defence Science and Technology Organization, Australia.

Use of a Random Array for High-Resolution Underwater Acoustic Imaging

David G. Blair
Maritime Operations Division, Aeronautical and Maritime Research Laboratory,
DSTO, PO Box 44, Pyrmont, N.S.W. 2009

Ian Bedwell
GEC-Marconi Systems, Faraday Park, Railway Rd, Meadowbank, N.S.W. 2114

S. D. Anstee
Maritime Operations Division, Aeronautical and Maritime Research Laboratory,
DSTO, PO Box 44, Pyrmont, N.S.W. 2009

and

Ultrasonics Laboratory, CSIRO Division of Radiophysics,
126 Greville St., Chatswood, N.S.W. 2067

Random arrays (Lo 1964, Steinberg 1976) have been utilized for twenty years in microwave systems, notably the radio camera and related synthetic apeture devices (Steinberg 1983, Steinberg and Subbaram 1991). However they have rarely been used in acoustic systems. Yet these sparse arrays have desirable properties; in particular, the resolution achieved is undiminished from that of a filled array of the same apeture. The main drawback is a raised sidelobe level at angular displacements beyond the first few sidelobes. In the continuous-wave case, the average intensity in these distant sidelobes is independent of angular displacement and is equal to $1/N$ (relative to the peak intensity), where N is the number of elements. But, for arrays whose apeture is sufficiently large compared to the wavelength, this level can be made quite low while preserving sparseness. Overall, random arrays are believed to be very cost-effective for high-resolution imaging, especially for two-dimensional (as opposed to one-dimensional) arrays.

We have been engaged with others on preliminary design work for an underwater acoustic camera using a random array. The proposed camera differs from the radio cameras commonly used in several respects. First, sufficient data is to be collected to form a three- rather than a two-dimensional image. (The image is to have of order 1000 x 1000 x1000 resolution cells or volume pixels, with the target body essentially filling the whole image.) Secondly, the bandwidth of the signal is to be comparable with the central frequency, rather than much smaller. Third, the image is to be of an angular field of order 90°x90°, rather than a much smaller angle.

There exists a fair-sized body of literature on random arrays developed for microwaves but applicable also to acoustic waves, including as topics self-calibration techniques and deconvolution technqiues for image enhancement. However, differences such as the three noted above may lead to modification in the methods and conclusions, particularly in regard to the peak distant sidelobe level and the degree of optimality of the random array comapred to deterministic arrays.

We have performed computer emulations of image-forming for array systems appropriate to the above design, wtih emphasis on the image of a point target. Included are near-field focussing using exact path lengths, and also the option of obtaining good range resolution, through either a short toneburst or a cross-correlated chirped signal. It is found that the performance of the random array is undiminshed by these includsions; in fact, both the average level and the peak level of the distant sidelobes are in general improved. Also theperformance of partially random arrays, constructed out of identical subarrays for ease of manufacture, has been investigated.

The development of a random array tile for acoustic imaging is well under way. The concept demonstrator to be produced consists of a "tile random array", a random linear array, a transmitting transducer, and conditioning electronics contained in a remote water/pressure-proof housing. The data is transferred via a fibre optic cable to a control and display computer. Each random array tile is 50mm x 50mm and contains 32 randomly placed receivers with integrated electronics. The elements are aboutone wavelength in diametre, which should give a 60° -3dB beamwidth. To control the beamforming the individual elements have to be within 50μm of true position. This technology is scalable to a full-sized 50cm diameter array, i.e. 10 tiles across a diameter.

Modelling will be presented to show the expected behaviour of the four tiles for both focussing and depth of focus. By introducing random sensitivites and phase errors to individual elements, the robustness of the design can be demonstrated.

REFERENCES

Lo, Y.T. (1964) A mathematical theory of antenna arrays with randomly spaced elements. *IRE Trans. Antennas Propag.,* **AP-12**, PP. 257-268.

Steinberg, B.D. (1976) *Principles of aperture and array system design – including random and adaptive arrays.* New York: John Wiley.

Steinberg, B.D. (1983) *Microwave imaging with large antenna arrays: radio camera principles and techniques.* New York: John Wiley.

Steinberg, B.D. and Subbaram, H.M. (1991) *Microwave imaging technqiues.* New York: John Wiley.

Constant False Alarm Rate Sonar

Andrew Madry
Thomson Sintra Pacific, Talavera Road, North Ryde NSW 2113

1. INTRODUCTION

The detection range of a sonar system is dependent on a number of environmental and sonar processing factors, together with the detection criteria that is applied. Generally the detection criterion is specified in terms of a probability of false alarm, P_{fa}, and probability of detection, P_d. Sonar performance modelling uses the signal to noise ratio required at the receiver for detection to determine detection range. It is often assumed that the noise distribution is Gaussian which can cause detection range calculations to be inaccurate if this assumption is wrong. A poor choice of noise distribution generally can lead to the detection process not being optimal. The purpose of this paper is to review the impact of some noise distributions, in comparison with the Gaussian, on the detection performance of a sonar system.

It sonar design it is often assumed that in a volumetric coverage the noise from cell to cell is both independent and identically distributed. The noise may be independent from cell to cell but the identically distributed assumption is likely to be false. This is due to the different types of noise contributing to the total, e.g. bottom or surface scattering, ambient noise and electronic noise.

When a fixed detection threshold is set, based on a particular noise distribution assumption, the false alarm rate depends on both the noise level and type of distribution. This leads to the concept of constant false alarm rate (CFAR) processing as is employed in radar systems. In an active sonar system it is relatively simple, for stationary targets, to implement constant probability of detection (CPD) processing in the detection algorithms by using multiple pings. This paper discusses the concepts of CFAR-CPD processing in a sonar system.

2. NOISE MODELS

A recent paper [1] has reported measurements of surface and bottom reverberation, surface and bottom forward scattering, and direct path propagation and demonstrated the complexity of the shallow water acoustic environment. Measurements were made using CW pulses at various frequencies and the amplitude of the signal envelope measured. It was found that the direct path signals followed Gaussian statistics and the bottom path signals were Rayleigh distributed.

Shallow water environments are often dominated by biological noise. In reference [2] the results of a study of ambient noise at frequencies up to 200 kHz have been reported. It was found that in temperate and tropical waters of depths less than about 60m the ambient noise is characterised by sharp transient sounds of snapping shrimps.

It is often difficult to find an accurate statistical description of non-stationary transient type noise. The appropriate probability density functions (pdf's) have a heavier tail as compared to that of the Gaussian pdf. The Laplace pdf is often used to characterise an impulsive noise type distribution [3].

3. CFAR PROCESSING

The sonar detection processing can use an algorithm to estimate the noise energy in the test cell and then adjust the detection threshold to reflect changes in this energy at different test cell positions. This technique, called CFAR processing, is commonly used in radar systems to improve performance in the presence of clutter. The threshold algorithms use detection cells near the target to estimate the background noise level. The threshold is then set to ensure the desired P_{fa}.

In a three dimensional sonar imaging system the test cell may be located in the water column or it may contain the sea surface or sea bottom. The probability distribution of noise in these different regions is likely to be different, as discussed above. Unless appropriate measures are taken the P_{fa} will vary across the cells in the sonar image. In addition to this all test cells may be influenced by locally generated noise such as the noise from snapping shrimp.

Receiver Operating Characteristic (ROC) curves have been calculated, using as an example a P_{fa} = 10-10. These are shown in figure 1 for noise with Gaussian, Rayleigh and Laplace pdf's. P_d is plotted as a function of the signal to noise ratio. Assuming that a P_d of 0.9 is required the appropriate threshold settings are shown in table 1.

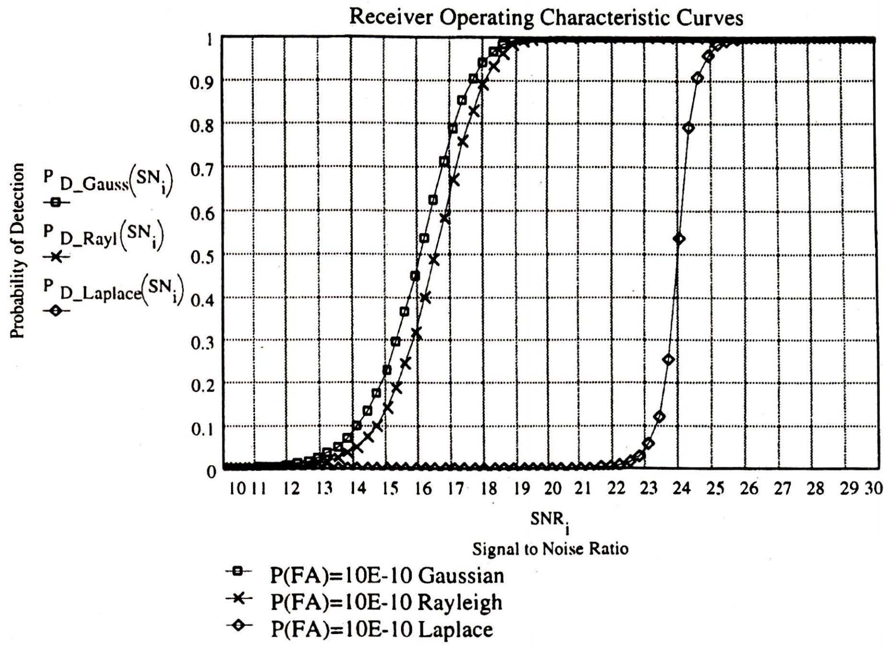

Figure 1. ROC Curves for $P_{fa} = 10^{-10}$ for Gaussian, Rayleigh-Rice and Laplace distributions.

When the detection threshold is set, the system achieves a certain P_{fa} and theoretical detection range. This assumes a particular probability distribution which may be chosen to be Gaussian. If the noise in fact follows another distribution, such as the Rayleigh, with the same noise power, either a higher P_{fa} or lower P_d occurs for the given detection threshold.

	Noise Distribution		
	Gaussian	Rayleigh	Laplace
Signal to Noise Ratio (dB)	17.7	18.1	24.6

Table 1. Required signal to noise ratio for $P_{fa}=10^{-10}$ to ensure Pd=0.9 for various noise probability density functions.

For a required P_d and a fixed detection threshold the difference between the Gaussian and Rayleigh distributions can be shown to change the P_{fa} by an order of magnitude. This can be the difference between the false alarms being acceptable and annoying. The effect of an impulsive type distribution such as the Laplace can be quite dramatic, as seen from table 1. Either detection range must be significantly reduced by setting a higher detection threshold or a much higher false alarm rate incurred. In practice the noise pdf may not be accurately described by the Laplace pdf due to considerations of the Central Limit Theorem discussed in reference [4]. This will be investigated further.

4. CPD PROCESSING

By using the CFAR technique the detection threshold is set appropriate for the noise pdf. However, by setting a higher detection threshold, to achieve constant P_{fa}, then for the same P_d, a lower detection range results. To achieve the same range a lower P_d would have to be suffered. The desired P_d can be recovered in an active sonar system by requiring more pings to confirm the presence of a target. Detection using multiple pings effectively reduces the detection threshold, in theory, by $5\log n$, for non-coherent detection, where n is the number of pings [4].

5. SUMMARY

Sonar performance is improved by characterising the type of noise distribution in the various cells of a sonar image. A technique whereby noise distributions are characterised adaptively has been developed to implement this and will be discussed. This is called a CFAR-CPD processing technique. Detection threshold levels may also be set appropriate to the level of threat as required by a sonar operator.

6. REFERENCES

[1] Wilson, M. A., Farwell, R. W. and Stanic, S. Statistics of Shallow Water, High Frequency Acoustic Scattering and Propagation. Oceans 93 Conference Proceedings.

[2] Cato, D. H. and Bell, M. J. Ultrasonic Ambient Noise in Australian Shallow Waters at Frequencies up to 200kHz. MRL-TR-91-23.

[3] Thompson, M. W. and Chang, H. S. Coherent Detection in Laplace Noise. IEEE Trans. on Aerospace and Electronic Systems. 30(2) 1994, 452-461.

[4] Urick, R. J. Principles of underwater Sound. McGraw Hill 1983.

Coherence Measurements for Imaging Evaluation at 4MHZ

Yue Li and David E. Robinson,
Ultrasonics Laboratory, Div. of Radiophysics, CSIRO, 126 Greville St, Chatswood, NSW 2067

Michael Bell,
Maritime Operations Division, Aeronautical and Maritime Research Laboratory,
DSTO, PO Box 44, Pyrmont, NSW 2009

Ian G. Jones,
GEC-Marconi Systems, Faraday Park, Railway Rd, Meadowbank, NSW 2114

In order to assess the ability to perform three-dimensional pulse-echo imaging at high resolution with ultrasound in seawater, measurements were made of observed coherence of 4 MHz pulses transmitted over a path of 1 m and received across an aperture of .5 m. The measurements were carried out at the MOD, DSTO wharf at Pyrmont on Sydney Harbour.

The proposed operational system will operate at 3.5 MHz with a bandwidth of at least 1 MHz over a range of 4 m with an acoustic receive aperture of .5m. Thus the system will be broadband, operating in the nearfield in pulse-echo mode. The medium aberrations which could cause degradation of the image data are:

- Refraction by local macroscopic variations in sound speed causing non-alignment in time of the received echoes (after correction for focus or geometric path length).
- Scattering from microstructural variations in sound-speed or density, or particulate matter causing changes in pulse shape or phase variations in longer pulses.

EXPERIMENTAL METHOD

The signal acquisition equipment consisted of a signal generator, power amplifier, and digitising oscilloscope controlled via a GPIB interface from a Sun SPARC 2 workstation running the TWODIMSY (proprietary to Ultrasonics Laboratory) signal and image processing software package.

The wet-end consisted of a wide-angle transmitter and two linear arrays for reception mounted on a steel frame. The receive aperture was 500 mm and the acoustic path length approximately 1 m. The transmitter was a spherical dome of 80mm radius of curvature and 50mm diameter. There were eight receive elements, four per array. The usable bandwidth was 3.5 to 4.5 MHz. Connection to the surface was by 15m of coaxial cable for each transducer element.

Several acquisitions were made at each depth, with both the transmitter axis and the receive line aperture horizontal. The process was repeated for another run with the transmitter axis horizontal and the linear aperture vertical.

Two signals were used for the measurements. A short pulse similar to that used in medical ultrasonic imaging, was used to assess the short-term coherence. A tone burst allowed conventional cross-correlation coherence measurements to be performed to establish uniformity of propagation during the pulse.

SIGNAL PROCESSING

For the short pulses, the time increment in the sampling of the pulse signals was 4 ns, corresponding to 6° of phase shift of the 4 MHz signal. As the path length to the individual elements was not equal, a calibrated time-shift was applied to the results, and the error was the time shift referred to the array centre. The range of variation of corrected relative arrival times gives a measure of the imaging ability of the system. Experience in the medical field suggests that random errors of within 30° (or 5 sample intervals) will have no noticeable effect on the main beam, but may raise the noise floor of the system.

The peak value of the normalised cross-correlation function between consecutive pulses received from the same transducer element for consecutive pings, or between elements for the same ping is a measure of the "fidelity" of the received pulses. The cross-correlation coefficient between consecutive pings for the same element should be close to unity. For inter-element cross-correlations, the difference between impulse responses causes a slightly lower value (in the range .9 to 1) to be obtained. The important parameter in this case is the variance of the coefficient due to fluctuations in the propagation path.

For the long tone bursts, the time increment in the sampling of the pulse signals was 40 ns, corresponding to 60° of phase shift of the 4 MHz signal.The effect of propagation errors on a long tone burst are fluctuations in the phase of the signal. This can be measured in two ways. The first is to assess the positions of the zero-crossings during the pulse against their "correct" positions and plot this error as a function of time during the pulse. For no distortion, the "error" value should remain within the range of zero to one sampling interval. The second is to take the first part of the tone burst (say the first one tenth) and cross-correlate it with the whole burst. Since the cross-correlation process is sensitive to phase and frequency variations, variations in the cross-correlation amplitude will reveal phase irregularities. The resulting cross-correlation characteristic should show a sine-wave of signal frequency with an envelope with a triangular ramp-up, flat top equal to unity, and a triangular ramp-down.

RESULTS

The arrival-time coherence at varying depths with the receive array vertical gave coherence errors less than 5 sample intervals or 30°, with the maximum RMS value for any element being about 10°, except between 1m and 2 m in depth. The range from 1 to 2 m depth coincides with the observed position of a 2 ms^{-1} change in sound speed in the water column. In this depth range, the coherence errors were consistently anti-symmetrical, and with the linear trend removed, the residual RMS error was less than 90°. The effect of the linear trend would be to shift the entire image by an angle less than 1°. With the linear trend removed, the remaining residual had a large symmetrical or focussing component. The amount of the "error" was equivalent to moving the position of the beam focus by less than 7 mm in depth at 1 m. This is within the focal zone which would normally be used for image-forming in medical equipment using fixed focal zones. The effect of the remaining residual error after the linear (rotation) and quadratic (focus) aberrations is to degrade the image by broadening the main beam and increasing clutter. As there are no data from intermediate positions on the receive aperture it is not possible to determine the extent of this residual error, although it appears to be within the 30° limit.

With the receive array horizontal, all errors were less than 30° in phase. The RMS error for any element was 10°.

For the short pulse signals, the cross-correlation coefficients for single elements were always in the range from .99 to 1with a variance below .001. For between-elem nt cross-correlation coefficients, the variance was below .01 in all cases. For the long tone pulses, neither the zero-crossing nor the cross-correlation analysis revealed any distortion in phase.received. The zero-crossing error was always either 0 or -1 (indicating the digitisation error, and there was no variation in the envelope of the cross-correlation. This indicates that negligible multipath due to micro-structure forward scatter was evident.

CONCLUSION

1. No evidence of forward scatter leading to multi-path propagation and pulse spreading has been observed. This is so for short pulses and long tone bursts.

2. No significant incoherence due to refraction in fine-scale microstructure has been observed. The arrival-times of pulses in the horizontal aperture are within 30° in phase.

3. A sharp change in vertical sound-speed profile (of 2ms^{-1} over 1m) did not affect the ability to image in the horizontal plane, even when at the discontinuity.

4. The sharp change in vertical sound-speed profile did affect the ability to image in the vertical plane. The linear gradient in arrival time would causes only an apparent shift of the image in the vertical direction (of about 1°). In many cases, the remaining shape of the arrival time function was equivalent to a focussing action. This will have only a slight de-focussing effect if present right across the aperture.

5. In regions of sharp vertical sound-speed profile, good-quality imaging can be obtained by ensuring that the aperture is not intersected by the discontinuity, and an inclined "look direction" is used from slightly above or below to image the target.

The conclusion is that in the conditions existing at the time of the measurements, signal incoherence due to inhomogeneity in the water path would not substantially affect ultrasonic high-resolution 3-D imaging at 4 MHz.

Application of Acoustic Coupled Normal Mode Modeling to Sonar Problems in Shallow Water

Warren W. Denner
Ching-Sang Chiu
and
James Miller
EOS Research Associates, Monterey, California

Coupled normal-mode propagation models may be best for assessing shallow water low frequency sonar system performance. It is possible to handle range dependent environments which are typically encountered in the littoral ocean. If thenumber of propagating modes of interest is limited the codes can be made to run efficiently on personal computers and work stations.

EOS Research Associates has developed a very powerful shallow-water modeling system which can readily be applied to a variety of Sonar problems. It is a broad-band coupled normal mode acoustic modeling and analysis system (BBCM-AMAS). The EOS-AMAS is a highly portable modeling system which runs in a variety of computer environments because it was developed for use in the popular MATLAB software. MATLAB is a user-friendly, high-performance, interactive analysis and visualization software, and is available for most PC's and UNIX workstations. Such availability makes the EOS-AMAS essentially machine-independent. We have coupled the model with a variety of environmental data bases to simulate sonar performance in a number of shallow water regions.

EOS-AMAS is capable of modeling the performance of sonar systems with mono-static or bi-static source and receiver-array geometries, and target directivity in a realistic ocean environment where sound speed, bathymetry and geoacoustic properties vary significantly in both the vertical and horizontal directions. Because EOS-AMAS uses fully-coupled mode propagation physics, it is highly efficient and accurate for the simulation of the performance of low-frequency, shallow-water active systems. In particular, it is extremely effective for studying system concepts that exploit the modal structure of a transmitted sonar signal. There are three types of input to EOS-AMAS:

1.) Sonar system specifications.
2.) Target characteristics.
3.) Environmental acoustic parameters.

The equipment input parameters include source and receiver array locations and configurations, shading and phasing of the arrays (or alternatively the beam patterns), the transmitted source signal in either the time or frequency domain, and signal processing gain.

Submarines and false targets are dealt with using two methods. One method treats a target as a simple omni-directional or directional point source with target strength and directivity specified. A more sophisticated technique involving the use of Helmholtz-Kirchoff integral is applied in conjunction with local plane wave decomposition of modes when target surface geometry, pressure and normal velocity as a function of the incident angle of a unit-amplitude plane wave are specified. The target model is completed with the addition of the target position, speed and heading.

The environmental input consists of sound speed and density profiles, sea-water and, sediment attenuation, and volume and boundary scattering losses. The input profiles, extending from the sea surface through the sediment to the rigid basement, and can be range- and azimuth-dependent, describing the ocean fields along different radials from the source site. The specification of variable bathymetry and multiple sediment layers are implicit. They are modeled by abrupt vertical changes in the sound speed and density in the input profiles. Other input environmental parameters include ambient noise level, noise spatial and temporal coherence, and boundary and volume scattering coefficients. Ambient sound and reverberation due to scatters constitute the background noise that limits the performance of a sonar system. It is not difficult to write codes in MATLAB that interface

EOS-AMAS to existing global or regional environmental data bases (e. g. BLUG, GEDM, etc.). The key is to arrange the extracted information/data in the input format required by EOS-AMAS.

The output of EOS-AMAS consists of simulated time-domain and frequency-domain sound pressure signals, modal arrival structure at selected positions, and plane wave or mode-beamformed output of the receiver array. A variety of derived sonarparameters and measures of system performance is also provided. The derived sonar parameters include transmission loss, reverberation level, Doppler gain, transmitting and receiving directivity indices, etc. System performance measures include signal excess, detection range, and probability of detection. All EOS-AMAS output can be visualized and analyzed interactively.

The principal component of EOS-AMAS is its unique propagation model which computes the propagation of sound from the source to the receiver or from the source to the target and then from the target to the receiver. It provides for a framework to relate the output at the receiver to selected environmental, source, receiver and target models.

In this paper we will present the physics in the EOS-AMAS propagation model, and show some example results of simulated systems performance in some shallow water areas.

Estimation of High Frequency Acoustic Scattering and Absorption in the Ocean

R. A. Thuraisingham
Maritime Operations Division, DSTO, Pyrmont, NSW 2009

Scattering and absorption of high frequency sound can result from several sources. These include suspended particles, air bubbles, changes in temperature and current, sea surface or bottom. This paper focuses it attention on acoustic scattering and absorption from suspended sand particles, air bubbles and temperature changes in the ocean. It looks at mechanisms that cause attenuation from suspended particles and provides estimates of attenuation and backscattering using suitable theoretical models at MHz frequencies and experimentally measured particle distributions. Attenuation, backscattering and dispersion of sound speed from wind generated air bubbles are next discussed and theoretical estimates given at MHz frequencies. In the case of temperature variations, intensity and phase changes from the mean temperature gradient, attenuation and fluctuations from the random temperature changes and the phase structure function are discussed.

1. SUSPENDED SAND PARTICLES

1.a Attenuation due to scattering

Studies on models to estimate scattering of sound due to sand particles showed the Rayleigh approximation to particles having radius larger than 44 μm and at frequencies above 3 MHz can lead to significant errors. The result from the non rigid model is always less than the rigid model by a factor of 2 or 3, while the inclusion of shear waves has an effect for large particles which have radius greater than 150 μm. Since large particles are present near the sea bottom, the most suitable model would be to consider the suspended material to be non rigid spheres with the inclusion of shear waves. The theory of Faran [1951] and Hickling [1962] is used.

1.b Viscous attenuation

When sound passes through a medium particles will oscillate with the fluid. If the medium is viscous then there is loss of acoustic energy due to drag. The theory of Lamb [1945] is used to estimate the viscous attenuation. The model of Ahuja [1970] also give reasonable results.

1.c Thermal attenuation

Sound attenuation due to thermal conduction is examined using the theory of Epstein and Carhart [1953].

2. AIR BUBBLES

2.1 Attenuation and backscattering

Air bubbles are one of the common acoustic scatterers and are present mostly near the surface within a depth of several metres. The bubble sizes vary from a few microns to a few hundred microns. Their number density range from a few per litre to hundreds per cubic centimetre. Although a single bubble may have little effect on transmission of sound, the cumulative effect of many can be pronounced. Scattering and absorption cross sections are obtained from bubble theory [Medwin, 1977] for ka very much less than one, and from the non rigid sphere approximation for intermediate and large ka, where k is the wavenumber and a is the radius of the particle. Bubble theory is valid only for ka less than one and at MHz frequencies this condition is not satisfied. The bubble population model of Hall [1989] is then used to obtain estimates of attenuation and back scattering of wind generated air bubbles at MHz frequencies.

2.2 Dispersion of sound speed

In the presence of air bubbles the speed of sound becomes a function of frequency. The theory of Wildt [1946, p473] and Medwin [1977] is used to estimate the sound speed dispersion. For ka comparable or greater than one, the change in sound speed is estimated using the theory of Liu [1991].

3. TEMPERATURE VARIATIONS

3.1 Intensity and Phase change from mean temperature gradient

Analytical expressions derived from deterministic ray theory is used to estimate intensity and phase changes due to refraction [Thuraisingham, 1994].

3.2 Attenuation, intensity and phase fluctuations from random temperature variations

Expressions based on the wave theory are used to estimate attenuation, intensity and phase fluctuations both for an isotropic and anisotropic correlation function. These expressions are valid for all ranges and frequencies [Thuraisingham, 1994].

3.3 Phase Structure function

The phase structure function gives the variance of the phase difference between two points caused by sound speed fluctuations. Expressions based on the stochastic ray model are used to estimate the phase structure function at MHz frequencies and short range (1-5 metres) [Thuraisingham, 1994].

4. REFERENCES

1. Ahuja, A. A., 1972 *Effect of particle viscosity on propagation of sound in suspensions and emulsions,* J. Acous. Soc. Am., 51, 182-191.

2. Epstein, S. P., and Carhart, R. R., 1953 *The absorption of sound in suspensions and emulsions. 1. Water fog in air,* J. Acous. Soc. Am., 25, 553-565.

3. Faran, J. J., 1951 *Sound Scattering by solid cylinders and spheres,* J. Acous. Soc. Am., 23, 405-418.

4. Hall, M. V., 1989 *A comprehensive model of wind-generated bubbles in the ocean and predictions of the effects on sound propagation at frequencies up to 40 kHz,* J. Acous. Soc. Am., 51, 1103-1117.

5. Hickling, R., 1962 *Analysis of echoes from a solid elastic sphere in water,* J. Acous. Soc. Am., 34, 1582-1592.

6. Lamb, H., 1945 *Hydrodynamics,* Dover publications, New York, 361-363.

7. Liu, K. C., 1991 *Wave scattering in discrete random media by the discontiuous stochastic field, 1: Basic method and general theory,* J. Sound and Vibration 147, 301-311.

8. Medwin, H., 1977 *Counting bubbles acoustically: a review,* Ultrasonics, Jan, 7-13.

9. Thuraisingham, R. A., 1994 *Models to estimate high frequency acoustic scattering due to thermal fine- and micro-structure of the ocean,* AMRL research report (in press).

10. Wildt, R., 1946 *Acoustic theory of bubbles,* US Navy Physics of Sound in the Sea, NDRC Summary Technical Report Div. 68 , Washington.

High Resolution Acoustic Seafloor Classification System for Mine Countermeasures Operations

Douglas N. Lambert, Donald J. Walter, David C. Young, Michael D. Richardson
Naval Research Laboratory, Stennis Space Center, MS 39529 USA

and

John C. Cranford
Neptune Sciences, Inc., Slidell, LA 70458 USA

ABSTRACT

A need exists in both the civilian and military communities for an automated seafloor classification system that can remotely and accurately estimate and map sediment properties for mine warfare/mine countermeasures, for a number of seafloor engineering applications, and for input to acoustic propagation prediction models. Over the past several years, the Naval Research Laboratory (NRL) has been developing a normal incidence, narrow beam width, and high resolution subbottom profiling system that has the capability to accurately predict, in near real-time, acoustic impedance and relate it to sediment type and a number of selected geotechnical properties of the upper several meters of the seafloor while in an underway survey mode (Lambert, 1988). This system is designated the Acoustic Seafloor Classification System (ASCS) and has evolved from the Echo Strength Measuring System (EMS) developed in the early 1980's by Honeywell ELAC of Kiel, Germany. A detailed description of the ASCS can be found in Lambert and Fiedler (1991). A recent development, designated the High Resolution Acoustic Seafloor Classification System (HR ASCS) has completely replaced the electronics portion of the original ASCS with a new hardware system having 16 bit resolution and a dynamic range in excess of 92 dB. An overview of this development can be found in Lambert, et al, (1993).

The HR ASCS consists of integrated hardware and software systems which provide the capability to accurately and remotely predict seafloor sediment properties in near real time. Using specialized software modules, it can a really predict mine impact burial potential during post-processing of the data. In order to understand how the system operates, it is necessary to describe the hardware and software components which comprise the HR ASCS.

HR ASCS HARDWARE

The HR ASCS is a new development by NRL and completely replaces the original EMS hardware with much greater resolution and capability. It is primarily used as a high frequency, short pulse length and narrow beam width subbottom profiling system. However, it has the capability to operate at virtually any frequency between 1 and 1000 kHz and with pulse lengths between a single wavelength and 16 ms. It also has the capability to output any wave form that can be digitized or it can output two frequency pulses simultaneously which allow it to also operate in parametric and FM chirp modes. The HR ASCS can be used to transmit and receive through virtually any transducer, such as the U.S. Navy's standard UQN-4 hull mounted fathometer.

The HR ASCS can be described as a high resolution seismic system because it is typically operated using a short pulse length (0.1 to 0.3 ms) and narrow beam width (6° and 12°) at 30 and 15 kHz, respectively. Bandwidth of the system with a 0.1 ms pulse length is 10 kHz. Minimum resolution at this pulse length is approximately 7.5 cm. The HR ASCS is a completely calibrated 16 bit data acquisition, data storage, and data processing system with a real dynamic range of > 92 dB. The outgoing and return pulse is digitized and stored at a rate of up to 125 kHz. A seismic record is displayed in 16 colors on a scrolling waterfall type computer monitor display (Fig.1). The colors represent an adjustable range of dB per color (typically 5 to 6 dB/color) of return signal intensity. The system is completely contained (except the transducer and a small power amplifier) in an inexpensive off-the-shelf 486 computer. Nearly all functions of the system frequency(ies), pulse length, power level, gains, display parameters, digitizing rate, etc,) are controlled or can be adjusted in real time from the keyboard. Integrated with the HR ASCS seismic system is Global Positioning System (GPS) navigation for real time mapping of sediment properties along survey tracklines.

In all environments, the HR ASCS produces a high resolution display of the energy returned (echo strength) from reflecting horizons in the upper 10 - 15 meters of sediment. The narrow beam width provides excellent horizontal resolution in the sense that the sediment being sampled is confined to a narrow vertical section. The narrow beam width also minimizes unwanted volume scattering returns. Because the HR ASCS is a high frequency system, it is well suited for delineating homogeneous sediments which contain discrete volume scatterers (i.e., gas bubbles as seen in Fig. 1). The high frequency, narrow beam width and low power requirements of the HR ASCS also make it an excellent candidate for use on Unmanned Underwater Vehicles (UUV) and Autonomous Underwater Vehicles (AUV) during routine environmental surveys and during clandestine operations. Because all of the raw return signal is digitized and stored, the data can be easily replayed and reprocessed for specific purposes.

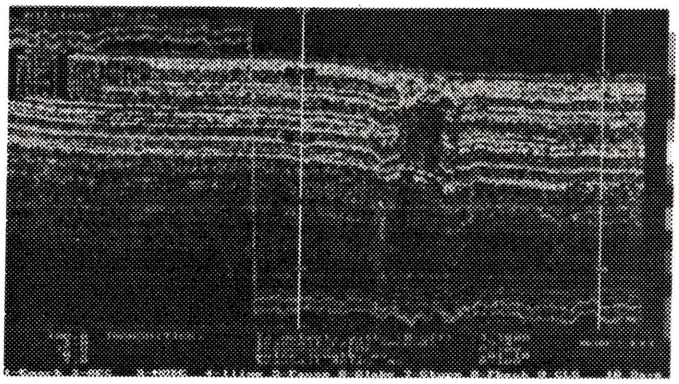

Figure 1. Example of a 15 kHz ASCS seismic profile from the Gulf of Mexico southeast of Ship Island. This data was collected using a 0.2 ms pulse length, 100 watt power level, and a 12° beam width. The distance between the solid white horizontal lines is five meters and one meter between the dotted white lines. Horizontal distance is approximately 2,000 m. Colors displayed are in steps of 5 dB of signal intensity (see color bar at right). Hot colors represent high reflectivity, cool colors low intensity. In this picture, the yellow and red layers are thought to be minor concentrations of biogenic gas, probably methane, lying along horizontal bedding planes in the sediment column. This sediment is a soft silty clay fairly rich in organic matter and cores previously taken in the area do not indicate the presence of sand lenses that would be reflective enough to produce the strong layered returns seen here. The high frequency and narrow beam of the acoustic signal provide for the excellent definition of the gas contained within the sediment. Note the large area in the right center of the record displaying very low reflectivity as indicated by the blue to brown coloration. This area appears to have been "homogenized", possibly due to the upward migration of gas bubbles. This structure is not a gas "wipe-out" because continuous layering is visible beneath it.

HR ASCS SEDIMENT CLASSIFICATION SOFTWARE

The HR ASCS sediment prediction software has the capability to remotely and accurately estimate and map sediment properties, with depth in the upper several meters of the seafloor, for a number of seafloor engineering applications and as input into acoustic propagation prediction models. Predicted sediment properties include reflectivity, acoustic impedance, sediment type, attenuation, compressional velocity, shear velocity, density, porosity, mean grain size and shear strength. To accomplish this, the software uses the digitized acoustic signals from the HR ASCS hardware and software systems to bin the measured return signal amplitude into ten adjustable width time windows which correspond to a series of depth increments in the sediment. This profile of sediment response echo strengths is used along with algorithms based on multilayer acoustic theory to compute an impedance profile of the sediment, for each ping, in near real time. Since the impedance (the product of density and sound velocity of the medium) is the property that determines the amount of energy reflected when sound energy passes from a medium of one impedance into another medium of a different impedance, it is possible to use the acoustic signal reflected from the seafloor to calculate acoustic impedance for each medium. The algorithms used consider transmission, reflection, and attenuation of the signal at each of the boundary (time interval) surfaces. These values of impedance are then used with a series of empirical relationships, originally developed by Hamilton (Hamilton, 1980 and Hamilton and Bachman, 1982) and later modified, to predict the above listed sediment geotechnical and geoacoustic properties in near real time and display them as a color scrolling waterfall-type display on the computer monitor (Fig. 2). In addition, the software produces a real time display of GPS navigation on a color plot of the survey tracklines being run. Each navigation point is plotted in a color which corresponds to the predicted value of surficial impedance for that geographic position. This gradually produces a near real time map of sediment impedance along the tracklines in the area being surveyed (Fig. 2).

The HR ASCS software will presently operate with 6-bit or 8-bit resolution digital data output from the EMS or from the new HR ASCS. In the latter case, the normal 16-bit resolution data stream has been shunted to 8-bits for sediment classification purposes. This will be upgraded in the near future to a full 16 bit resolution (this requires modification of the HR ASCS software for acquisition, storage, and processing). Operating on a second 80486 microprocessor-based microcomputer in the DOS operating environment, the sediment properties prediction software is designed to be user friendly yet extremely flexible in its capabilities for near real time prediction of seafloor geotechnical properties and the mapping of these properties for numerous military and civilian applications.

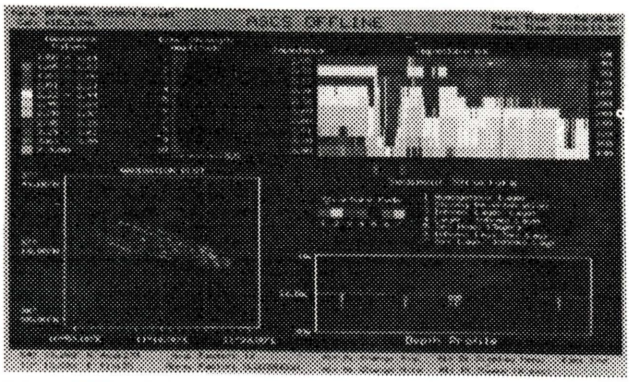

Figure 2. An example of the ASCS sediment prediction software scrolling display screen. Displayed is a prediction of impedance with depth in the sediment (for the last 288 pings) with a digital display of the last ping's values, a computer interpreted prediction of sediment structure, transducer altitude above the seafloor (scrolling display), a plot of the ships tracklines determined from an integrated GPS receiver with the positions shown in color dots that correspond to the last pings surface layer of predicted impedance, and an oscilloscope type display of the raw echo strength. All predicted sediment properties can be similarly displayed in near real time while running a survey.

In order to produce areal maps of the sediment properties predicted along tracklines, a significant amount of post processing of the data is required. This is due to the fact that very high density data is collected along the tracklines but no data is collected in the areas between them. It is therefore necessary to estimate sediment properties in the areas not traversed through the use of gridding algorithms. These gridding algorithms interpolate the sediment property data at evenly spaced "grid nodes" over the area of interest that has been surveyed. Because the HR ASCS data is processed into 10 intervals with depth in the sediment, it is necessary to produce a series of 10 grids which are geographically registered to each other, over the area of interest. From these, interpolated vertical profiles of the sediment property are produced by stacking the 10 interval values at each geo-referenced grid node. These profiles can then be used to make three dimensional sediment properties maps of the area or to make areal predictions of potential mine burial using the DSE/CSS Impact Burial Prediction Model (Hurst, 1993) (Fig. 3).

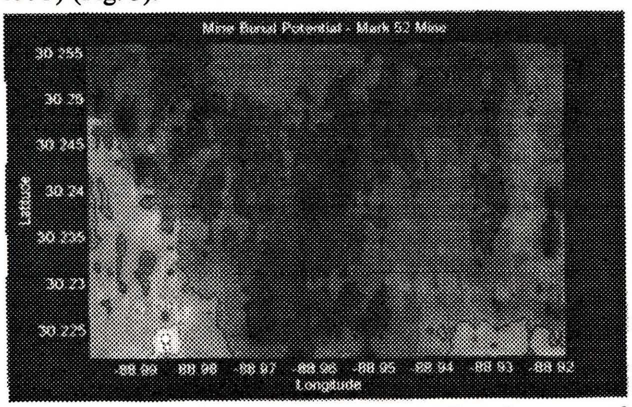

Figure 3. Mine burial potential map developed from ASCS trackline data over the Ship Island Testbed. Red colors indicate complete burial for a MK52 dummy mine impacting the seafloor in a horizontal orientation. The Yellow color indicates areas where the mine would partially bury. The white color indicates an area where the m ine would lie proud of the seafloor. The yellow and white portion on the left of the map cover the Gulfport Ship Channel and dredge spoil areas which consist of sand and muddy sand. The red area of the map consists of relatively soft silty clay sediments.

REFERENCES

Hamilton, E. L., (1980). Geoacoustic Modeling of the Sea Floor, Journal of the Acoustical Society of America, v. 68, no. 5, pp. 1313-1340.

Hamilton, E. L. and R. T. Bachman, (1982). Sound Velocity and Related Properties of Marine Sediments. Journal of the Acoustical Society of America, v. 72, no. 6, pp. 1891-1904

Hurst, Robert, (1993). NZ Defence Force, Defence Scientific Establishment, Aukland, New Zealand, Personal Communication

Lambert, D. N., (1988). An Evaluation of the Honeywell ELAC Computerized Sediment Classification System, Naval Ocean Research and Development Activity, Stennis Space Center, Report 169.

Lambert, D.N. and Fiedler, H., (1991). Methods of High resolution remote Seafloor Characterization. Proceedings of MTS 91, v. II, Marine Technology Society Conference, Nov. 10-14, 1991 New Orleans, LA, pp. 1004-1011.

Lambert, D.N., J.C. Cranford, and D.J. Walter, (1993). Development of a High resolution Acoustic Seafloor Classification Survey System. In Acoustic Classification and Mapping of the Seabed, an Underwater Acoustics Group Conference held at the University of Bath, Bath England, 14th-16th April, 1993. Proceedings of the Institute of Acoustics, Vol. 15, Part 2, pp. 149-156.

Sea Bed Roughness Classification from Processed Side Scan Sonar Data

W. R. Arcus and J. D. Penrose
Centre for Marine Sciences and Technology, Curtin University of Technology,
PO Box U1987, Perth, Western Australia, 6001

INTRODUCTION

Rough surface scatter is important in many areas of application including sonar, radar and remote sensing generally. In marine acoustics, scattering from the sea surface and sea bed is often the dominant masking factor against which a target must be detected. The study of sea bed roughness potentially has applications in areas as diverse as sediment movement and acoustic propagation studies as well as for mine counter-measures.

The Centre for Marine Science and Technology, in association with Fugro Survey Pty. Ltd and the Department of Industry Technology and Commerce, have been conducting research into the acquisition of side scan sonar data, in order to characterise sea bed roughness using various signal processing techniques, in near real time.

Attention has been given to the several methods in which information on surface roughness may be inferred from backscattered signals. These include features of the leading and trailing edge of an echo pulse and various parameterisations based on higher order statistics of an ensemble of pulses, including spectral composition. Studies to date have included - acoustic principles behind scattering phenomena, approaches to numerical modelling and the development and trials of a prototype near real time side scan sonar data acquisition and processing system.

Particular attention has been given to the nature of the modulation of the envelope of an acoustic return pulse. This approach has arisen as a natural extension of earlier work undertaken at Curtin University (Penrose *et. al.*, 1984), which showed the limitations emerging from an approach which employed the variation of backscattered echo amplitude with incident angle to infer surface roughness. A similar approach has also been used with some success, undertaken at the University of Bath in the United Kingdom (Pace and Gao, 1988), to characterise sea bed types by geological composition such as sand, mud, clay, gravel, stones and rock. Other researchers such as Chivers *et. al.* (1990) have derived geological classification by utilising roughness and hardness indices for vertical incidence echo sounding.

THE REAL TIME SYSTEM REQUIREMENTS

The system developed to date utilises a PC based (80486 (50 MHz) minimum) platform with a 16 channel, 200 kHz throughput Analog to Digital Converter (ADC) card. It is designed to acquire and log data in real time and process the acoustic data in near real time. It was clear from the start that to achieve full real time processing, some form of accelerator or digital signal processing (DSP) card would be required. By utilising demodulation methods to acquire the echo envelope directly, much of the data processing and storage overheads have been reduced. The system logs vessel position data (from Fugro's Differential GPS system) and utilises Kalman filtering to provide a best estimate of position.

Fugro Survey Pty. Ltd. owns and operates two types of side scan sonars as part of its Australian off-shore operations, namely the EG&G models 259 and 260 side scan sonars. The interface electronics packages, which include modules for demodulation, threshold level detection and amplification for use with the two sonar systems, have been designed and built.

DATA PROCESSING ALGORITHMS

Various corrections need to be applied to the data, such as time varied gain (TVG) and slant range correction, depending upon the sonar system being used. For example, the model 260 provides TVG in the tow fish and therefore slant range correction need only be applied to the raw data.

Reut *et. al.* (1985) and Pace and Gao (1988) define two spectra of particular interest when examining backscattered spectral composition namely, the log power and log normal power spectra given by the two respective equations below.

$$P_L(f) = \frac{\log\left(A.\overline{P}(f)/P_m + 1\right)}{\log(A+1)} \qquad P_{NL}(f) = \frac{P_L(f)}{\int^{f_{NY}} P_L(f)df}$$

Here, P_m is the maximum value of the average power spectrum, A is an arbitrary constant chosen to best enhance any spectral features and f_{ny} the Nyquist frequency. Pace and Gao *ib. id.* used $A = 10^4$ and further defined feature space classifiers by examining ratios of integrated spectral regions (of the normalised log spectra). They were able to show surface types may be classified by geological type using this method.

In the studies at hand, the authors are particularly interested in the characteristics of the spectral composition of the normalised log power spectra, for a given surface classification with varying roughness. It should be noted that many factors can potentially affect the spectral composition including the very process of slant range correction and variations in the tow fish position before backscattering is even considered.

EXPERIMENTAL TRIALS

Initial trials have been conducted off the coast of Western Australia to allow real side scan data to be acquired for algorithm development and to test acquisition and logging functionality of the system. The developed interface electronics package was also able to be tested.

Two sites of interest were identified and examined. The first was in the Sepia Channel, where a relatively uniform sand wave field was evident and the second in Cockburn Sound which was a relatively smooth uniform sea bed (with respect to the insonofying wavelength). The sites were surveyed by side scan initially and sonar data collected. Divers then make a visual inspection of the two areas of sea bed in order to acquire representative stereophotographs - therefore allowing nominal surface statistics to be determined.

Figures 1 and 2 show average log power spectra for the two sites with figure 3 showing the difference spectrum. It should be noted that significant structure is noted in figure 3 around the 2 kHz spectral region where the nominal surface statistics indicate.

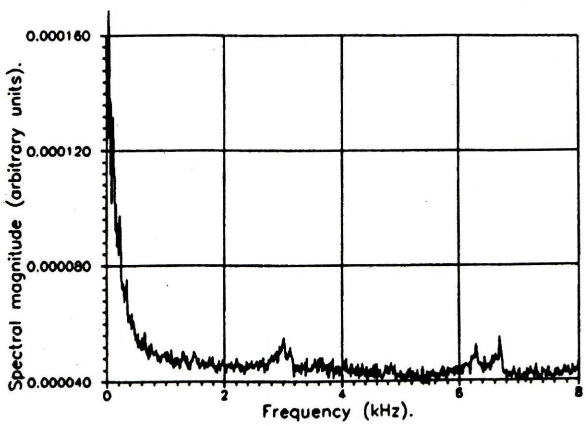

Figure 1. Average log normal power spectra for Cockburn Sound.

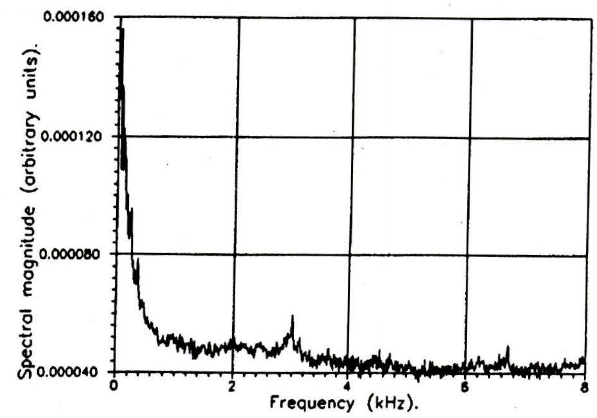

Figure 2. Average log normal power spectra from Sepia Channel.

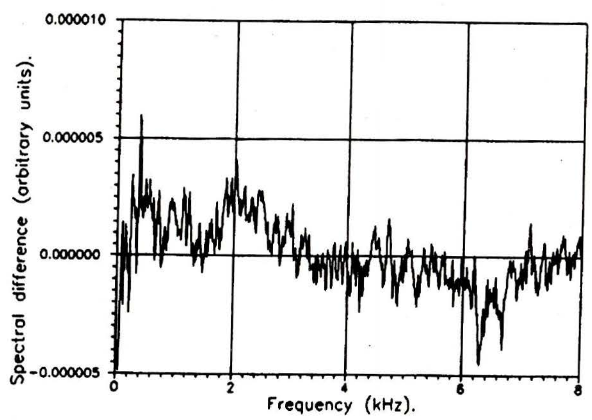

Figure 3. Differences in the average log normal power spectra for the Sepial Channel and cockburn Sound sites.

CONCLUSION

Work continues in being able to quantify roughness, however results to date suggest that for similar surface types, differences in roughness can be distinguished from the log normal spectra and that variations in the Pacian feature classifiers may be able to be used for this purpose.

Another sea trial is expected soon with modified interface electronics and algorithms implemented in the real time prototype system.

REFERENCES

Chivers, R. C., Emerson, N. and Burns, D. R., 1990: 'New Acoustic Processing for Underway Surveying.', The Hydrographic Journal, No 56, April, 9 - 17.

Pace, N. G., and Gao, H., 1988: 'Swathe Seabed Classification', IEEE J. Oceanic Eng., **13**(2), April., 83- 90.

Penrose, J. D., White, B. A., Palumbo, D., Wells, J. B., and Collins, L. B. (1984): 'Monte Carlo Modelling of Scattering in Underwater Acoustics.', Bulletin Aust. Acoust. Soc. **12**(2), 39 - 45.

Reut, Z., Pace, N.G., and Heaton, M.J.P., 1985: 'Statistical Properties of Sidescan Sonar Signals and the Computer Classification of Seabeds.', Proc. Inst. Acoust., **7**(3).

ROXANN - Remote Data Acquisition and Classification of Seabed Surface Material Types from Echo Sounder Signal Returns

A. Williamson and F. Ogilvie
Marine Micro Systems Ltd., Aberdeen, Scotland

1. INTRODUCTION

The subject of seabed classification covers considerably more than identifying the presence of mud, sand and rock on the seabed and intermittently locating this information on a chart. Seabed classification is an ancient art with a fascinating history and one which today offers new dimensions for hydrography and many other disciplines.

It is perhaps a cliché, yet in the context of seabed sensing we need to remind ourselves that there is no place on the earth's surface as remote as the seabed. Indeed in some cases, we know more about what is deep under the seabed than we do about the actual surface.

The parallel with space exploration is most topical with the recent television programs celebrating the 25th anniversary of the Apollo landings on the moon. The seabed is as infrequently visited by humans as the earth's orbit but, unlike space, the more time we spend on investigating the seabed, the more we discover, such as unknown organisms, and new life forms associated with the volcanic vent on the mid-Atlantic Ridge.

As with any form of exploration, first we must establish yardsticks for what we are observing and then work out why and for whom we acquire seabed material data. Classification is always user defined.

2. HISTORY OF SEABED CLASSIFICATION

For hundreds of years, seabed classification has been used for safety and navigation. Gravel, shingle or hard boulder clay - all these are poor holding ground and ever since Roman times (e.g. St. Paul's shipwreck on Malta), anchoring has been the last resort safety measure for mariners.

Less well remembered is the use of seabed classification for navigation. Approaching a lee shore after a long passage, perhaps without sun or star sights for days or even weeks, as the vessel came "into surroundings" the recess in the base of the lead weight would be smeared with tallow grease so that the finer particles of the seabed surface would adhere to the lead and enable surface examination of the seabed material on recovery.

Until the recent advent the terminology used as a result of this classification method could be found in common use on navigation charts. There are still some quaint references in the standard UK Hydrographic Office's Mariner's Handbook however, for example the definition for pebbles reads as "water rounded material of from 4 to 64 mm in size - i.e. from the diameter of the top of a man's thumb to the diameter of his clenched fist when viewed sideways."

3. TODAY'S NEEDS

New demands have emerged from different sectors, together with new sensing technology to broaden the subject of seabed classification. One can list sectorial needs as follows:

- Environmental
- Fishery habitat
- Commercial fishing
- Dredging/coastal engineering
- Defence
- Seabed engineering.

4. SUMMARY

From this overview of seabed classification, it is appropriate to compile a wish list of features of an ideal seabed classification system, accommodating, as far as possible, the different needs already outlined.

We may look at preferred features of such a system as follows:

- Capable of remote sensing
- Unambiguous numerical classification
- Automatic, not dependent on subjective interpretation
- Real-time, capable of integration into data acquisition systems
- Portable for post processing
- Capable of accommodating different user classifications
- Minimal operational deployment restrictions
- Not dependent on depth, vessel speed, sea state
- Robust marinised hardware.

Current seabed data acoustic acquisition techniques such as side scan sonar and echo sounders produce images of the seabed and by definition require the human brain to 'imagine' the result and produce profile images and 3D graphics and by human input give images of the seabed surface.

Video is currently also used in limited applications primarily because of the expense of deployment and recovery. Video image is subjective to the viewer and any two scientists may classify the seabed differently.

Divers are also used, but due to cost, only in a limited number of applications. The result, although superior to grab sampling, is also subjective.

5. ROXANN

Roxann hardware was developed for the specific purpose of meeting the wish list criteria. The system is fully patented in many countries - including Australia.

The field-proven RoxAnn system represents a genuinely significant advance in remote sensing technology.

RoxAnn can be easily fitted to the existing ship's echo sounder without affecting its operation and requires no additional work through the hull of the vessel, and can be configured to supply user specific applications - i.e. RoxAnn simply gives you as much or as little information as you want. The system may be operated at an average operating speed of 15 knots in underway surveying and an electronic gimble ensures clean data acquisition even in rough states.

Unambiguous numerical RoxAnn data is objective and directly processable into colour coded results against geographic position, depth and profile in either 2 or 3D. Data can be displayed in real-time or saved onto disk to enable assimilation with grab samples.

6. ROXANN - HOW?

RoxAnn extracts two indices: one from the first echo (E1) and one from the second echo (E2). These are then used in combination to identify the seabed surface. In shallow water multiple echoes may be observed depending on the transmit power of the echo-sounder and the noise level of its receiving electronics. Each echo must however include at least one stage of non-specular reflection from a signal to be able to return to the transducer.

Using information from the first and second echo, observed via the dedicated parallel receiver connected across the terminals of the transducer of an echo-sounder, ground discrimination can be successfully achieved when the vessel is under full steam.

Incorporation of the processing into a flexible digital environment, linked to the navigation system of the vessel permits rapid detailed survey work to be achieved and displayed on a chart on the computer screen.

In terms of ground truthing, a demand for a detailed quantitative analysis can only be achieved by direct measurement and this raises the question of obtaining a seabed material sample that is representative and not only of the localised area from which the sample was taken but also of a significant region surrounding the sampled area. Therefore, the precision with which a particular piece of ground needs to be labelled can only be defined by the application for which the information is needed.

The relevant acoustics are complex. It takes knowledge from three areas of underwater acoustics that are usually discussed as separate specialties - namely seabed (surface) scattering, sea surface scattering and sub-bottom reverberation.

6.1 SELECTION OF PARAMETERS E1 AND E2

The practical question that arises is how information on the seabed material type that is clearly present in the echoes returning to the echo sounder transducer can be extracted by signal processing in the most efficient way. With a view to effective display and indeed practicality of implementation, all the potential descriptive parameters - whether acoustic or topographical have been condensed into two indices; E1, derived from the first echo and E2 derived from the second echo.

The whole of the second echo is integrated to provide E2, which is primarily a measure of hardness. The integration is performed after swept gain has been applied to the received signal to eliminate dependence, the effect of depth on the index E2. The strength of the specular reflection to the seabed will depend not only on the characteristic acoustic impedance mismatch but also on the shear wave velocity and the attenuations at the seabed.

Not so for normal incidence

Furthermore, roughness will tend to diffuse the reflection, diminishing the purely specular part.

The differences are due in part to the different characteristic acoustic impedances and in part to the inherently greater capability of harder substances to be rough. To process the first echo to obtain the index E1, it is clearly necessary to minimise the contributions of competing mechanisms such as sub-bottom reverberations.

The relative magnitude of the oblique back scattering and the sub-bottom reverberation in contributing to the first echo is determined primarily by the angular beam pattern of the transducer and secondarily by the nature of the ground.

If a narrow beam transducer is used, as is common in many surveying applications, the sub-bottom reverberations will dominate the first echo. Softer ground, presenting a lower acoustic impedance discontinuity to the normally incident acoustic wave in the water, will permit more energy to be transferred to the bottom to produce reverberations. This can lead to the observation that soft ground produces longer trails on the first echo than hard ground.

The magnitude of the normal reflection contains essentially the same information as the index E2 derived from the second echo. To obtain complementary information from the first echo to be encapsulated in the indices E1 it appears wise to try to isolate the component caused by the oblique back reflection.

The first condition is to use a transducer with an adequate beam width. The second condition is to minimise the potential contribution of sub-bottom reverberation.

E1 and E2 are derived from the echo train returning to the transducer. E1 can be seen to be related to roughness (in combination with hardness), while E2 is primarily related to hardness (moderated by roughness).

Each seabed produces a particular pair of values of E1 and E2, which will change as the vessel moves from one ground type to another. A general empirical classification can be derived as shown (slide/overhead) where the range of combinations are delineated by closed areas. The patented trade name for this type of display is the **RoxAnn Square .**

Some Progress in Underwater Acoustic Geo-Mapping Technology

Shuying Zhang
Shanghai Acoustics Laboratory, Academia Sinica 456 Xia-Mu-Qiao Rd., Shanghai 200032, PRC

1. INTRODUCTION

Since 1964 the Shanghai Acoustics Laboratory, Academia Sinica (SALAS) has been working on a series of projects to develop various underwater acoustic geo-mapping (profiling) equipments. Based on studies and developments of geo-acoustic signal processing techniques and underwater impulsive sound-sources, several kinds of geo-sonar systems have been developed. Also some new progress in geo-mapping technology has been made in recent years.

2. GEO-SONAR SYSTEMS FOR DIFFERENT USES

A. High resolution geo-sonar systems

Three types (QPY-1, GPY AND PGS) of high resolution geo-sonar systems have been successively developed with specifications of resolution 0.1-0.3m and penetration 50-100m, and mainly used for geological surveys in marine engineering, such as harbour construction, waterway dredging, platform building etc., also used for exploitations of marine resources and geological studies of upper sediment layers. Particularly GPY has been an industrial product and most extensively used in China.

The key to developing a high resolution geo-sonar system with good quality of geo-mapping is to have a strong impulsive sound-source with good output signature (a peak following very short ring) and good directional pattern (very low sidelobes and back-radiation). The acoustic arrays composed of 4 or 6 small size boomers, which has been verified to be a satisfied sound-source, were invented and applied to the above mentioned geo-sonar systems. Appropriately adjusting the size of the radiating plate and the electrical parameters (inductivity and capacity) of the boomer, the frequency-band of sound transmission can be varied in the range of 0.5-8 kHz, and the source level reaches 210dB.

Excepting good sound-sources, some effective techniques of geo-acoustic signal processing have also been developed and applied, such as: 1. multi-section time-varying gain-controlling for the compensations of transmission losses caused by spherical spreading and sound absorption in sediments respectively; 2. sea-bottom tracking for the automatic operation of the geo-sonar system. 3. time-varying filtering for increasing the ratio of echo signal to background noise (S/N) and reducing multiples, and 4. synthetic aperture processing for enhancing S/N and improving the resolution along the navigation line.

B. Deep penetration geo-sonar system

A huge acoustic profiling system, the DDCI-I geo-sonar system, has been developed with specifications of resolution 10-30 m and penetration 1000 m, and used for geological surveys in different areas of the West-Pacific Ocean. This system mainly consists of: 1. an electrical spark unit of 30,000 Jules, 2. an empennag-like underwater electrode with an equally-spaced coaxial construction between four pairs of positive (at the centre) and negative (at the edges) poles, 3. an echo-processing unit involving the above-described several processing techniques, 4. a 50m long streamer with 20 hydrophones separated by 2m between each other, 5. a graphical recorder and a tape recorder.

Valuable profiling records of hundreds of nautical miles have been obtained by this system at the continental shelf and a slope areas of the East China Sea. In addition, a significant discovery is that a more than 500 m thick sediment layer exist at the area of the Ryukyn Trench where the water depth is over 6700 m. Also some profiling records for finding manganese nodules in a certain area of the Pacific Ocean, where the water depth is 5400 m, were obtained.

C. Acoustic suspended-sediment monitoring system

Recently the acoustic method based on sound back-scattering principle has been applied to monitoring suspended-sediments in water. The main advantage of this method is to be able to automatically and continuingly observe the real-time concentration profiles of suspended-sediments without disturbing the environmental conditions around the observed spot. Thus the acoustic method is quite suitable for the dynamic observations of suspended-sediments and the studies of sediments migration and deposition at different areas, such as the mouth of river, waterway, bay and reservoir. Also, this method can be effectively used for monitoring polluters and planktons in water.

Essentially a suspended-sediment monitoring system based on the acoustic method is just a high-frequency geo-sonar system. According to different requirements, two types of the acoustic suspended-sediment monitoring systems, ASSM-1 for fixed-spot observations and ASSM-2 for on boat observations, have been developed by SALAS, and remarkable performances demonstrated through practical applications at the mouth of the Yangtse River.

The two types of ASSM systems are mainly composed of a signal transmitter, a back-scattering echo receiver, 1 or 2 underwater transducers and a micro-computer set. In ASSM-1, a four-pod framework is involved. On the framework, two underwater transducers (0.5 and 1.5 MHz) for upwards and downwards observations, a pressure case for containing electronic circuits, and 4 sensors for measurements of water temperature, water depth, current speed and direction, are mounted at appropriate positions respectively. In ASSM-2, only one underwater transducer (0..5 MHz) for downwards observations, which hangs into water from a side of boat during the process of observation, is applied.

In ASSM 1 and 2, the sound pulse transmitting, the back-scattering echo receiving and processing etc. are automatically operated by the micro-computer according to several selectable programs. On the screen of a displayer, the two-dimensional (depth in vertical and time in horizontal) concentration profile of suspended-sediments, where the magnitudes of concentration are expressed with different colours, can be directly displayed in real-time. On this colourful picture, a belt of mark with 16 kinds of colours is attached, and the above mentioned 4 hydrographical parameters displayed at the beginning of every 3 minutes. Through further processing to the observed data, e.g. compensation of sound transmission loss, in situ calibration of scattering intensity to real concentration, averaging of the data wit h a variable time-depth window etc., the two-dimensional concentration profile of suspended sediments can be printed out in a data table and a set of curves. The specifications of ASSM-1 and ASSM-2 are as follows: 1. maximal monitoring depth 10m (2m), 2. depth-resolution of concentration profile 20cm (2cm), 3. time-resolution of concentration profile 1 sec., 4. beam-width of observed region 1.5°, and 5. concentration range being able to be quantitatively measured 0.1-10kg/m3, where the values in curves are suitable to the downwards observation of ASSM-1.

3. DEVELOPMENTS OF NEW TECHNIQUES IN ACOUSTIC GEO-MAPPING

A. Pulse-compression technique with complementary coding signals

The problem about applying the pulse-compression technique with complementary coding (c.c in abbreviation) signals to acoustic profiling has be considered. No. theoretical side-lobes in the output signature is the feature of using c.c. signals. This is exactly a strong point superior to using chirp and pseudorandom signals, which have been applied to modern active sonar and geo-sonar systems. Thus, applying the pulse-compression technique with c.c. signals to acoustic profiling is able to improve the quality of profiling records not only with high resolution and deep penetration, but no false reflections as well.

A prototype instrument including an 8 unit c.c. signal generator and a corresponding correlation processor has been made. In practical acoustic profiling the way to use the pulse-compression technique with a c.c. signal is to generate and process the two parts of the c.c. signal, Sa(t) and Sb(t), alternately (each of them involves 8 polarity-coding pulses to form a complementary pair). The outputs displayed on the profiling records are the real-time sums of their auto-correlation functions, Xa(t) + Xb(t), Xb(t) + Xa(t), successively. Consequently excepting a single peak (the main-lobe), no side-lobes can be seen on the output signatures because of the definition of a complementary pair.

A problem, which needs to be discussed in practical applications, is that the travel-times of echoes from a certain sediment layer can be different due to the up and down movements of the underwater acoustic transmitting and receiving transducers of a geo-sonar system under the action of wave. In the case where the wave is very strong, the variations of intervals between every two adjacent units in a c.c. signal should be counted in. As a result, not only Xa cannot be added with Xb exactly one by one in time (called de-complement effect), but also the signatures of both Xa and Xb theirselves may be distorted considerably (called de-correlation effect). Through computer simulations, it has been confirmed that the de-complement effect caused by the wave modulation can be completely eliminated by a simple echo travel-time correlation effect of wave modulation be ignorable in the cases where the wave-height h<1.5 m and the wave-period T> 1 sec. (i.e. below sea-state 4).

B. Pattern recognitions of acoustic profiling records

It is known that the pattern characteristics of acoustic profiling records corresponding to different kinds of marine sediments must be different. According to these differences, specialists can carry out the geological interpretations to the profiling records, and the geological classifications to the profiled sediments. Based on practical experiences accumulated by some specialists and through an intensive analysis of some typical profiling records, seven pattern characteristics with three different states for each have been summed up and shown in Table 1.

Table 1. Pattern characteristics of acoustic profiling records

Characteristic	code name	State 1	State 2	State 3
1. darkness between layers	A	light	mid	dark
2. variation of darkness between layers	B	no	slow	fast
3. size of scanning points between layers	C	small	mid	large
4. smoothness of sub-bottom line	D	smooth	mid	rough
5. thickness of sub-bottom line	E	fine	mid	thick
6. undulation of sub-bottom line	F	little	mid	great
7. shape of lines between layers	G	disjointed	jointed	unappearing

Moreover the standard pattern characteristics appearing on the acoustic profiling records corresponding to 10 categories of marine sediments have also been concluded as follows:

1. mud	A1,B1,C1,D1,E1,F1,G3
2. mud with silty sand	A1, B1,C1, D1, E1, F1, G1
3. mud with sandy clay	A1, B1,C1, D1, E1, F1, G2
4. mud and sand	A1, B1,C2, D2, E2, F1, G1
5. silty and fine sand	A2, B2,C1,D2,E3,F1,G1
6. gravel and coarse sand	A3, B3,C3,D3,E3,F1, G3
7. densified fine sand	A3,B2,C2,D2,E1,F1,G3
8. clay	A3, B2,C2,D2,E3,F2,G3
9. sandy clay	A3,B2,C2,D2,E3,F2,G1
10. rock	A3,B3,C2,D3,E3,F3,G3

Note: A1 represents the patter characteristic A with state 1, and so on.

From the statistical average of a large amount of acoustic profiling records, the weight of each pattern characteristic and state thereof in making a judgement of the geological category of sediments has been determined. Consequently, a computerised pattern recognition system (i.e. an expert system) has been developed by means of the Zadeh's fuzzy set theory with fuzzy logic reasoning. Through inquiring about the pattern characteristics appearing on acoustic profiling record being interpreted and then computing the so-called approximating factors of this record to the standard ones corresponding to the above-mentioned 10 categories of marine sediments respectively, the geological classification of sediment layers can be derived according to selecting the maximal approximating factor for each layer.

High-Frequency Acoustic Bottom Backscatter from a Well Defined Patch of Sea Floor

Martin W. Lawrence
Maritime Operations Division Defence Science and Technology Organisation

A valuable parameter for use in acoustic modelling is the strength of the backscatter of acoustic energy from the sea floor, for a range of angles of incidence. Conventional measurements of acoustic backscatter use a hydrophone in a fixed location, using change of the angle of the transducer to obtain the different angles of incidence. A necessary result of this process is that the hydrophone ensonifies different patches of the sea floor for the different angles. While this gives a measure of the general dependence of backscatter strength on grazing angle, it does not give it for a single patch of sea floor. Thus variations in the backscatter strength will be caused not just by the differing angle, but also by the differing reflectivity of different patches of the sea floor.

A system has been developed that avoids this problem. It is applicable to backscatter at high frequencies, where the wavelength is small. The apparatus moves the location of the transducer as the angle changes, so that the transducer always looks at the same patch of sea floor. The apparatus, illustrated in Figure 1, is based on a cubic framework with the transducers mounted at the apex of an A-frame that pivots near one edge of the base. The transducers point towards the pivot axis. Thus as the A-frame rotates, the transducers continue to point at the same patch of sea floor. The cubic frame has no metal bars in the vicinity of the acoustic beam.

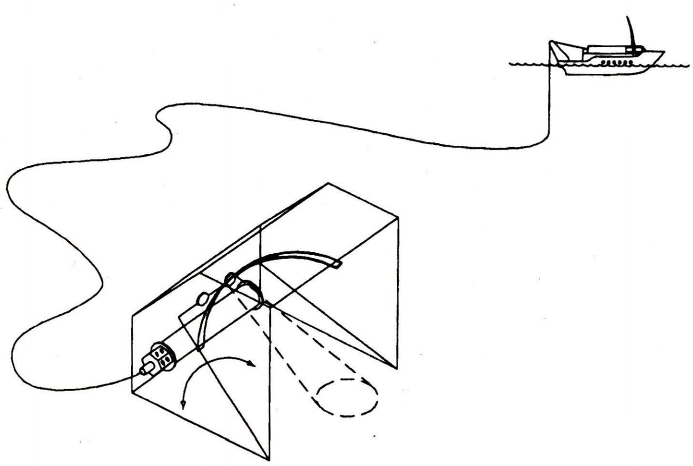

Figure 1. Apparatus for measurement of acoustic bottom backscatter.

There is an electronics canister mounted on the structure. This electronics package is under control from the sea surface via an umbilical cable. The underwater package generates the acoustic signals, receives and amplifies the reflected signals, controls the position of the Aframe and controls the stereo cameras. The signals are passed up the umbilical cable to the sea surface, where they are digitised and stored. The movement of the A-frame is achieved via a chain drive, with its position being determined by a system of magnets and a Hall effect sensor. This has proved to be a very robust and accurate system.

Using this apparatus measurements have been made of the acoustic backscatter from the sea floor at frequencies of 100 and 200 kHz, over a range of grazing angles from 4° to 90°. The beamwidth of the transducers is 14° and 12°, respectively. The transmitted signal is a tone burst 0.3ms long. The patch of sea floor used in the bottom backscatter measurement is delineated by a combination of beam width and time delay on the acoustic pulse.

A pair of underwater cameras is used to take stereo photographs of the region of the sea floor from which the acoustic backscatter is measured. Analysis of these photographs then produces a topographic map of the area from which the scattering occurs.

One question of importance in acoustic bottom backscattering is how much of the backscatter occurs at the surface of the sediment as compared to backscatter from inhomogeneities within the volume of the sediment. This is important in that to acoustically characterise a region of sea floor by using geological measurements, it is necessary to know whether to concentrate on surface or sub-surface properties of the sediment.

The current experimental technique provides a means for determining which of these mechanisms is dominant at the frequencies used and for the locations surveyed. A model is under development for calculating the backscatter from the deterministic surface (measured by stereo photography). Comparison between model and experimental results should provide insight into the relevant mechanism.

Changing the surface topography of the sea floor can also provide insight into the scattering mechanism. First, backscatter measurements are made with the sea floor in its natural state, then a diver smooths the sea floor and the measurements are repeated on exactly the same patch of sea floor (except that hills and valleys have been smoothed away).

The advantages of the technique described here lie around the measurement of the same patch for all angles and the ability to very accurately characterise the sea floor and even to modify it. A disadvantage of the technique is the relatively short acoustic path length, which means that near field considerations come into play. Also the small size of the area measured means that this technique is not appropriate for surveying large areas of sea floor.

The apparatus has been used a number of times. On any given deployment, great reproducibility of results is observed. Although at this early stage the analysis is not complete, an example of the results is given in Figure 2 for two independent runs at each frequency for the same patch of sea floor. For this figure, points are plotted at intervals of 0.2°, with approximately 70 acoustic measurements being included in each plotted point. It is evident that even the fine structure of the results is highly consistent from one run to the next.

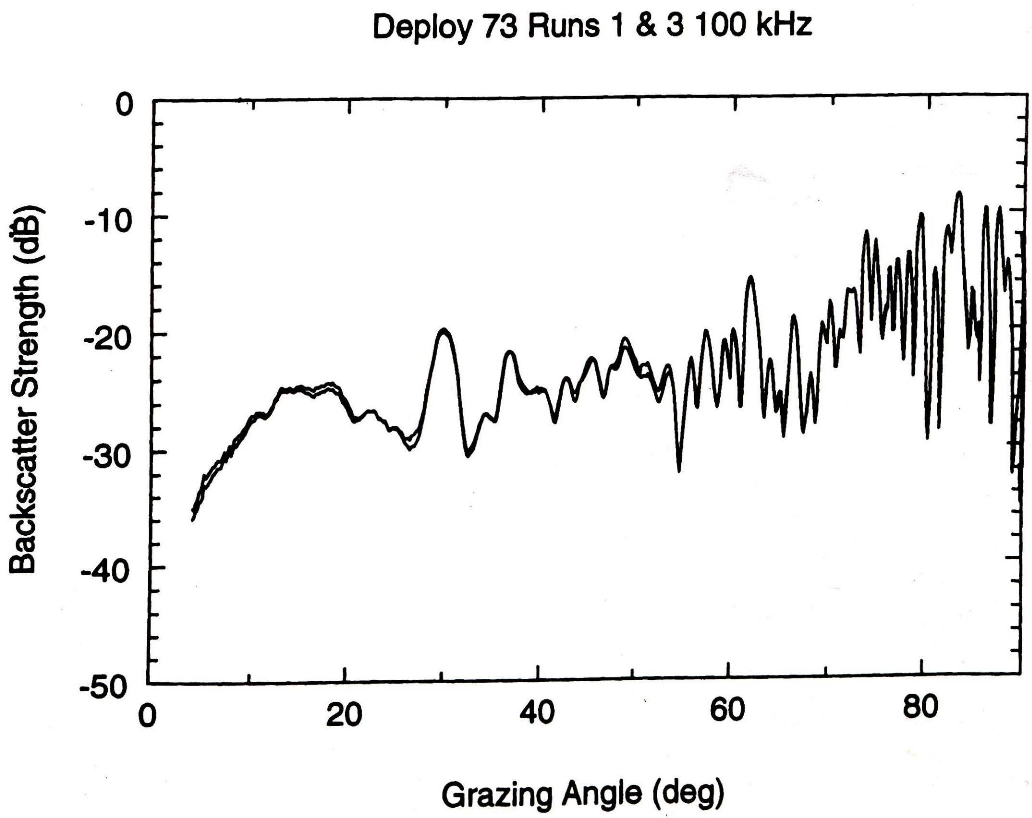

Figure 2. Acoustic bottom backscatter strength as a function of grazing angle, for a single site.

In summary, the described technique for studying the acoustic characteristics of the sea floor has been demonstrated to give results of high quality. Detailed analysis of the results is continuing.

The effect of seabed rigidity on bottom reflections: implications on mode excitations by a bottom-lying source in the ATOC project

Zhiyong Zhang
Defence Scientific Establishment, Auckland Naval Base, Auckland, New Zealand

INTRODUCTION

Acoustic Thermometry of Ocean Climate (ATOC) is an international research project aiming to monitor ocean climate change by measuring the travel times of acoustic signals transmitted over long distances[1]. The ATOC experiment expects to measure the travel times of the lower order modes. For logistic convenience, acoustic sources are to be placed on the seabed. Because lower order modes are well trapped, they penetrate little into the seabed and have small amplitudes at the sea bottom. Therefore there are concerns about the excitation of lower order modes by a bottom-lying source and about the role shear waves play in the excitation of these lower order modes[2,3,4].

In this paper, mode excitations by a bottom-lying source were directly linked to the phase of the bottom reflection coefficient. Bottom reflections were analyzed using the concept of effective depth[5]. Shear wave effects were assessed for a wide range of realistic seabed parameters. When the shear wave speed is less than the sound speed in the water, seabed rigidity reduces the mode excitations. When the shear wave speed is much larger than the sound speed, seabed rigidity moderately enhances mode excitations.

Part of the work here was contained in a report sent to the ATOC Program Office[6]

RESULTS

The effect of seabed reflections on waterborne sound propagation can be simulated by reflections from a pressure release boundary located an `effective depth' below the seabed[7, 8,5]. The effective depth of a seabed represents the difference in reflection properties between the seabed and a pressure release bottom. For a bottom-lying source, the effective depth can be viewed as the distance that the source is away from a pressure release surface. A seabed with a larger real effective depth means the phase of its reflection coefficient has a larger difference from $-\pi$ and thus supports larger excitations of the modes by a bottom-lying source.

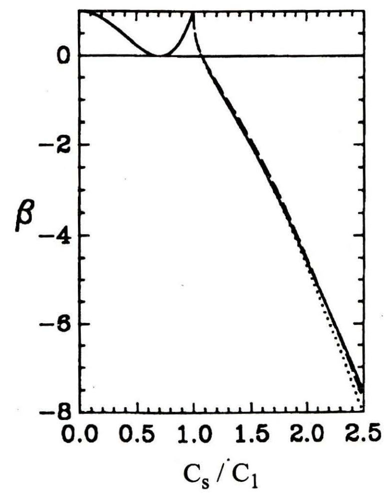

Figure 1. The factor β . For c_s/c_l <1, β values depend only on c_s/c_l. For c_s/c_l > 1, β values are shown for three types of rocks (⋯sedimentary rock, — —limestone, —— basalt).

Ignoring seabed inhomogeneity, Zhang[9] gives the following expression for the real effective depth ΔH at zero grazing angle for solid seabeds:

$$\Delta H = \frac{\rho_2 \lambda_1 \beta}{2\pi\rho_1(1 - c_1^2/c_2^2)^{1/2}} \tag{1}$$

Where ρ_1, c_1 are the density and sound speed of the water, $\lambda_1 = (c_1$ /frequency) is the sound wavelength in the water, ρ_2, c_2 are the density and compressional wave speed of the seabed. The effect of seabed rigidity is represented by the factor β :

$$\text{if } c_s < c_1, \ \beta = (1 - 2c_s^2/c_1^2)^2 \qquad (2)$$

$$\text{if } c_s > c_1, \ \beta = \frac{(1 - 2c_s^2/c_1^2)^2 - 4(c_s/c_1)^4}{(1 - c_1^2/c_s^2)^{1/2}(1 - c_1^2/c_2^2)^{1/2}} \qquad (3)$$

where c_2 is the shear wave speed in the seabed.

The factor β in Eq.(2) is also given in Ref.[2] and is valid only for $c_s < c_1$. For $c_s > c_1$, β is given as in Eq.(3). Figure 1 shows the β factor computed from Eqs.(2,3). For $c_s < c_1$, β depends only on the ratio c_s/c_1. For $c_s > c_1$, β also depends on the ratio c_1/c_2; a nominal value of c_1 = 1500 m/s was assumed and the relations from Hamilton[10,§I] were used to link the wave speeds c_2 and c_s.

Figure 1 shows that β rapidly drops to being negative after c_s exceeds c_1 and the three types of rocks give about the same β value for the same shear wave speed. For c_s/c_1 <1.3 (the most frequent case in underwater acoustics), $|\beta| \leq 1$ and the generation of shear waves reduces the mode excitations. At $c_s/c_1 = 0.7$, $\beta \approx 0$ and hence a seabed with $c_s \approx$ 1000m/s support little mode excitations.

For c_s/c_1 >1.3, $|\beta|$ >1 and seabed rigidity enhances the mode excitations moderately.

Equations (1,3) show that soft fluid-like seabeds with $c_1/c_2 \approx 1$ have large positive effective depths and hard rock seabeds with $c_s \gg c_1$ have large negative effective depths.

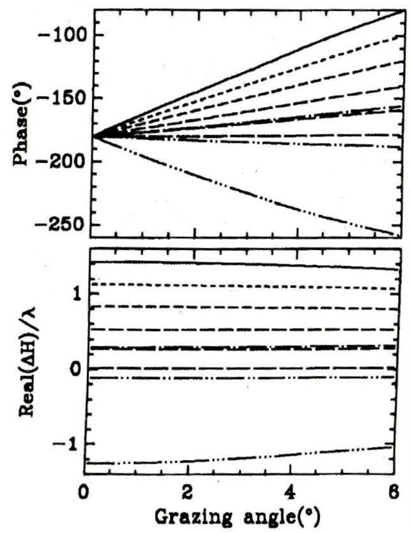

Figure 2. Reflection coefficients and real effective depths versus grazing angle for various seabed parameters. (—JK1, dash length increases from JK2 to JK6, —• JK7, —••AUC, —•••JK8).

Figure 2 shows the phases of the reflection coefficients and the real effective depths versus grazing angle for some typical model parameters. JK1 to JK8 are the eight typical seabeds in Table I of Jensen & Kuperman [11] and AUC is the hard seabed used in the second example of Ref.[12]. The effective depths were normalized by the sound wavelength in the water with water sound speed being taken as 1500 m/s. Attenuation in water was assumed negligible and attenuation in the seabed were included using complex wave speeds.

Only results to a grazing angle of 6 degrees are shown because for a typical ATOC scenario, a water depth of 1000 meters and a source frequency of 70 Hz, modes 1 to 10 correspond to grazing angles from zero to about 6 degrees.

As the seabed goes from JK1 to JK6, the phases approach $-\pi$ and the corresponding effective depths decrease from about $1.4\lambda_1$ to about zero. Seabed JK6 has c_s=1000m/s and has the smallest effective depth. Seabeds AUC and JK8 have $c_s > c_1$ and have negative effective depths.

Seabed JK1 has the largest positive real effective depth and seabed JK8 has the largest negative real effective depth. This is because for both seabeds the phase of their reflection coefficient deviates most from $-\pi$ at low grazing angles.

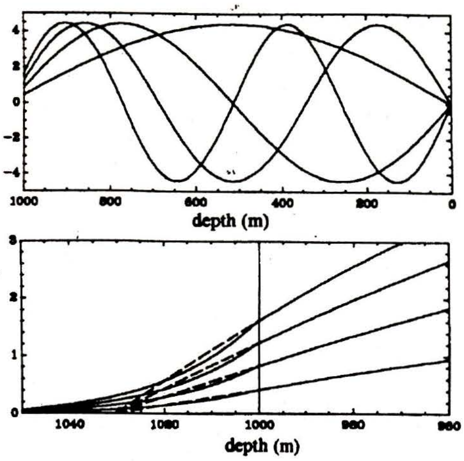

Figure 3. Mode functions (modes 1 to 4) for seabed JK1.

KRAKEN
Computes BL
& takes account
of $G = G(z)$.
"BOUNCE"

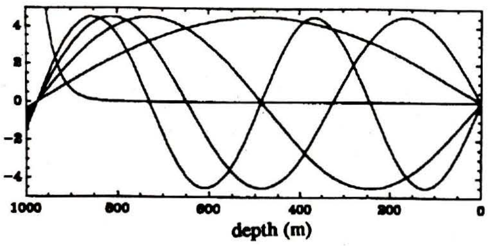

Figure 4. Mode functions (modes 0 to 4) for seabed JK8.

Figures 3,4 show the mode functions for an isovelocity water of 1000 meters and a frequency of 70 Hz. Seabed JK1 has a positive effective depth and the mode functions appear to have a common zero *below* the water-seabed interface. Elevating the source above the seabed will increase the mode excitations.

Seabed JK8 has a negative effective depth and the mode functions of the acoustic modes have a common null above the water-seabed interface. The interface mode (mode 0) also appears to be strongly excited by a bottom-lying source. Figure 4 shows that for seabed JK8 elevating the source appears to have a negative effect: *decreasing* the mode excitations.

SUMMARY

- Seabeds with larger effective depths support greater excitations of lower order modes by a bottom-lying source.
- When seabed inhomogeneity can be ignored, usually seabed rigidity reduces the mode excitations, but for hard rock seabeds high rigidity enhances the mode excitations moderately.
- Very soft seabeds or very hard rock seabeds appear to support larger mode excitations. However, soft seabeds may not be suitablefor source installations and very hard seabeds may have strong excitation of interface waves.
- Two effects are worth watching out for when installing the ATOC sources:(1) a seabed with shear wave speed around 1000 m/s supports little mode excitations by a bottom-lying source, (2) elevating the source above a very hard rock seabed may decrease the mode excitations.
- At acoustic frequencies, most seabeds have shear waves speeds less than the water-sound speed and thus excitation of shear waves is less likely to be of much help in putting energy into lower order modes.

REFERENCES

1. W. H. Munk and A.M.G. Forbes. Global ocean warming: An acoustic measure? *J. Phys. Oceanogr.*, 19:1765-1778, 1989.
2. W. H. Munk. It's the shear velocity, stupid! *ATOC Occasional Notes,* Number 8, May 1993.
3. W. H. Munk. It's the slope, stupid! *ATOC Occasional Notes,* Number 13, September 1993.
4. M. Dzieciunch. The sea floor and modal excitation. *ATOC Occasional Notes,* Numbe 12, August 1993.
5. Z. Y. Zhang and C.T. Tindle. Complex effective depth of the ocean bottom. *J. Acoust. Soc. Am.*, 93:205-213, 1993.
6. Zhiyong Zhang. Effect of shear waves on the mode amplitudes at the sea bottom. Technical report, Department of Physics, University of Auckland, June 1993.
7. D. E. Weston. A Moire fringe analog of sound propagation in shallow water. *J. Acoust. Soc. Am.*, 32:647-654, 1960.
8. D.M.F. Champman, P.D. Ward, and D.D. Ellis. The effective depth of a perkeris ocean waveguide, including shear wave effects. *J. Acoust. Soc. Am.*, 85:648-653, 1989.
9. Z.Y. Zhang. *Approximations for acoustic reflection from solid seabeds.* PhD thesis, The University of Auckland, February, 1993.
10. E. L. Hamilton. Geoacoustic modelling of the sea floor. *J. Acoust. Soc. Am.*, 68:1313-1339, 1980.
11. F. B. Jensen and W. A. Kuperman. Optimum frequency of propagation in shallow water environments, *J. Acoust. Soc. Am.*, 73:813-819, 1983.
12. Juan I. Arvelo and Herbert Uberall. Adiabatic ormal-mode theory of sound propagation including shear waves in a range-dependent ocean floor. *J. Acoust. Soc. Am.*, 88:2316-2325, 1990.

PA-1 Parametric Transmitter and its Applications

Lesun HUA, Honglie LING, Jiazhong HU and Ketang CHEN
Shanghai Acoustics Lab, Academia Sinica 456 Xia-Mu-Qiao Rd., Shanghai 200032, PRC

1. INTRODUCTION

During past three decades, parametric acoustic arrays have been extensively researched and some prototype parametric sonars reported. However, real products are still rare nowadays. In order to provide customers with reliable and multi-functional equipment, a PA-1 parametric acoustic transmitter has been developed in our lab. It is specially suitable for 3D high-resolution detection system and can also be utilised in those cases that the sharp beam-width and/or broad transmitting frequency-band are claimed and the large scale of the array is not permitted.

2. CONFIGURATION

Model PA-1 parametric transmitter is composed of a rectangular sound projector and an electric transmitter (Fig.1). An optional stepping motor rotating unit may also be presented for the use of mechanical beam-scanning. The array consists of one hundred sixty PZT-8 compound-bar transducers (Fig.2). The radiating area of each element is 1.5cm$*$1.5cm. Its design guarantees a very broad frequency band (q=3.3) and the lowest nonlinear transmission of the transducer itself. Considering the requirement of electro-steering, all elements are divided into ten groups and each group has its own feed lines.

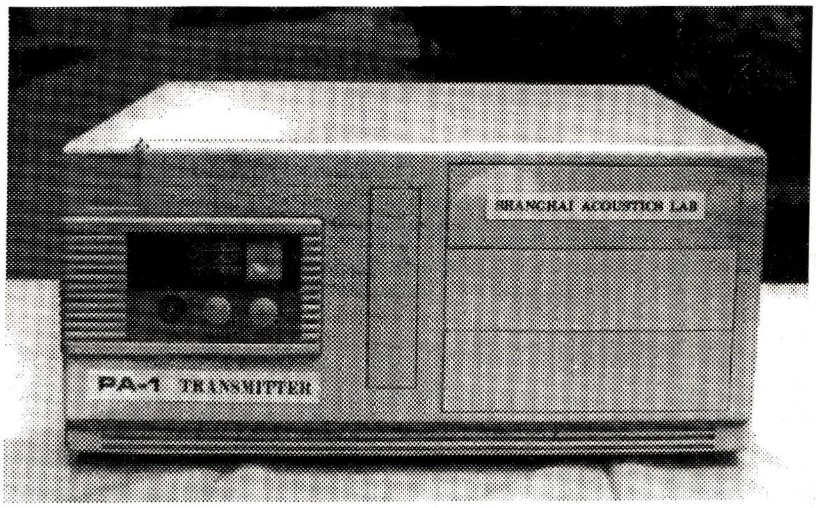

Figure 1. PA-1 transmitter

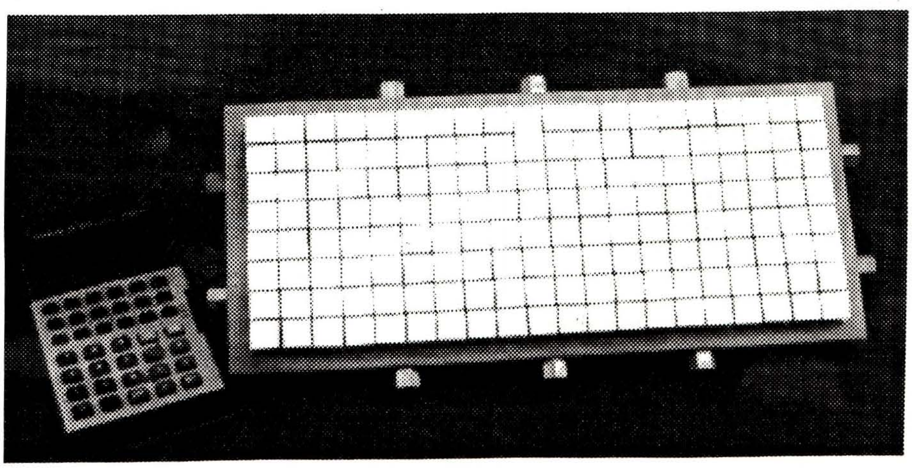

Figure 2. PA-1 parametric acoustic array

3. MAIN FEATURES

The specifications of PA-1 parametric transmitter are as follows:

1) mean primary frequency	100kHz
2) maximum primary acoustic power	2*4kW
3) projector dimensions	30cm*12cm
4) primary beamwidth	2.5 degree*6.5 degree or 5 degree*13 degree
5) difference frequency	2-30 kHz
6) difference frequency source level	204dB (when difference frequency = 7kHz)

Because our task is to offer customers a versatile and reliable equipment, special considerations were adopted. In fact, PA-1 can bear a sound power density up to 12.5 Watts per square centimetres, yet the beam-pattern of the difference frequency remains as good as that of low power density. Compared with the result of literature (1), that the half-power beamwidth enlarged from 1.5 degree of low power density to 7.5 degree at the density of 10 watts per square centimetres, the improvement is obvious. The second feature of PA-1 is its broadband operating ability. The 3dB bandwidth of the transducer is more than 30kHz, so that the difference frequency can extend from 30kHz down to 2 kHz or even less. The third feature is its reliability. A ruggedized structure of transducers guarantees PA-1 can work in any field adverse circumstances. Besides, PA-1 is a portable apparatus. The array with 160 elements weighs 9kg only. And the electric transmitter (12 kg) is a portable unit too.

4. POSSIBLE APPLICATIONS

A. 3D subbottom Profiling

A strip array is originally designed for this purpose. The sharp beam pattern and the broadband transmitting ability present high resolution both in the depth and horizontal. By means of electrical and/or mechanical beam scanning, the three dimensional sea-bottom topography is easily realised. In case of detecting subbottom buried objects such as boats, pipelines, mines, isolated stones and so on, 3D detection is much more effective than the conventional 2D sub-bottom profiling. A lot of research work about using oblique incident difference frequency wave for the detection of sand-buried objects has been conducted by Professor Xu of our lab.

B. Multi-beam and multi-frequency echo sounder

The difference-wave level of PA-1 is sufficient to implement a general-purpose multi-beam echo sounder. The advantage is its side-lobe suppression and the small array dimensions.

Besides, because of the PA-1's broad-band performance, a multi- frequency echo sounder can be realised with only one transducer.

C. Chirp sonar

PA-1 might be an ideal transducer to a chirp sonar which needs a very broad band in low frequency.

D. Underwater communications

PA-1 might be quite beneficial to underwater communications. Its narrow beam-width can substantially decrease multipath distortions. With this and its broadband performance, it is possible to transmit data with high baud rate.

E. Underwater sonovision

The conventional underwater imaging system, such as ROV's sonar suffers from a restriction of array dimensions. Usually, engineers have to make a compromise between resolution and range, sacrificing the former for the latter or vice versa. However, if PA-1 is used, this contradiction could be solved.

5. ACKNOWLEDGEMENT

We are indebted to Professor Shuying Zhang for his permission to publish the work about PA-1.

6. REFERENCES

1. R.H. Nichols, "Finite amplitude effects used to improve echo sounder", J.A.S.A., Vol. 50, pp. 1086-7, 1971.

2. W.L.Konrad, "Design and performance of parametric sonar systems", AD-A016242, 1975.

3. Wen-sen Liu and Zen-xia Xu, "Propagation of the difference frequency wave generated by a truncated pametric array through a water-sediment interface", J.A.S.A., Vol. 89, PP. 92-7, 1991.

Experiments in Deconvolution of Sub-Bottom Profiler Records

R. B. Hurst
Defence Scientific Establishment, Auckland Naval Base, Auckland, New Zealand.

INTRODUCTION

A typical acoustic sub-bottom profiler system uses a transducer such as a boomer as a sound source, and an array of hydrophones (often an "eel" floating in the sea surface) to pick up the acoustic echoes from the sea floor. The signals consist of normally reflected pulses from the sea floor. The shape of the received pulse, $g(t)$, is the transmitted pulse, $f(t)$, convolved with an impulse response $h(t)$ corresponding to the process of normal reflection from the sediment, and then further convolved with another function $e(t)$ that is the impulse response of the hydrophone system.

The impulse response $h(t)$ for the sediment reflection process is closely related to a "reflectance function" that is in turn related to vertical structure in the sediment. The relective function $r(z)$ is given approximately as,

$$r = 0.5 \; d/dz \; (\ln \mathbf{Z}) \tag{1}$$

where $\boldsymbol{Z}$ is the acoustic impedance $\rho\, c$ of the sediment at depth z, and ρ and c are respectively the mass density and sound propagation speed. This equation applies to a continuous variation of $\boldsymbol{Z}$ with depth. (For *discontinuities* in $\boldsymbol{Z}$, the usual Rayleigh formula for the amplitude reflection coefficient applies.)

The relationship between the reflectance $r(z)$ and the sediment impulse response $h(t)$ is given implicitly, approximatley, by the equation

$$h(\tau)\, d\tau = r(z)\, dz$$

where τ is the two-way sound travel time to depth z in the sediment. (The equation is approximate because multiple reflections within the sediment structure have been ignored.) If the sound speed were constant with depth in the sediment (not usually true in practice) then $h(\tau)$ and $r(z)$ would be linearly related.

Most commonly the echo signal is recorded essentially as received, in its convolved form, on a graphics recorder or similar. What is usually required from the measurements is the reflectance function $r(z)$, representing the sediment structure. The function $g(t)$ serves as an estimate of $r(z)$, within a proportionality factor. The convolutions with the other two functions $f(t)$ and $e(t)$ have the effect of confusing the interpretation, particularly when high resolution and quantative results are required.

This paper describes two applications where the effects of the convolutions have been removed, in order to obtain quantative measurements of the reflectance, the underlying acoustic impedance, and the sediment mass density. The basis of our deconvolution method is the well known result [1] that the operation of convolution in the time domain "maps" onto multiplicat ion in the frequency domain. Using upper-case symbols to denote the Fourier transforms of lower-case time-domain functions, then

$$G(f) = a.F(f).H(f).\,E(f)$$

(The factor a allows for changes in the amplitudes of the signals due to spherical spreading and different amplifications of $f(t)$ and $g(t)$.) Thus, deconvolution cna be effected by division of the functions in the Fourier domain. An important constraint, however is that this can not be done at frequencies where F and E are zero or very small. This may mean that some frequency components may be missing from the estimate of $h(t)$.

APPLICATION OF DECONVOLUTION TO DETERMINING DENSITY PROFILES:

The first application is a technique we have developed for estimating mass density profiles in the topmost 1m of sediment, by processing the signals from a commercial sub-bottom profiler system. The signals are received, not using the usual eel array of hydrophones but instead a single hydrophone positioned about 1.6 m below the sound source. An essential feature is that both the transmitted pulse and the seafloor echo are monitored.

The signals are typically sampled at 41.6 kHZ. The pulses are captured within time windows typcially consisting of 64 or 128 samples, for convenience in using the FFT algorithm. The deconvolution is effected by dividing the Fourier transform of the echo pulse by that of the transmitted pulse. Because the same hydrophone is used to monitor both *f(t)* and *g(t)*, the effect of the hydrophone impulse response on the signals in effect cancels when the quotient of the transforms is formed.

After deconvolution, the estimate of *h(t)* is corrected for spherical spreading and for the different amplifications that were applied to *f(t)* and *g(t)*. also a very important adjustment is made, of the DC level. This is required because of the constraint on frequency-domain deconvolution noted earlier: the hydrophone signals do not extend to indefintely low frequencies. However the correct representation of the lowest frequencies contained in *h(t)* is essential. As can be seen from equation (1), the reconstruction of an impedance profile from h(t) involved an integration, and the result is dominated by the lowest frequencies. The DC adjustment uses the principle of causality. The impulse response *h(t)* should certainly be zero prior to the return of the very first part of the echo from the sediment. The time windows are chosen so that the earliest tru echo is part-way into the time window containing h(t). The DC level can then be adjusted so that this early part of the estimate is in fact zero.

After these corrections the impulse response is regarded as equivalent to the impulse response for plane wave reflection from the sediment. The next step is subtraction of the multiple reflections within the sediment structure, using an algorithm equivalent to one that has been published [2]. (Usually this is a rat her minor correction.) The output from this algorithm is, within a scale factor, equivalent to the reflectance function of the sediment, but sampled at equal increments of two-way travel time τ rather than depth. From this, the impedance profile $Z(\tau)$ is estimated.

The final step, estimating a density profile from the impedance profile, uses empirical observations that impedance and density are very highly (although non-linearly) correlated [3,4] for shallow-water marine sediments, across a wide variety of compositions and grain sizes.

The system is in routine use as part of DSE's investigations of sediments for mine countermeasures. Figure 1 shows a "screen dump" from the profiling software. Typically, the pulses are processed as averages of batches of 50 to 100. A profile is calculated every 30 to 60 seconds. Figure 2 shows some representative examples of profiles obtained using the system. The vertical resolution in the profiles is typically a few cm and the depth is limited to about 1 m with the present sound source. These parameters follow directly from the spectrum of the boomer - the deconvolution using Fourier techniques is possible between frequencies of approximately 600 Hz and 15 kHz.

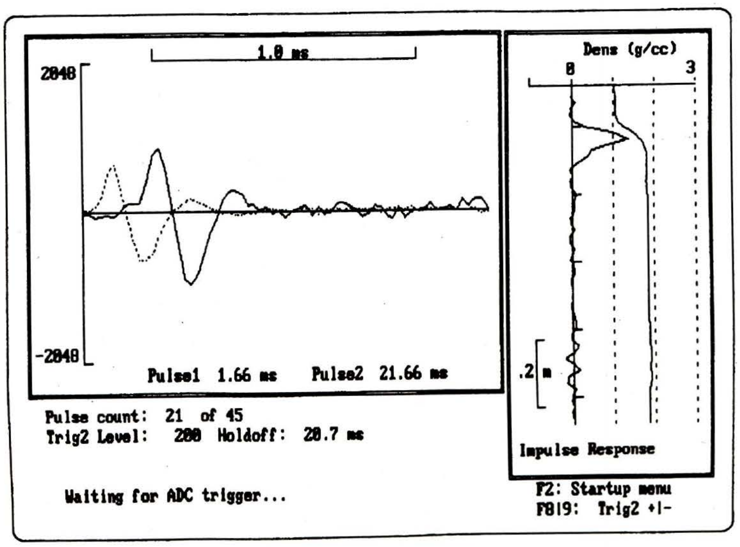

Figure 1. A "screen dump" (minus the colours) from the sediment density software. The left-hand window shows an oscilloscope-type display of the transmitted pulse (dotted trace) and the seafloor reflection (solid trace), for a typical single pulse. The right-hand window displays the impulse response and sediment density profile resulting from the processing of the previous average of 45 pulses.

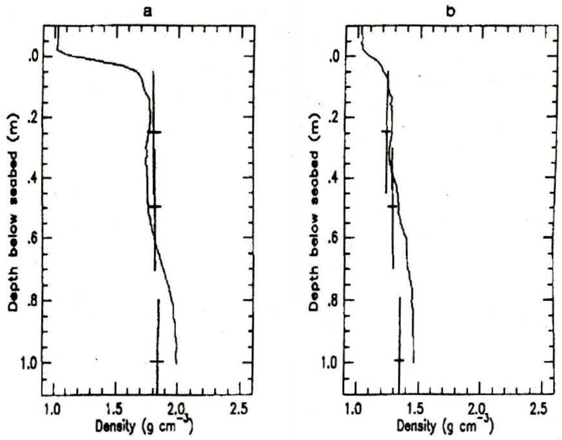

Figure 2. Two typical density profiles otained in the Hauraki Gulf near Auckland. Ground truth measurements are also shown. These were made using a Troxler density measuring system, which uses g-ray scattering. The vertical and horizontal bars represent respectively the approximate vertical resolution of the Troxler system, and its measurement uncertainty.
a. A profile of a sediment consisting of fine sand with some mud; b. A profile of soft mud.

HIGH-RESOLUTION SUB-BOTTOM ACOUSTIC PROFILES

A related technique has been used for enhancing the resolution of conventional sub-bottom profiler records. The same transducer configuration is used as for the density profiling. The processing proceeds as before, through deconvolution. However in this application the processing ends with the calculation of sediment impulse response. As there is no attempt to recover absolute values of acoustic impedance, the absence of low-frequency components of $h(t)$ can be tolerated. Consequently much longer time windows can be chosen for capturing the pulses. The result of t he deconvolution is a high-pass filtered version of h(t), but extending to much greater depths in the sediment.

Figure 3 shows an example of this type of processing. In this case an accurage measurement was required of the thickness of a lens of dredging spoil. The deconvolution processing allowed the measurement to be made with a resolution of a few cm. Interestingly, the sense of the reflectance (i.e. non-inverted or inverted echoes) is readily apparent in the processed records. This allows horizons of higher or lower acoustic impedance to be identified. This information would be completely obscured in a conventional recording of the sub-bottom profiler record.

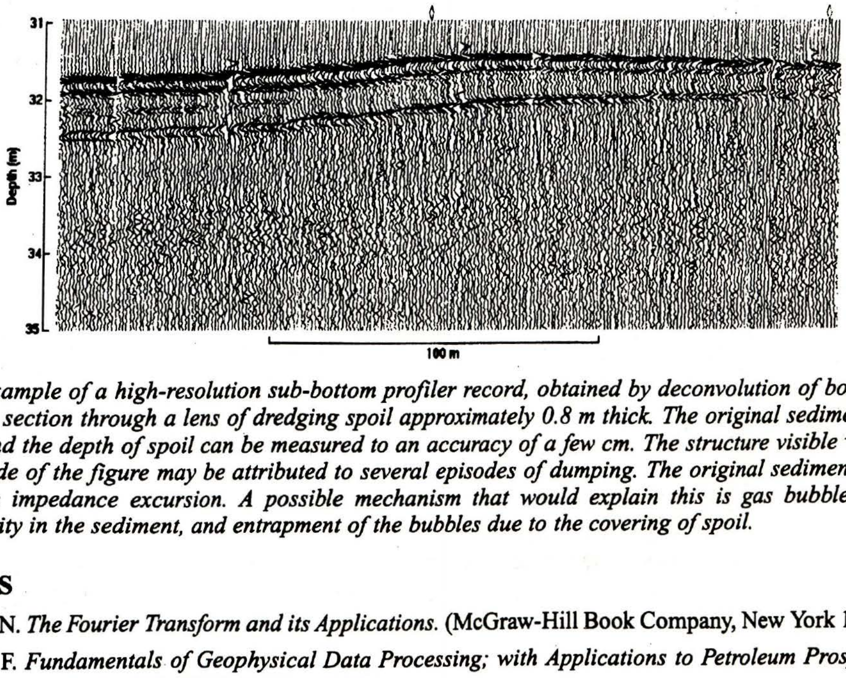

Figure 3. An example of a high-resolution sub-bottom profiler record, obtained by deconvolution of boomer signals. The record shows a section through a lens of dredging spoil approximately 0.8 m thick. The original sediment surface can be readily seen, and the depth of spoil can be measured to an accuracy of a few cm. The structure visible within the spoil at the left-hand side of the figure may be attributed to several episodes of dumping. The original sediment surface shows a strong negative impedance excursion. A possible mechanism that would explain this is gas bubble generation from biological activity in the sediment, and entrapment of the bubbles due to the covering of spoil.

REFERENCES

1. Bracewell, R N. *The Fourier Transform and its Applications.* (McGraw-Hill Book Company, New York 1978), 2nd ed, p187.
2. Claerbout, J. F. *Fundamentals of Geophysical Data Processing; with Applications to Petroleum Prospecting.* (McGraw-hill Book Company, New York 1976), p158.
3. Richardson, M D and Briggs, K B. On the use of acoustic impedance values to determine sediment properties *in* Acoustic Classification and Mapping of the Seabed, Proc IOA, 15, part 2, pp154-24 (1993).
4. Hurst, R B. Sediment density profiles from reflections of boomer pulses. *in* Acoustic Classification and Mapping of the Seabed, Proc IOA, 15, part 2, pp229-236 (1993).

Comparison Of Acoustic Seafloor Classification (ASCS) and In-Situ Geoacoustic (ISSAMS) Data Collected from a Variety of Sediment Types in Kiel Bay, Germany

Michael D. Richardson, Douglas N. Lambert, Kevin B. Briggs and Donald J. Walter
Geosciences Division, Naval Research Laboratory
Stennis Space Center, MS 39529-5004 USA

The Naval Research Laboratory has developed two systems to remotely characterize near-surface sediment physical and geoacoustic properties. Sediment properties determined using these remote and in situ measurement systems are compared with standard laboratory-determined sediment properties for a variety of sediments types in Kiel Bay, Germany. The comparisons were made as part of the Office of Naval Research (ONR) Coastal Benthic Boundary Layer (CBBL) Program. The CBBL program is a 5-year basic research program that addresses the physical characterization and modeling of benthic boundary layer processes and the subsequent impact of these processes on seafloor properties that affect mine countermeasures. One of the naval objectives of the CBBL program is the improvement of remote acoustic sediment classification.

The High-Resolution Acoustic Seafloor Classification System (HR ASCS) utilizes a normal incident echo sounder to classify surface and subbottom sediments. The system can be best described as a high-resolution seismic system which typically operates using short pulse lengths (0.1 to 0.3 ms) and narrow beam widths (6° and 12°) at 30 and 15 kHz, respectively (Lambert et al., this workshop). Echo strength returns are used to predict, in real-time, acoustic impedance and relate impedance to a variety of sediment physical and geotechnical properties. Predicted sediment properties include reflectivity, acoustic impedance, sediment type, density, porosity, compressional wave velocity and attenuation, shear wave velocity, mean grain size and shear strength.

The In-Situ Sediment Acoustic Measurement System (ISSAMS) allows direct in situ measurement of sediment compressional and shear wave velocity and attenuation using pulse techniques. Geoacoustic probes, which are mounted on the In-Situ Sediment Acoustic Measurement System, are inserted into the sediment hydraulically. The entire operation is controlled and monitored in real-time from the surface. Data is collected and processed by a wet-side computer and transmitted to the surface for waveform display and analysis. Video cameras both monitor insertion of probes and provide preliminary indication of sediment type. A seabird CTD is used to measure bottom water temperature, salinity and sound speed. Sediment compressional wave velocity and attenuation are measured over pathlengths of 40 to 110 cm and at depths of between 0 to 50 cm below the sediment-water interface. Transmit pulses are driven utilizing 58-kHz pulsed sine waves and time delays and voltages are used to determine values of velocity and attenuation between identical radial-poled ceramic cylinders. Actual values of compressional wave velocity and attenuation are calculated by comparison of received signals transmitted through the sediment with those transmitted through seawater overlying the sediments. Shear wave velocity and attenuation are measured, using a similar pulse technique, between bimorph bender elements mounted in flexible silicone rubber mounts and driven at 100 to 2000 Hz. Shear wave measurements are made over the same pathlengths and at the same depth intervals as for compressional wave properties

A comparison of remote (HR ASCS) and direct in-situ (ISSAMS) measurements, using these two sediment classification systems, is made for a variety of sediments in Kiel Bay surveyed during July, 1994. In addition to in-situ and remote acoustic estimates of sediment physical and geoacoustic properties, box core and gravity core samples were collected for laboratory measurement of sediment physical and geoacoustic properties. Subcores from the gravity and box core samples are analyzed for sediment bulk properties including mean grain size, porosity, and bulk and grain density. Compressional wave velocity and attenuation are also measured on cores prior to determination of sediment bulk properties.

Preliminary data suggest good agreement among laboratory, remote and in-situ determination of sediment physical and geoacoustic properties. Kiel Bay contains glacial marine deposits which range from very soft muddy deposits, which collect in water depths greater than 20 meters, to winnowed glacial tills at bathymetric highs. Free methane bubbles were present in the soft muddy sediments of Eckernforde Bay. Outcroppings of relict glacial till sediments are clearly evident as a highly reflective surfaces in the HR ASCS records. The gradual change of sediments, with water depth, from glacial till, to hard sand, muddy sand, sandy mud and mud is shown as decreased impedance in the HR ACSC records (Fig. 1). Numerous subbottom layers of higher impedance were noted in the unconsolidated sediments and correspond to coarser sediment layers in the gravity core samples. These coarser sediments are deposited during erosional and depositional events that are common in Kiel Bay. The presence of glacial till underlying unconsolidated mud and sandy surface sediments is also clearly evident in the HR ASCS records, except when obscured by acoustic turbidity created from scattering from methane bubbles. Considerable lateral and vertical variability in methane gas bubble concentration was noted for the softer silty-clay sediments.

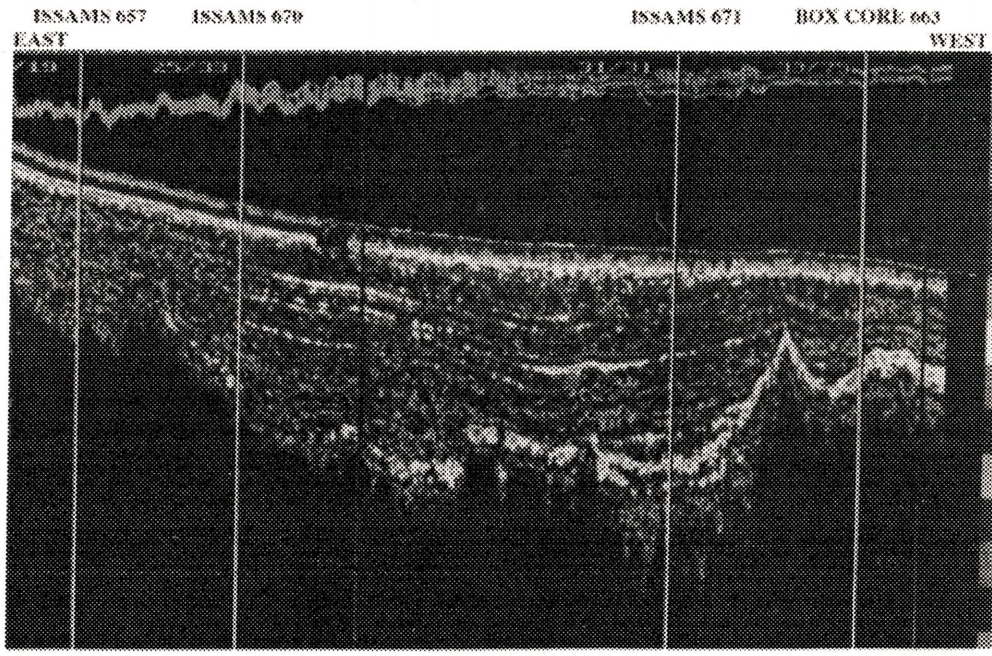

Figure 1. High Reolution Acoustic Seafloor Classification System (HR ASCS) 15 kHz seismic record across a portion of Kiel Bay, Germany. This data was collected using a 0.2 ms pulse length, 100 watt power level, and a 12° beam width. The vertical scale (depth) lines are shown as solid white horizontal lines which are five meters apart; the horizontal dotted lines indicate one met er intervals. Horizontal distance is approximately 2450 meters across the tracklines. Colors are displayed in steps of 6 dB of signal intensity (see colour bar at right). Hot colors represent high reflectivity, cool colors lower reflectivity. Surface sediment reflectivities transition from a highly reflective sand to a muddy sand at the left portion of the record and to a less reflective mud at the right portion. This transition is indicated by the change in color at the sediment-water interface and by the echo strength lines at the top of the record. Layered muds underlie these surficial sediments to a variable depth of up to three meters. A highly reflective glacial till underlies these deposits throughout the area. The glacial till is indicated by the highly irregular (red to yellow) surface at the lower limit of the acoustic return. Locations of the ISSAMS measurements and a box core along the trackline are shown by the yellow verticals lines on the record.

Laboratory and in-situ compressional wave velocities ranged from a low of 1440 m s^{-1} in the soft muds of Eckernforde Bay to 1652 m s^{-1} in fine sands in central Kiel Bay. In-situ shear wave velocities ranged from 5 to 40 m s^{-1} over the same sediment types. Compressional wave attenuation was lowest in the soft muds (k = 0.1) and highest in the fine sand sediments (k = 0.4 to 0.6). Sediment porosity in fine sand was measured to be 41-42 %. Soft muds near and Eckernforde Bay varied from 80 to 90 % in surface layers to as low as 65 % in lenticular sandy mud layers. Muddy sands and sandy muds with porosity values ranging from 44 to 75 % comprised the sediments of the transitional stations between central Kiel Bay to Eckernforde Bay. Direct in-situ measurements and box core or gravity core sampling were not attempted from coarser glacial till sediments.

Modelling Shallow Water Sea Beds

C. T. Tindle,
Physics Department, University of Auckland, Bag 92019, Auckland, New Zealand

The propagation of underwater sound in shallow water is dominated by multiple reflections from the sea bed. The effect of the sea bed can be described in terms of a plane wave reflection coefficient which can include the effects of attenuation and any layered structure within the ocean bottom. At low frequencies the effects of interface roughness are negligible and the reflection coefficient contains all the information about the ocean bottom which is required to determine the acoustic field.

The difficulty associated with using a reflection coefficient to describe the sea bed is that it is essentially unmeasurable because it is defined in terms of infinite plane waves at a single frequency. Multiple reflections and finite source-receiver geometry make direct measurements of the reflection coefficient impossible in shallow water.

In most practical cases there exists a critical angle. Sound which meets the bottom at a steep angle has a small reflection coefficient and its energy is rapidly lost to the bottom. Sound at low grazing angles is strongly reflected and is transmitted to large distances. In all cases the reflection coefficient approaches unity as the grazing angle approaches zero. These common features for the reflection coefficient means that approximations can be obtained which are useful in a variety of situations.

The simplest theoretical description of the propagation of sound in shallow water is in terms of normal modes. At low frequencies there are only a few such modes, each with its own phase velocity and attenuation derivable from the mode eigenvalue. Therefore the propagation is characterised by only a few parameters and it is not surprising that fairly simple models of the ocean bottom are quite successful. Any model which gives a good approximation to the reflection coefficient will give a good approximation to the normal mode parameters and a good description of the propagation.

The simplest model for shallow water propagation is the two fluid model of Pekeris with real mode eigenvalues. The original model did not include attenuation but this can be included as a perturbation or as a complex sound speed. In either case the eigenvalues become complex. This model has the main features of shallow water propagation.

The inherent simplicity of the two fluid model means that it is convenient to approximate a real sea bed by an equivalent fluid.1 The parameters of the equivalent fluid are chosen as those which give the most useful approximation to the reflection coefficient and are not necessarily equal to the corresponding parameters of the actual sea bed.

If a water layer of density ρ_1 and sound speed c_1 lies over a solid bottom of density ρ_2, compressional wave speed c_2, shear wave speed c_s, compressional attenuation α_2, and shear attenuation α_s then the bottom can be approximated by a fluid of density ρ_2', sound speed c_2' and attenuation α_2' given by

$$c_2' = c_2$$

$$\alpha_2' = \alpha_2 + \frac{8\alpha_s c_2 c_s^3(1-c_1^2/c_2^2)}{c_1^4(1-2c_s^2/c_1^2)} + \frac{4\omega c_2 c_s^3(1-c_1^2/c_2^2)^{3/2}(1-c_s^2/c_1^2)^{1/2}}{c_1^5(1-2c_s^2/c_1^2)^2}$$

$$\rho_2' = \rho_2(1-2c_s^2/c_1^2)^2\left[1 - \frac{(\alpha_2')^2 c_1^2(1+2c_1^2/c_2^2)}{2\omega^2(1-c_1^2/c_2^2)^2}\right]^{-1}$$

where ω is the angular frequency. This approximation is useful provided $c_s < 600$ m/s and the resulting reflection coefficient is frequency independent because α_2 and α_s are proportional to frequency. The three terms in α_2' arise respectively from attenuation of compressional waves, attenuation of shear waves and energy loss due to the generation of shear waves.

Another useful approximation is to replace the bottom by an equivalent fluid of complex density.[2] The required values are

$$c_2' = c_2$$

$$\alpha_2' = \alpha_2$$

$$\rho_2' = \rho_2\left[\left(1 - \frac{2}{(c_1/c_s + i\alpha_2 c_1/\omega)^2}\right)^2 + \frac{i4[1-(c_1/c_2+i\alpha_2 c_1/\omega)]^{1/2}[(c_1/c_s+i\alpha_s c_1/\omega)^2-1]^{1/2}}{(c_1/c_s+i\alpha_s c_1/\omega)^4}\right]$$

This approximation also gives a reflection coefficient which is independent of frequency and works well provided $c_s < 1000$ m/s. The notion of complex density may seem strange but the objective here is to get a good approximation to the reflection coefficient. Complex density arises naturally in the physics of porous media.

When the ocean bottom contains well defined layers it may be necessary to consider a more detailed layered model. The reflection coefficient of the bottom can then become strongly dependent on frequency as reflections from the top and bottom of a layer move in and out of phase. The corresponding effect for normal modes is that the amplitude of of a mode within a layer can be quite large when one or more loops of the mode function fit exactly into the layer.

Resonant effects within layers can lead to strong attenuation of some of the normal modes. The corresponding normal mode eigenvalues have a large imaginary part and this can cause difficulties for numerical searches. With multiple solid layers the usual correspondence between the mode number and the number of zeros of the mode function is lost.

A method of finding the normal modes systematically[3] is to define reflection coefficients R_1 and R_2 looking upwards and downwards respectively at some suitable depth. The product R_1R_2 is then a complex function of the ray angle of the plane waves or, equivalently, the horizontal wavenumber. A function f can be defined as

$$\phi = -\frac{i}{2}\ln(R_1R_2)$$

and corresponds to half the complex phase of R_1R_2. The normal mode eigenvalues occur at positions where ϕ is real and a multiple of π. The eigenvalues can thus be found by following the curve along which ϕ is real.

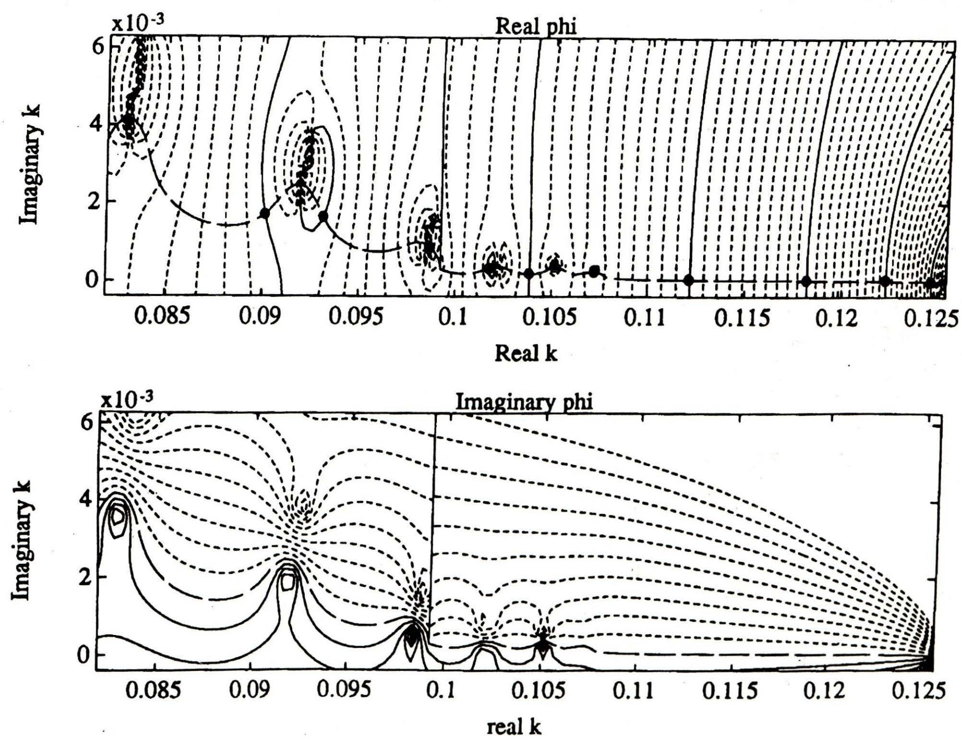

Contours of the phase function ϕ in the complex wavenumber plane. The dots show the normal mode eigenvalues.

The figure shows contours of the function f for a representative shallow water case in which a 200 m layer of water lies over a 250 m solid sediment with a solid basement underneath. The sediment has density 2 gm/cc, compressional wave speed 1750 m/s and shear wave speed 350 m/s. The corresponding parameters for the basement are 2.1 gm/cc, 1900 m/s and 550 m/s. All waves in the sediment and basement have attenuation of 0.2 dB/l. A propagation frequency of 30 Hz is assumed.

In the upper part of the figure the dashed lines show contours of Re(ϕ) in steps of 0.1π and the solid lines show steps of π. The lower figure shows contours of Im(ϕ) in steps of 0.2. Dashed contours are negative and solid contours are positive. The zero contour is given by the long dashed line and is reproduced in the upper figure. The intersection of the long dashed line and the solid contours are the normal modes and are identified by the solid dots.

The search for normal mode eigenvalues is reduced to following the line Im(ϕ)=0. Locating the eigenvalues is simple because the function f is monotonic along the line. The method has the advantage of avoiding the two dimensional search for complex eigenvalues which can be required when multiple solid layers are present.

The method also locates the leaky modes. The solid line at Re(k)=0.099 is the Pekeris branch cut and modes to the left of this line are leaky modes.

REFERENCES

1 C. T. Tindle and Z. Y. Zhang, An equivalent fluid approximation for a low shear speed ocean bottom. J. Acoust. Soc. Am. 91 3248-3256 (1992).

2 Z. Y. Zhang and C. T. Tindle, Approximate methods for shallow water acoustics with solid sea beds. J. Acoust. Soc. Am. 93 2395 (1993).

3 C. T. Tindle and N. R. Chapman, A phase function for finding normal mode eigenvalues over a layered elastic bottom. J. Acoust. Soc. Am. 96 accepted.

Dividing Australian Shallow Waters into Acoustic Propagation Loss Zones

Dr. A. I. Larsson
Maritime Operations Division, DSTO Aeronautical and Maritime Research Laboratory
Salisbury, S.A. Australia

Acoustic propagation loss is the amount of acoustic energy lost between an acoustic source and an acoustic receiver. This energy loss plays a major part in determining the distance that a sound signal is detected with clarity. In certain circumstances, it is valuable to know the range of propagation loss values at particular distances and where a particular value of propagation loss at a particular range is expected to be located. Showing the variation in propagation loss within a region at every location on a map is a difficult task, especially when the region to be examined, is a vast area like the Australian shallow waters. For this situation, the simplest way to display or model the variation in propagation loss and its locations is a map of acoustic propagation loss zones. At each location within each acoustic propagation loss zone, the propagation loss values at a particular distance should be within specific values.

This propagation loss at a fixed distance can change seasonally or daily though. This is caused by the seasonal or daily variations in the factors that affect propagation loss. The major factors that affect propagation loss are water depth, the water's sound speed profile and the acoustic characteristics of the sea bed.

Water depth does not vary significantly with range (distance) on continental shelves but on the continental slopes the water depth does vary significantly with range. This presentation will only consider range independent water depths. Therefore continental slopes are excluded. Shallow water is defined as a body of water with water depth less than two hundred metres.

The water sound speed profile is the major cause of the seasonal and daily changes in propagation loss. Usually it is consistent with range. The seasonal and daily variation in the sound speed is due to the temperature change in the water. The sound speed profiles chosen for this type of survey of propagation loss are ones that are representative for a particular season and representative for an area of one square degree of latitude and longitude.

The sea bed acoustics does affect the propagation loss significantly in shallow water. This is due to the acoustic waves reflecting off the ocean floor more regularly with range than in deep water. The ocean floor acoustic properties are constant with time in terms of years. The dividing of the ocean floor into acoustic bottom zones is a good basis to making propagation loss zones. Within each zone the acoustic properties of the ocean bed are considered relatively constant.

The majority of sea floor data available in the Northern Australian waters is in terms of the grain size distribution of the sediment on the surface of the ocean floor. This data was gathered by the Ocean Science Institute. (There is some other data available for some regions.) This mean grain size distribution is the only data used for dividing the ocean floor into acoustic sea floor zones. This data consisted of a grain size category distribution of gravel, sand, silt, clay and mud. Not all these categories were present in each sample.

The sand category is defined as grains with its diameter between 2 to 0.062 mm. The category of silt is defined as grains with diameters between 0.062 to 0.004 mm and Clay is defined as grains with diameters less than 0.004mm. Gravel is defined as grains with diameters greater than 2mm and mud is defined as grains with diameters less than 0.062 mm.

The definition of the phi value of a particle is the negative of the log to the base 2 of the particle diameter in millimetre [11]. The phi value assigned to the distribution category of gravel, sand, silt, mud and clay were -3, 2, 5, 7 and 12 respectively. The mean distribution grain size of each sample was calculated using these values and the distribution of the categories of each sample.

The region to be surveyed was divided into half degree boxes (1/2 lat by 1/2 long). The averaged mean grain size for a box was calculated by averaging the mean distribution grain size of the samples that were taken at locations within a box. Boxes with similar averaged mean grain size values which were adjoining each other, were grouped together to form an acoustic sea floor zone.

These averaged mean grain size values were converted to seabed acoustic parameters in order to predict or calculate propagation loss. These acoustic parameters required depend upon the model used for predicting propagation loss. For SUPERSNAP (which divides the seabed into two layers, the top layer which is in contact with the water is called the sediment and the lower layer which is called the base rock), the parameters are :- 1) the compressional wave speed profile of the sediment, 2) the compressional wave attenuation of the sediment, 3) the thickness of the sediment, 4) the density of the sediment, 5) the compressional speed of the base rock, 6) the compressional wave attenuation of the base rock, 7) the shear wave speed of the base rock, 8) the shear wave attenuation of the base rock, and 9) the density of the base rock.

A paper by Hamilton [1] was the first premise used, which converted mean grain size values to acoustic parameters of the sea floor. Bachman's [2] revisions of Hamilton's compressional sound velocity equations were used for this paper. Propagation loss was then calculated using the formulas from the above papers to convert averaged mean grain size to acoustic parameters for a homogeneous base rock. There was no sediment used in these calculations as no depth of sediment can be found from the averaged mean grain size. The parameters were inserted into SUPERSNAP for a scenario where experimental propagation loss was measured and recorded in M. Hall report [3] [4]. These experiments were conducted in the region of interest.

The theoretical results produced propagation loss lower than the experimental results. At one particular site in M. Halls report [3], the experimental propagation loss at 10 km for 32 Hz was 110 dB and 80 dB for 500 Hz. At 15 km the 32 Hz propagation loss was so high it could not be recorded but at 500 Hz it was 83 dB. Using Hamilton's results in SUPERSNAP for the site, the results were, that no modes were produced at 32 Hz and for 500Hz at 10km the propagation loss was 73 dB coherent and 67dB incoherent. At 15km for 500Hz the results were 70dB coherent and 71dB incoherent. The averaged mean grain size for this site was 7.4 phi. At another site where the averaged mean grain size was 2.2 phi, the comparison was better. M. Hall report [4] gives 66dB for 32Hz at approximately 10km and 78dB for 500Hz at 10km. Using Hamilton's results in SUPERSNAP the results for 32Hz at 10km were 67.2dB for coherent and 69.4 for incoherent addition of modes. For the 500 Hz case the results were 60.6dB for coherent addition of modes and 64.7dB for incoherent addition.

These results show poor agreement between the models and actual experiment results. This was a common experience at other sites mentioned in M. Hall reports. One possible reason for the poor agreement is shown by a comparison of the mean grain size distribution collected in the Timor Sea to that collected by Hamilton. Hamilton had his samples [6] distributed as shown in Figure 1 on a Clay-Silt-Sand graph. The bureau of mineral resources, geology and geophysics [11] collected samples in the Timor sea whose distributions of grain sizes are also shown in Figure 1. These figures show different grain category distributions but the mean grain sizes of these distributions can be the same. The Timor sea distribution shows a lack of silt and this lack of silt may have an effect on the propagation loss results.

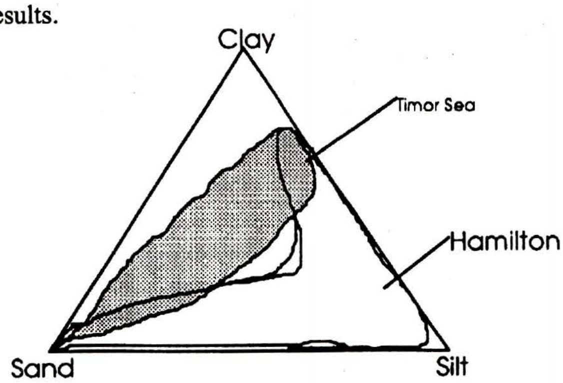

Figure 1: Grain size distributions

The major reason to explain the poor agreement, is that this method does not consider the underlying structure of the sea bed. A reflective sub-layer just beneath the sea floor can reflect a lot of energy back into the water layer. The mean grain size measurements will not take this into account.

The comparison of the transmission loss results shows that Hamilton produced an ocean floor that is more reflective, than what the experimental results show. These results show that the ocean floor is more absorbing of the sound energy than predicted by Hamilton et al. An alternative technique was contrived, to predict a more absorbing ocean floor from mean grain size values, which hopefully would give a better result. The technique was to have the base rock properties as that of Hamilton's paper and a layer of sediment upon the base rock that is a more absorbing material.

This material which is the sediment, was modelled upon the papers of Jenkins[5], Nobes et al [8], Carlson et al [9] and Milholland et al [7]. The method contrived for developing a more absorbent ocean floor used Wood's equation for the sediment's sea floor surface compressional sound speed. This though requires the porosity of the sediment. The porosity of the sediment can be found by the mean grain size. A relationship of porosity verses mean grain size derived from Bachman's [2] empirical formula for the compressional sound speed ratios written in terms of mean grain size and the formula written in terms of porosity.

This relationship is

porosity =0.83922-0.512033*sqrt(0.011054Mg^2-0.23475Mg +1.20595)

where Mg is the mean grain size in phi units and porosity is in fraction that is porous. The sediment density comes from Milholland [7] which has conducted some measurements at deep water sites near New Guinea. This gave the formula as the density in gm/cc of the sediment as 2.68 -1.65*porosity in fraction portion.

The wood's equation is based on the parallel spring model and is given in Nobes et al [8]. It is derived upon the harmonic mean of the spring constants of the particles and water.

Nobes gave the grain wave speed as 4370m/s and the density of the grain material to be 2.68g/cc.

The sediment was modelled with a sound speed profile based upon the equation by Carlson et al [9], which has the compressional sound speed in the sediment varying with depth. The formula presented was Vc(d)=Vc(0)exp(-0.33*d) where Vc(0) is the sediment compressional velocity at the surface. The Vc(d) in the above expression is the sediment sound speed at depth d metres deep in the sediment. This compressional wave velocity of the sediment was restricted to a maximum of the sound speed calculated from Bachman's formulae that is the compressional speed of the base rock. The thickness of the sediment was the depth at which the compressional speed of the sediment reached the base rock's compressional wave speed. The rest of the acoustic parameters remained the same in the sediment as that of the base rock.

This model allowed more energy into the sediment. The results this new model produced for the 7.4 phi value site were for the 10 km:- 112 dB for 32 Hz and 102 dB for 500 Hz, and for the 15 km range, 118.9 dB for 32 Hz and 123 dB for 500 Hz. The 2.2 phi value site produced at 10km were, 76.5 dB coherent modal addition for 32 Hz and 72.7 dB incoherent, and for 500 Hz at 10km, 72.7 dB coherent addition and 64.5 dB incoherent. This type of model does allow more energy into the sediment and increases the propagation loss, but sediment depths are large. This model though, does have some reasonable agreement with the experimental propagation loss measured but it is not in good agreement with the experiment.

The compressional velocity profile of the sea bed is an important parameter to know when calculating propagation loss in shallow water, and it is required to be known to some depth. The error in propagation loss caused by not knowing the compressional sound speed in the sea bed beyond a specific depth depends on the amount of acoustic energy reaches that depth. A.O.Williams [12] investigated the error in the last mode N, if a perfect reflector was placed at a specific depth hn. The major factor, that comes from this paper is that the amount of error is directly proportional to the density ratio of the water over the sediment density. It is also exponentially decays with the unknown depth.

REFERENCES

1. Hamilton, E.L.,(1980), Geoacoustic modeling of the sea floor, J.Acoust. Soc. Am 68, 1313-1340
2. Bachman,R.T.,(1989), Esatimating velocity ratio in marine sediments, J.Acoust.Soc.Am 86,2029-2032
3 Hall,M.V.;Carter,J.C. and Prenc,S. (1992) Shallow Water Transmission Experiments in the Timor and Arafura Seas, DSTO Australia, Technical Report, To be Published
4. Hall, M.V.; Prenc, S. (1993), Measurements and Modelling of Acoustic Transmission Loss in the Timor Sea and the North-West Australian Continential Shelf, Technical Report To be Published
5. Jenkins,C.J. (1991) A review of Seafloor Acoustic Properties for the Tasman Sea and South-west Pacific Univ. Syd. Ocean Sci. Inst. Rep., 45, 1-72.
6. Harris P.T. and Baker E.K. (1988) A review of Seabed sediments, Morphology and acoustic properties of the outer continential shelf and upper slope, northern Australia (Gladstone to Dampier) Univ. Syd. Ocean Sci. Inst. Rep., 33, 1-121.
7. Milholland,P., Manghnani, M.H., Schlanger,S.O. and Sutton,G.H. (1980), Geoacoustic modeling of deep-sea carbonate sediments, J.Acoust.Soc.Am. 68,1351-1360
8 Nobes,D.S.,Villinger,H., Davis,E.E. and Law,L.K.(1986), Estimation of Marine sediment bulk physical properties at depth from seafloor geophysical measurements. J.Geophys.Res 91 14033-14043.
9. Carlson,R.L.,Gangi,A.F. and Snow,K.R. (1986), Empircal reflection travel time versus depth functions for tyhe deep sea sediment columns, J1. Geophys Res.,91 8249-8266.
10. Orsi T.H., (1991) Equations for estimating sound velocity and velocity ratio of marine sediments: Brazil Basin (NW South Atlantic).J.Acoust.Soc.Am. 90, (5) 2851-2853
11. van Andel T.H., Veevers J.J., (1967) Morphology and Sediments of the Timor Sea, Dept. of National Development, Bureau of Mineral Resources, Geology and Geophysics, Bulletin No 83
12. Williams Jr., A.O., (1976) Hidden depths: Acceptable ignorance about ocean bottoms, J.Acoust.Soc.Am 59,1175-1179.

Options for a Database of Audio-Frequency Acoustic Seabed Properties in the Ocean Areas Around Australia

Marshall V Hall
Maritime Operations Division, DSTO Aeronautical and Maritime Research Laboratory
17 Jones Bay Road, Pyrmont, NSW, 2009 Australia

INTRODUCTION

Sonars that are used for detecting vessels such as ships or submarines normally work within the frequency band that extends from a few tens of Hertz to around 10 kHz. This band is similar to the audio-frequency band over which the human ear is sensitive. Audio-frequency sound waves travelling between sonar and target often interact with the seabed, especially at the lower frequencies. At the lower end of the band, sound waves may penetrate 100 m into the seabed and still return to the water column to significantly affect the total transmitted signal. The acoustic properties of the seabed vary significantly with geographic position, depending primarily on whether the seabed is rock, sand, or mud, and whether it is uniform or heavily stratified. In order to predict and optimise the performance of sonars over oceanic regions, it is therefore necessary to possess a geographical database of the parameters that are needed for calculating the amplitude of the sound signals that have interacted with the seabed.

SEA-FLOOR TOPOGRAPHY: PHYSIOGRAPHIC PROVINCES (PP)

The feature of the seabed that was first studied in a widespread manner was its topography or ìreliefî. Heezen and Menard (1963) described the Continental Margin, the Ocean-Basin Floor, and the Mid-Oceanic Ridge as the 3 major topographic features of the ocean floor. These were subdivided into a total of 21 physiographic provinces (PP), of which the following are represented in the nearby waters north of Australia:

- Continental shelf
- Continental slope
- Continental rise
- Abyssal hills
- Abyssal plains
- Plateaus
- Ridge-trench complex
- Ridge-basin complex
- Seamounts and islands.

The first world-wide acoustic database, which was developed by the US Navy in the 1970ís, consisted of charts of the ocean in which the seabed is divided into 9 classes of Bottom reflection Loss (BL). The classes have associated Bottom Loss versus grazing angle functions, curves of which have been presented by Urick (1983). These charts were based on measurements in the North Atlantic of BL at ìhigh-frequenciesî (a few kilohertz). Correlations between BL and PP were observed in the North Atlantic Ocean data, and charts of BL in other oceans were drawn on the basis of these results[1].

SEDIMENT THICKNESS (ST)

Measurements of BL at low frequencies (less than 1 kHz) did not show a correlation with PP, but appeared to correlate with sediment thickness (ST), at least in the North Pacific Ocean (Spofford, 1980). World-wide data on ST became available during the 1970's. In the nearby waters north of Australia for example, the total two-way travel time (TWTT) through the sediment varies from 0.1 sec (in the Argo Abyssal Plain) to 12 sec (off shore near Port Moresby). Initially the seabed was divided into 3 classes, and for each class, curves of BL as a function of grazing angle (for frequencies from 25 to 800 Hz) have been presented by Spofford (1980). The seabed is generally assigned Class 1 (low BL) if the sediment TWTT is at least 0.4 s, Class 2 (medium BL) if TWTT is between 0.2 and 0.4 s, and Class 3 (high BL) if it is a continental shelf or TWTT is less than 0.2 s[2].

REVIEW OF THE PHYSIOGRAPHIC-PROVINCE AND SEDIMENT-THICKNESS ACOUSTIC DATABASES [3]

- All continental shelves are represented by single values for IBHF and IBLF, thus giving the impression that there will be no spatial variation in BL over a continental shelf. Shallow water TL has been found to vary significantly with geographic position however, even when effects due to the surface or water column have been allowed for (Hall and Carter, 1992, and Hall and Tavener, 1994). In addition, the regression equations contained in the US Navy program COLOSSUS indicate a trend for TL (at frequencies greater than 100 Hz) to be greater over mud than over sand seabeds.

• The values for BL predicted by the PP and ST databases do not correlate well with the acoustic measurements that have been made. Ereaux (1994) surveyed acoustic measurements of BL in waters north of Australia that had been reported (primarily by M W Lawrence and coworkers). Results at around 40 locations (for a grazing angle of 15∞ and a frequency of 4 kHz) were noted and compared with the corresponding PP database values for the particular locations. Similarly, results at 16, 63, 250 Hz, and 1 kHz were compared with the corresponding ST database values. As may be seen from Fig. 6 of Ereauxís report, at no frequency is there a significant positive correlation between the measured and predicted values for BL[4] .

SEABED GEOLOGY AND GEOPHYSICS DATABASE

A geological/geophysical database would contain profiles of geological parameters from which geoacoustic parameters could be calculated, and also profiles of geoacoustic parameters obtained geophysically. Calculations of the missing geoacoustic parameters would either use physical models, such as that due to Biot (Stoll, 1989), or regression equations, such as those published by Hamilton (1980) and Bachman (1989).

Two important questions are:

(i) are the models and/or regression equations sufficiently accurate, given a complete description of the geology of the seabed?

It is unfortunately the case that the Biot model currently has little predictive use. Stoll (1989) adds arbitrary corrections to have it yield realistic values for absorption (McCann, 1994). The regression equations obtained by Hamilton and Bachman (for the geoacoustic parameters in terms of geological parameters such as mean grain size, or porosity) all have associated with them large residuals around the mean, sufficient to place an unacceptable uncertainty on the predicted values. For example, from Fig. 19 of Hamilton (1980) it may be seen that for a mean grain size of 2.5 phi, the measured absorption coefficients ranged between a minimum of 0.3 and a maximum of 0.6 dB/km/Hz (a ratio of 2).

(ii) Are there sufficient data spread over the geographic area of interest from which the required acoustic properties may be calculated?.

To address this issue, DSTO funded Dr Chris Jenkins of the University of Sydney to create a geological database for the nearby waters north of Australia. From mid-1993 to early 1994, this database (NAUST6) was applied to determine whether it would enable BL to be predicted with more accuracy than do the PP and ST databases. Algorithms were developed for the reflectivity of a half-space in terms of its grain size or porosity profiles (Hall, 1994), and the resulting values of BL in deep water were compared with measured data (as the other database predictions had been). The findings of the evaluation are described in Ereaux (1994). As may be seen from Fig. 8 in Ereauxís report, there is no significant correlation between the calculations and measurements. One reason for this poor result appears to be the paucity of geological data <u>below</u> the sea-floor (as distinct from the many results at the sea-floor).

In addition, TL has been measured in shallow water at around 24 sites in northern waters (in 1990 and 1993). The acoustic measurements were supplemented by oceanographic data and samples of sediment. The TL results have been compared with calculations based on the mean grain size of the sediment samples and Hamilton/Bachman regression equations. As reported by Hall and Carter (1992) and Hall and Tavener (1994), the calculated values for TL were found to be generally poor indicators of the measured results. One reason for this is considered to be that the sediment is unlikely to be uniform. Based on the small number of cores that have been taken over the northwest continental shelf as a whole, it seems likely that the sedimentís mean grain size will vary significantly in the first metre or two beneath the sea-floor. Large tracts of the North-west shelf, for example, consist of a pavement of limestone overlain by a sand layer whose thickness varies between zero and a metre (Jones, 1973).

DATABASE OF ACOUSTIC PARAMETERS ESTIMATED USING "MATCHED TL PROCESSING"

Geoacoustic profiles can be derived from Transmission Loss [TL] measurements using "matched TL processing" to minimise the RMS error between predicted and measured values for TL at a given position (Chapman, 1994). DSTO's measurements of TL can be utilised if they are analysed by an inverse process to yield a database of "effective geoacoustic profiles" (EGAPís). Not all TL data are eligible to make a contribution to this process, since for seismic studies to be useful, the source and receiver should be close to or on the sea-floor, and the region to be studied must be carefully selected so as to contain little horizontal variation (Whitmarsh, 1994). There is also the problem of non-uniqueness: the likelihood that more than one equally valid EGAP may exist for a given set of TL data at any position. In addition, the calculated EGAP will depend on the TL model used to obtain it, especially if incoherent scattering had been a significant component of the measurements. There would also be a large measurement program to fill in the geographic gaps that have been left by the (many) measurements made so far. In spite of these problems, it seems that overall this kind of database would be more accurate than those based on topography or geology have been.

REFERENCES

Bachman R T (1989) Estimating velocity ratio in marine sediment. Journal of the Acoustical Society of America 86, 2029 - 2032.

Chapman N R (1994). Personal communication.

Ereaux K (1994) NAUST Database Evaluation (unpublished Contractor Report). Sydney: DSTO Materials Research Laboratory.

Hall M (1994) Program DBASE-BL (unpublished DSTO Computer program)

Hall M V and Carter J (1992) Measurements and modelling of acoustic Transmission Loss in the Timor and Arafura Seas (unpublished DSTO manuscript)

Hall M V and Tavener S (1994) Measurements and modelling of acoustic Transmission Loss in the Timor Sea and the North West Australian Continental Shelf (unpublished DSTO manuscript)

Hamilton E L (1980) Geoacoustic Modeling of the Sea Floor. Journal of the Acoustical Society of America 68, 1313 - 1340.

Heezen B C and Menard H W (1963) 12. Topography of the deep-sea floor. In M N Hill (Editor), The Sea - Ideas and observations on progress in the study of the seas. Volume 3 The Earth beneath the Sea - History. New York and London: Interscience Publishers.

Jones H A (1973). Marine geology of the northwest Australian continental shelf (Bulletin No. 136). Canberra: Bureau of Mineral Resources, Geology and Geophysics.

McCann C (1994) [University of Reading, England]. Private communication.

Spofford C W (1980) Interim Bottom-Loss values and geographic assignment based upon sediment thickness (unpublished manuscript)

Stoll R D (1989) Sediment Acoustics. Berlin: Springer Verlag.

Whitmarsh R B (1994) [Institute of Oceanographic Sciences, Wormley, England]. Personal communication.

---

[1] In the FACT and RAYMODE Transmission Loss (TL) programs, these classes are denoted by the parameters IBHF and BOTNUM respectively (both are integers from 1 to 9).

[2] In the FACT program, these classes are denoted by the parameter IBLF. RAYMODE does not have a facility for using IBLF (at low frequencies, it uses smooth profiles of the geoacoustic parameters density, compressional sound-speed and compressional absorption).

[3] These databases are known in the Australian Navy as the "Tactical Environmental Support System (TESS) BL Database"

[4] Several measured BLís reported have an unphysical negative value (eg. -10 dB), particularly at the lower frequencies. This phenomenon occurred because in the analysis of the measured signals, the rays that had been refracted within the seabed were interpreted as having being reflected at the sea-floor.(In deep water, rays that penetrate a highly porous seabed are refracted by the sound-speed gradient and return to the water column where they form a caustic, a narrow region of high intensity. At low frequencies, less than 50 Hz say, such rays can dominate the rays reflected at the sea-floor.) There is thus a problem in comparing TESS and measured values for BL, but this should not substantially reduce the value of the correlation between these two parameters. In modelling seabed interaction, FACT treats only the reflection at the sea-floor and neglects rays that penetrate the sediment.

Application of a Database/GIS of Australian Seafloor Properties to Naval Acoustic Modelling

CJ Jenkins & GA Rawson
Ocean Sciences Institute, Sydney University

It is clear from theoretical work and a large body of experimental data that the acoustic properties of the seafloor vary with textural, compositional and structural changes to seabed materials. It seems plausible then, that a classification of the acoustics useful to naval operations could be drawn from a database of seafloor properties using tools like Geographic Information Systems (GIS). Despite some significant successes, a number of at-sea experimental results indicate that the endeavour is still in early stages. Since 1989, OSI has been steadily constructing a database of Australian seafloor properties, which now includes information on sediment textures, compositions, acoustic and geotechnical properties and seafloor structure for over 10000 sample sites. The project is a joint one with the RAN AODC, but addresses also the needs of the offshore engineering, environmental management and geoscience research. The database is has a relatively mature structure and is equipped with tools of dictionary, units conformance, reformatting and modelling; the addition of new data, quality checking and software refinements is a continuing process.

Several groups are currently using the OSI AUSEABED database for modelling acoustic interaction but they adopt different approaches (see other papers, this conference). A crucial question at this stage is the form of the outputs from such modelling, whether: (i) acoustic seafloor classification, (ii) models of the acoustic response along defined tracks; or (iii) maps of navy operational factors such as the detection "shadow zones" around vessels. These formats/approaches are linked, since the classifications need to be verified by range experiments, which in turn feed into operational products.

At OSI we have briefly investigated how the database might be used for naval acoustics, with the following steps: (i) draw on AUSEABED for surface sediment data on textures, presence of rock, carbonate contents, porosities etc., with enhancement of the raw database using look-up-tables based on Hamilton, Stoll, the ODP, etc.; (ii) use the down-core data to assess the variability of sediment textures and properties in general as a function of water depth and land proximity in different sectors of the seabed; (iii) apply that variability expressed as a variance to the surficial data to model the sub-seabed properties of regions; (iv) apply Biot theory (Stoll descriptions) to that sub-seabed models to obtain basic acoustic parameters; (v) apply certain seabed roughness scales, water column sound velocities and seafloor gradient data (from bathymetry); (vii) run a simple acoustic prediction model for a semi-quantitative value of acoustic response at several frequencies and grazing angles.

Obviously, there is a great deal of modelling involved in the process. Actual ground-testing is required and will probably suggest major alterations to find the most appropriate method of modelling. Furthermore, the results will be applicable only on regional scales. As the AUSEABED database matures we look forward to decreasing the importance of modelling relative to actal data, and also to improving the closeness of the modelled and experimental data.

Measurement of Acoustic Properties of Marine Sediments

J.I.Dunlop and P. Thomson
School of Physics, University of New South Wales, Sydney 2153

Mathematical models for characterising the propagation of acoustic signals in shallow water require an understanding of the acoustic properties of the sea-floor. These models generally require as input values such acoustic properties of the seabed sediments as sound speeds and attenuation constants and, particularly for the more sophisticated models, values for shear wave velocity and attenuation. There are considerable difficulties in measuring these properties due to a lack of suitable techniques and to the remoteness and inaccessibility of the seabed. Much work has therefore been done making measurements of these properties on laboratory samples extracted from the seabed (Hamilton 1980, Richardson 1994). These are then related to such physical properties of the sediment as density, grain size etc. (Backmann 1985) in the hope that acoustic characteristics can be predicted from the geological features of the seabed.. There are however considerable uncertainties in these procedures, particularly in the accuracy and precision of these predictions and there usefulness to propagation models.

Most propagation models are related to low frequency propagation and as most of the acoustic parameters are frequency dependent there are often discrepancies between laboratory measurement procedures and the requirements of the mathematical models. There is also the ever present problem of sediment disturbances due to the sampling process. This can range from slight in the case of a simple sleeve sample from a soft surface sediment to severe in the case of a grab sample from the depths. The effect of the former problem can be corrected for to some extent using theories of sediment propagation such as Biot's (Dunlop 1989) but the latter problem appears insoluble.

In this paper we examine prevailing measurement techniques and their application to a selection of samples from the Australian continental shelves.

LABORATORY TECHNIQUES

Sound speed may be readily determined from measurements of the transit times of acoustic pulses through a length of sediment. The need for high precision in values of sound speed (better than 1%) requires that the acoustic signal be a high frequency wave packet (usually several hundred kilohertz) with its corresponding short rise time. The inaccuracy of the length measurement can be overcome by making comparative measurements in sediment and interstitial fluid. Low frquency measurements are more difficult — there being an unacceptable loss of precision for pulse measurements below 30 kHz. An impedance tube technique (Dunlop 1992) working at 1 kHz suffered similar lack of precision.

Determination of sound attenuation may be measured with the same high frequency pulse techniques to an acceptable precision (5%). The impedance tube technique offers the same precision at an attractive lower frequency, but is best suited to in-situ measurement.

Shear wave speed may be measured with a similar pulse transit timing. The frequencies that may be used are much lower (1 kHz) and the precisions acceptable due to the usually low shear wave speed in sediments. Shear wave speed in a well defined section of seafloor sediment can also be determined from in-situ or large tank Scholte wave experiments(Jessup et al 1994).

MEASUREMENT EQUIPMENT

Three piezoelectric transducers of 340 kHz resonance frequency were fabricated into a speed measurement frame as indicated in Fig 1. The electric signal, a wave packet at the resonance frequency, was applied to the transmitter and the signals received at the receivers was captured and displayed in a digital recorder. The time interval between the signals of about 20 us corresponding to a transit distance of 50 mm could be measured to a precision of 0.05 us. The accuracy of the technique was calibrated using measurements on water at different temperatures and found to be about 0.2 %

The magnitudes of the two signals was used to determine the acoustic attenuation constant of the propagation medium. The accuracy of the technique was calibrated using measurements on glycerol, the attenuation in which may be determined from its viscosity, and found to be about 5 %.

Sound Speed Frame

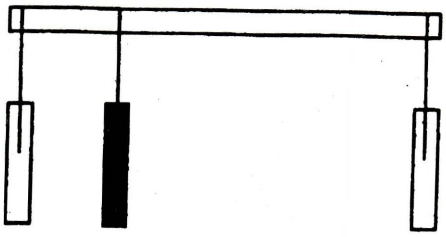

Figure 1.

Shear wave measurements were made using a similar measurement frame and piezo electric transducers of 1 kHz resonance frequency. Considerable difficulties were experienced with this measurement due to two factors. Firstly a strong dilatational signal was produced in addition to the shear signal and reverberated in the medium. Thus separation (in time) of the two signals was required, a successful example of which is shown in Fig. 2. The accuracy of the technique was calibrated from measurements on jelly, the shear modulus of which could be measured using tensile testing equipment. The accuracy was found to be about 10 %. The second problem relates to the coupling of the transducers to the medium. This was so non-reproducible that it was difficult to measure signal magnitudes with any certainty and thus prevented any accurate measurement of shear wave attenuation constants.

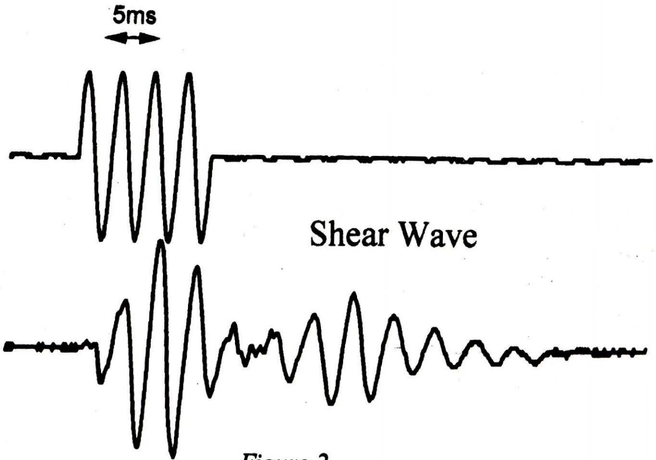

Figure 2.

MEASUREMENTS

Core samples taken from several shallow water sites in Australia's northern waters were investigated and the three acoustic parameters measured at different positions in the cores corresponding to different depths. The geological properties and history of the samples had been well documented at the Ocean Science Institute of the University of Sydney. These properties were then used to correct the measurements for frequency.

CORRECTIONS TO HIGH FREQUENCY MEASUREMENTS

Both sound speed and attenuation constant are dependent on the frequency of measurement, showing dispersion in a transition frequency zone controlled primarily by the fluid permeability of the sediment (Dunlop 1989). The measurement frequency of 330 kHz can be considered to be in the high frequency regime for almost all sediments. Sediment properties corrected to the low frequency regime would describe the properties at frequencies below from 5 kHz for coarse sand to frequencies below say 30 kHz for finer sediments such as clay silts.

The correction procedures involve appplication of Biot theory with suitable values substituted for the critical parameters: structure factor (g), which accounts for the apparent increase in fluid inertia caused by random orientation of the pores in the sediment, and permeability to fluid flow (k) — both estimated from the porosity of the sediment and grain size analysis; skeletal frame modulus — estimated from the shear modulus of the sediment, obtainable from its shear velocity speed and porosity.

REFERENCES

Bachman R.T. (1985) "Acoustic and physical relationships in marine sediments", J. Acoust. Soc. Am., 78, 616-621.

Dunlop J.I. (1989) "Propagation of acoustic waves in marine sediments: a review", Exploration Geophysics, 19, 523-535.

Dunlop J.I. (1992) "Measurement of acoustic attenuation in marine sediments by impedance tube", J. Acoust. Soc. Am.,91, 460-469.

Hamilton E.L. (1980) "Geoacoustic modelling of the seafloor", J. Acoust. Soc. Am 68, 1313-1340.

Jessup B.L., Lee L., Kimura M. & Dunlop J.I. (1994) "Wave propagation in the shallow water environment", Proceedings of Conference "Acoustic classification and mapping of the seabed", Inst. of Acoustics, Bath, U.K. p287-294.

Richardson M. (1994) "On the use of acoustic impedance values to determine sediment properties", Proceedings of Conference "Acoustic classification and mapping of the seabed", Inst. of Acoustics, Bath, U.K. p15-24.

ISSAMS: An In Situ Sediment Acoustic Measurement System

Michael D. Richardson
Marine Geosciences Division, Naval Research Laboratory
Stennis Space Center, MS 39529-5004 USA

Sean R. Griffin and Francis B Grosz
Omni Technologies, Inc., Metaire, LA 7001 USA

INTRODUCTION

Knowledge of sediment geoacoustic properties is of fundamental importance for prediction of stability of marine slopes, consolidation behavior of sediments, strength of marine foundations, mine burial, and scattering and propagation of acoustic energy from and within sediments. In the past, near surface sediment geoacoustic properties have been measured in situ using probes deployed by scuba divers, from research submersibles and remotely from surface ships; between and down boreholes using explosive and various vibratory techniques; with various seismic reflection and refraction techniques; from direct path and inversion measurement of surface waves; and in the laboratory using geotechnical techniques related to the stress/strain behavior of sediments.

It is our intent to develop a remote method to measure in-situ shear and compressional wave velocities and attenuation in surficial marine sediments. It is within this surficial zone (upper 50 cm of sediment) that the most active and rapid diagenetic changes in sediment properties occur. ISSAMS, as described herein, is capable of making rapid, direct in-situ measurements of sediment geoacoustic properties in the upper 50 cm of shallow-water marine sediments. We have included information on early development stages to justify the current measurement configuration and will present concepts for further development.

ISSAMS has passed through five developmental stages. During the first stage, individual probes were tested to determine beam pattern, frequency response, signal attenuation, and coupling characteristics within the sediment. During second stage, we tested for potential acoustic coupling between probes and the deployment frame, and determined probe penetration resistance within the sediment. The scuba diver deployed third stage was used to test the measurement system in a range of sediments commonly found on the continental shelf, including soft muds, hard packed sands and loose gravels. The fourth stage was a diver-independent shallow-water geoacoustic measurement system which was hardwired to surface electronics via a 100 m electro-mechanical cable. In this system, probes were driven into the sediment by self weight. The current version of ISSAMS was developed by Naval Research Laboratory (NRL) to allow rapid, remote collection of in-situ sediment geoacoustic data. ISSAMS has the capability to remotely measure sediment shear and compressional wave velocity and attenuation, near bottom water conductivity, temperature and depth and to provide live video of system operations. Acoustic velocity and attenuation measurements are made using a pulse technique with shear and compressional wave probes separated at distances from 40 to 110 cm. Water conductivity, temperature and depth measurements are made using a Seabird CTD and live video is provided by two underwater cameras. All data is collected by remote electronics and displayed in real-time by topside electronics. One of the primary advantages of ISSAMS is that the system can be deployed without divers as previous systems have required, allowing measurements to be made at greater depths (up to 300 meters) and with greater frequency. The next version of ISSAMS will include additional geotechnical measurement capabilities including sediment electrical resistivity, penetration resistance and pore pressure.

ISSAMS MECHANICAL DESCRIPTION:

ISSAMS is an aluminum and stainless steel structure used to hydraulically deploy geoacoustic and geotechnical measurement probes in coastal marine sediments. The large size (3 m high, 2 m square footprint) and weight (approximately 1 metric ton) is required to make measurements over the variety of sediments found in coastal marine waters (Fig. 1). The outer frame acts as a guide for a hydraulically driven inner frame to which 4 compressional and 4 shear wave probes are mounted. The inner frame has a 60 cm stroke allowing the probes to be completely drawn into the protective outer frame at any time during deployment. Once the ISSAMS is placed on the seafloor, probes are pushed into the sediment at depths ranging between 0 to 50 cm. This allows for gradient measurements to be obtained. The inner frame allows for probe mounting separations of between 40 and 110 cm. Around the entire base of the structure is a 30 cm wide plate which serves a dual purpose. When ISSAMS is deployed on a soft mud, this plate increases the surface area to better distribute weight and keep ISSAMS from sinking into the sediment. On hard packed sands, however, additional weight may have to be attached to the plate to help insert the 8 geoacoustic probes into the sediment.

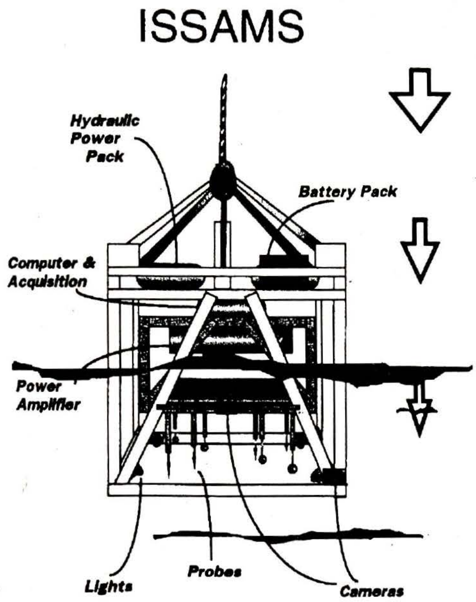

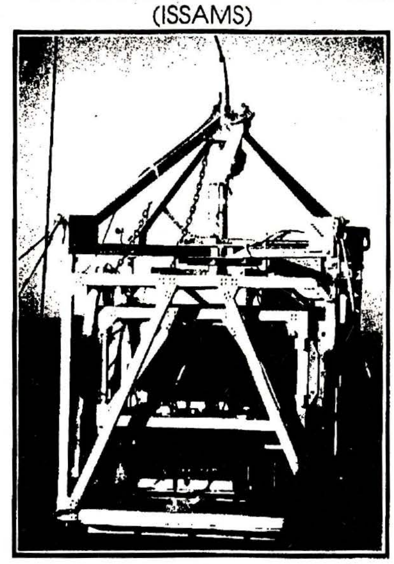

Figure 1. Simplified drawing and photograph of the In Situ Acoustic Measurement System (ISSAMS)

ISSAMS ELECTRONICS:

ISSAMS electronics consists of both top side and bottom side electronic suites connected by a single, electro-mechanical coaxial cable. The top side system provides remote control, system power, storage and display. An IBM compatible computer system provides control, display, signal analysis and storage. Standard NTSC color television and VCR are used to display and store real-time video of the deployment of the system and movement of the probes into the sediment. A commercially available 20 amp, 200 VDC switching power supply is used to provide 150 VDC power to the bottom side electronics. The only custom components are a low-pass filter to reduce power supply switching noise and an interface box which combines/separates data, video and 150 VDC power. The interface box accepts filtered 150 VDC power and a RS-422 data stream from the top side computer, converts the RS-422 to FSK and then combines the two signals. Output from the interface box is RS-422 data converted from the bottom side FSK signal and NTSC video on a 64 MHz carrier (channel 3). A custom written software program integrates the system operation.

The ISSAMS bottom side electronics consists of a hydraulic power pack, bottom side interface electronics, Seabird CTD, black and white camera, color camera, a 24 VDC sea battery, computer system and power amplifier. Most bottom side electronics are housed in 4 pressure canisters. The sea battery, the CTD and the cameras are separate commercially available units for which interfaces have been developed. The hydraulic power pack consists of a 24 VDC powered, hydraulic motor located in a pressure canister. Control commands from the top side are received by the bottom side computer which controls the hydraulic motor. Position feedback information is provided by a potentiometer built into the hydraulic cylinder. Limit switches are located at the top and bottom stroke of the inner frame to stop the frame from moving past preset positions. An additional feature of the hydraulics system is automatic retraction of the probes from sediment if the 150 VDC top side power is lost. This is a safety mechanism to protect the probes from being destroyed if an electronics failure occurs when the probes are in the sediment. Power to run the hydraulic motor is provided by the sea battery.

The interface electronics consists of an assortment of electronics. Included in this canister is a FSK modem, hydraulic control relays, DC-DC power converters, video amplifiers and video modulators. The FSK modem converts the RS-422 data from the bottom side computer to a FSK signal and converts the FSK signal from the top side computer to a RS-422 data stream that the bottom side computer accepts. The DC-DC power converters down convert the 150 VDC to the various DC voltages required by the bottom side electronics. The hydraulic control relays perform the hydraulic control discussed in the above paragraph. These are not included in the cylinder with the hydraulic motor due to the flammable nature of the hydraulic fluid. Lastly, the video modulators and video amplifiers condition the signals from the cameras for transmission to the top side. Control circuitry selects the desired camera since the color camera is pointed downward to provide a view of the sediment and the black and white camera is directed horizontally to provide a view of probe position.

The amplifier electronics is housed in a separate canister. Programmable gain amplifiers (0 - 60 dB) are used to amplify the probe received signals. This is in addition to the 40 dB of gain that each probe's preamplifier provides. Transmit probes are driven by a 350 watt power amplifier. These amplifiers are conduction cooled to prevent thermal damage.

The bottom side digital electronics system controls the functionality of ISSAMS. This unit contains a function generator, two 12-bit, 1 Msample/second A/Ds, one low speed, 12-bit A/D a parallel I/O card and an IBM PC compatible computer system. The software running on this computer can control the pulse length, frequency and amplitude of the transmitted shear or compressional wave signals. Signals from 20 Hz to 100 kHz are synthesized by the function generator. The receive sample rate can be adjusted from 1 ksample/second to 1 Msample/second. The high speed A/Ds are simultaneously triggered with the function generator to provide an accurate signal velocity measurement. RS-232 serial communications is used to collect data from the CTD. The parallel I/O and low speed A/D are used to provide feedback and control of the ISSAMS subsystems.

ISSAMS PROBES:

ISSAMS uses a single radial-poled ceramic element in each of the 4 compressional wave probes. The compressional wave probes have a modular design which allows for easy repair and for the use of probe tips made of different materials (Fig. 2). The current probes have a resonant frequency of 58 kHz which is the frequency which most measurements are made. Both transmit and receive compressional wave probes are identical except for a 40 dB gain pre-amplifier in the receive probes.

The shear wave probes used on ISSAMS are single, bimorph bender elements potted in a stainless steel frame with soft urethane (Fig. 2). A thin, higher derometer polyurethane is used as a resilient outer coating to protect the ceramic during insertion. Transmit and receive shear wave probes are identical, except for a 40 dB gain pre-amp located in the receive probes. Frequencies from 70 Hz to 2 kHz are used to make measurements with these probes. The shear probes are mounted to the ISSAMS frame using a neoprene filled mount to reduce mechanical coupling between transmit and receive shear wave probes.

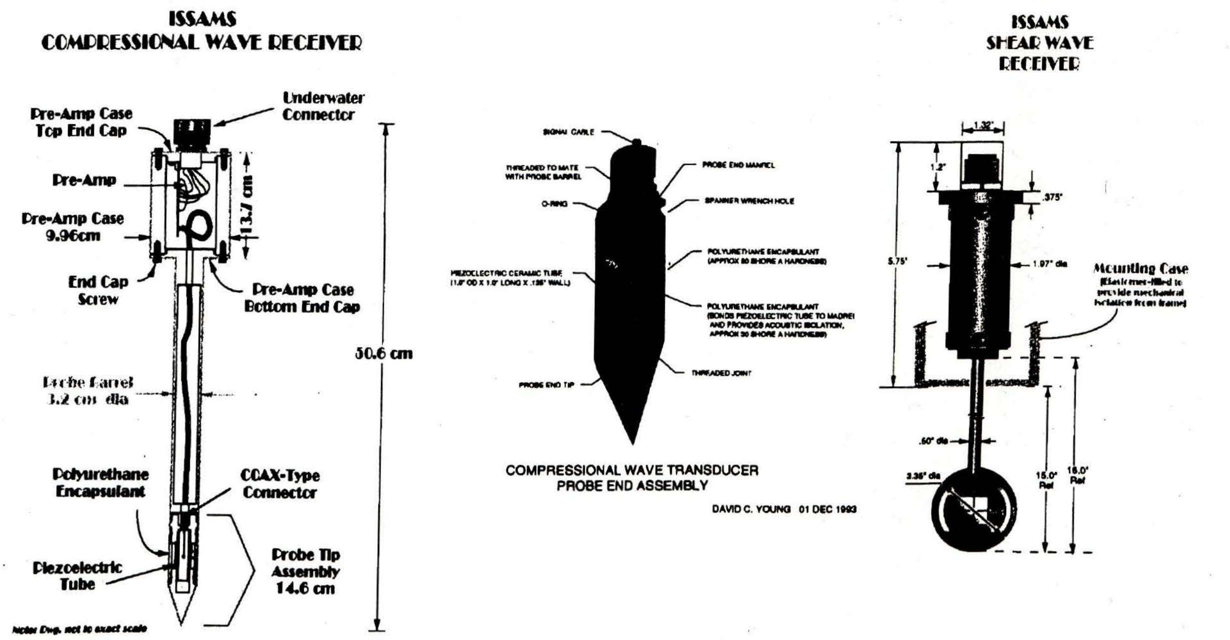

Figure 2. Mechanical drawings of ISSAMS compressional and shear wave probes

ISSAMS DATA:

Examples of shear and compressional wave signals will be provided along with the methodology and equations used to calculate sediment geoacoustic properties. Plots of CTD data will be included. In addition, top and bottom side video from the Kiel, Germany deployment of ISSAMS will be shown.

Global Acoustic Propagation

W. A. Kuperman
University of California, San Diego, Scripps Institution of Oceanography, La Jolla, CA 92093-0701

Global propagation in the oceans was demonstrated in a 1960 Perth to Bermuda Experiment [1,2]. Acoustic models have subsequently shown their capability to model propagation over such antipodal propagation paths. That sound deterministically propagates such long distances has encouraged scientists to propose global tomographic schemes. A controlled source experiment, the Heard Island Feasibility Test (HIFT) [3,4] organized by Walter Munk and collaborators demonstrated that coherent signals could be detected utilizing gain from pulse compression signal processing schemes. HIFT preceded and motivated the present efforts to develop a global network of acoustic sources and receivers for the purpose of measuring global warming and possibly other large scale geophysical phenomena. This global tomograhic effort, Acoustic Thermometry of the Ocean (ATOC), seeks to utilize long range acoustic paths to average over mesoscale ocean phenomena and measure warming via acoustic travel times. Central to these aims, an ability to accurately model long range ocean acoustic propagation is necessary. That the acoustic modeling field [5] is growing in sophistication can be illustrated by a recent ambitious modeling attempt. A global acoustic model was applied to predicting the planetary scale acoustic propagation excited on Jupiter by the impact of the Comet Shoemaker-Levy 9 [6]. Below is a parochial summary of some recent work in the area of global acoustics to be presented in this talk.

Approximately 13000 s after the detonation of each TNT charge near Perth, a pair of arrivals separated by approximately 30 s was recorded on the Bermuda receivers. Adiabatic mode theory was used to calculate phase speeds (c(n), n=1,2...) for local modes as a function of latitude and longitude from existing ocean data bases. From c(n) and Snell's law, we find the horizontal path taken by mode n. The three-dimensional acoustic wave field may be represented as a sum over normal modes each possessing two-dimensional (horizontal) propagation characteristics. Adiabatic mode theory assumes that the ocean waveguide varies so slowly in the horizontal that energy in mode n at a given location remains totally in mode n as the signal propagates through the waveguide. Calculation of the vertical normal modes yields the horizontal phase speed for each mode including dependencies on ocean and bathymetric parameters.

Upon integration of the ray equations (on the non spherical earth surface) derivable from adiabatic normal mode theory [2], it was found that each of the several modes possesses multiple eigenray solutions for the Perth-Bermuda path. Thirty years after the experiment, this most recent analysis produced the following unexpected but quantitatively sound interpretation of the Perth-Bermuda experiment: The first of each double arrival is a signal along a shorter and faster northern path, with the second being along a longer and slower southern path. The pulse widths at the receiver are consistent with the calculated levels of dispersion in the ocean waveguide along the propagation path. Computed time of arrivals were within 5 s (the experimental accuracy) of the 13360 stime of propagation.

The parabolic equation (PE) method [7] which accounts for coupling of energy between modes involves approximating the full wave equation with a one-way wave equation that may be solved efficiently. The PE method is accurate because its assumptions about how sound propagates are generally applicable to the ocean: energy is mostly outgoing and the speed of sound varies gradually with horizontal directions. For a hybrid global propagation modeling approach, once the horizontal propagation paths are determined, the PE model can be used to solve for the outgoing wave field in the two-dimensional space defined by depth and horizontal range along the propagation path. This approach provided computational predictions consistent with the recent HIFT experimental results [8]. In particular, mode coupling (as determined by projecting PE results onto local normal modes) caused by the acoustic interaction with the Antarctic Circumpolar Current and/or bathymetry, for example, at the New Zealand Plateau were significant factors in accurately explaining observations at both point receivers as well as arrays.

Recent progress in global acoustic modeling have taken some novel directions. An adiabatic PE method [9,10] was developed that solves the horizontal equation for each mode with the PE method rather than the above mentioned ray like computation. An attempt to extend this approach to develop a coupled mode PE is underway. Such a model would include horizontal redirection of modes which are generated along a path because of a bathymetrically and/or an oceanographically caused mode coupling interaction. Modal representations have an advantage in attempts to model pulse propagation. That is because the modes, being the fundamental constituents of the field, tend to be the quantities that are most interpolatable across frequency.

The most ambitious application of global modeling was an attempt to predict acoustic effects of the Jovian impact of the Comet Shoemaker-Levy 9 [6]. The comet fragments were expected to explode in an atmospheric deep sound channel with 900 m/s sound speed minimum. Initial infrared measurements indicated a circular ring expanding at a rate of about 900 m/s. The main Jovian environmental factor expected to dominate propagation is the zonal reversing wind structure in the atmosphere. Modeling predicts that the far field will be dominated by the effect that energy in the sound channel will be pinched into well defined beams formed in wind cells to the east and west of the impact cites. Though not yet observed in preliminary analysis not aimed at detecting this phenomena, the fact that a wave with an acoustic speed was detected provides hope that interplanetary acoustic tomography is not just a whimsical thought.

REFERENCES

[1] W. H. Munk. W.C. O'Reilly, and J.L. Reid, "Australia-Bermuda sound transmission expeeriment (1960) revisited," J. Phys. Oceano. 18. 1976 (1988).

[2] K. D. Heaney, W. A. Kuperman, and B. E. McDonald, "Perth-

Bermuda sound propagation (1960): Adiabatic mode interpretation," J. Acoust. Soc. Am. 90, 2586 (1991).

[3] A. B. Baggeroer and W. Munk, "The Heard Island Feasibility Test," Physics Today 45(9), 22 (1992).

[4] W. Munk et al: A series of papers in the October 1994 issue of the Journal of the Acoustical Society of America

[5] F. B. Jensen, W. A. Kuperman, M. B. Porter and H. Schmidt, "Computational Ocean Acoustics," AIP Press, New York (1994). [ISBN 1-56396-2090-8].

[6] M. D. Collins, B.E. McDonald, W. A. Kuperman, and W. L. Siegmann, "Jovian acoustics and Comet Shoemaker-Levy-9" J. Acoust. Soc. Am., submitted, 1994.

[7] M. D. Collins, "A split-step Pade' solution for the parabolic equation method," J. Acoust. Soc. Am. 93, 1736-1742 (1993)

[8] B.E. McDonald, M.D. Collins, W.A. Kuperman, and K.D. Heaney, "Comparison of Data and Model Predictions for Heard Island Acoustic Transmissions," J. Acoust. Soc. Am. 96, 2357-2370 (1994).

[9] M.D. Collins, "The Adiabatic Mode Parabolic Equation," J. Acoust. Soc. Am. 94, 2269-2278 (1993).

[10] M. D. Collins, B. E. McDonald, K. D. Heaney, and W. A. Kuperman, "Three-dimensional effects in global acoustics," J. Acoust. Soc. Am., submitted, 1994.

Techniques for Measuring the Minimum Detectable Signal in a Passive Sonar Processor

R. L. Dawe, A. Grigorakis and E. J. Parker
Maritime Operations Division, Aeronautical and Maritime Research Laboratory,
Defence Science and Technology Organisation, P.O. Box 1500, Salisbury S.A. 5108, Australia.

1. INTRODUCTION

The work described here was part of a project undertaken by the Defence Science and Technology Organisation, which had the aim of measuring the end-to-end performance of passive sonar processing systems under controlled conditions. This would enable operators to quantify the current performance of a sonar system and to allow quantification of the effect of changes in the system due to software upgrades and hardware alterations.

Three methods of measuring the minimum detectable signal (MDS) were developed and then applied to an experimental sonar processing system which had been configured for use in detecting omnidirectional narrowband signals against a variable background of noise.

2. EQUIPMENT AND PROCEDURE

Test data was introduced to the processor via an RF signal generator at a level which ensured that the receivers did not overload and that added electronic noise was low. The signal was FM demodulated, processed and the results finally presented on either a video display or hard copy device. The signal to noise ratio (SNR) at the receiver was taken as being the same as that at the input to the modulator of the RF signal generator, which contributed negligible noise.

A sampling rate of 1600 Hz was used as well as analogue to digital (A/D) conversion to 10 bits. Time domain automatic gain control on the radio receiver output kept the signal and noise within the A/D converter's range. A Hanning window was applied prior to all FFT analyses. A spectral automatic gain control process, effectively display whitening, was applied to both video screens and printouts. The displays showed relative power levels as a grey scale plotted on a time versus frequency graph.

Two separate tests were performed. The first test, designated MDS1, used white noise and covered a frequency band arbitrarily set at 600 Hz wide. The second test, designated MDS2, used shaped noise to more closely simulate typical sea noise and covered the same frequency band as test MDS1. The shaped noise was a simulation of passing Urick's interpretation of noise characteristic of sea state 3 with medium shipping through an omnidirectional sonobuoy and demodulating with a flat response receiver. Tests MDS1 and MDS2 were each divided into 12 sessions, with each session consisting of 14 one minute periods, hereafter called 'sets'. The task of the test subjects was to identify by observation of the video displays, using agreed guidelines, what narrowband signal frequencies were present in each set.

The first two sets of each session constitute complete tests in themselves and were included in order to develop a quick performance test. For the first set of each session, called the Staircase set, 12 sinusoidal signals approximately evenly spread across the test frequency band were used, as shown in figure 1(a). The SNRs of the adjacent signals increased by 1 dB with increasing frequency. The second set of each session, called the Random Stair set, used 12 sinusoidal signals having the same SNRs as the Staircase set but having their frequencies randomly spread across the test band, as shown in figure 1(b).

Each of the remaining twelve sets, called Equal SNR Random Frequency (ESRF) sets, used a number of sinusoidal tones of equal SNR randomly spread across the test frequency band, as shown in figure 1(c). The SNR was different for each of the ESRF sets. These twelve sets covered approximately the same SNR range as the Staircase and Random Stair sets, and provided at least 50 samples at each SNR per test subject. The number of tones used in each ESRF set varied randomly between 6 and 12.

To avoid edge effects the pixels near each end of the video display did not contain signal lines. Signal duration was 60 seconds in all cases, with a break of approximately 8 seconds between sets of signals to allow separation of test formats to be visible to the subjects and to prevent data overlap during the data integration time in the processor.

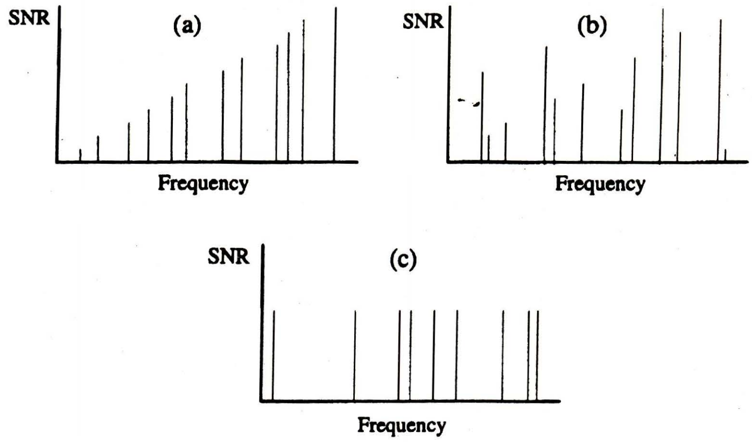

Figure 1. Sample SNRs used for each of the three measurement techniques: (a) is the Staircase set, (b) is the Random Stair set and (c) shows one of twelve ESRF sets.

The signal to noise ratio (SNR) is the ratio, expressed in dB, of the mean signal power of a single tone to the mean spectral density of the noise at the frequency of the tone. The minimum detectable signal (MDS) is the SNR at the receiver input corresponding to a given probability of detection (PD) and probability of false alarm (PFA). In this experiment MDS values have been referred to PD=50% for a signal tone and PFA=0.01%.

For the Staircase and Random Stair methods it was assumed that the expected number of lines detected would be a linear function of the MDS (measured in decibels), such that each additional line detected would be indicative of a 1 dB lower MDS. With a correction to normalise to a false alarm rate (FAR) of 1 in 10000, this could be expressed in dB as, $MDS = M + 1 - N + C_f$, where M is the maximum SNR (dB), N is the number of lines correctly detected and C_f is a correction factor which may be obtained from figure 2. The correction factor C_f arises because any value of MDS must be quoted for specific pairs of values of PD and PFA. Such a correction allowed all values of MDS to be compared using a common basis, even though different test subjects had different FARs during the experiment.

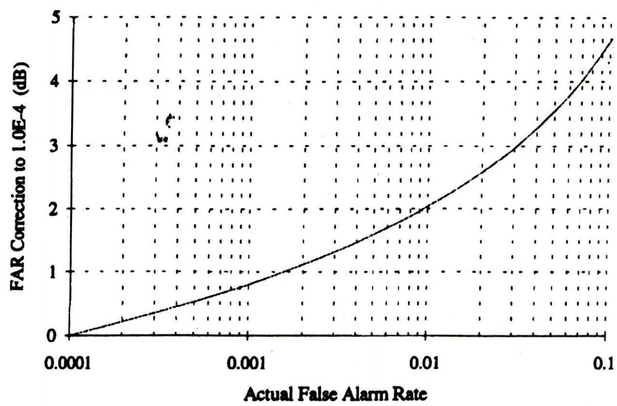

Figure 2. MDS correction for false alarm rate, assuming a Gaussian distribution.

The false alarm rate, FAR, was determined for each test subject by dividing the number of false alarms by the number of opportunities for a false alarm. On each display there were L signal lines (tones) superimposed on the noise background, with each line having a frequency tolerance bandwidth of β. As L varied from display to display in the ESRF part of this experiment and 666 pixels were available to contain signal lines, then the approximate number of opportunities for a false alarm was given by 666 - βL_{av}, where L_{av} is the average number of signal lines generated per display. For the Staircase and Random Stair $L_{av} = 12$ in each case, while $L_{av} = 9$ for the ESRF method. The tolerance bandwidth β, measured in pixels, is due to the line marking uncertainty and fuzziness arising from statistical noise fluctuations. In this experiment a value of 14.7 for was used in both the MDS1 and MDS2 tests. Hence the FAR could be calculated from

$$FAR = F/(666 - \beta L_{av}) \qquad (1)$$

where F was the number of false alarms produced by the test subject.

For each subject/display/test/session combination the probability of detection was plotted against SNR and the false alarm rate was calculated using eq. (1). A minimum squared error fitted cumulative normal distribution function was applied to the experimental data. This function provided a smoothed result from which the mean, corresponding to PD=50%, was extracted. An estimate of MDS corrected to a PFA of 0.01% was obtained from each plot by adding the FAR correction obtained from figure 2 to the SNR corresponding to PD=50%.

3. RESULTS AND DISCUSSION

Table 1 shows corrected statistics obtained from all of the measurements in tests MDS1 and MDS2 using Staircase, Random Stair and ESRF signal sets, averaged across all test subjects. An arbitrary shift relative to an input baseline has been applied to all MDS values: this does not affect the relation of the results to each other. The mean values of MDS for each test are averaged over all test subjects using both hard copy printouts and video display measurements. The rows marked 'Video' and 'Print' are averaged across all subjects for that display mode only. The standard deviations associated with each mean value are also based on combined statistics from (a) both video and hard copy printout display types for tests MDS1 and MDS2, or (b) across all subjects for the specific display type of video or hard copy printout.

GROUP	RELATIVE MDS ± STD. DEV. (dB)		
	Staircase	**Random Stair**	**ESRF**
MDS1	-1.7 ± 1.6	-1.3 ± 1.5	-1.8 ± 0.5
MDS2	-1.9 ± 1.2	-1.6 ± 0.8	-1.8 ± 0.4
Video	-1.5 ± 1.6	-1.2 ± 1.2	-1.6 ± 0.5
Print	-1.7 ± 1.4	-1.5 ± 1.2	-2.0 ± 0.4

Table 1. Combined statistics obtained from all measurements. All MDS and standard deviation values are in dB.

The decrease in standard deviation of MDS values as the progression is made from Staircase to Random Stair to ESRF techniques is a direct reflection of the increasing elaboration of the measurement technique. This indicates the Staircase and Random Stair methods can give reliable and consistent results and, as they are relatively quick and easy to implement, should provide a viable method for determining major changes in processor performance. Using a confidence interval of two standard deviations (2σ) as a guide, performance changes of 3dB or greater should be apparent using the Staircase and Random Stair techniques.

The relatively small standard deviation in ESRF measured MDSs indicates that this technique could be used to measure end to end system performance, and also changes in performance following either hardware or software changes, to within 1.0dB based on a 2σ confidence interval.

The difference in average test subject performance resulting from the change from white gaussian noise (test MDS1) to a spectrum representative of typical ocean conditions (test MDS2) was found to be negligible, being within one standard deviation of uncertainty for each technique. This similarity of measured MDS values is attributed to the automatic gain controls (AGCs) used in the processor, which are typical of those used in operational processors. With AGC in place and functioning properly, use of Gaussian noise appears to be adequate for performance testing and detection studies.

It was found that the false alarm rate (FAR) for the ESRF technique was not significantly dependent on SNR. This means that, in general, subjects did not vary their detection performance when confronted with particularly easy or difficult detection opportunities. This consistency was crucial to producing reliable statistics, and was a consequence of providing clear guidelines for calling detections and practice with feedback prior to starting the experiment to allow subjects to stabilise their performance. The FAR for the ESRF technique was unaffected by changing from a video display to a hard copy display.

As a guide, to achieve either a Staircase or Random Stair standard deviation of 1.5 dB per MDS experiment per test subject required approximately 8 minutes of studying displays followed by one hour of analysis. Achieving an ESRF standard deviation of 0.5 dB per MDS experiment per test subject took approximately 3 hours studying displays, which then needed approximately 2 days to analyse.

Future work planned in this area is to automate parts of the analysis process to save time, refinement of the signal generation techniques, and an extension of the work to apply to acoustic systems processing directional information.

Acoustic Tracking of Non-Vocalising Whales Using the Scattered Field of Vocalising Whales

Nicholas C. Makris [1] and Douglas H. Cato [2]
[1] Naval Research Laboratory, Washington, D.C. 20375 U.S.A.
[2] Maritime Operations Division, Defence Science and Technology Organisation, PO Box 44 Pyrmont, NSW 2009, Australia.

There are considerable difficulties in tracking whales and making behavioural observations because they are submerged most of the time. Visual monitoring is therefore limited to the small proportion of time that whales appear at the surface to blow, and even then they may not always be detected when visibility is affected by weather or sea conditions. Whales make extensive use of sound and the potential exists to track vocalising whales acoustically over large distances (> 100 km), because of their high source levels. This has recently received much attention in the underwater acoustics community, and some US Naval facilities have been made available for this purpose [see abstracts of papers presented at Acoustical Society of America Meeting: J. Acoust. Soc. Am., 95, 2851-2854 (1994)]. These techniques are, however, confined to those individuals that are vocalising at any time, and this is often only a small proportion of the stock.

This paper describes a method of tracking and monitoring the behaviour of all whales in a herd by using the vocal whales as active sources and detecting the echoes from the non-vocalising whales. It presents asimulation of acoustic monitoring of humpback whales migrating along the east coast of Australia using a towed array.

The observations of Paterson and Paterson (1984, 1989) of humpback whales passing Point Lookout on Stradbroke Is. (off Brisbane) were used to model the spatial distribution of whales. The proportion of whales singing and the characteristics of the sounds were determined from recordings in the same area (Cato, 1991). Source levels were based on the measurements in the northern hemisphere (Winn et al, 1971; Thompson, Cummings and Ha, 1987), which were consistent with local observations. These were in the range 175-188 dB re 1 micropascal. A spectral model for scattering from an object in a waveguide (Makris et al 1994) based on the method of Ingentio (1987) is used to determine the scattered field from the whales. The dimensions are chosen to give an effective target strength of close to 0 dB, which is probably a conservative estimate. Measurements of humpback whale target strengths by Love (1973) at 10 and 20 kHz gave 7 dB and -4 dB for the side and head aspects, respectively, of an adult and +2 dB for side aspect of a juvenile. The dominant frequencies of the humpback vocalisations are in the order of a few hundred hertz and it is possible that some resonance mechanism is used to generate the sounds which would also provide enhanced target strengths at the same frequencies.

Waveguide noise is modelled using the method of Kuperman and Ingenito (1980) which calculates the spatial properties of sea surface generated ambient noise. Simulations were made a towed array of 128 hydrophones spaced at half wavelength intervals at 200 Hz, running parallel to the line of whales. The results indicate that localisation of non-vocal whales is plausible for towed arrays within roughly 10 km of the herd in typical ambient noise conditions. The use of time domain matched filtering may significantly extend this range by making use of the direct signal from the vocalising whale to match the scattered signals.

REFERENCES

Cato, D.H. (1991) Songs of humpback whales: the Australian perspective. Mem. Qd. Mus. 30(2), 277-290.

Kuperman, W.A and Ingenito, F. (1980) Spatial correlation of surface generated noise in a stratified ocean. J. Acoust. Soc. Am., 67, 1988-1996.

Ingenito, F. (1987) Scattering from an object in a stratified medium. J. Acoust. Soc. Am., 82, 2051-2059.

Love, R.H. (1973) Target strengths of humpback whales. J. Acoust. Soc. Am. 54, 1312-1315.

Makris, N.C, Ingenito, F. and Kuperman, W.A, (1994) Detection of a submerged object insonified by surface noise in an ocean waveguide, J. Acoust. Soc. Am., 96,1703-1724

Payne, R.S. and McVay, S. 1971. Songs of humpback whales. Science. 173: 585-597.

Paterson, R. and Paterson, P. 1984. A study of the past and present status of humpback whales in east Australian waters. Biol. Conserv., 29: 321-343.

Paterson, R. and Paterson, P. 1989. The status of the recovering stock of humpback whales Megaptera novaeangliae in east Australian waters. Biol. Conserv. 47: 33-48.

Thompson, P.O., Cummings, W.C. and Ha, S.J. (1986) Sounds, source levels and associated behaviour of humpback whales, southeast Alaska. J. Acoust. Soc. Am, 80, 735-740.

Winn, H.E., Perkins, P.J. and Poulter, T.C. (1971). Sounds of the humpback whale. Proc. 7th Annual Conf. on Biol. Sonar. 7: 39-42. Menlo Park: Stanford Research Institute.

Vertical Reconstruction of Sound Fields from Data Measured Along a Radial

C. J. Price
Defence Scientific Establishment, Devonport Naval Base, Auckland, New Zealand

This paper examines a method of reconstructing along a sound field generated by a point source in an ocean. It is assumed that measured sound field data along a radial is available at one, or at most a few depths. The reconstructed field is defined on the vertical slice of ocean containing this radial. It is also assumed that no detailed knowledge of the bottom is available. The basic nature of the approach is as follows.

Consider an oceanic environment with a constant sound speed profile, and cylindrical symmetry about an isotropic monochromatic source. The acoustic velocity potential ψ can be shown to satisfy the Helmholtz equation $\nabla^2 \psi + k^2 \psi = 0$, where k is the wavenumber, and where $\psi = 0$ on the surface. In place of any boundary information from the ocean floor ψ is known at one or a few depths along part of a radial emanating from the source. Using r to denote the horizontal distance from the source and z as depth, the known data is

$$\psi(r, z_i) = f_i(r) \quad \forall r \in [\ell, u] \quad \forall i \in 1, \ldots, N.$$

Assuming that the decaying modes are neglible in the region of interest, on using the standard exponential approximations to Hankel functions when $r\xi$ is large, ψ can be expressed in the form

$$\psi = \frac{1}{\sqrt{r}} \int_{\xi=-k}^{k} e^{i\xi r} \sin(z\sqrt{k^2 - \xi^2})\, A(\xi)\, d\xi$$

The data fitting conditions then become

$$\sqrt{r}\,\psi(r, z_i) = F_i(r) \quad \forall r \in [\ell, u] \quad \forall i = 1, \ldots, N \text{ where } \sqrt{r} f_i(r) = F_i(r)$$

An estimate of the field is sought along a radial at some depth. For the moment, the case where the data is only known at one depth is considered. For convenience, the following quantity is defined.

$$D = \sin(z\sqrt{k^2 - \xi^2})A(\xi) \qquad \forall \xi \in [-k, k]$$

The depth dependence means that it is now necessary to find D explicitly. Now

$$F_i(r) = \int_{\xi=-k}^{k} e^{ir\xi} D(\xi, z_i)\, d\xi$$

On defining $D(\xi) = 0 \;\forall |\xi| > k$, $2\pi F_i$ is the inverse Fourier transform of D. In practice, F_i is only known at a finite number of points of the interval $[l, u]$, and so the inverse Fast Fourier Transform must be used to calculate D. It is expected that the waves with the largest magnitudes are nearly horizontally travelling waves moving outwards from the source. If the number of points at which F_i is known is insufficent to provide information about all wavenumbers $|\xi| \leq k$, then a frequency shift was applied to the data in order to ensure that D is calculated for the most important wavenumbers. Once D has been found at the appropriate depth, the estimate of the field can then be calculated by the FFT.

The cases where the sound speed is a function of depth, and where measured data is known at more than one depth will also be discussed in the talk. Some results will also be presented.

Shallow Water Acoustic Propagation from a Source in the Sea-bed

G.D. Wills, C. L. Morfey, P. A. Nelson
Institute of Sound and Vibration Research, University of Southhampton, England SO17 1BJ

INTRODUCTION

The method of plane wave decomposition is being used to model acoustic propagation in shallow water from a point source in the sea-bed. The interest in this work was prompted by the need to model blast waves emanating from explosive charges buried in boreholes, which are used to fragment unwanted bedrock. The water channel is assumed to be a homogeneous medium of constant depth, and the point spherical source is located below the rock-water boundary. By using the analytical decomposition of a spherical wave into plane wave components (Brekovskikh[1]), the wavenumber spectrum incident on the rock-water boundary is calculated. This wavenumber spectrum is then multiplied by a transfer function, which relates the field at a particular location in the shallow water to the plane wave components incident on the boundary. After inverse spatial transformation using the Hankel transform, the resulting pressure due to the spherical source is given as a single, one-dimensional integral. This integral is of a similar form to the expression arrived at by Brekovskikh for the case of having a point score located within the water channel, and in fact the denominator is identical. Inverting the denominator as an infinite series produces a summation of integrals, or images, with each image corresponding to the exact pressure produced after a certain number of reflections from the water surface and sea-bed. It is well known that the images come in groups of four when the point score is within the water channel. When the point score is located within the sea-bed, the images come in groups of two. Solving individual integrals of this form has been treated by Plumpton et al.[2], who used saddle point analysis to calculate the field reflected back from a fluid-fluid interface. Westwood[3] allowed the angular dependent reflection co-efficient to influence the location of the saddle points, and consequently included the reflected lateral wave and evanescent field in the saddle point formulation. Westwood was then able to calculate the pressure in flat and sloping shallow water waveguides by adding together such integrals[4].

THE CURRENT RESEARCH

Rather than taking the analytical approach of Westwood, the integrals are solved numerically using reliable adaptive integration routines and advanced computational power. It is not necessary to evaluate each individual image integral and then add them together, since the single integral that the image formulation converges to can be evaluated directly. This is possible because the integrand is finite-valued at all points, and leads to an obvious saving in computational time. There is however one point in the integrand, corresponding to plane waves travelling within the water at grazing incidence to the sea-bed, at which the integrand has a value of 0/0. The limiting value of the integrand at this point has been calculated using l'Hopital's rule, enabling the integration routine to continue without any problems. By integrating the real and imaginary parts separately, complete contour plots of the pressure in the water channel are produced for both the case of the point source in the sea-bed and the point source in the water. The effect of shear waves in the sea-bed is also incorporated into the model by using the fluid-solid plane wave reflection and transmission co-efficients in the integrands.

An experiments has been conducted to validate the results produced by the integration routine. This involved using a hydrophone as an impulsive source in a scale model shallow water channel of 12.5 cm depth. A stepper-motor controlled linear traversing system was used to move a receiving hydrophone, and to thus measure the propagation loss as a function of increasing radial distance. Excellent agreement was found between the measurements and the theoretical predictions.

This paper presents details of theoretical approach, and presents results of the theoretical predictions in both the frequency and time domains. Comparison will then be made with the experimental results.

REFERENCES

[1] L.M. Brekovskikh, Waves in Layered Media. (Academic Press, New York, 1980), 2nd ed.

[2] N.G. Plumpton, and C.T. Tindle, "Saddle point analysis of the reflected acoustic field," J. Acoust. Soc. Am. 85, 1115-1123 (1989).

[3] E.K. Westwood, "Complex ray methods for acoustic interaction at a fluid-fluid interface", J. Acoust. Soc. Am. 85, 1872-1884 (1989).

[4] E.K. Westwood, "Ray methods for flat and sloping shallow water waveguides", J. Acoust. Soc. Am. 85, 1885-1894 (1989).

Echo Processing Algorithms for the Remote Acoustic Sensing of Sea-Ice Thickness

A. J. Duncan*, J. D. Penrose*, G. Bush*, I. Allison**
* Centre for Marine Science and Technology, Curtin University of Technology,
PO Box U1987, Perth, Western Australia, 6001.
** Antarctic CRC and Australian Antarctic Division, GPO Box 252C, Hobart 7001.

INTRODUCTION

In 1993 the Centre for Marine Science and Technology at Curtin University designed and built two Upward Looking Sonars (ULS) for the Australian Antarctic Division. The sonars were designed to be moored up to 200 metres below the sea surface and to determine the draft of the sea-ice passing over them (the depth of ice below sea level) by comparing the distance to the underside of the ice, determined from the round-trip travel time of an acoustic signal reflected from the ice, to the depth of the sonar below sea level, determined from a precision pressure sensor. The sonars record this information together with water temperature at the sonar, instrument tilt and various acoustic receive signal statistics which are intended to assist in distinguishing between reflections from ice and open water. Specifications are given in Table 1.

Table 1. Curtin University Upward Looking Sonar: Specifications

Maximum operating depth	200 metres
Maximum survival depth	400 metres
Active operational capability	2 years
Data storage	1 Mbyte EEPROM (expandable to 2 Mbytes)
Acoustic transducer beamwidth (between half power points)	2.5 degrees
Acoustic centre frequency	300 kHz
Acoustic timing resolution	8 microseconds (equivalent to 6 mm ice thickness change)
Pressure transducer resolution	100 Pa (equivalent to 10 mm sea level change)
Temperature measurement resolution	0.025 C
Tilt measurement resolution	0.1 degrees
Weight in air	300 kg (including buoyancy)
Physical dimensions	0.7 x 0.7 x 1.8 m
Operating temperature range	-10 C to +40 C

The prospect of global warming has recently increased the need for quantitative data on the polar sea-ice. Sea-ice, even when thin, stops most of the turbulent heat flux between the ocean and the atmosphere, and greatly changes the surface albedo. The sea-ice mass budget involves latent heat and drives the thermohaline circulation of the Southern Ocean. The only present practical means of obtaining sea-ice thickness data, apart from manual drilling, is with ULS either deployed on under ice moorings or on under water vehicles. Recognising the crucial role of ice thickness data in verifying climate simulations, the World Climate Research Programme has promoted an international Ice Thickness Monitoring Project. In support of both its own climate research priorities and thisinternational project, the Australian Antarctic Division has purchased two ULS units and may purchase a further three.

After initial trials off the Western Australian coast the two sonars were deployed in Antarctic waters from RSV Aurora Australis in January 1994. The first was deployed on the continental shelf in 520 metres of water and the second 200 km to the north in 3260 metres. Moorings for the sonars were designed and supplied by the CSIRO Division of Oceanography. Two current meters were included in the 520 metre mooring, and one in the 3260 metre mooring. The sonars are due to be recovered during the 1994/5 summer.

The Curtin ULS have been designed for deep operation (200 m) and pressure resistance (400 m). However, operating at this depth introduces uncertainties in the acoustic depth calculation because of unmeasured changes in temperature and salinity of the water column above the instrument. Fortunately the Antarctic sea-ice cover is not continuous: open water leads of tens of metres widthoccur regularly, and if the difference between an open water reflection and ice reflection can be discriminated, these leads will provide spot calibration points for the acoustic depth calculation. A considerable percentage of the Antarctic pack is also very thin (less than 0.2 m) and, although difficult to measure with a ULS, this ice is thermodynamically very different from open water. Hence the Curtin units also record pulse echo statistics and can sample the entire received waveform to provide data to develop methods to better discriminate thin ice from no ice.

SIGNAL TO NOISE RATIO ENHANCEMENT

The precise acoustic signal timing requirements for this system and the decision to use an acoustic frequency comparable to that used in other instruments necessitated the use of the relatively high acoustic centre frequency of 300 kHz, which is well above the frequency at which optimum signal to noise ratio is obtained when echo ranging over 200 metres. Calculations indicated that to achieve adequate signal to noise ratio from short, wideband acoustic bursts would require prohibitive peak transmit powers, and so an alternative had to be found.

The signal to noise ratio at the receiver output can be improved for a given peak power by using a signal and receiver with a narrow bandwidth, but this makes accurate arrival time measurement impossible. An alternative approach is to transmit a long signal, of length T seconds, which has been modulated in some way so that it has a wide bandwidth, B. The received signal is correlated against a replica of the transmitted signal yielding a sharp correlation peak at a delay corresponding to the acoustic travel time. The signal to noise ratio at the correlator output is about a factor of BT greater than that at its input.

If the return signal originates from a single acoustic scatterer the correlator output will contain a number of small peaks in addition to the main peak. These peaks are known as range sidelobes and depend on the autocorrelation properties of the transmitted signal. The geometry of the ULS dictates that the received signal is made up of contributions from a large number of scatterers at slightly different ranges from the sonar. In this case the correlator output depends on the relative phases of the signals from the different scatterers, and the range sidelobes can sum to produce significant amplitudes, making identification of the first genuine correlation peak difficult. Figure 1, which is based on computer simulations, illustrates this by comparing the correlator output for a 31 bit pseudo random binary sequence (PRBS) phase modulated signal to the result obtained for a short tone burst with the same bandwidth. In both cases the signal to noise ratio is infinite.

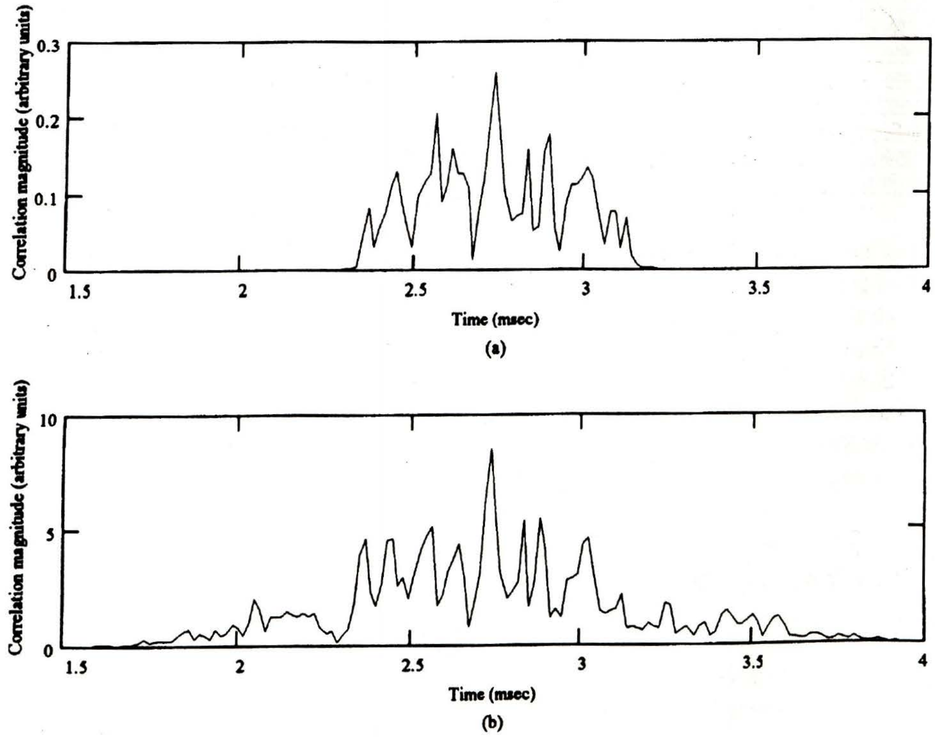

Figure 1. Simulated correlator outputs when the signal is scattered from a rough surface with an amplitude of 0.12 metres rms at a range of 200 metres from the sonar. In (a) the transmit signal is a 27 microsecond tone burst, while in (b) it is an 826 microsecond tone burst phase modulated by a 31 bit PRBS.

ULS SIGNAL PROCESSING ALGORITHMS

The Curtin ULS has been designed so that it can transmit both simple sinusoidal signals and phase modulated signals. The bandwidth and gain of the receiver are under processor control and the receive signal is quadrature demodulated to preserve all information about the incoming signal. The two quadrature channels are simultaneously sampled by analog to digital converters.

To obtain the necessary time resolution and signal to noise ratio it was decided to use replica correlation and an 826 microsecond long transmit signal phase modulated with a 31 bit pseudo random binary sequence. In order to reduce the number of samples of the receive signal that had to be correlated against the replica of the transmit signal to a manageable level it was decided to use a two stage measurement. In the first stage a 1 ms long tone burst is transmitted which is received with a 1 kHz receiver bandwidth (one sided) and sampled at 3 kHz. The amplitude of the received signal is calculated as a function of time and a threshold, based on a running average of the noise level, is used to determine the approximate arrival time.

The PRBS modulated signal is then transmitted and received with a bandwidth of 20 kHz and a sampling frequency of 62.5 kHz. The approximate arrival time is used to time gate the receiver sampling. The samples of the received signal are correlated with a replica of the transmit signal and an arrival time is calculated based on a threshold given by the larger of: 3.75 times the average of the first 50 samples (assumed to be noise), and 0.625 times the average of the two highest peaks in the correlator output. The first of these thresholds was derived from standard receiver operating curves and gives acceptable false alarm and detection rates for low signal to noise ratio situations. The second threshold was derived empirically from computer simulations and field trial data to give an acceptable compromise between triggering on range sidelobes and rejecting genuine correlation peaks.

When a sonar is readied for deployment up to five measurement schedules may be specified. Each schedule specifies a fundamental time interval for making pressure, travel time and tilt measurements, together with intervals for making optional measurements such as recording complete receive signals.

CONCLUSIONS

The recovery of the two sonars is awaited with great anticipation. If all goes well the sonars will contain a wealth of unique data on the acoustic and physical properties of sea-ice.

REFERENCES

Kvambekk, A. S. and Vinje, T., "Ice Draft Recordings from Upward Looking Sonars in the Fram Strait and the Barents Sea in 1987/88 and 1990/91", Norsk Polarinstitut, rapportserie Nr. 79, Oslo 1992.

Untersteiner, N. and Moritz, R. E., "Ice Thickness Distribution", Polar Science Center, Applied Physics Laboratory, University of Washington, final report on contract N00014-87-K-0035, 1989.

The Sensitivity of Acoustic Measurements to Climate Change

Matthew Dzieciuch
Scripps Institution of Oceanography

1. INTRODUCTION

Acoustic Thermometry of Ocean Climate (ATOC) measures the integrated heat content of a path through an ocean basin by recording the travel time perturbations of low frequency sound waves. Anthropogenic CO2 in the atmosphere is expected to heat the oceans. A relevant question is: What is the signal-to-noise ratio of the CO2 warming signal versus the ambient signal? A couples ocean-atmosphere general circulation model was run wi th no CO2 increase and with CO2 doubling. The GCM output was then used as an input to an acoustic propagation model. The acoustic time series can then be analyzed for climatic trends. The control run is used tō estimate the ambient noise processes on long term scales. The spatial properties of the CO2 signal are nonuniform and therefore maps of the signal strength are also constructed.

2. THE GREENHOUSE EXPERIMENT

A computer experiment to simulate the effects of the anthropogenic CO2 increase in the atmosphere was run at the NOAA Geophysical Fluid Dynamics Laboratory[1,2]. In short, a coupled ocean-atmosphere model was spun up until it reached quailibrium. Then two different integrations were performed. First a control run was run for one thousand years where the level of CO2 was held constant. Secondly, a 500 year integration was performed with CO2 growing at a compounded rate of 1% per year, corresponding to the current rate of growth (doubling CO2 in 70 years). The model output analyzed here are the yearly average temperature on a gride scale of about 4.5 degrees in the horizontal and 12 depths in the vertical.

3. MODEL ANALYSIS

The model was analyzed by decomposing the output into empirical orthogonal functions. If we represent the output by

$$A(x, t) = \sum_i \lambda_i u_i(x)\, v_i(t) = U \Lambda V^T, \tag{1}$$

where x is the space (row) index and t is the time (column) index, we can separate the output into the product of spatial and temporal functions. Since the time index is much shorter than the spatial index, (500 vs. 40*96*12), it is convenient to form the covariance matrix in the following fashion

$$C = A^T A = V \Lambda^2 V^T. \tag{2}$$

Next find the eigenvalues and the temporal eigenvectors by solving

$$C v_i = \Lambda_{ii}^2 v_i. \tag{3}$$

Finally the spatial EOF's can be constructed by forming the product

$$u_i = \frac{1}{\Lambda_{ii}} A v_i. \tag{4}$$

For a lucid account of this type of analysis see Fukumori and Wunsch[3].

Figure 1 shows the results of this decompostition. The upper panels show the fraction of variance explained by the eigenvalues. The first eigenvalue explains 15.0% of the variance anc can be attributed to computational drift in the control run associated with the difficulties in correctly modeling the fluxes of heat, water, and momentum that couple the atmosphere and ocean GCM's. For the purposes of this study this EOF will be ignored since it does not represent any real climate physics. The 2nd eigenvalue explains 4.5% of the remaining variance and can be associated with an ENSO phenomena. The spatial EOF of this mode is shown in Figure 2. Note the strong oscillation pattern along the equatorial Pacific.

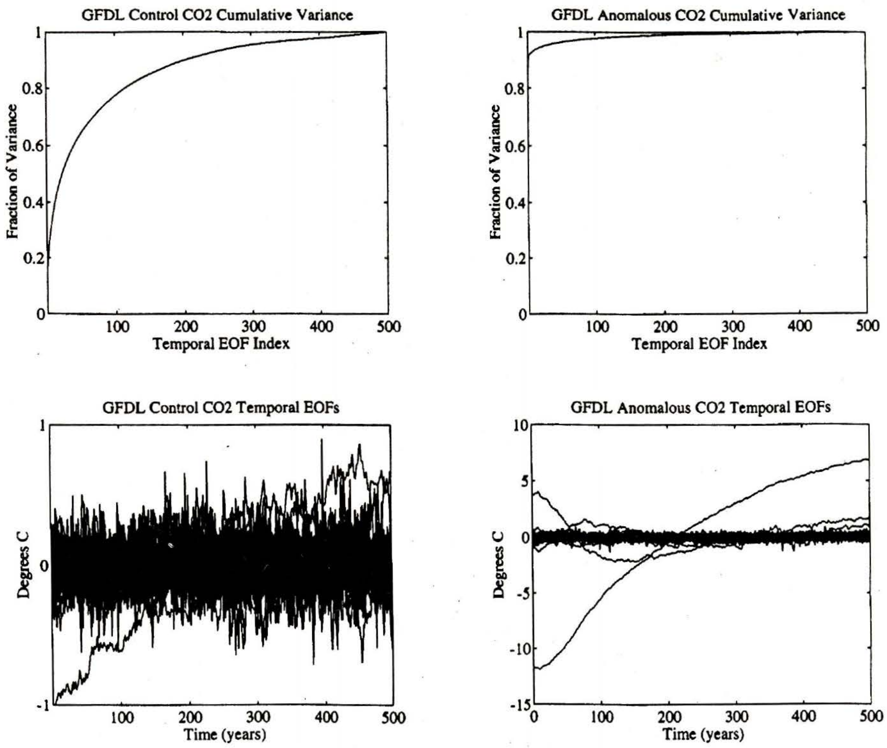

Figure 1

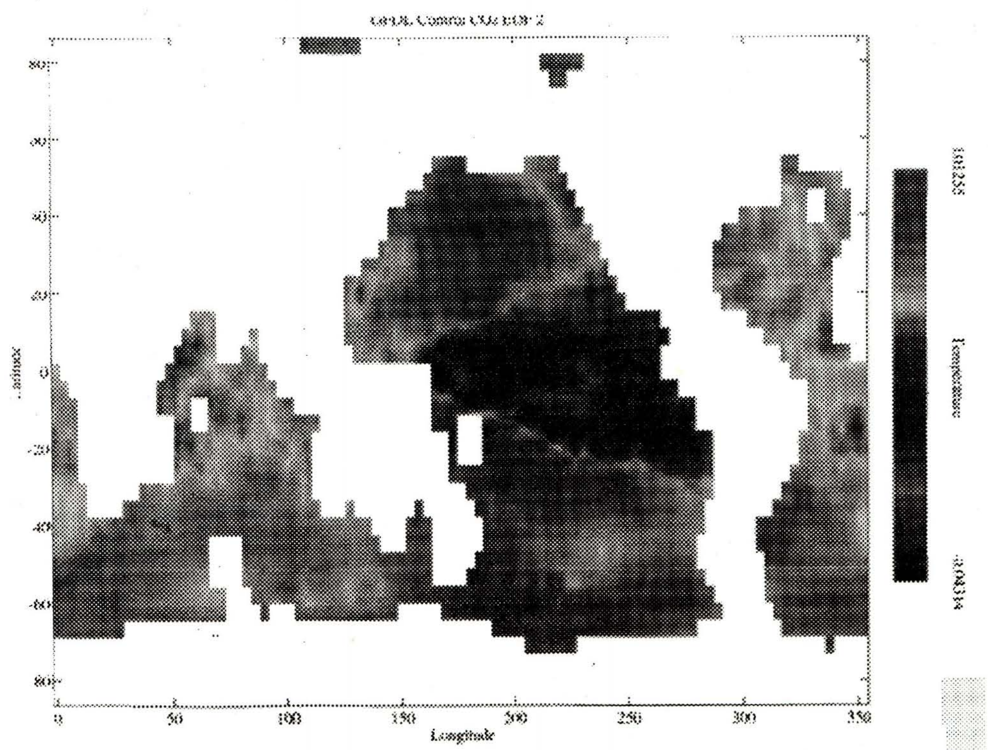

Figure 2

4. ACOUSTIC SENSITIVITY

The primary difficulty of coupling an acoustic model to the output of the climate model is the lack of vertical resolution. This can be overcome by using the Levitus climatology as a base state and considering the climate EOF's as perturbations. When one does this it is possible to make a map of the group velocity sensitivity of an acoustic mode to a particular climate EOF. Shown in Figure 3 is the spatial response of acoustic mode 1 at 75 Hz to the first greenhouse EOF. Although the response is fairly uniform for this case. The responses of other acoustic modes do show considerable spatial variability.

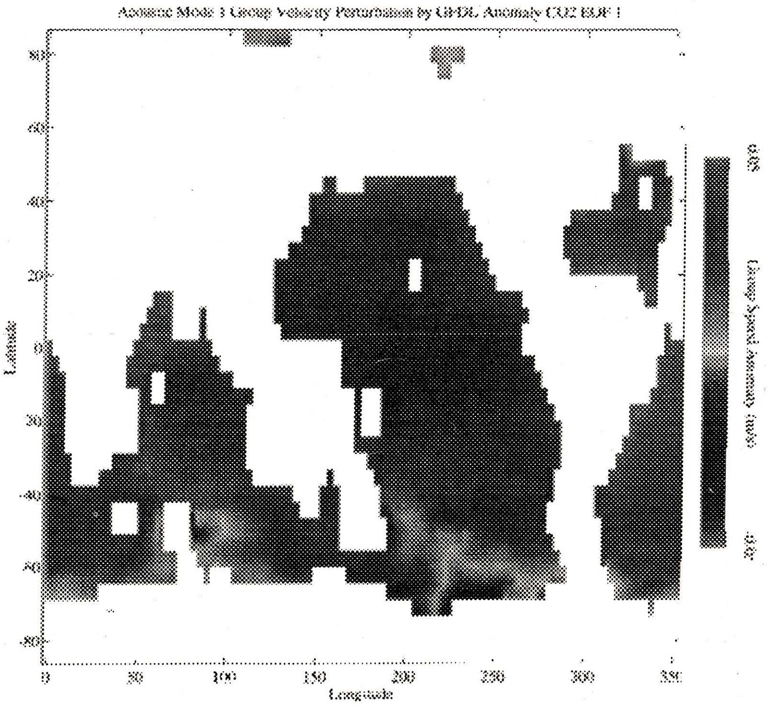

Figure 3

5. REFERENCES

1. S. Manabe, R. Stouffer, M. Spellman, and K. Bryan, "Transient Responses of a Coupled Ocean-Atmosphere Model to Gradual Changes of Atmosphere CO_2. Part I. Annual Mean Response", *Journal of Climate*, v. 4, pp. 785-818. August 1991.

2. S. Manabe, M. Spellman, and R. Stouffer, "Transient Responses of a Coupled Ocean-Atmosphere Model to Gradual Changes of Atmosphere CO_2. Part II: Seasonal Response", *Journal of Climate,* v. 5, pp. 105-126. February 1992.

3. I. Fukumori and C. Wunsch, "Efficient representation of the North Atlantic hydrographic and chemical distributions", *Progress in Oceanography,* v. 27, pp. 111-195. 1991.

4. S. Levitus, "Climatological Atlas of the World Ocean", NOAA Professional Paper 13. U.S. Dept. of Commerce. 1982.

Hydroacoustic Verification of the Comprehensive Test Ban Treaty

Martin W. Lawrence
Maritime Operations Division Defence Science and Technology Organisation

A Comprehensive Test Ban Treaty (CTBT) on nuclear weapon explosions is being negotiated under the auspices of the United Nations. At present the CTBT is in the latter stages of negotiation. Verification of the absence of nuclear explosions is an important aspect of the CTBT.

Seismic monitoring for verification purposes has been investigated for a number of years. In the last twelve months or so, interest has arisen in other verification techniques. These techniques are of importance if they can provide backup for the seismic technique, by such things as reducing false alarm rate, increasing classification certainty and filling holes in seismic coverage of either location or type of explosion. Hydroacoustic (underwater acoustic) monitoring has real promise and is being studied for its applicability to verification of compliance with the CTBT.

Australia is taking a leading role in the treaty negotiations. The Department of Foreign Affairs and Trade (DFAT) is the lead Australian agency in the negotiation of the CTBT. DFAT is being supported on seismic monitoring by the Australian Seismological Centre (part of the Australian Geological Survey Organisation) and on hydroacoustic monitoring by the Defence Science and Technology Organisation (DSTO).

Hydroacoustic methods would have significant synergetic benefits once combined with seismic monitoring techniques, potentially:

- reducing significantly the number of ambiguous events registered by the global seismic network in respect of natural underwater events; and,
- enabling small island masses in large oceanic areas to be monitored for possible underground testing without the need to deploy new but most likely relatively inefficient seismic systems there to fill known areas of lower detection confidences.

For events that occur in oceanic regions, hydroacoustic techniques are far more sensitive than seismic techniques. Studies have shown that a large proportion of the oceanic events which are recorded on hydroacoustic systems are not detected on land based seismic systems. The hydroacoustic signal from small explosions (e.g. 1 kilogram) has been routinely observed across major oceans. Thus there is excellent sensitivity for detecting even the smallest nuclear (underwater) explosions by using hydroacoustic techniques.

Hydroacoustics has the ability to precisely locate the site of an explosion in the water. A single hydroacoustic station can be designed to give a precise direction from the station to the event. Accuracies of fractions of a degree have been reported. Hence if two stations observe the same event, the position of the event can be determined with considerable accuracy.

Hydroacoustics should also be more capable of discriminating between underwater explosions and other events, than is the seismic technique. This results from two phenomena. The first is the presence of a characteristic bubble pulse signature for underwater explosions. This phenomenon results from an oscillating gas bubble and will not be present in events without such a gas bubble. The signature of this bubble pulse has been observed at large distances from an explosion, showing that this characteristic can be used even if the event is detected at considerable range.

The other phenomenon which facilitates event identification by hydroacoustic techniques is the relatively wide bandwidth of information contained in hydroacoustic signals (that is relative to seismic signals). A wide bandwidth signal is inherently more capable of containing information that could be used to perform event identification. The frequency range of seismic systems is limited to a few Hertz (cycles per second) due to the preferential absorption of the higher frequencies on passage of the waves through the Earth. In contrast, because absorption is much less during propagation through water, hydroacoustic signals contain useful energy up to a frequency of 50 to 100 Hertz.

Simultaneous examination of hydroacoustic and seismic measurements of the same event will also enable improved identification. A signal which originates in the ocean will be relatively stronger at a hydroacoustic receiver than a seismic receiver when compared to the relative levels for an event under the ocean floor (such as an earthquake).

Hydroacoustics is the best verification technique for underwater explosions. However, it will also perform well for explosions on islands or near to coasts. It will also perform well for air blasts over the ocean. In each of these cases there is good coupling of the explosive energy into the ocean, before the energy has dissipated.

Hydroacoustics has some potential to make a contribution to detection of underground tests at sites distant from the coast. However, the technique is not at its best here, and there are a number of technical issues that are not well developed.

Other events that can be regarded as having potential to cause ambiguity in identification include both man-made and natural events. The man-made events include explosives used for mineral exploration and other purposes. Hydroacoustics is not able to discriminate between a nuclear explosion and a conventional explosion of the same magnitude. In the normal course of events explosions in the ocean that are large enough to be confused with nuclear explosions are very rare. Natural events that may cause ambiguity problems include earthquakes, volcanoes, meteorites and biological noises. In each of these cases the hydroacoustic signature will differ from that of an explosion. Of the natural events, it appears that explosive volcanism may have the greatest potential for creating a "false alarm".

At the time of writing, the form of the hydroacoustic monitoring stations has not been decided. There are a number of contenders, such as fixed arrays cabled to the shore, moored buoys, and drifting buoys. The network of stations will include some existing stations built for other purposes as well as some new stations. There is relationship between the monitoring for CTBT verification and other programs such as Acoustic Thermometry of the Ocean Climate (ATOC), Global Acoustic Monitoring for Ocean Temperature (GAMOT), SOund SUrveillance System (SOSUS) and the Missile Impact Locating System (MILS). The CTBT verification systems will draw on knowledge (and systems) from these and other programs.

Other technical issues being considered include communication data rates, data storage requirements, signal processing and integration of hydroacoustic with seismic data.

In summary, the use of hydroacoustic techniques will be necessary to provide international verification of treaty obligations with reliable detection, identification and location of nuclear explosions in the oceanic environment.

An Indian Ocean Source-Receiver Network for ATOC

John Penrose[1] and Andrew Forbes[2]

[1] Curtain University, Perth

[2] Scripps Inst. Oceanography, La Jolla, CA)

INTRODUCTION

A global network of acoustic sources and receivers (Figure 1) was proposed in the early stages of planning for ATOC as a "first guess" array that would cover all the major ocean basins. Uwe Mikolajewicz (MPI, Hamburg) has conducted an EOF analysis of 107 paths which the network generates, to determine the effectiveness of such an array 107 paths which the network generates, to determine the effectiveness of such an array in detecting a climate signal against a background of ambient variability. In parallel with this work, the Pacific demonstration network (sources at Kauai and Pt. Sur) was designed to detect variability, primarily in the North Pacific. Global extensions to the Pacific network will have to wait until the next phase of ATOC, when we have analysed the rich data set expected from the Pacific network over the next two years, but it is not too early t o consider how we might extend acoustic coverage into the Indian Ocean. There is no special priority implied for the Indian Ocean over the Atlantic in this discussion. It simply reflects the authors' active involvement in forward planning for the Southern Hemisphere (sub) Working Group of ATOC. John Gould (IOS, Wormley) is similarly concentrating on future acoustic coverage of the Atlantic.

INDIAN OCEAN NETWORK

In choosing locations for the sources, several factors were considered:

- favourable local bathmetry
- maximum number of unimpeded paths
- availability of electrical power
- availability of support personnel

Receivers can be placed with more freedom than sources, since power requirements are not as great and some receivers can be autonomous, moored systems. The receivers along the Antarctic coast are most likely to be autonomous, to overcome the difficulty of cabling through the nearshore zone of destructive sea ice. Locations for these where chosen to be near existing Antarctic Stations which are visited at least annually by re-supply ships, which could be used to deploy or recover simple, autonomous receivers.

Two sub-Antarctic receivers are proposed, at the Kerguelen Islands and Macquarie Island, which are sparsely but sufficiently populated to provide maintenance support.

Several additional considerations weigh on the feasibility of an Indian Ocean extension in the near term:

- availability of a source
- availability of cable
- laying of cable to power a source
- finding a suitable source site
- availability or receivers
- funds

A third Alliant Tech source is currently available, and may not be required in the Pacific. There is also the possibility that a Russian source may be available as a low-cost "evaluation" option.

Telstra, the Australian overseas telecommunications company, has embarked on a program of replacing coaxial, copper cored deep ocean cables with fibre-optic cables. They are prepared to donate the required length of cable to power the proposed Cape Leeuwin source, from their inventory of recovered, redundant coax cable.

A source located 42 n. miles due west of Cape Leeuwin (the south west extremity of Australia) would ensonify 75% of the Indian Ocean (at axial depth) and parts of the Southern and South Pacific Oceans (see Figures 2-5). These plots show the ocean regions ensonified by a Cape Leeuwin source at axial depth and 1000m below axial depth. Bathymetric features such as oceanic ridges and seamounts, and of course, islands and continents, cast acoustic shadows, shown as white areas.

There is an excellent shore facility available at the Cape Leeuwin Light Station with sufficient power and a suitable building for the shore installation and cable termination.

South Africa, France, India and Australia have agreed to support receivers in the Indian Ocean and Indonesia is also a likely candidate. Simple, autonomous receivers of the type described by Spindel (ATOC Occasional Note #7) could be used at the majority of receiver locations around the rim of the Indian Ocean.

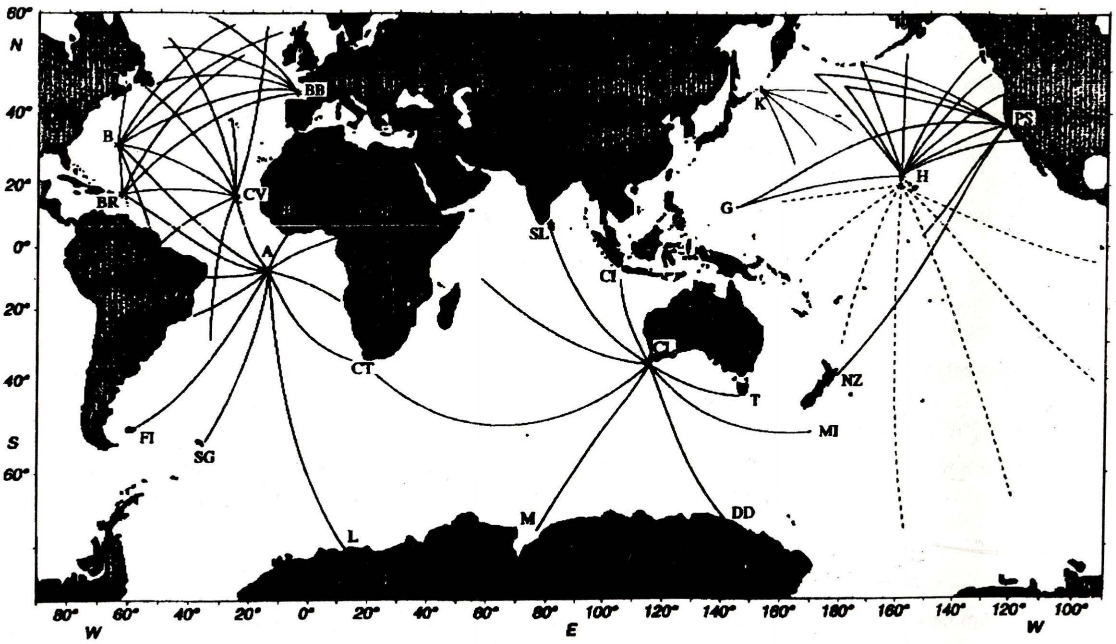

A - Ascension (UK)
B - Bermuda (UK)
BB - Bay of Biscay (Spain)
BR - Barbuda (UK)
(r) CI - Christmas Island (Australia)
CL - Cape Leeuwin (Australia)
(r) CT - Cape Town (South Africa)
CV - Cape Verde
(r) DD - Dumont D'Urville (France)
(r) FI - Falkland Islands (UK)
(r) G - Guam
H - Hawaii
K - Kuril Islands (Russia)
(r) L - Lazarev (Russia)
(r) M - Mawson (Australia)
(r) MI - Macquarie Island (Australia)
(r) NZ - New Zealand
PS - Point Sur
(r) SG - South Georgia (UK)
(r) SL - Sri Lanka
(r) T - Tasmania (Australia)

Figure 1.

Evaluation of an ATOC Line from Shot Waveshapes

Leon Krige, Geoff Brundrit, David Palmer, Andrew Forbes and Kurt Metzger
Institute for Maritime Technology, Simon's Town, 7995 South Africa
Department of Oceanography and Meteorological Laboratory,
4301 Rickenbacker Causeway, Miami FL 33149 USA
CSIRO Marine Laboratory, Hobart, Tasmania 7001, Australia
Department of Electrical Engineering and Computer Science,
The University of Michigan, Ann Arbor, MI 48109-2122 USA

ATOC-FACT (Acoustic Thermometry Of OceaN Climate -- Feasibility: Ascension - Cape Town) consisted of a series of shot tests aimed at establishing the feasibility of an ATOC acoustic path between Cape Town and Ascension (Figure 1). There is possibility of this line being blocked by the cones of Seamount Bonaparte (-105m) and St. Helena and the path depth will be limited over the Walvis Ridge. Seamount Gratton (-72m), some 2 degrees south and east of St. Helena is another potential source of topographic interference. ATOC-FACT was designed to determine the effect of these bathymetric features, thereby reducing the risk in future ATOC decisions. Acoustic transmission from the Cape Town sites to Bermuda and Australia could also be explored.

1. THE EXPERIMENT

The experiment took place on 23,30 November and 1 December 1992. Eight acoustic charges were detonated at five sites on a line extending 300 nm south west of Cape Town (Figure 1). In an attempt to place the charges as close as possible to the local sound channel axis, tethered charges were deployed from a tender to a surface vessel and triggered from the surface (Table 1 - not shown). Shot positions and times were recorded using Global Positioning System receiver. Receptions at Ascension were recorded with GPS time markers. Shortcomings of the experiment were the inability to consistently place the charges on the axis of the sound channel and the failure, after the third shot, of the on-site hydrophone for determining the detonation depth. The experiment was complicated by the presence of a warm water ring which depressed the sound channel (Figure 1).

The inner shelf sites were chosen because of their relatively good accessibility to cables from shore. Successful receptions from these sites would demonstrate the feasibility of reciprocal acoustic paths to Ascension and Bermuda. The sites beyond the shelf edge were chosen so as to provide a reference acoustic path clear of the potential topographic interference from Seamount Bonaparte and St. Helena.

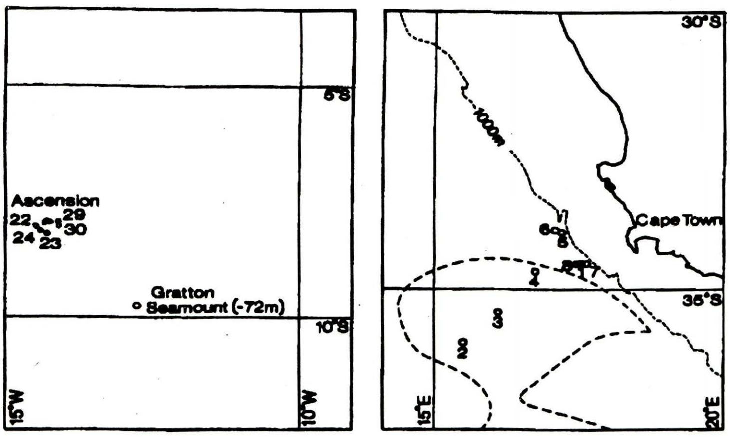

Figure 1. The eight shot sites offshore from Cape Town and the five receiver sites around Ascension. The extent of the arm water Agulhas ring at shot sites 2,3 and 4 is indicated by the dashed line.

2. THE OCEANOGRAPHIC SETTING

The climatological mean sound speed profiles [1] are essentially identical over the entire propagation pat h with a minimum Co of 1481 metres per second centred at approximately 800m. For a range independent sound channel, the relation between the ray group velocity Cg (the ratio of horizontal range to travel time) and the ray phase velocity Cp (the sound speed at the upper and lower turning depths) takes the simple form: Cg - Co = 1/3 (Cp - Co). This expression enables the maximum turning depth of rays to be estimated from the waveform duration.

3. RESULTS

Shot 2 was received by the Australian fisheries research ship, the Southern Surveyor, off the south coast of Tasmania. All eight shots were received at both Ascension and Bermuda. Signals from all eight shots were digitised and recorded from five hydrophones at Ascension (Figure 1). The spectra of the receptions show the bubble frequency associated with each shot. The shot depth can be estimated from this frequency and the charge size. These shot depth estimates, combined with estimates of the depth of the local sound channel axis, give approximate values for the relative displacement of shot depth above the channel axis, (Table 1). This provides depth estimates to make up for the on-site measurement failure.

A charge detonated on the axis of the sound channel will result in a waveshape with an increasingly steep upslope to a peak followed by a near-vertical downslope. If the charge is detonated above the axis, the sound near-axis components are excluded and the sharp peak of the waveform is cut off [2]. Figure 2 shows the reception at the Ascension hydrophones from shot 1, which was placed in the sound channel. Apart from differences in amplitude, the waveshapes received at the hydrophones are similar for each shot.

The peak intensity of the shots detonated in the channel axis (shots 1 and 7), the minor cut-off peaks (4,5,6 and 8) and major cut-off peaks (2 and 3) can be seen in Figure 3. The duration of the direct arrivals for each shot can be estimated. From this, the group velocity for the propagation path can be estimated, which, in turn, enables the depth of the critical bathymetry to be found. The overall results are shown in Table 2 (Not shown).

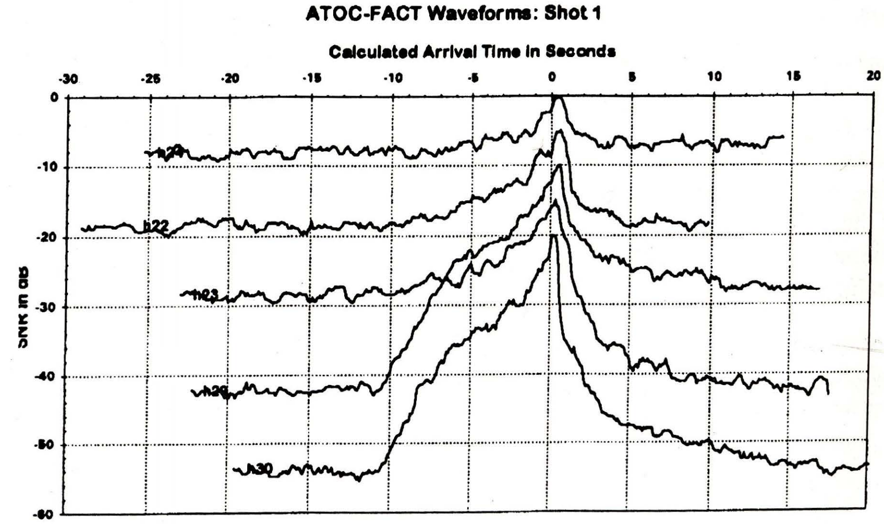

Figure 2. Relative signal shape reception at each hydrophone for shot 1; the peaks are shifted successively by 5 dB for clarity.

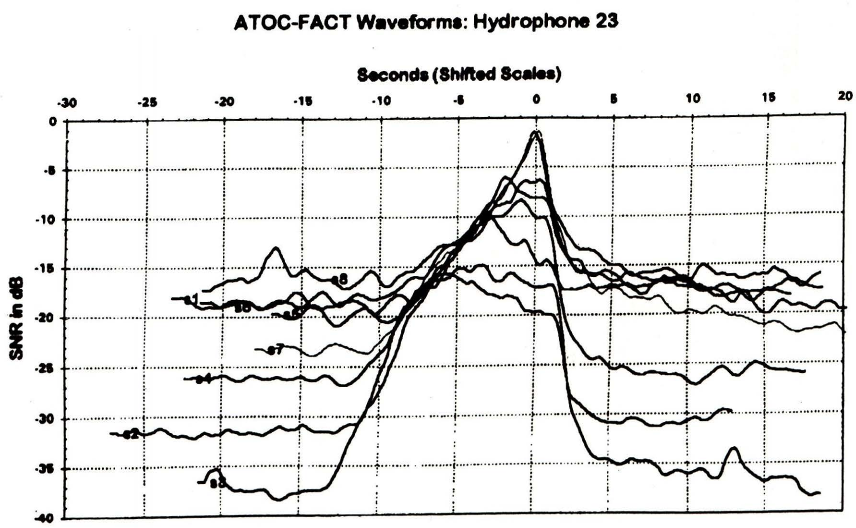

Figure 3. Relative signal shape reception for each shot at hydrophone 23; the intensity peaks are offset to fill in the supposed full signal.

4. CONCLUSION

For most of the lines the rays are limited to a depth of approximately 2000 m. This is consistent with the depths expected across the Walvis Ridge. Some of the easter shelf edge lines to hydrophones 24 and 22 have been greatly attenuated. These weak signals, in contrast to the stronger signals at the nearby hydrophone 23, suggest a narrow obstruction located close to Ascension, possibly Seamount Gratton. Seamount Bonaparte and St. Helena apparently did not interfere with the transmissions. It appears that the Cape Town to Ascension line is usable as part of the global ATOC network, provided care is taken to avoid interference from Gratton seamount.

The excellent reception facilities at Ascension and the multiplicity of ATOC-FACT lines with adequate time, position and depth information, have resulted in a data set which can be processed to determine some of the parameters of a potential ATOC line. The availability of affordable computers and software has made it practical to do precise processing of data sets such as these.

REFERENCES

1. D.R. Plamer, T.M. Georges, J.J. Wilson, L.D. Weiner, J.A. Paislay, R. Mathiesen, R.R. Pleshek and R.R. Mabe. Reception at Ascension Island, South Atlantic of the transmissions from the Heard Island Feasibility Test. Journal of Acoustic Society of America. (In press).
2. G.M. Bryan, M. Truckam and J.I. Ewing. Long range SOFAR Studies in South Atlantic Ocean. Journal of Acoustic Society of America. 35(1963) 273-278.

Acoustic Detection of Supercooled Antarctic Water

J. D. Penrose*, T. J. Pauly**
*Centre for Marine Science and Technology, Curtin University of Technology,
PO Box U1987, Perth, Western Australia, 6001
**Australian Antarctic Division, Hydroacoustics Marine Science Section,
Channel Highway, Kingston, Tasmania, 7050

INTRODUCTION

Ice crystals can form in the ocean water column when the water temperature falls below the local freezing point. Such crystals, while often associated with surface cooling processes, have been reported at depths to 250m [Dieckmann et al., 1986] and have been assigned a variety of roles in oceanic processes. As with other ice formation from saline water, the generation of a solid phase of frazil ice is expected to involve some salt rejection with a consequent formation of associated water of higher than ambient salinity. The comparatively low salinity ice crystals will rise towards the surface and in doing so can provide a vertical transport mechanism for microbiological organisms while the rejected high salinity water sinks. Such a mechanism has been proposed by Ushio and Wakatsuchi [1993] as a source of sub-surface supercooled water derived from surface processes in open water areas in sea-ice regimes. Dieckmann et al. [1986] noted returns on a 30kHz echo sounder from ice crystals of average diameter 20mm and thickness 0.5mm at a location approximately 25km from the edge of the Filchner Ice Shelf in Antarctica and surmised that the production of underwater ice platelets is probably a characteristic feature of the ice shelf barrier in the Southern Ocean, where the formation of deep supercooled water may be a frequent or continuous process. Jenkins and Doake [1991] have proposed that supercooled water at depth may be generated by melting processes underneath ice shelves, coupled with a suitable ambient density profile. This paper reports on an extensive series of field measurements in Antarctica, in which acoustic scatter from ice crystals in the water column led to the discovery of a substantial region containing sub-surface supercooled water. The location of the supercooling observed suggests a source mechanism associated with shelf melting processes. A fuller account of the work described in this paper is given in Penrose et al (1994).

During the period January-March 1991, the Australian Antarctic research vessel "Aurora Australis" carried out a marine science program in the region of Prydz and MacKenzie Bays, Antarctica, here collectively referred to for brevity as Prydz Bay. This program included continuous biomass measurement, a suite of CTD stations and biological net casts in the study area.

During the study program several classes of echo record became apparent. Some, due to krill and other biota as revealed by net hauls yielded echo returns showing significant spatial variability of up to 40 dB in volume backscattering strength S_v over horizontal length scales ranging from tens to hundreds of metres.

Here: $$S_v = 10\log s_v = \sum_i N_i\sigma_i \qquad (1)$$

N_i is the number per unit volume of scatterers with acoustic cross section σ_i. Other echograms indicated relatively uniform intensity returns over longer length scales extending in some cases over kilometres of track passage, indicating that the scattering centres involved were comparatively uniformly distributed through the water volumes involved.

Echograms showing such spatial uniformity in backscattering strength encountered in the vicinity of the Amery Ice Shelf edge suggested the possibility of ice crystals as acoustic backscatter targets. Accordingly two experiments were carried out in regions yielding comparable echogram character to the near-shelf returns, but well away from the shelf edge, to test this hypothesis. No surface ice was present at the sites of these experiments. In each experiment a rectangular mid-water trawl (RMT) of frontal opening area 8m^2 was deployed at the central depth of strong returns as indicated on the echo sounders. In both cases ice crystals were recovered in the net with no significant biological component in the catch. The crystals were roughly disk shaped, with diameters in the range 10-25 mm and thickness of approximately 1 mm. Thus, ice crystals were recovered from depths in the range 50-250m, with no evidence of surface ice, solely on the basis of the form of the echograms. Echo sounder records of the complete two month long cruise in the Prydz bay region were then reviewed for evidence of similar echo traces possibly arising from ice crystals. Particularly attention was directed to records which showed spatial uniformity in the volume backscattering parameter S_v over length scales comparable to the echograms associated with the trawl experiments noted above.

EVIDENCE OF SUPERCOOLING

Figure 1 shows a map of the study area with 1000m depth contour indicated between 66S and 67S latitude. Trackplots containing echograms of a spatially smooth character are indicated by the solid line segments shown. The three regions shown within the dotted lines contained supercooled water as assessed from CTD profiles which were taken at half degree spacing over the area.

Figure 2 shown the results of a CTD profile taken within the largest such region and also shows a plot of freezing temperature with depth and the region over which the echo trace arising from ice crystals occurred. This CTD profile was taken at one of the locations where ice crystals were gained from net hauls. Significant supercooling occurs over approximately 200 m of the depth range in this example which was typical of the profiles used to generate the estimates of supercooling regions shown in Figure 1.

The results shown in Figure 1 suggest that the western edge of Prydz Bay contained, during the period of the cruise, a significant population of ice crystals associated with a plume of supercooled water. A possible explanation for the location of this plume is as a consequence of the dominant clockwise gyre in the bay reported by several investigators. Such a current may flow under the Amery Ice Shelf and give rise to the conditions for the formation of frazil ice at depth. Under such conditions, water from the beneath the shelf emerges at temperatures such that any movement to the surfaces causes it to become supercooled as a consequence of the variation of freezing point with depth. Such movement towards the surface may arise from buoyancy effects alone or as a consequence of topographical forcing but may, as in the example shown in Figure 2, not reach the surface, which remain ice free. The plume of supercooled water joins the circulation outside the shelf edge at a depth determined by the local density balance.

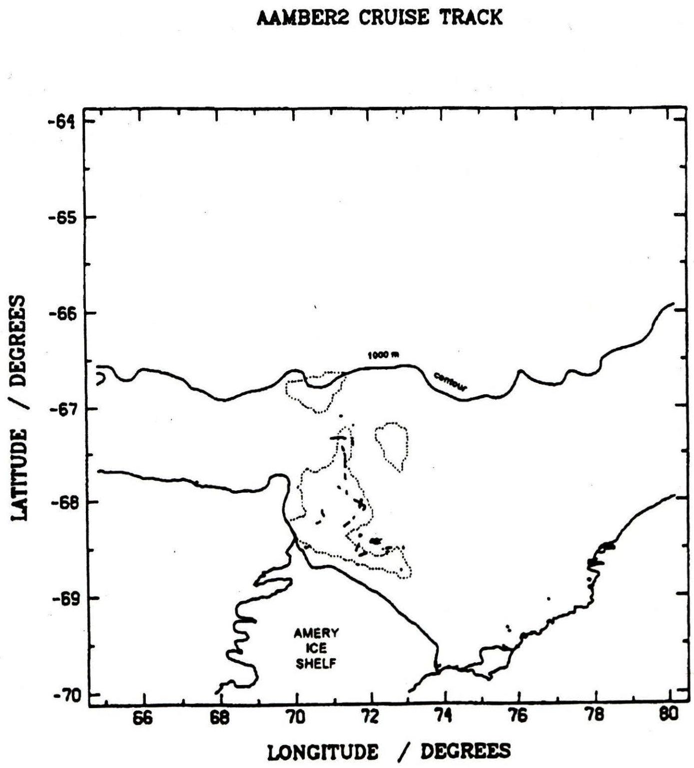

Figure 1. Regions containing supercooled water, as determined from CTD data and echograms assigned as arising from ice crystals (solid line segments)

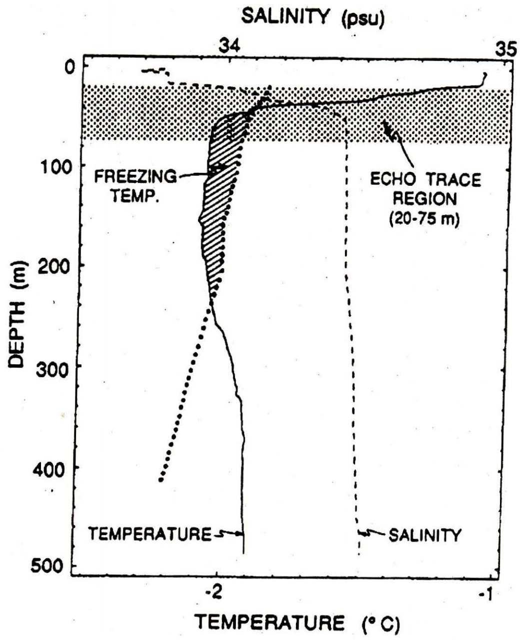

Figure 2. CTD record taken at Latitude 68°3'00"S, Longitude 71°42'00"E February 25, 1991, in conjunction with a net haul yielding ice crystals

CONCLUSIONS

The nature of acoustic backscatter from sub-surface aggregations of ice crystals has been shown to be a guide to the presence of supercooled water beneath the Antarctic sea Surface. Such supercooling may arise in principle as a consequence of shelf-ice melting processes [Jenkins and Doake, 1991] or from surface processes [Ushio and Wakatsuchi, 1993]. In this case, the location of the supercooled water is consistent with a source associated with the Amery Ice Shelf, given what is known of the circulation pattern in Prydz Bay. The match between supercooled water locations derived from CTD profiles and those assigned on the basis of echogram character is partial, suggesting that improved echogram classification procedures to better distinguish between ice crystals and biological targets would permit improved detection of supercooled water volumes. It is possible that in the regions surveyed which did contain supercooled water, but were not assigned as ice crystal regions on the basis of echogram appearance, ice crystals did exist, but have been interpreted incorrectly as biological targets. Such a process has significance for the conduct of acoustic biomass surveys in polar waters.

REFERENCES

Dieckmann, G, G. Rohardt, H. Hellmer, and J. Kipfstuhl, The occurrence of ice platelets at 250 m depth near the Filchner Ice Shelf and its significance for sea ice biology, *Deep Sea Res.*, 33(2), 141-148, 1986.

Jenkins A. and Doake, C.S.m., Ice-ocean interaction on Ronne Ice Shelf, Antarctica, *J. Geophys. Res.*, 96, 791-813, 1991.

Penrose, J.D., Conde, M., and Pauly, T.J., Acoustic detection of ice crystals in Antarctic waters, *J. Geophys. Res.*, 99, 12,573-12,580. 1994.

Ushio, S. and Wakatsuchi, M., A laboratory study on supercooling and frazil ice production processes in winter coastal polynyas, *J. Geophys. Res.*, 98, 20, 321-20,328, 1993.

Marine Animals and Man-Made Noise

Robert D. McCauley
Department of Marine Biology, James Cook University, Townsville, Qld., 4811

Man-made noise in the marine environment is produced by many different sources and hence encompasses a variety of noise types and levels of exposure. Some of the more common sources include commercial shipping, fishing vessels, private vessels, offshore seismic surveys, harbour dredging and blasting operations. Each of these sources has its own defining noise characters, such as signal duration, waveform, spectral content and source levels.

Many of these sources may expose marine animals to high noise levels (or shock waves in the case of explosives) and so potentially produce physiological or behavioural effects. Such effects may, or may not, have environmental and commercial consequences. Environmental groups and the general public have shown a pre-occupation with possible impacts on marine mammals, such as the recent outcry over the proposed ATOC or ocean temperature experiments, or reactions to offshore seismic surveys. In Australia the recent rise of whale watching from a cottage industry employing a few small operators, to a million dollar concern, has seen a corresponding rise in concern over the short and long term effects of vessel noise on the targeted whales. Commercial fishing operations may be affected by the behavioural interactions between target or by-catch species and the noise generated by fishing boats or their gear. Commercial fishing groups have expressed concerns over the avoidance of some fin-fish species from the sound fields produced during offshore seismic survey operations and the implications for catch rates. Aquaculture operations attempt to rear fish and invertebrates, often in extremely noisy environments, with scant knowledge of the implications of exposing the animals to continually high noise levels.

A full spectrum of the short term implications of exposure to high levels of noise includes: a) lethal effects such as produced by the shock wave of explosives; b) sub-lethal or pathological effects such as damage to hearing systems or stress related effects; c) behavioural effects such as repulsion or avoidance from the source, disturbance to normal behaviour patterns, or attraction to the source; d) interference with acoustic communication by direct masking of signals or the raising of acoustic thresholds; e) no direct effect at all; or f) indirect effects caused by abundance or behavioural changes to another critical species, such as prey.

To fully assess the implications of noise exposure on marine animals requires a considerable amount of information, much of which is simply not available. For example very few structured experiments have been undertaken on the effects of rearing marine animals in noisy environments. Even when information is available it may be difficult to interpret, to make generalisations from or to apply to other species. This may be particularly true for behavioural reactions where responses to a given noise may vary considerably within a species, dependant on such factors as the animals pre-exposure physiological state, behavioural state or habituation. Some of the variables important in assessing effects include: a) the noise character, such as spectral content and noise duration; b) the sound levels experienced by the animal, thus requiring a knowledge of source levels, local sound propagation conditions and ambient noise; c) the frequency of exposure and any habituation which may occur; d) the hearing capabilities of the species concerned, particularly the overlap in best hearing frequency range and spectral content of the source; e) the ability of the animals hearing system to cope with high levels of continuous, repetitive or transient noise exposure; f) the range of behavioural reactions likely; and g), biological features which may increase the risks of exposure, particularly breeding or spawning events and post-natal care periods.

A considerable amount of noise is generated naturally in the marine environment. Sources include wind, rain, hail, sleet, surf, earthquake events, ice movements and marine animals. The levels produced by some of these sources may be very high, and akin to or greater than many of the more common man-made noises in the ocean, except in the immediate vicinity of such sources. But the historical exposure of marine animals to naturally high noise levels suggests that their hearing systems are physically adapted to cope with at least short term exposure to very high levels. This may be particularly true of some marine mammals which are continually exposed to high noise levels produced by themselves or co-specifics. Anecdotal evidence of some species of marine mammals deliberately approaching noisy vessels or operating air-gun arrays supports this.

Two examples are given of some known effects of specific noise types: vessel noise; and seismic-survey noise. Several studies have been undertaken at the Norwegian Institute of Marine Research on the reactions of fin-fish to fishing vessel noise (eg. Olsen et al, 1982, Ona and Godo, 1990). A general flight reaction has been observed to an approaching vessel, consisting of either a lateral movement away from the vessel or downward directed swimming to form a compacted layer at depth or on the bottom. Such reactions are observed from ranges of several hundreds of metres and may be sustained for up to 10 minutes (Engas et al, 1993). The implications for the bycatch component of the northern Australian bottom-trawl prawn fishery, which operates in shallow water where vessel noise will be significant, have not been investigated.

Offshore seismic surveys involve the firing of intense (to 255 dB re 1microPa- m) 'shots' at intervals of 6-20 s. In 1992 an average of 70-90 thousand km per three months (or ~2.8-3.6 million shots) of seismic surveys were conducted in Australian waters. McCauley (1994) presents a review of the effects and implications of such surveys. Some general effects of such shots on marine animals, with increasing range from the source air-gun array, are: range 1-10 m, lethal effects on plankton, including larval fish and invertebrates; range 10-100 m, possible pathological damage to hearing systems of fish and marine mammals, maximum audible range for some invertebrates (eg. crustaceans); range 100-1000 m, startle and alarm responses in fish and marine mammals, strong behavioural reactions; range 1-10 km, behavioural reactions of fish and marine mammals including avoidance by baleen whales and some fish species; range 10-100 km more subtle behavioural effects with increasing range, but avoidance of sound field observed for some baleen whales and fish at ranges to 30 km; range 100-1000 km, in moderate-good propagation conditions, signal still above ambient.

These reactions give some idea of the scale of short term effects. To gauge long term effects and implications one needs to consider the frequency and severity of exposure, the 'susceptibility' of populations to forced behavioural changes or interference with communication signals, and the proportion of the population exposed. For example the forced deviation of humpback whales say 20 times at 5 km per deviation, is insignificant when compared with their annual migration from the southern ocean up and down the east or west coast. But the operation of air-gun arrays in enclosed bays where humpback calves spend time feeding and mothers resting, may have significant negative repercussions for the population.

In closing this brief review it is worth reiterating many of the unknowns involved in assessing the impact of man-made noise on marine animals. Without elaborating, some of these include: the levels, character, frequency of exposure and persistence of sources; sound propagation conditions and ambient noise levels; fundamental aspects of marine animal hearing, such as frequency range and threshold levels; the conditions required for pathological damage to auditory systems or to induce stress; behavioural reactions to various noise types and levels; habituation; situations which may render individuals or populations 'at risk'; the effects of interfering with communication signals; and finally synergistic effects, or the combined influence of all man-made sources on marine animals.

REFERENCE

Engas A., Lokkeborg, S., Ona, E. and Soldal, A.V. (1993). Effects of seismic shooting on catch-availability of cod and haddock. Norwegian Institute of Marine Research, Fisken Og Havet, NR. 9 -1993, ISSN 0071-5648

McCauley, R.D. (1994). Seismic surveys. In Swan, J.M., Neff, J.M., Young, P.C., (Eds.), Environmental implications of offshore oil and gas development in Australia - The findings of an independent scientific review. pp 19-122, APEA, Sydney, 695 pp.

Olsen, K., Angell, J., Pettersen, F. and Lovik, A. (1982). Observed fish reaction to a surveying vessel with special reference to herring, capelin and polar cod. FAO Fish Rep. 300:131-138

Ona, E., and Godo, O.R. (1990). Fish reaction to trawling noise: the significance for trawl sampling. Rapp. P.-v. Run. Const. int. Explor. Mer. 189:159-166

Geoacoustic Classification of the SW Pacific Seabed

Robin K H Falconer
GeoResearch Associates Ltd, P O Box 137, Waikanae, New Zealand

At frequencies below 1000Hz, and particularly below 100Hz, the properties of the seafloor, the sediments and the basement below it have a significant impact on acoustic propagation. To provide information for a variety of low frequency propagation models that the New Zealand Defence Scientific Establishment uses we have defined values throughout the SW Pacific for a range of parameters of relevance. These include sediment and basement P and S wave velocity, density, attenuation and roughness. Values are specified at key depths e.g. seafloor, shallow, mid depth and base of t he sediment, and in the basement. A total of 20 parameters are specified. The area classified is the SW Pacific extending from the equator to 60 S from 140 E to 160 W. The area has been divided into about 100 geoacoustic provinces. Each province comprises an area within which the acoustic parameters of the seabed, other than water depth and sediment thickness, can be assumed constant. For each province we have a general text description of the province and the factors that influence the values for each type of parameter, and a separate table that lists low, high, and best estimate values for each of the parameters. The province boundaries have been digitised and the provinces, defined as polygons, and their parameter values are stored in a PC Arcinfo GIS. The Defence Scientific Establishment selects and reformats data as appropriate to a range of computation models. There is not sufficient knowledge of the properties of the seabed available to accurately define most parameter values, so of necessity classification is based on inferences based on factors such as: morphology, plate tectonic setting, ocean circulation, basement and sediment age, and sedimentation history. Direct sampling from the Deep Sea Drilling Project provides valuable data for specific sites that can be extrapolated to other areas, and geophysical and geological research cruise data provide broader coverage. General literature or seabed properties is also used. The paper describes the data base, the rationale used, and some of the practical issued involved in defining geoacoustic provinces and in specifying parameter values.

PROGRAMME FOR CONFERENCE

Monday Morning:

10.00 Opening : VC John Nyland
10.10 PLENARY : Kibblewhite

11.00 MEDICAL (R145)

Warren
Carpenter
Loupas/Gill
Carpenter
Zhou/Guan

NOISE

Kibblewhite/Wu
Cato/Taverner
Edwards et al
Rodgers et al
Schultz et al
McCauly/Cato

Monday Afternoon:

IMAGING 1

02.30 Robinson, Buckingham, Jones
Jaffe, Baker, Anstee

06.00 Reception at Castellorizieian Club

Tuesday Morning:

IMAGING 2 (R31)

09.00
Battle et al
Battle et al
Haywood
Blair et al

FISHERIES

Kloser
Coombs
Pauley/Penrose
Waring et al

11.00 PLENARY: Kuperman

IMAGING 3 (R31)

Madry
Denner et al ✓
Thuraisingham ✓
Li et al

REMOTE SENSING 1

Dawes et al ✓
Makris/Cato
Price
Wills et al ✓

Tuesday Afternoon:

IMAGING 4

02.00 Lambert, Walter, Young & Richardson
Arcus/Penrose
Williamson/Olgivie
S Y Zhang/Hua

SEABED 1

1540 Martin Lawrence 79
1600 Z Zhang 81
1620 Bob Hurst 86
1640 Robin Falconer p. 133

Finish lecture 05.00 sharp

REMOTE SENSING 2 (R31)

Duncan et al
Dzieciuch
Penrose/Pauley

06.30-07.00 Embark Darling Harbour for dinner cruise

Wednesday Morning:

09.00 PLENARY: Richardson

SEABED 2

Tindle
Larrson
Hall
Jenkins
Richardson et al
Dunlop/Thompson

REMOTE SENSING 3 (R31)

Lawrence
Krige
Penrose/Forbes
McCauley

12.00-12.10 Closing

TABLE 1.1 GEOACOUSTIC PARAMETERS

APBM	dB/m/kHz	P wave attenuation of basement
APM	dB/m/kHz	P wave attenuation, average for sediments
APT	dB/m/kHz	P wave attenuation near the top of the sediments
ASB	dB/m/kHz	S wave attenuation of lower part of the sediments
ASBM	dB/m/kHz	S wave attenuation of basement
COCW	-	Ratio vel in sediment to vel in water at seafloor
DENB	gm/cm3	Average density of the sediments
DENBB	gm/cm3	Bulk density of basement May be average of deeper section than DENBM
DENBM	gm/cm3	Density of basement
DENM	gm/cm3	Density at base of sediments
DENT	gm/cm3	Sediment density near the top of the sediment
GVP	(km/sec)/km	Gradient of P wave velocity, for the whole sediment column, weighted towards upper part.
HSED	m	Thickness of sediments
ROBM	-	Roughness of basement, Arbitrary scale, Smoothest 1, Roughest 5.
ROT	-	Roughness of the seafloor. Arbitrary scale, Smoothest 1, Roughest 5.
VPT	km/sec	P wave velocity near the top of the sediments
VPB	km/sec	P wave velocity at base of sediments
VPBM	km/s	P wave velocity of basement
VSB	km/sec	S wave velocity at base of sediments
VSBM	km/s	S wave velocity of basement

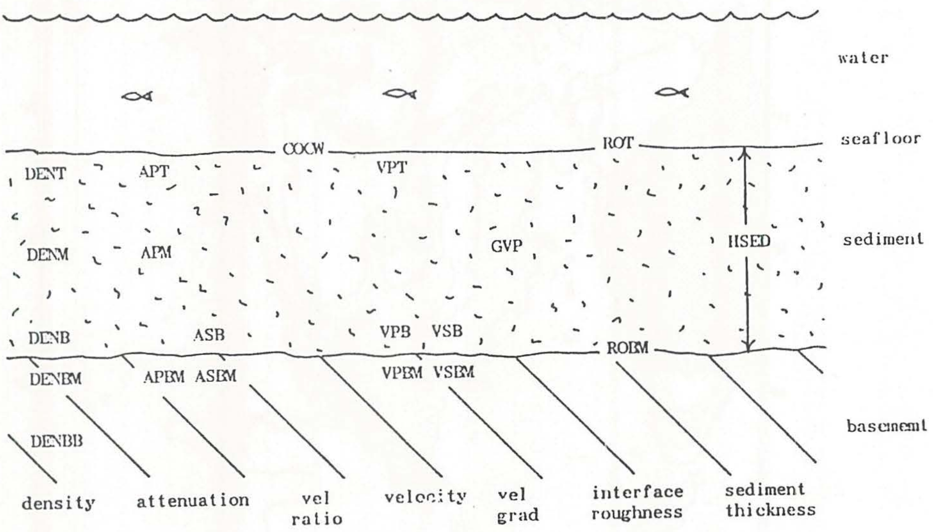

The geoacoustic parameters used.

GeoResearch Associates

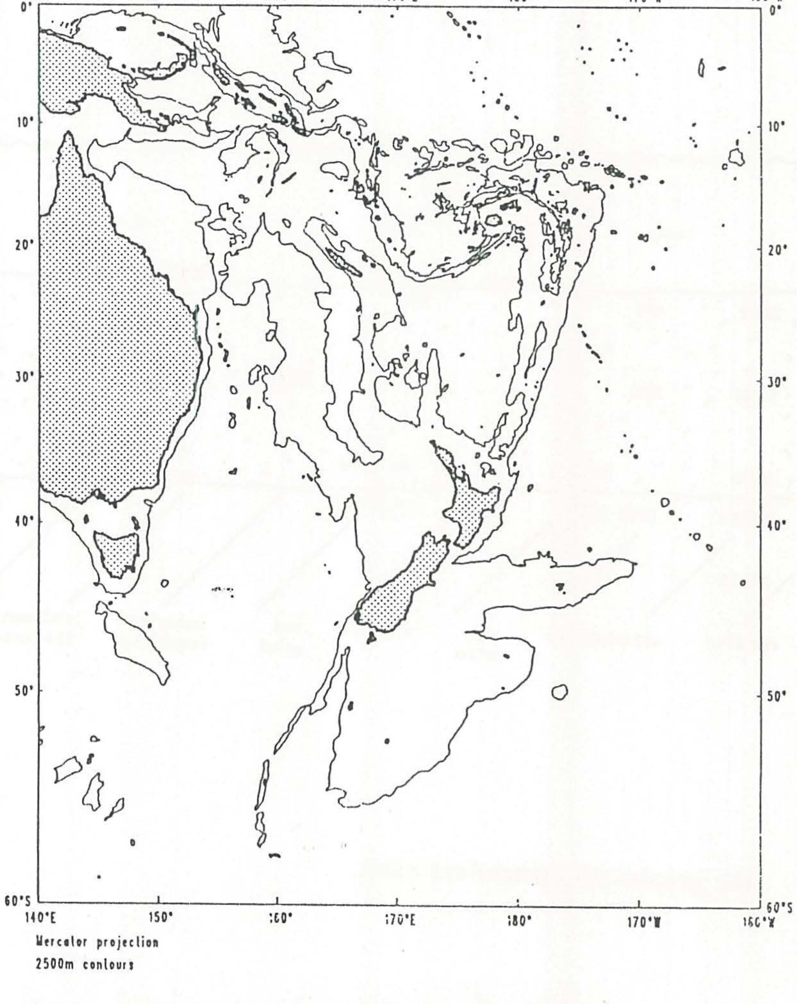

The area for which geoacoustic classification has been carried out. The 2500m outlines most major features.

GeoResearch Associates

Geoacoustic Classification of the SW Pacific Seabed

Robin K H Falconer
GeoResearch Associates Ltd
P O Box 137, Waikanae, New Zealand

At frequencies below 1000Hz, and particularly below 200Hz, the properties of the seafloor, the sediments and the basement below it have a significant impact on acoustic propagation. To provide information for a variety of low frequency propagation models that the New Zealand Defence Scientific Establishment uses we have defined values throughout the SW Pacific for a range of parameters of relevance. These include P and S wave velocity, density, attenuation and interface roughness for sediment and basement. Values are specified at key depths eg seafloor, shallow subbottom, mid depth and base of the sediment, and in the basement. A total of 20 parameters are specified.

The area classified is the SW Pacific extending from the equator to 60 S from 140 E to 160 W The area has been divided into about 100 geoacoustic provinces. Each province comprises an area within which the acoustic parameters of the seabed, other than water depth and sediment thickness, can be assumed constant. For each province we have a general text description of the province and the factors that influence the values for each type of parameter, and a seperate table that lists low, high, and best estimate values for each of the parameters. The province boundaries have been digitised and the provinces, defined as polygons, and their parameter values are stored in a PC ArcInfo GIS. The Defence Scientific Establishment selects and reformats data as appropriate to a range of computation models.

There is not sufficient knowledge of the properties of the seabed available to accurately define most parameter values, so of neccessity classification is based on inferences based on factors such as: morphology, plate tectonic setting, ocean circulation, basement and sediment age, and sedimentaton history. Direct sampling from the Deep Sea Drilling Project provides valuable data for specific sites that can be extrapolated to other areas, and geophysical and geological research cruise data provide broader coverage. General literature on seabed properties is also used used. The talk will describe the data base, the rationale used, and some of the practical issues involved in defining geoacoustic provinces and in specifying parameter values.

Acoustic Imaging and Remote Sensing

International Conference on Underwater Acoustics

University of New South Wales

5th,6th,7th December 1994

Sponsored by

Australian Acoustical Society

Dec 94

Australian Academy of Science

GEC-Marconi

The role of underwater acoustics in the economic exploitation of marine resources and in defence is of vital interest to Australia's needs.

Recent advances in acoustic imaging and remote sensing technology have added new capabilities to both the assessment of marine biological resources and the mapping and classification of the sea-bed.

After the previous two successful conferences on underwater acoustics held at UNSW in 1984 and 1988, it was felt that due to the rapid rate of developments in research and technology another major meeting was warranted. The theme of the present conference is similar to that of the previous two, but provides a greater emphasis on imaging and remote sensing.

Program

Several renowned international speakers will attend, including Jules S. Jaffe from SCRIPPS - "Underwater imaging in 3D"- and Shu-yin Zhang from Academia Sinica -"Low frequency imaging in sediments"

The Conference will open on Monday at 10:00 am following registrations, and close at 12:00 noon on Wednesday. There will be a welcome reception on Monday evening and a Sydney harbour dinner cruise on Tuesday evening. A Technical exhibit by industry will be displayed at the venue for the duration of the conference.

Venue and Accommodation

The conference will be held in the Physics Theatre at the University of New South Wales. The University campus is located approximately 6 km from Sydney airport. Accommodation will be available in two university colleges and at three local motels.

Registration Fee

A registration fee of approximately $180 will include Conference handouts, catering, the reception and dinner cruise. Accommodation will be charged separately and will be advised in registration forms to be circulated in August.

Abstract Submission

If you wish to present a paper at the Conference you are advised to submit an extended abstract by 12 July 1994 --- 2-3 pages (1000-2000 words) to include diagrams and references for issue in the proceedings of the Conference. A full paper can be produced for circulation at the conference or for submission to ***Acoustics Australia*** for publication in a future issue on underwater acoustics.

Layout: Please supply one hard copy of your abstract, including good quality diagrams with captions, and a copy of the plain text on a 3.5" floppy disk, IBM compatible or Macintosh.

The themes of the Conference will be as follows:

- *Ultrasonic Imaging*
- *Sonar*
- *Acoustic Vision*
- *Sea-bed Characterisation*
- *Remote Sensing*
- *The Noise Environment*
- *Acoustic Technologies in Fisheries.*

AUSTRALIAN ACOUSTICAL SOCIETY

International Conference on Underwater Acoustics

5 to 7 DECEMBER 1994

EXPRESSION OF INTEREST

Please complete this form, and return to:

Dr. J.I. Dunlop, Conference Organiser
c/o School of Physics
U.N.S.W.
Box 1 Kensington 2033
N.S.W. Australia

NAME:..
(include given name)

ORGANISATION: ....

POSTAL ADDRESS: ....

....

....

Tel: .... Fax: ....

email: ....

I hope to attend the conference and would be pleased to receive a registration form in August 1994 ☐

I enclose 2-3 page extended abstract and disk ☐

UNDERWATER ACOUSTICS CONFERENCE

in

SYDNEY

Further Information

John Dunlop, School of Physics,
University of New South Wales, Box 1,
Kensington 2033
Tel: (02) 385 4575
Fax: (02) 663 3420
Email: jid@newt.phys.unsw.edu.au